The effects of inflammation on the regeneration and degeneration of axons in the CNS

Francia Carolina Acosta Saltos
University College London

A thesis submitted for the degree of

Doctor of Philosophy (Neuroscience)

to University College London

2014

Declaration

I, Francia Carolina Acosta Saltos, confirm that the work presented in this thesis is my own. Where information has been derived from other sources, I confirm that this has been indicated in the thesis.

Abstract

Microglia have neurotoxic and neuroprotective effects. The aim of the current project was to investigate the effects of perineuronal microglial activation on axonal regeneration in adult rats and the effects of prolonged neuroinflammation on foetal mouse brain.

In contrast to the PNS, the CNS only displays limited axonal regeneration after injury and little perineuronal inflammation. Inflammation around the cell bodies of axotomised neurons has been demonstrated to promote CNS regeneration.

Polyinosinic:polycytidylic acid (Poly I:C) is an inflammatory agent. Following delivery of Poly I:C into the motor cortex and a concomitant C4 dorsal corticospinal tract (CST) injury, rats exhibited more CST axons in the cervical spinal cord and less retraction from the injury site than controls. Following facial nerve axotomy, Poly I:C injections adjacent to the facial nucleus accelerated functional recovery.

Viral vectors carrying Granulocyte Macrophage Colony Stimulating Factor (GM-CSF) were injected into motor cortex. GM-CSF virus reduced retraction of corticospinal axons from a spinal cord injury site. Behavioural studies of forelimb movements showed that C4 injury had a greater impact on fine distal movements, particularly reaching and grasping, which are known to be controlled by the CST. Treating rats with GM-CSF virus showed a trend towards improved forelimb sub-movements and significantly aided the reaching function recovery.

Perinatal activation of periventricular phagocytes has been suggested to result in white matter damage, causing persistent motor disabilities. Transuterine injections of control or GM-CSF virus targeting the lateral ventricles of mice at gestational day 14, resulted in a widespread virally-transduced cells. Greater numbers of phagocytic and activated microglia were present in the areas of viral transduction. There was increased inflammation in the periventricular white matter. Although, the level of transduction remained relatively constant with increasing time, inflammation decreased, suggesting that GM-CSF toxicity is high before or around birth.

Acknowledgements

I profoundly thank my supervisor Professor Gennadij Raivich for giving me the opportunity to embark on the exciting journey of scientific discovery. His support and guidance during the four years of my PhD have been invaluable.

A special thanks to my supervisor Professor Patrick Anderson for teaching me the techniques that were essential for this project. I am very grateful for his insights, suggestions and attention to detail that were important in creating this thesis.

I thank my supervisor Professor Adrian Thrasher for sharing with me his expertise during the first year of my PhD.

I am deeply thankful to my supervisor Dr Mariya Hristova for her constant help, kindness and encouragement particularly at the end of my PhD. Thank you for giving me some of your precious time to check work on this thesis.

Thanks to Dr Roman Gonitel, Dr Alejandro Acosta Saltos, Dr Ahad Rahim, Dr Simon Waddington, Dr Li Ying and Professor Geoffrey Raisman for teaching me various techniques that were essential for this project.

Thanks to all of my colleagues at the Molecular Immunology Unit, Institute of Child Health. I am particularly thankful to Dr Conrad Vink and Dr Marlene Carmo for teaching me more about lentiviral vector production.

To my fellow PhD students Laura Thei, Smriti Patodia and Eridan Rocha Ferreira- I whole heartedly thank you for all those wonderful moments we shared in the lab and in ULU.

I thank all the students I had the pleasure to work with, Dr Catherine Pringle, Seetal Chavda, Elisabeth Thubron, Lucas Topham, Harmony Ubhi, Ainkaran Santhirasekaram, Victoria Boggiano, Kim Lyons and Devavrata Joshi.

I would like to thank my family for their love and unconditional support. Thanks for being so caring and for your constant encouragement.

This degree was funded by a Natalie Rose-Barr PhD studentship from International Spinal Research Trust and GlaxoSmithKline. Thanks for the generous support.

This thesis is dedicated to my mum, dad and brother

Francia, Ramon and Alejandro

Table of Contents

List of Figures

List of Tables

Abbreviations

abl	Abelson Murine Leukemia Viral Oncogene Homolog 1
Akt	Akt also known as Protein Kinase B (PKB)
ATF3	Activating Transcription Factor 3
BBB	Blood Brain Barrier
BDA	Biotinylated Dextran Amine
BDNF	Brain-Derived Neurotrophic Factor
bFGF	Basic Fibroblast Growth Factor
c/EBP	CCAAT-Enhancer-Binding Protein
cAMP	Cyclic Adenosine Monophosphate
cGMP	cyclic Guanosine Monophosphate
CGRP	Calcitonin Gene-Related Peptide
ChP	Choroid Plexus
CNS	Central Nervous System
CNTF	Ciliary Neurotrophic Factor
CON	Control
cPPT	Central Polypurine Tract
CSF	Colony Stimulating Factor
CSPGs	Chondroitin Sulphate Proteoglycans
CST	Corticospinal Tract
DAMPS	Damage-Associated Molecular Patterns
DAPI	4',6-Diamidino-2-Phenylindole
DREZ	Dorsal Root Entry Zone
DRG	Dorsal Root Ganglion

EGF	Epidermal Growth Factor
eGFP	enhanced Green Fluorescent Protein
eNOS	endothelial Nitric Oxide Synthase
EP	Endogenous Peroxidase
EPO	Erythropoietin
ERK	Extracellular Signal Regulator
G-CSF	Granulocyte-Colony Stimulating Factor
GFAP	Glial Fibrillary Acidic Protein
GM-CSF	Granulocyte-Macrophage Colony Stimulating Factor
GTPase	Guanosine-5'-Triphosphatase
HEK-293T	Human Embryonic Kidney 293T Cells
hipp	Hippocampus
IBA-1	Ionized Calcium-Binding Adapter Molecule 1
ICAM1	Intercellular Adhesion Molecule 1
IFN	Interferon
IGF-1	Insulin-Like Growth Factor 1
IL	Interleukin
iNOS	Inducible Nitric Oxide Synthase
IRES	Xiap-Derived Internal Ribosome Entry Site
JAK2	Janus Kinase-2
JNK	Jun-N-Terminal Kinase
LIF	Leukemia Inhibitory Factor
LPS	Lipopolysaccharide
LTRs	Long Terminal Repeats
MAC-1	Complement Receptor Macrophage-1

MAG	Myelin-Associated Glycoprotein
MAPK	Mitogen Activated Protein Kinase
MCP	Monocyte Chemotactic Protein
M-CSF	Macrophage-Colony Stimulating Factor
M-CSFR	Macrophage-Colony Stimulating Factor Receptor
MDA-5	Melanoma Differentiation-Associated Protein 5
MDFs	Macrophage Derived Factors
MERTK	MER Receptor Tyrosine Kinase
MFI	Median Fluorescence Intensity
MHC	Major Histocompatibility Complex
MIP	Macrophage Inflammatory Protein
Mst3b	Mammalian Sterile 20-Like Kinase-3b
MTT	3(4,5-Dimethythiazol-2-Yl)-25-Diphenyltetrazolium Bromide
mTOR	mammalian Target of Rapamycin
NF-kappa B	Nuclear Factor Kappa Light Chain Enhancer Of Activated B Cells
NG2	Neural/Glial Antigen 2
NGF	Nerve Growth Factor
NMJ	Neuromuscular Junction
NO	Nitric Oxide
NOD	Nucleotide-Binding Oligomerization Domain
NT-3	Neurotrophin-3
Omgp	Oligodendrocyte-Myelin Glycoprotein
PAMS	Pathogen-Associated Molecular Patterns
PBS	Phosphate Buffered Saline
PDGF	Platelet-Derived Growth Factor

PI3K	Phosphatidyl-Inositide-3 Kinase
PKA	Camp-Dependent Protein Kinase
PNS	Peripheral Nervous System
Poly I:C	Polyinosinic:polycytidylic Acid
PRRs	Pattern Recognition Receptors
PVL	Periventricular Leukomalacia
PXY	Pyramidal Decussation
RANTES	Regulated On Activation, Normal T Cell Expressed And Secreted
RGC	Retinal Ganglion Cells
RIG-I	Retinoic Acid Inducible Gene-I
RRE	Rev Response Element
SCI	Spinal Cord Injury
SFFV	Spleen Focus-Forming Virus
STAT	Signal Transducer And Activator Of Transcription
STR	Striatum
TCR	T-Cell Receptor
TdT	Terminal Deoxynucleotidyl Transferase
TGF	Transforming Growth Factor
TLRs	Toll-Like Receptors
TNFR	Tumour Necrosis Factor Receptor
TNF-α	Tumour Necrosis Factor Alpha
TRN	Thalamic Reticular Nucleus
TUNEL	Terminal Deoxynucleotidyl Transferase Dutp Nick End Labeling
vCAM	Vascular Cell Adhesion Protein
VE	Ventricular Epithelium

VSVG	Vesicular Stomatitis Virus Glycoprotein
WM	White Matter
WPRE	Woodchuck Hepatitis Post-Transcriptional Regulatory Element

CHAPTER ONE

INTRODUCTION

Axons in the central nervous system (CNS), which include those of the spinal cord, normally fail to regenerate after injury. However, it is well documented that peripheral nervous system (PNS) axonal regeneration is vigorous and is often associated with structural and functional recovery (Cajal, 1928). There are three main theories that seek to explain this dichotomy: first, presence of inhibitory molecules in the CNS; second, lack of neurotrophic support in the CNS environment; and third, intrinsic inability of CNS neurons to mount an appropriate cell body response to axotomy.

Peripheral Nerve Regeneration after Injury

Cell body response

Morphological changes

The neuronal cell body undergoes a range of morphological changes following axonal injury. The Nissl bodies, which are large accumulations of granular endoplasmic reticulum and free ribosomal rosettes (Lieberman, 1971), disperse in the cytoplasm (chromatolysis), the nucleus is displaced from the centre of the neuron to the periphery, the nucleolus is enlarged, the cell body swells, and the synaptic terminals retract from the cell body (Lieberman, 1971). In addition there is an increase in the number of organelles such as ribosomes and mitochondria (Lieberman, 1971). The cell body response reflects the switch in metabolic priority from making neurotransmitters to the synthesis of materials that are necessary for axonal repair and growth (Grafstein, 1975).

Molecular Changes

Following peripheral nerve injury, axotomised neurons undergo a molecular response which drives axonal regeneration. They increase the expression of growth-associated proteins including adhesion molecules, axonal transport molecules, cytoskeletal components, secreted growth factors and cytokines. There is also an increase in energy, amino acid, iron and lipid metabolism

(Holtmaat et al., 1998; Lieberman, 1971; Raivich and Makwana, 2007), and changes in the expression of ion channels and transporters, particularly those for calcium (Arteaga et al., 2004; Hudmon et al., 2008; Wu et al., 2008). This molecular response is initiated by signals from the injury site that act on intracellular pathways which ultimately influence gene expression.

INJURY SIGNALS

Axonal injury generates three types of signals that exert effects on neurons. First, injury transiently opens the axonal membrane permitting the influx of ions (Yoo et al., 2003), which cause depolarisation and transmission of injury mediated action potentials. Second, axotomy produces a discontinuation in the axonal transport which normally brings neurotrophic signals to the neuronal cell body (Raivich et al., 1991b). Third, injury exposes the axon to neurotrophic intracellular contents of adjacent cells (Elde et al., 1991; Kirsch et al., 2003; Sendtner et al., 1997) and other molecules from the inflamed neural environment (Lindholm et al., 1987); these can be retrogradely transported to the neuronal cell body (Hanz et al., 2003).

MAPK AND OTHER EARLY SIGNAL ENZYMES

Intracellular signalling enzymes are involved in propagating the signals derived from injury site within the injured neuron. In vitro studies have demonstrated that neurite outgrowth is influence by signalling involving mitogen activated protein (MAPK), Jun-N-terminal (JNK), and extracellular signal regulator (ERK), abl, AKT and p38 protein kinases, as well as cAMP, and cAMP-dependent protein kinase A (PKA) (Lindwall and Kanje, 2005; Perlson et al., 2005).

In vivo, JNKs become activated rapidly after peripheral nerve injury and are retrogradely transported with their upstream kinases (Lindwall and Kanje, 2005). Deletion of JNK1 and JNK2 genes mildly delays functional recovery after facial nerve injury (Ruff et al., 2012).

Mammalian sterile 20-like kinase-3b (Mst3b) is a protein kinase activated by PKA (Zhou et al., 2000). In vitro, Mst3b is essential for neurotrophin-stimulated axon outgrowth (Irwin et al., 2006). In vivo, removal of Mst3b abolishes neurite

outgrowth by retinal ganglion cells and reduces axonal regeneration after peripheral nerve injury (Lorber et al., 2009).

Peripheral axotomy causes a decrease in the activated form of Ras, a small GTPase involved in the activation of mitogen activated proteins (Makwana et al., 2009). Neuronal overexpression of active Ras in vivo increases central sprouting emanating from the injured motor neurons (Makwana et al., 2009).

Phosphatidyl-Inositide-3 kinase (PI3K) expression (Ito et al., 1996) and activation of Akt, its main target protein kinase, is induced by axotomy (Murashov et al., 2001; Owada et al., 1997). In vivo, deletion of the p110 delta catalytic component of PI3K reduces Akt activation, slows down axonal regeneration and mildly delays functional recovery (Eickholt et al., 2007).

TRANSCRIPTION FACTORS

The cytoplasmic signalling cascades brought about by axonal injury are followed by an increased nuclear localisation and activation of proteins involved in gene transcription. Numerous axotomy-induced transcription factors have been identified. These include: c-Jun, Jun-D, activating transcription factor 3 (ATF3), P311, Sox11, several members of the CEBP family and STAT3 (de Heredia and Magoulas, 2013; Fujitani et al., 2004; Jankowski et al., 2009; Mason et al., 2003; Nadeau et al., 2005; Schwaiger et al., 2000). In contrast, the expression of other transcription factors can be reduced, including islet-1 (Hol et al., 1999), Fra-2 and ATF-2 (Herdegen et al., 1997; Robinson, 1996).

AP-1

c-Jun is consistently upregulated in all models of successful regeneration (Herdegen et al., 1991; Jenkins and Hunt, 1991; Lindwall and Kanje, 2005; Mason et al., 2003; Raivich et al., 2004). Neuronal injury increases JNK-mediated c-Jun phosphorylation (Herdegen et al., 1998; Kenney and Kocsis, 1998). Application of JNK inhibitor to explanted injured dorsal root ganglions (DRG) reduces neurite outgrowth (Lindwall et al., 2004). However, in vivo removal of phosphorylation sites in the c-Jun protein does not affect peripheral nerve regeneration (Ruff et al., 2012). Nonetheless, neuronal deletion of c-Jun dramatically reduces the expression of regeneration-associated genes, the

speed of target reinnervation and the recovery of motor function (Raivich et al., 2004). In addition, deletion of c-Jun blocks post-axotomy perineural sprouting (Makwana et al., 2010), reduces neuronal cell death and inhibits the activation of neighbouring microglia and recruitment of lymphocytes (Raivich et al., 2004).

ATF3 is axonally transported from the injured distal stump (Lindwall and Kanje, 2005) and may act as a retrograde injury signal similar to STAT3 (Lee et al., 2004a). In vitro, ATF3 encourages neurite outgrowth. In vivo, the overexpression of ATF3 leads to increased expression of regeneration-related genes and an earlier onset of axonal regeneration (Seijffers et al., 2006). ATF3 is highly localised in the neuronal nucleus after axotomy but is cytoplasmic in the absence of injury (Bontioti et al., 2006; Campbell et al., 2005) Interestingly, nuclear localisation of ATF3 after axotomy appears to depend on the presence of c-Jun (Raivich, 2011).

STAT3

Early after peripheral nerve injury there is a transient increase in STAT3 expression, activation and nuclear translocation (Schwaiger et al., 2000) in the cell bodies of the injured neurons. STATs can be activated by signalling pathways induced by several cytokines and growth factors including IL-6, LIF, CNTF, G-CSF, G-CSFR, EPO, EGF, IGF-1, and BDNF, as well as NGF withdrawal and the presence of free radicals, excitatory neurotransmitters and other inflammatory mediators released after injury (Dziennis and Alkayed, 2008). STAT3 is phosphorylated at the proximal stump of the injured axon and retrogradely transported to the neuronal cell nucleus (Lee et al., 2004a). Conditional mutant mice lacking STAT3 specifically in their neurons have a profound reduction in expression of other neuronal regeneration-associated genes, speed of axonal regeneration, functional recovery and target reinnervation (Patodia and Raivich, 2012a).

C/EBP

C/EBPβ is upregulated and phosphorylated after neuronal injury and has an important role on the expression of regeneration-associated genes (Nadeau et al., 2005). In vitro, c/EBP delta-deficient primary sensory neurons demonstrate impaired axonal growth, and a reduced response to a conditioning lesion (de

Heredia and Magoulas, 2013). In vivo, c/EBP delta also appears to have a role in the response to facial nerve axotomy (Patodia and Raivich, 2012a). Other signalling pathways involved in axonal injury such as the JAK/STAT pathway may also converge on the c/EBP family (Jiang and Zarnegar, 1997).

SOX11

SRY-box containing gene 11 can drive expression of neurite growth associated genes (Bergsland et al., 2006; Jankowski et al., 2006). In vivo, SOX11 is upregulated after axotomy (Boeshore et al., 2004; Jankowski et al., 2006; Jankowski et al., 2009).In vitro, inhibition of SOX11 decreased DRG regeneration following axotomy (Jankowski et al., 2006). In vivo, knocking down SOX11 reduces the number of regenerating DRG axons and diminishes the injury induced ATF3 levels by half (Jankowski et al., 2009).

P53

p53 is a regulator of the expression of growth cone guidance molecules and their receptors (Arakawa, 2005). Overexpression of dominant negative p53 leads to growth cone collapse in primary cortical neurons and a decrease in neurite outgrowth, together with reduced expression of growth cone-associated genes (Di Giovanni et al., 2006; Tedeschi et al., 2009). In contrast, over-expression of wild type p53 leads to increased growth cone size (Qin et al., 2009). In vivo, p53 knock out mice show decreased target muscle reinnervation after nerve injury (Di Giovanni et al., 2006).

NUCLEAR FACTOR KAPPA LIGHT CHAIN ENHANCER OF ACTIVATED B CELLS

High levels of NF-kappa B can be observed in the injured neuron after peripheral nerve injury (Ma and Bisby, 1998; Pollock et al., 2005). Like STAT3 and ATF3, it responds to stimuli in neurites and travels retrogradely to affect gene transcription. NF-kappa-B can enhance or inhibit neurite growth depending on its phosphorylation status. Phosphorylation of NF-kappa B by the IκBα subunit IKK-β results in reduced neurite growth, whilst neurons lacking IKK β activity show increased neurite growth (Gutierrez et al., 2008).

DOWNSTREAM EFFECTOR MOLECULES

Changes in intracellular signalling and the regulation of transcription after peripheral nerve injury lead to the expression of molecules which encourage successful axonal regeneration. These include adhesion molecules, neuropeptides and cytoskeletal adaptors (Patodia and Raivich, 2012b).

ADHESION MOLECULES

Adhesion molecules enable the axon to interact with the bands of Büngner as the axon elongates (Grumet, 1991; Shapiro et al., 2007). Among the numerous adhesion molecules up-regulated by axons following injury, α7β1 (Raivich et al., 2004; Werner et al., 2000) and CD44 (Lin and Chan, 2003; Nagy et al., 1998) have been identified as the in vivo downstream targets of regeneration-associated transcription factors. Deletion of neuronal c-Jun or STAT3 is associated with a reduction in the expression of α7β1 integrin (Patodia and Raivich, 2012b; Raivich et al., 2004; Ruff et al., 2012). There are significant delays in axonal regeneration following facial nerve crush injury in mice in which the α7 subunit is globally deleted (Jones et al., 2000). In addition, preliminary data suggests that the deletion of β1 integrin is associated with a reduction in axonal regeneration speed, similar to that seen in α7 knockout mice (Patodia and Raivich, 2012b). Following facial nerve axotomy, CD44 expression is abolished in mice lacking neuronal c-Jun (Ruff et al., 2012) and STAT3 (Patodia and Raivich, 2012b). Inhibition of CD44 reduces axon outgrowth from noradrenergic neurons grafted into the anterior chamber of the eye (Nagy et al., 1998) and produces significant defects in routing of retinal axons through the optic chiasm (Lin and Chan, 2003)

NEUROPEPTIDES

Axonal injury leads to an increase in the expression of neuropeptides, molecules involved in cell signalling via their action on G-coupled receptors. The expression of the neuropeptides calcitonin gene-related peptide (CGRP) and galanin is regulated by transcription factors c-Jun and STAT3. Mice deficient in neuronal c-Jun and STAT3 fail to upregulate CGRP and galanin following facial nerve axotomy (Patodia and Raivich, 2012b; Raivich et al., 2004; Ruff et al., 2012). The absence of galanin reduces the rate of sciatic nerve regeneration following a

crush injury and was associated with long-term functional deficits in the injured animals. In addition, cultured DRG from galanin deficient mice show deficits in neurite number and length (Holmes et al., 2000). Knocking down CGRP expression, by delivery of siRNAs to the sciatic nerve injury site, was also associated with significant disruption to axonal growth (Toth et al., 2009).

CYTOSKELETAL ADAPTORS

Cytoskeletal adaptors are present in growth cones and are involved in cytoskeletal remodelling (Baas and Ahmad, 2001). Increased expression of the adaptor molecules, GAP-43 and CAP-23, is induced by nerve injury and regulated by regeneration-associated transcription factors (Bomze et al., 2001; Goslin and Banker, 1990). Following nerve injury, GAP-43 and CAP-23 mRNA are upregulated in axotomised neurons (Mason et al., 2002). Mice deficient of c/EBPβ show reduced upregulation of GAP-43 following injury (Nadeau et al., 2005). Similarly, axotomy-induced expression of CAP-23 is reduced in mice lacking c-Jun (Patodia and Raivich, 2012b). Functionally, global deletion of GAP-43 results in defective neuronal pathfinding during development, leading to a grossly abnormal adult CNS in mice (Strittmatter et al., 1995). Similarly, CAP-23 knock out mice fail to produce stimulus-induced nerve sprouting at the adult neuromuscular junction (Frey et al., 2000), and show reduced axonal regeneration following facial nerve axotomy (Anderson et al., 2006).

Axonal Response

Distal end

Following peripheral nerve injury the portion of nerve distal to the injury site undergoes Wallerian degeneration. This process is already noticeable around 24 hours after nerve lesion (Perry and Brown, 1992; Stoll and Muller, 1999) . There is rapid breakdown of the axoplasm, with granular disintegration of the axonal cytoskeleton (Bignami and Ralston, 1969; Trojanowski et al., 1984). The myelin sheath becomes fragmented and breaks down into fatty spheroids (Lassmann et al., 1978). Schwann cells detach from myelin sheaths and begin to clear myelin and axonal debris (Hirata et al., 2002; Perry and Brown, 1992). However, this process is predominantly taken over by infiltrating macrophages (Tanaka et al., 1992), which are recruited by Schwann cells through the release of cytokines

(Tofaris et al., 2002). Debris clearance eliminates some factors associated with myelin (e.g. MAG) which might otherwise inhibit axonal growth. This begins the process of turning the distal nerve into an environment that promotes regeneration.

Schwann cells proliferate as they lose axonal contact and are stimulated by macrophages secreted cytokines (Karanth et al., 2006). They then line up within the hollowed endoneurial tubes forming the bands Büngner, pathways that will later support regenerating axons (Bungner, 1891) by secreting neurotrophic factors (Funakoshi et al., 1993; Lindholm et al., 1987; Meyer et al., 1992), and expressing adhesion molecules and their receptors (Fawcett and Keynes, 1990; Martini and Schachner, 1988).

Proximal end

At the proximal nerve stump, injury also causes axonal degeneration with macrophage invasion and myelin breakdown but this is limited to the area most proximal to the lesion site (Grafstein, 1975; Lieberman, 1971).

Injury transiently opens the membranes of cells within the nerve, exposing the injured axonal tip to the intracellular contents of other axons and Schwann cells (Kirsch et al., 2003; Sendtner et al., 1997). With the arrival of axoplasm containing cytoskeletal components and organelles, the proximal end of the axon seals and forms a bulbous swelling at the tip (Meller, 1987; Vallee and Bloom, 1991).These axonal swellings eventually give rise to some of the axonal sprouts which are tipped by growth cones (Cajal, 1928).

Growth cones are highly dynamic sensory structures at the tip of sprouts (Spira et al., 2003). The growth cone looks like a webbed foot; it has a swollen central area from which processes called lamellipodia and filopodia extend (Fawcett and Keynes, 1990). Growth cones grow towards their target tissues aided by the mechanical and chemical guidance from the bands of Büngner (Ide, 1996).

SPROUTING

In addition to the sprouting observed at the tips of regenerating axons, growth cones can arise more proximally: at the nodes of Ranvier (Cajal, 1928), distal part of dendrites (Fenrich et al., 2007) and sometimes even at the level of the injured

neuronal cell body (Linda et al., 1985; Makwana et al., 2010). Nerve injury can also promote sprouting from adjacent uninjured axons (Nurse et al., 1984); (Nguyen et al., 2002; Tanigawa et al., 2005). Sprouts which arise closest to the injury site can enter the distal nerve stump along with those arising directly from the injured axonal tip (Mackinnon et al., 1991; Morris et al., 1972).

Successful axonal regeneration leads to the reinnervation of target synapses (Magill et al., 2007). In motor axon regeneration, this process appears to occur in a step wise manner. The fastest regenerating axons reach the muscle and sprout, a single regenerating axon forming synapses on many denervated neuromuscular junctions. Subsequent arrival and sprouting of more axons, results in many NMJs receiving axonal endplates from more than one regenerating axon. This phenomenon has been termed NMJ polyinnervation. Ultimately, pruning abolishes polyinnervation and each NMJ is innervated by a single axon (Magill et al., 2007). Mono-innervation of NMJs is associated with good functional recovery (Magill et al., 2007).

Upon reinnervation of targets, Schwann cells remyelinate the regenerated axon providing them with the property of saltatory nerve conduction (Ide, 1996). However, the diameter of regenerated axons, their conduction velocity and excitability remain below normal levels for a long time following regeneration (Fields and Ellisman, 1986). Figure 1 summarises the changes that occur following injury to peripheral neurons.

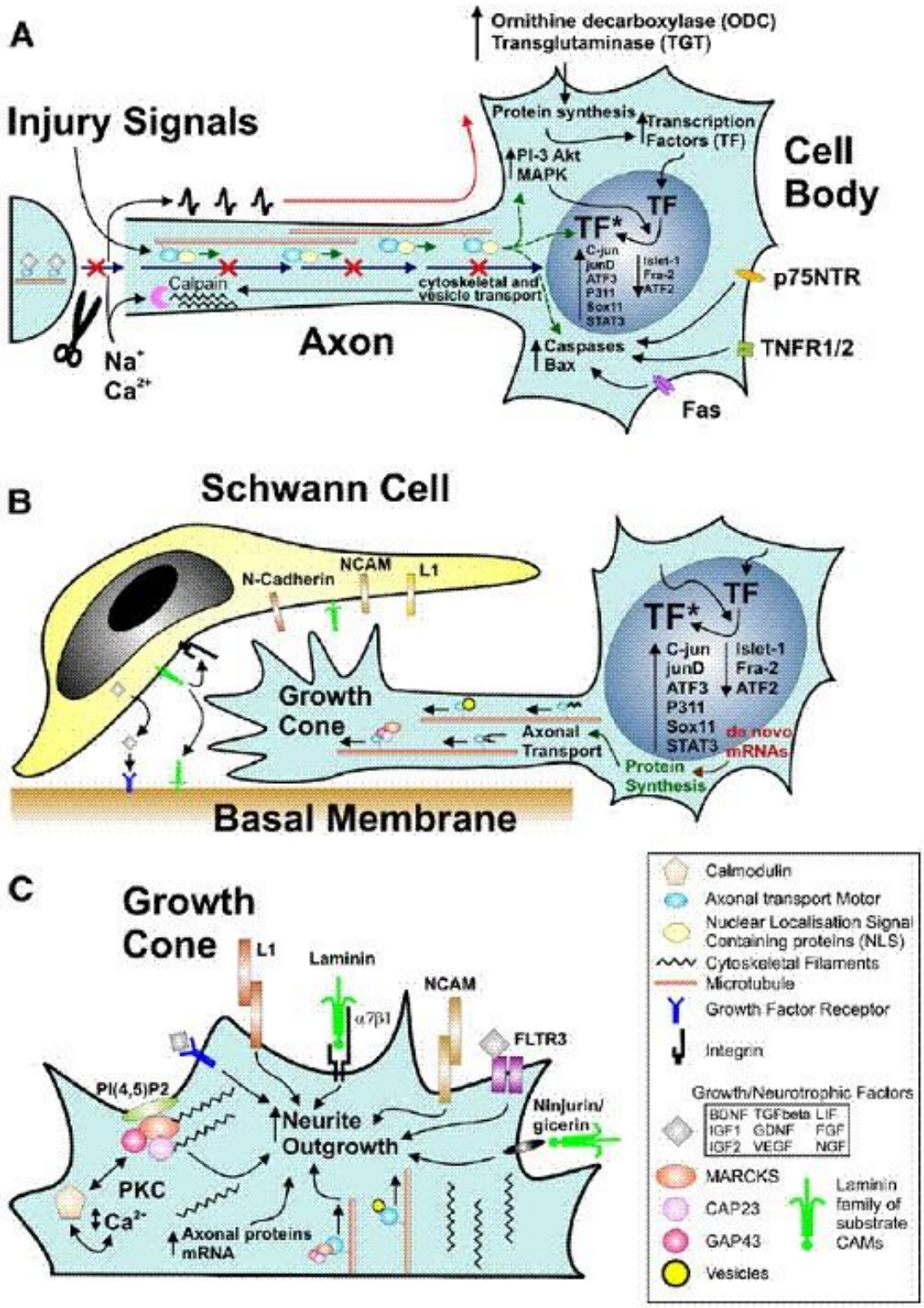
A
Ornithine decarboxylase (ODC)
Transglutaminase (TGT)
Injury Signals
Protein synthesis
Transcription Factors (TF)
PI-3 Akt
MAPK
Cell Body
TF
TF*
C-jun
junD
ATF3
P311
Sox11
STAT3
Islet-1
Fra-2
ATF2
p75NTR
Calpain
cytoskeletal and vesicle transport
Axon
Caspases
Bax
TNFR1/2
Fas
Na+
Ca2+
B
Schwann Cell
N-Cadherin
NCAM
L1
Growth Cone
Axonal Transport
de novo mRNAs
Protein Synthesis
Basal Membrane
C
Growth Cone
L1
Laminin
NCAM
α7β1
FLTR3
PI(4,5)P2
Neurite Outgrowth
Ninjurin/ gicerin
PKC
Ca2+
Axonal proteins mRNA
Calmodulin
Axonal transport Motor
Nuclear Localisation Signal Containing proteins (NLS)
Cytoskeletal Filaments
Microtubule
Growth Factor Receptor
Integrin
Growth/Neurotrophic Factors
BDNF TGFbeta LIF
IGF1 GDNF FGF
IGF2 VEGF NGF
MARCKS
CAP23
GAP43
Vesicles
Laminin family of substrate CAMs

Figure 1: Summary of cellular mechanisms involved in successful regeneration: injury-induced signalling (A); cell body response involved in axonal growth (B); and molecular mechanisms of neurite outgrowth at the growth cone (C). (A) Axonal trauma induces a cessation of normal trophic retrograde transport (blue arrows), a rapid influx of cations resulting in an antidromal train of action potentials (red), and exposure to injury signals transported retrogradely via proteins containing nuclear localization signals (green), that may act in synergy to induce the biochemical activation in the neuronal cell body. This regeneration programme includes enzymes regulating mRNA metabolism—ODC, TGT, intracellular cascades such as MAP kinases and PI3K-Akt, and complemented by enhanced nuclear localization and phosphorylation or other forms of activation (*) for a host of transcription factors (TF) including c-Jun, etc., as well as numerous molecules that regulate cell death, including death domain carrying membrane proteins (p75, TNFR, fas) as well as cytoplasmic caspases and bcl-2 family members. At the cut axon, the rapid influx of Ca2+ causes calpain activation and cytoskeletal remodelling that results in structured accumulation of anterogradely transported vesicles and cytoskeletal components, transforming the axon tip into an extension-competent growth cone. (B) Regenerating neurons undergo transcription factor-dependent changes in mRNA and protein synthesis that result in the production and anterograde transport of vesicles and proteins (cell adhesion molecules, cytoskeleton, growth-associated proteins such as the GMC family members GAP43, CAP23 and MARCKS), that are needed for interacting with the local cell adhesion and guidance molecules (L1, NCAM, N-cadherin, laminin etc.) and extending the axonal growth cone along the Schwann cells and the basal membrane substrate of the peripheral neural tubes. (C) A brief overview of signals regulating neurite outgrowth at the axonal growth cone. This can involve a variety of interactions via preferentially homophilic (L1, NCAM) or heterophilic cell adhesion ligands (laminin, alpha7 beta1 integrin, ninjurin/gicerin), a variety of growth factors and their receptors such as FGF and FLTR3, and the phosphoinositol-4,5-diphosphates – PI(4,5)P2 – that associate with the GMC family of calcium/calmodulin ligands and Protein Kinase C (PKC) and regulate actin cytoskeleton polymerization, organization and disassembly. The anterograde axonal transport of vesicles, signalling molecules, cytoskeletal proteins and their mRNA plays a critical role in providing structural and regulatory components for axonal elongation. From Raivich and Makwana (2007).

The rate of nerve regeneration and functional recovery

In the first 2 to 7 days following nerve injury, there is a delay in axonal regeneration, which is associated with the initial retrograde degeneration of proximal axon and slow axonal growth through the nerve injury scar (Forman and Berenberg, 1978; Gutmann et al., 1942; Sunderland, 1947). Having crossed the scar, axonal fibres grow at a rate between 1 to 4 mm per day (Bisby and Keen, 1985; Forman and Berenberg, 1978; Gutmann et al., 1942). Estimates of the rate of axonal regeneration depend on the method used for its measurement (Raivich and Makwana, 2007).

Complete anatomical target reinnervation following sciatic nerve transection occurs after 6 weeks in mice (Magill et al., 2007) and after 10 weeks in rats (Sinis et al., 2009). At these times, functional recovery is robust and almost complete in mice (Magill et al., 2007) but minimal in rats (Sinis et al., 2009). In fact, functional recovery in the rat is minimal even up to 16 weeks after peripheral nerve transection (Bendella et al., 2011; Hadlock et al., 2010; Knox et al., 2013).

The overall rate of axonal regeneration after peripheral nerve injury can be accelerated by the use of conditioning lesions (McQuarrie et al., 1977) and electrical stimulation of the proximal stump of severed peripheral nerves (Al-Majed et al., 2000a; Brushart et al., 2002). However, these procedures only marginally increase functional recovery in the rats after peripheral nerve transection, despite increasing the speed of anatomical regeneration (Hadlock et al., 2010; Zhang et al., 2013).

The poor functional recovery in rats despite robust axonal regeneration has been explained by inaccurate target reinnervation. Collateral axonal sprouting at the nerve transection site (Ito and Kudo, 1994) results in highly branched axons innervating multiple inappropriate targets (Bendella et al., 2011; Dohm et al., 2000; Sinis et al., 2009). In addition, terminal motor axon sprouting at the neuromuscular junctions leads to poly-innervation of NMJs rather than normal mono-innervation (Guntinas-Lichius et al., 2000; Sinis et al., 2009).

Polyinnervation of NMJs and collateral sprouting remain up to 16 weeks post nerve transection in rats and are associated with poor functional recovery (Bendella et al., 2011). Interestingly, when rat peripheral nerve is crushed instead of transected, robust functional recovery is achieved (Zhang et al., 2013) and no NMJ polyinnervation or inappropriate multiple target innervation by axons is observed (Magill et al., 2007).

Changes following CNS axonal injury

Although some functional recovery occurs following partial spinal cord injury, tracts which are damaged almost invariably fail to demonstrate successful regeneration. This failure has been most commonly explained by the fact that the environment presented to an injured CNS projecting axon is highly inhibitory to regeneration and lacks the neurotrophic support that is characteristic of the injured PNS

Axonal die back

After spinal cord injury axons are known to undergo a series of changes. Like in the PNS, distal CNS axon ends undergo Wallerian degeneration (Cajal, 1928). However, the ends of the axons in the proximal stump die back and fail to regenerate. The distance that axons die back increases as time passes: at week

one the mean die back distance that CST axons die back is 1.4mm and at 16 weeks it is approximately 4.1mm. However, the majority of axons stop dying back after 4 weeks, at approximately 2.5mm from the injury site. Nonetheless, a minority of axons continue to die back for much longer distances (Seif et al., 2007).

The proximal endings of severed spinal axons develop into spherical swellings known as terminal bulbs (or retraction bulbs), which are clearly seen within one day after injury and persist for many months (Fishman and Kelly, 1984b; Pallini et al., 1988; Pasquale-Styles et al., 2003). Terminal bulbs contain dense accumulations of axoplasmic organelles (Borgens et al., 1986; Fishman, 1987; Hill et al., 2001). The formation of axonal retraction bulbs may involve the increase in axoplasmic flow in axons following trauma. The constant pushing force produced by this flow is thought to be a contributor to the end bulb swelling, and subsequent rupture that is characteristic of axon tips as they undergo die back (Jacob and McQuarrie, 1996; Kao et al., 1977; Kreutzberg, 1995).

Small axonal swellings (varicosities) are also present sporadically along the length of the injured and adjacent uninjured axons. They are filled with axoplasmic organelles including mitochondria. They normally occur at least every 3-10 um along the axon (Shepherd and Harris, 1998) and can be distinguished from end bulb by their size. Axonal swellings greater than 6 um^2 can be identified as a terminal bulb, while those smaller being varicosities (Seif et al., 2007).

Axonal Sprouting

Axons undergoing die-back do engage in regenerative attempts in the form of axonal sprouting but these attempts are transient and rarely lead to axonal elongation (Hill et al., 2001; Li et al., 1994). About 30% of injured corticospinal axons mount an initial growth response, some between 6 to 24 hours after lesion. During this early growth phase axons seem to grow in two different modes: elongation in which the axons advance fast and straight, and branching in which numerous small lateral outgrowths form. Branching seems to be initiated when elongation stalls or when it is quenched from the beginning. It allows the axon to navigate outside pre-established axon pathways (Bareyre et al., 2004; Kerschensteiner et al., 2005). Neither mode of growth, however, allows axons to

advance substantially closer to their original targets. Figure 2 summarises the changes that CNS axons undergo following injury.

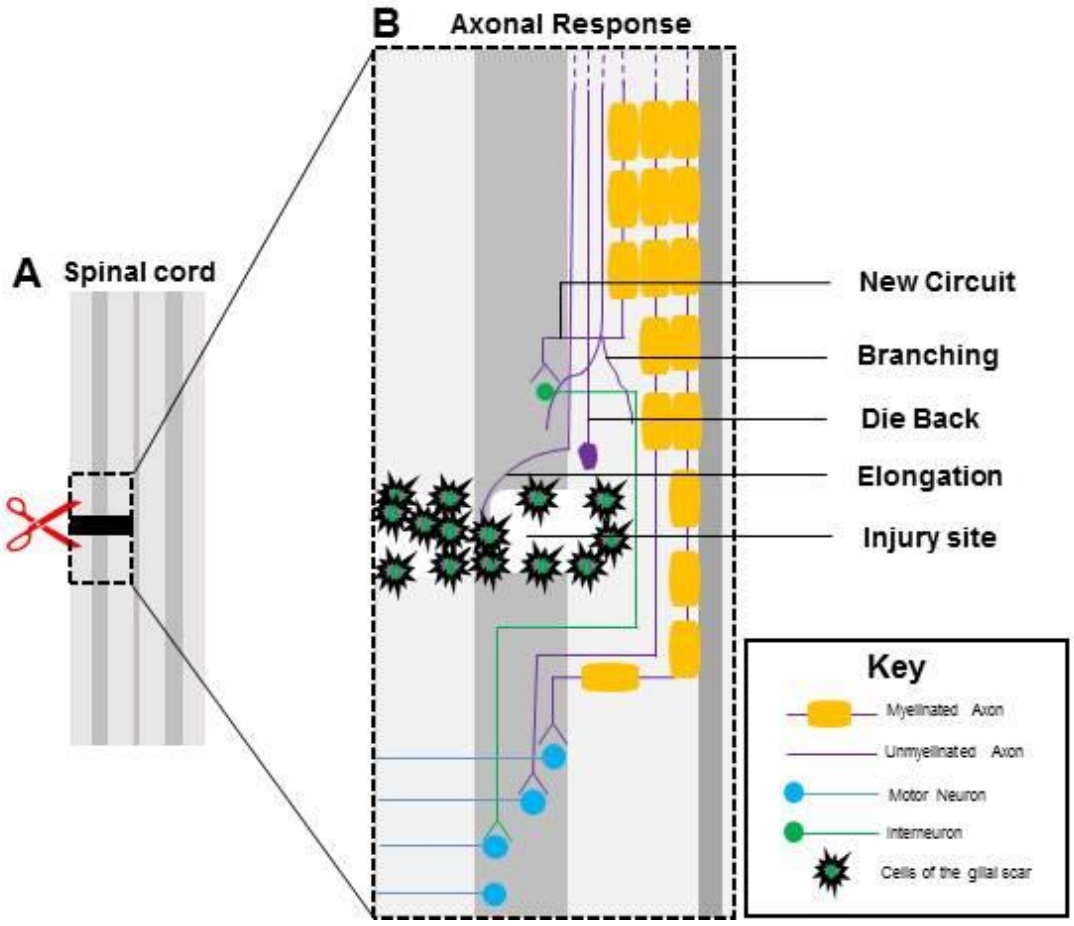

Figure 2: Axonal changes following spinal cord after injury. **A:** Diagram shows a longitudinal section through the rodent dorsal corticospinal tract after cervical spinal cord injury. **B:** Diagram depicts the axonal response following injury. Descending axons are interrupted by injury. Some axons form new circuits with motor neurons via interneurons. Axonal branching and elongation is also evident. However, axons do not grow for long distances. Axons that fail to regenerate die back. Edited from Thuret et al., (2006).

The injury site

Following spinal cord injury in the rat, microglia take on an activated phenotype (Anderson et al., 1982), they upregulate molecules including the MHCI and II, complement receptor C3, and the macrophage activation marker ED1 (Flaris et al., 1993) and they later take on a phagocytic morphology (Andersson et al., 1991). Microglial activation starts in the epicentre of injury and spreads moderately into the spinal grey matter and white matter (Dusart and Schwab, 1994).

Astrocytes become hypertrophic, they proliferate and show a pronounced increase in expression of GFAP (Obrien et al., 1994). After one week post injury, GFAP-positive astrocytes accumulate at the margins of the lesion to form a scar between the intact tissue and wound (Reier and Houle, 1988). At longer time points post injury, astrocytes build a very dense network of processes (Reier and Houle, 1988).

Infiltration of a number of different cells proceeds in waves (Blight, 1985; Dusart and Schwab, 1994). The first consists of the influx of polymorphonuclear granulocytes. The granulocyte entry to the lesion site and adjacent tissue is seen within the first few hours, is highest at 24 hours and disappears by 3 days post injury in the rat (Dusart and Schwab, 1994). Invading neutrophils are involved in the production of oxygen radicals undergoing oxidative burst (McCord, 1987) and neurophagia (Means et al., 1978). The second involves the infiltration of predominantly monocytes/macrophages (Blight, 1985; Bunge et al., 1994). Their primary role is to phagocytose cell debris (Perry et al., 1993). Relatively few lymphocytes appear at spinal cord injury sites (Popovich et al., 1993). There is also infiltration of Schwann cells, meningeal cells and fibroblasts into the injury site (Blakemore, 1975). Schwann cells have been implicated in the remyelination of axons (Blight and Young, 1989) and produce neurotrophic factors (Brown et al., 1991) , which may promote axonal regeneration. Meningeal cells may play a role in establishing a glial limitans at the boundary of the scar (Carbonell and Boya, 1988). Fibroblasts originating from the meninges (Maxwell et al., 1990) or overlying connective tissue also invade the lesion site to some degree (Krikorian et al., 1981).

In the later stages of spinal cord injury in rats, phagocytic macrophages disappear from the lesion site and leave behind a cerebrospinal fluid-filled cyst surrounded by scar tissue (Madsen et al., 1994). At this later stage, GFAP-positive hypertrophic astrocytes surround the margin of the lesion, with their end feet forming multi-layered stacks at the border between intact tissue and the wound (Reier and Houle, 1988). A summary of the different cells found in the injury site is found in figure 3.

Molecules inhibitory to axonal growth

Numerous molecules have been found to inhibit axonal regeneration or repel regenerating axons in the CNS. Molecules with the most significant role in axonal regeneration generally fall into three categories: those associated with the meningeal/glial scar, (chondroitin sulphate proteoglycans -CSPGs), axonal guidance molecules (semaphorins and ephrins), and those related to CNS myelin (Nogo, MAG, OMgp).

Inhibitory molecules in the meningeal/glial scar

CSPGs are proteoglycans comprising of a core protein with variable numbers of glycosaminoglycan side chains. CSPGs may have their effects by activating the Rho-A signalling pathway within injured axons (Monnier et al., 2003). CSPGs are characteristically distributed in and around the lesion site and are expressed both by invading meningeal cells and by glia (Tang, 2003).

Vigorous axonal growth is inhibited by the expression of CSPGs (Snow et al., 1990). Dorsal root ganglion neurons transplanted within the degenerating dorsal columns of rats with spinal cord injuries regenerated only up to the outskirts of the lesion site, which expressed high levels of chondroitin-6-sulphate (Davies et al., 1999). In addition, following injury to the central process of the DRG, the axons extend up to the dorsal root entry zone (DREZ) then were repelled back towards the DRG (Cajal, 1928). The inhibition of growth past the DREZ is associated with high levels of expression of CSPG, NG2 and tenascin-C (Zhang et al., 2001). However, deletion of NG2 is not associated with regeneration or improved recovery (Donnelly et al., 2012; Hossain-Ibrahim et al., 2007), although lentiviral vector-mediated knockdown of NG2 does promotes neurite outgrowth in culture models of glial scars (Donnelly et al., 2010).

Further evidence for the inhibitory role of CSPGs comes from experiments using chondroitinase ABC, a bacterial enzyme that can remove their glycosaminoglycan side chains (Hynds and Snow, 1999; McKeon et al., 1995; Snow et al., 1990). Chondroitinase ABC infusion encouraged corticospinal tract regeneration past the lesion site in rats following a crush injury to the dorsal columns of the cervical spinal cord (Bradbury et al., 2002). Chondroitinase ABC had similar effect on mice encouraging more regenerative sprouts to enter the injury site following CST lesions (Carter et al., 2008). Furthermore, when chondroitinase ABC was applied to the site of injury to the dorsal spinocerebellar and rubrospinal tracts there was apparently impressive axonal regeneration beyond the injury site and into distant spinal segments (Yick et al., 2003; Yick et al., 2004).

Axonal guidance molecules

Semaphorin

Several repulsive guidance cues may be involved in regulating axonal regeneration (Anderson and Lieberman, 2000). Semaphorins, a large family of secreted and membrane-bound glycoproteins, are expressed widely in the CNS (de Wit and Verhaagen, 2003; Dickson, 2002; Kruger et al., 2005). Semaphorins have been categorised into 8 classes by their sequence similarity and structural features (Pasterkarnp and Verhaagen, 2006). Plexins and neuropilins act as receptors for semaphorins, to induce signalling cascades involving, Rho family GTPases (Liu and Strittmatter, 2001), cyclic nucleotides, redox signalling (Terman et al., 2002), eicosanoids (Mikule et al., 2003) and cyclic GMP (Song et al., 1997).

Following injury to spinal cord motor pathways, the corticospinal and rubrospinal tracts express receptor components for class 3 semaphorins. This makes them susceptible to scar-derived semaphorins (De Winter et al., 2002; Lindholm et al., 2004; Pasterkamp and Verhaagen, 2001). Of the different semaphorins, the soluble semaphorin 3A (Sema 3A) has been frequently investigated in regeneration of the spinal cord. When injured ascending dorsal column axons are stimulated to regenerate into a transection lesion site, they avoid areas of Sema3A expression (Pasterkamp and Verhaagen, 2001). Furthermore,

interfering with Sema3A signalling, by injecting galectin-1 (Gal-1) to the injury site of mice with a complete lesion of the lower thoracic spinal cord, has been reported to promote axonal regeneration and functional recovery (Quinta et al., 2014).

Ephrins

Ephrins are major contact-dependent guidance molecules in the development of the nervous system, which bind to the Eph family of receptor tyrosine kinases (Pasquale, 2005). The predominant effects of ephrins are repulsion of migrating cells and growth cones (Kullander et al., 2001; Williams et al., 2003). The principal mediators of ephrin-induced repulsion are the Rho family of small GTPases, particularly RhoA (Kullander and Klein, 2002). Eph and ephrin expression (Bundesen et al., 2003; Fabes et al., 2006; Figueroa et al., 2006; Miranda et al., 1999) has been implicated in gliosis, scar formation, cell death and inhibition of axonal regeneration.

Following partial spinal cord transection, ephrin B2 is upregulated by reactive astrocytes, while its corresponding receptor EphB2 is upregulated by meningeal cells (Bundesen et al., 2003). Ephrin B2 deficient mice, showed reduced astrogliosis, smaller glial scar, exhibited increased regeneration of injured corticospinal axons and accelerated motor function recovery after spinal cord injury (Ren et al., 2013).

Astrocytes in the injured rat spinal cord express EphA4 (Cruz-Orengo et al., 2006; Cruz-Orengo et al., 2007; Fabes et al., 2006). EphA4 knockout mice exhibit more axonal regeneration following spinal cord injury (Goldshmit and Bourne, 2010). In addition, infusion of a peptide antagonist of EphA4 around the injured spinal cord increased corticospinal axonal sprouting and enhanced behavioural recovery after injury (Fabes et al., 2007). Furthermore, 2-week administration of EphA4 blockers in mice with spinal cord injury promoted substantial axonal regeneration, functional recovery by 5 weeks, and a reduction in astrocytic gliosis (Goldshmit et al., 2011). In contrast, in other studies knockdown of EphA4 failed to enhance regeneration (Cruz-Orengo et al., 2007; Herrmann et al., 2010)

Myelin-derived inhibitors

Myelin proteins affecting axonal outgrowth include Nogo (Chen et al., 2000), myelin-associated glycoprotein (MAG) (McKerracher et al., 1994) and

oligodendrocyte-myelin glycoprotein (OMgp) (Wang et al., 2002), but also include semaphorins, ephrins and CSPGs.

Nogo-A was identified as a myelin-associated neurite outgrowth inhibitor (Chen et al., 2000). Nogo-A is found in CNS Myelin, it is expressed by neurons and oligodendrocytes, but not astrocytes or Schwann cells (Josephson et al., 2001). Nogo-A downregulates cytoskeletal systems responsible for neurite growth and long-term potentiation (Pernet and Schwab, 2012). Antibodies against Nogo promote recovery after spinal cord injury in rats (Liebscher et al., 2005) and monkeys (Freund et al., 2007). Blockade of Nogo-A or its receptors enhances sprouting and plasticity of surviving white matter tracts in injured spinal cords (Freund et al., 2009; Harel et al., 2010; Hoogewoud et al., 2013). Nogo A/B deficient mice demonstrate an abundant number of corticospinal axons sprouting past the injury site and improved locomotor function after spinal cord injury (Kim et al., 2003). Likewise, following unilateral pyramidotomy, corticospinal tract regeneration and forelimb motor function is significantly improved in Nogo-AB or knockouts (Cafferty and Strittmatter, 2006).

The myelin-associated proteins, Nogo-A, MAG and OMgp, work in synergy to inhibit axonal regeneration and functional recovery following spinal cord injury. Mice deficient of OMgp (Ji et al., 2008) and MAG (Bartsch et al., 1995) show limited axon growth following corticospinal tract injury and no enhancement in behavioural recovery (Cafferty et al., 2010). However, Nogo-A deletion is associated with more regeneration of injured corticospinal and raphespinal axons, as well as greater behavioural recovery than MAG and OMgp knockout mice. But, the triple-mutant mice exhibits greater axonal growth and improved locomotion than Nogo-A deficient mice (Cafferty et al., 2010). Although these findings have not always proven repeatable (Lee et al., 2010). A summary of the inhibitory molecules in the spinal cord following injury is found in figure 3.

Neurotrophins

Neurotrophins contribute to the successful regeneration of axons in injured peripheral nerves (Funakoshi et al., 1993; Heumann et al., 1987; Naveilhan et al., 1997; Sendtner et al., 1994).

The neurotrophin family consists of nerve growth factor (NGF) (Cohen, 1960), brain-derived neurotrophic factor (BDNF) (Barde et al., 1982), NT-3 (Hohn et al., 1990), and NT-4/5 (Berkemeier et al., 1991). Neurotrophins bind to tyrosine kinase receptors TrkA, TrkB, and TrkC and to the low-affinity p75 neurotrophin receptor (Boyd and Gordon, 2001; Cui, 2006).

There is increased expression of neurotrophins and their receptors following spinal cord injury. In rats, BDNF and NT-3 is upregulated early after crush injury to the spinal cord (Hayashi et al., 1997). In the transected spinal cord of young adult cats and rats there is increased expression of trkB mRNA and protein several days to weeks after the lesion (Eidelberg et al., 1977). Expression of low-affinity NGF receptor is also found in the scar tissue, motoneurons, and blood vessel-associated cells after ventral funiculus (cat) or contusion injuries (rat) (Reier et al., 1992; Risling et al., 1992).

Increasing the levels of neurotrophins in the injured spinal cord augments the regenerative potential of injured CNS axons. Injections of NT-3 to the lesion site of adult rats with spinal cord injuries substantially increases sprouting from the injured CST. However, NGF and BDNF have weak or no effect on axonal sprouting, respectively (Mukhopadhyay et al., 1994). NT-3 promotes axonal sprouting but its application alone results in fibres remaining 1mm away from the injury site. However, combined delivery of NT-3 and an antibody against myelin-associated neurite growth inhibitory proteins (IN-1) promotes long distance elongation of injured fibres caudal to the spinal cord injury site (Mukhopadhyay et al., 1994). Furthermore, grafts expressing a gradient of NT-3 along the spinal cord injury site in rats, promote axonal elongation past the lesion site (Taylor et al., 2006).

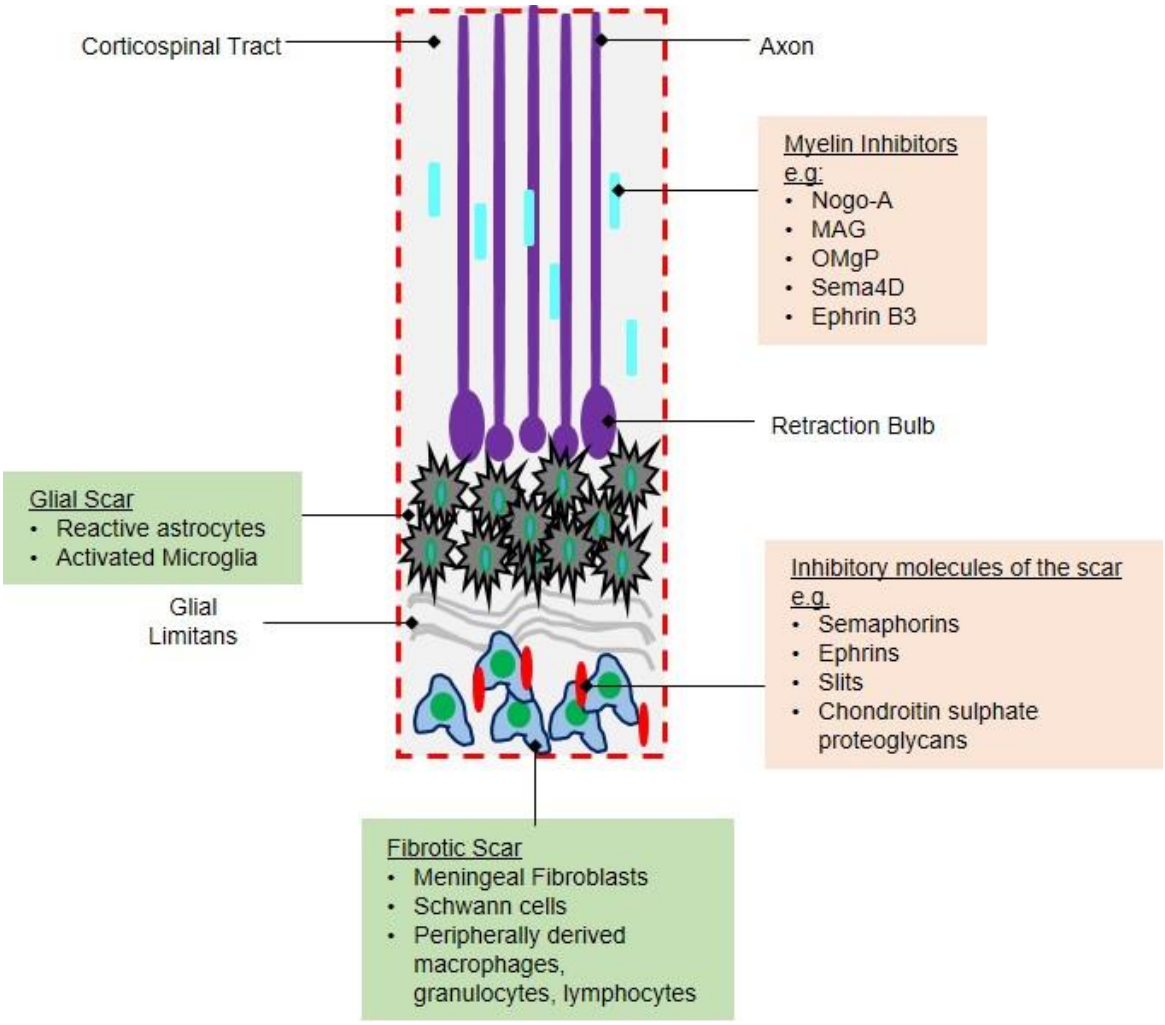

Figure 3: Axonal growth is prevented by the glial and fibrotic scar as well as inhibitory molecules in the spinal cord. After spinal cord damage, reactive astrocytes and microglial cells form the glial scar, and cells invade the injury site to form the fibrotic scar, which together create a physical barrier to axonal growth. Preventing axonal regeneration are various inhibitory molecules found in myelin and the fibrotic scar. Diagram edited from Schwab et al., (2006).

Role of corticospinal tract in skilled limb movement

Skilled motor function is dependent on both the direct action of lower motor neurons on muscles and their control by neurons in the brain and spinal cord. Spinal cord injury can result in damage to a number of structures involved in motor control.

Skilled Motor Function

Behavioural studies have demonstrated that rats are able to carry out skilled movements, such as reaching and grasping food, using an individual forelimb (Whishaw et al., 1981; Whishaw et al., 1986; Whishaw and Kolb, 1988; Whishaw and Pellis, 1990; Whishaw et al., 1992).

The skilled task of food reaching involves a sequence of actions which include: locating food using olfactation, positioning body in front of food source, lifting, aiming, advancing, pronating the paw as the limb is advanced, and opening the digits, grasping, supinating and releasing the food as the limb is withdrawn (Whishaw and Pellis, 1990). To execute food reaching successfully, proximal and distal forelimb muscles must work together in a coordinated manner (Holstege, 1991).

Corticospinal Tract

The corticospinal tract (CST) has an important role in the fine motor control involved in skilled movements. Other structures that also exert influence include the striatum, substantia nigra, red nucleus, and dorsal columns (McKenna and Whishaw, 1999; Whishaw et al., 1986; Whishaw et al., 1991; Whishaw et al., 1993; Whishaw et al., 1998).

The CST originates from layer V in the motor cortex, descends through the internal capsule and forms the pyramids at the brainstem. At the level of the spinal cord, it is found divided to the dorsal, ventral, lateral and dorsolateral components. The dorsal component comes from the contralateral motor cortex and contains 95% of descending axons in rodents. The ventral component originates ipsilaterally and contains less than 5% of all CST axons. The lateral and dorsolateral components together only represent around 2% of the CST (Weidner et al., 2001).

CST projects to both dorsal and ventral horns. Most of the CST fibres end in the dorsal horn or in the intermediate laminae of the ventral horn with very sparse direct connections to the motor neurons in laminae IX (Armand, 1982). Single corticospinal neuron axons make synaptic contacts within many of the spinal cord laminae and extend through several spinal segment (Kuang and Kalil, 1990).

In general, activation of proximal forelimb muscles is generated primarily by neurons of the medial motor neuron column in the spinal cord, and distal forelimb muscles are innervated primarily by neurons of the lateral motor neuron column (Holstege, 1991).

Effects of neural lesions on skilled movement

Skilled forelimb movements in reaching depend on a number of neuroanatomical areas.

Lesions to the motor cortex in rats result in reduced reaching success using the contralateral forelimb proportionate to increasing injury size in the contralateral forelimb. Severe defects are found in pronation and supination of the contralateral limb, with milder effects on aiming, advancing and lifting (Whishaw et al., 1991), as well as digit use (Castro, 1972b). Injury to the striatum and dopaminergic substantia nigra results in similar contralateral deficits as those seen with motor cortex lesions (Whishaw et al., 1986).

Pyramidal tract injury results in a less severe impairment of skilled reaching motor function but with a deficit pattern similar to that following large motor cortex injury (Whishaw et al., 1993). Loss of dorsal or ventral CST results in similar deficits, with greater severity following dorsal CST injury (Weidner et al., 2001). However, the functional effects of injury to individual dorsal or ventral components of the CST are mostly transient with recovery in reaching behaviour occurring weeks after injury (Weidner et al., 2001).

Injury of the red nucleus results in deficit in limb guidance, pronation, supination and aiming which are similar deficits to those seen after CST injury. In addition red nucleus injury results in loss of arpeggio grasping movements seen in food reaching. Deficits that result from injuries of both red nucleus and CST are additive (Whishaw and Gorny, 1996; Whishaw et al., 1998).

The sensory information from the dorsal columns also plays an important role in reaching movements. Injury results in deficits similar to those seen after CST or red nucleus injury indicating the importance of sensory feedback in skilled limb movement. However, these deficits are very short lived with rapid functional recovery after dorsal column injury (McKenna and Whishaw, 1999).

Experimental lesions used in spinal cord injury research can encompass damage to any of the structures described above and therefore can cause different levels of functional loss. In this regard, it is important to note that CST injury can also inadvertently be associated with injury to the grey matter. Dorsal CST lesions can be associated with major damage throughout the medio-lateral extent of the grey matter, Rexed's laminae V, VI and VII. This type of grey matter injury results in deficits very similar to those seen after CST injury but which are permanent (Yamamoto et al., 2009).

Spontaneous recovery

As described above, spontaneous functional recovery can occur following CST injury. There is evidence that this can happen through behavioural compensatory mechanisms or through structural compensation mediated by uninjured motor pathways (Weidner et al., 2001; Whishaw et al., 1991; Whishaw et al., 1993).

Normally, reaching for food involves a number of specific component submovements which culminate in the end point of the rat placing food in its mouth. However, success in this end point may be achieved using alternate motor strategies, without carrying out certain submovements in the reaching process. Part of the fast recovery of end point success seen after CST injury has been explained by behavioural compensation using whole body movements (Weidner et al., 2001; Whishaw et al., 1991; Whishaw et al., 1993).

Another mechanism of functional recovery occurs over a more protracted time period and appears to involve structural changes. Spontaneous functional recovery has been demonstrated in the spinal cord after injury that spares components of the CST. After unilateral lesion of a pyramid, where all components of the CST are injured, there is irreversible loss of certain submovements of the reaching action. However, injury limited to the dorsal CST, sparing the ventral component, is associated with recovery of function of these

submovements. Spontaneous functional recovery appears to be mediated by axonal sprouting from the uninjured ventral CST terminating on motor neuron pools in the lamina IX (Weidner et al., 2001).

Treatments for spinal cord injury

Therapies treating spinal cord injury mainly focus on producing or improving functional recovery. The therapeutic strategies that have been examined in animal models and clinical trials are based on cellular, molecular and rehabilitative approaches. Cellular therapeutic interventions aim to bridge any cyst or cavities and replace dead cells at the injury site, and provide a favourable environment for axon regeneration (Table 1-blue columns). In addition, molecular therapeutic interventions aim to promote axonal growth, enhance conduction and protect neurons from secondary cell death (Table 1-orange columns). Finally, rehabilitative therapies use peripheral input to maintain the spinal circuitry below the lesion site active and functional Table 1-green column). Many of these therapies have shown moderate functional recovery as well as axonal regeneration in rodents, canine, non-human primates and humans (Thuret et al., 2006). The therapy type, intervention and observed effects in various animal models are summarised in table 1.

Table 1: Summary of the observations following different therapeutic interventions in animals and humans with spinal cord injury. Columns highlighted in blue, orange or green are therapies based on cellular, molecular or rehabilitate approaches, respectively

Therapy Type	Intervention	Observed effects
Transplantation of peripheral nerve	• Avulsed peripheral nerves are implanted into the spinal cord. • Various combinations of this therapy involve the implanting the nerve and the local delivery of anti-inflammatory drugs, vertebral wiring, fibrin glue, acidic fibroblast growth factor, the transplantation of bulbar olfactory ensheathing cells, or bone-marrow-derived mesenchymal stem cells.	• **In rats:** Functional recovery is improved and axonal regeneration is evident following peripheral nerve implantation (Cheng et al., 1996; Cheng et al., 1997; Lee et al., 2002b; Lee et al., 2004b). • **In non-human primates:** No functional recovery but some spinal axons regenerate after inserting peripheral nerves into the spinal cord (Levi et al., 2002). • **In humans:** Some functional recovery is found when peripheral nerves were implanted, however some studies lacked control patients (Amr et al., 2014; Cheng et al., 2004; Tabakow et al., 2014).
Transplantation of Schwann cells	• Schwann cells from the peripheral nerve are injected as suspension or implanted into channels containing extracellular matrix into the spinal cord. • Therapies that involve the transplanting of Schwann cells and a concomitant delivery of neurotrophins, a steroid, or olfactory ensheathing glia have also been tested.	• **In rats:** Spinal cord injury cavitation is reduced when shawnn cells are transplanted into the spinal cord. Sensory and spinal neurons with cell bodies near to the graft enter the implants and become myelinated (Bamber et al., 2001; Takami et al., 2002; Xu et al., 1995). Some but not all studies found functional improvement (Pearse et al., 2004a; Takami et al., 2002).
Transplantation of olfactory nervous system cells	• Cells from the embryonic and adult olfactory bulb or mucosa are transplanted after spinal cord injury.	• **In rats:** Functional recovery and/or CNS regeneration has been reported after transplanting cells from the olfactory bulb. Transplantation of these cells can also enhance myelination (Li et al., 1997; Li et al., 2003; Lu et al., 2001a; Plant et al., 2003; Ramon-Cueto et al., 2000). However, some studies show that CNS regeneration and functional recovery not always occurs (Ramer et al., 2004; Riddell et al., 2004; Ruitenberg et al., 2005; Takami et al., 2002).

		• **In humans:** Improvement of motor and sensory function has been reported following treatment, but studies do not include controls (Amador and Guest, 2005; Guest et al., 2006; Huang et al., 2003).
Transplantation of embryonic CNS tissue	• After spinal cord transection, foetal spinal cord is transplanted into the lesion site. At the same time neurotrophic factors can be delivered at the injection site.	• **In rats:** Few axons regenerate but terminate at the transplant border (Bregman et al., 1997; Jakeman and Reier, 1991). Functional recovery has also been observed following the transplantation of embryonic tissue (Bregman et al., 2002; Coumans et al., 2001; Kunkel-Bagden et al., 1993).
Transplantation of embryonic stem/progenitor cells	• Multipotent progenitor cells and stem cells have the ability to differentiate into many cell types. These cells can be injected into the site of injury. • The cells can also be pre-differentiated to a desired lineage before transplantation.	• **In rodents:** Modest functional recovery is found after transplanting stem or progenitor cells (Cummings et al., 2005; McDonald et al., 1999; Ogawa et al., 2002; Teng et al., 2002). Transplanting neuron- and glia- restricted precursor cells resulted in the reduction of the cavity size, the presence of cells with characteristics of neurons and the sparing/sprouting of axons (Mitsui et al., 2005). Early delivery of oligodendrocyte-restricted stem cells to the injury site enhanced myelination and improved motor function (Keirstead et al., 2005). • **In non-human primates:** Improvements in behavioural recovery were evident after transplanting human neural progenitor cells (Iwanami et al., 2005).
Transplantation of adult	• Cells transplanted into the spinal cord after injury, include those from the adult bone marrow (haematopoietic stem cells and bone marrow stromal cells) or neural progenitors cells, which are isolated from the	• **In rodents:** Transplantation of bone marrow-derived stem cells promotes functional recovery (Hofstetter et al., 2005; Koda et al., 2005; Koshizuka et al., 2004; Wu et al., 2003).

stem/progenitor cells	dentate gyrus, subventricular zone or spinal cord.	Treating mice with neural progenitor cells results in the differentiation of these cells into astrocytes or oligodendrocytes (Cao et al., 2001; Shihabuddin et al., 2000; Vroemen et al., 2003). Neural progenitor cells taken from the brain of mice and then transplanted into the rat spinal cord changed to oligodendrocytes that remyelinated injured axons, and promoted functional recovery (Karimi-Abdolrezaee et al., 2006).
Transplantation of activated macrophages	• Blood-derived macrophages are activated by exposing them to peripheral nerve segments or skin pieces of the same animal. Activated microglia are then transplanted into the spinal cord injury site.	• **In rats:** Activated macrophages injected into the spinal cord injury site were associated with axonal regeneration through the injury site and improvement of hind limb function (Bomstein et al., 2003; Rapalino et al., 1998). In line with this study, injecting an inflammatory agent (GM-CSF) into the microglia has shown to promote axonal regeneration and functional recovery (Huang et al., 2009). . However, it has also been shown that activating microglia with another pro-inflammatory agent (zymosan) can have deleterious effects on hindlimb function (Popovich et al., 2002). In addition, depleting macrophages in rats with spinal cord injury show improved functional recovery, spared white matter and reduced tissue cavitation (Popovich et al., 1999). These studies delineate the negative as well as the positive properties inflammation can have on spinal cord regeneration. • **In canines:** There was no functional recovery or axonal regeneration following the transplantation of activated microglia injected into the injury site.
Neuroprotective therapies	• Animals with spinal cord injury receive intravenously injections of a chosen neuroprotective substance.	• **In rodents:** intravenous injection of an antibody against a cell adhesion molecule found on neutrophils and macrophages

		reduces secondary damage and improves motor function (Baptiste and Fehlings, 2006). Additionally, injecting the antibiotic minocycline, after spinal cord injury, reduces cell death and improves motor function in rats and mice (Lee et al., 2003; Stirling et al., 2004; Teng et al., 2004).
Delivery of growth factors	• Different growth factors have been tested on spinal cord injury models including, BDNF, GDNF, NGF, NT3, NT4 and NT5. These growth factors have been delivered to the injured spinal cord by transient injection, continuous infusion or insertion of an artificial carrier saturated with neurotrophic factors. Other methods to promote a prolonged expression of the growth factors in the spinal cord involve transplanting fibroblasts that have been transduced with genes to encode growth factors, or delivering adenoviruses and lentiviruses that carry the genes for the neurotrophic factors.	• **In rats:** Delivery of NGF is associated with the regeneration of coerulospinal axons (Grill et al., 1997b; Tuszynski et al., 1996), NT3 promotes corticospinal axon growth (Grill et al., 1997a), BDNF improves functional recovery and axonal growth of rubrospinal, reticulospinal, vestibulospinal, raphespinal, and local sensory and motor neurons (Jin et al., 2000; Jin et al., 2002; Liu et al., 1999; Lu et al., 2001b). Delivery of NT3 and BDNF enhances bladder and hindlimb function after spinal cord injury (Blitts et al., 2003; Mitsui et al., 2005). In addition, treating rats with GDNF promotes motor and dorsal column sensory axon elongation and remyelination (Blesch and Tuszynski, 2003). BDNF or GDNF and NT-3 expression induced axonal elongation and sprouting into the spinal cord injury site (Blesch and Tuszynski, 2007).
Modulation of cAMP or small GTPases	• Substances known to affect or interact with cAMP or GTPases can be given orally, systemically or locally in the spinal cord after injury.	• **In rodents:** Elevating the levels of cAMP and transplanting foetal tissue (Nikulina et al., 2004) or Schwann cells (Pearse et al., 2004b) into the injury site, improves functional recovery following spinal cord injury. Factors that limit axonal regeneration signal trough Rho and Rac GTPases (Jain et al., 2004; Niederost et al., 2002; Schweigreiter et al., 2004). In rats inhibition of Rho is associated with axonal regeneration and some functional

		recovery (Dergham et al., 2002). However, this could not be replicated by another study (Fournier et al., 2003). Nonetheless, inhibiting Rho kinases accelerated functional recovery following spinal cord injury (Dergham et al., 2002; Fournier et al., 2003; Hara et al., 2000; Sung et al., 2003; Tanaka et al., 2004). The safety of elevating cAMP and inhibiting GTPases must be further studied in bigger animal models to determine its therapeutic value.
Modulation of myelin-derived inhibitors	• Following spinal cord injury factors that modulate myelin inhibitors can be delivered to the spinal cord.	• **In rodents:** Axonal regeneration and functional recovery has been reported in animals that have been treated with an antibody against Nogo following spinal cord injury (Bregman et al., 1995; Schnell and Schwab, 1990; Schnell and Schwab, 1993; Thallmair et al., 1998; von Meyenburg et al., 1998; Z'Graggen et al., 1998). In addition, deletion of Nogo-A, deletion or inhibition of Nogo-receptor promotes axonal regeneration and functional recovery. However, some have been unable to replicate these findings (Guest et al., 1997; Oudega et al., 2000). • **In non-human primates:** Treating marmoset monkeys with Nogo-A antibody promoted corticospinal tract regeneration after spinal cord injury (Fouad et al., 2004).
Modulation of inhibitory molecules of the glial scar	• Local infusion of substance to alter the inhibitory molecules found in the spinal cord injury site.	• **In rodents:** Infusion of bacterial enzyme chondroitinase ABC, which degrades the inhibitory chondroitin sulphate, improves axonal regeneration and functional recovery after spinal cord injury (Bradbury et al., 2002; Moon et al., 2001). Application of chondroitinase ABC and transplantation of peripheral nerves into the spinal cord resulted in CNS axons to extend into the peripheral nerves (Yick et al., 2000). Also, the delivery of chondroitinase ABC and transplantation of hemichannels containing Schwann cells into the spinal cord promoted the

		growth of injured axons beyond the hemichannels (Chau et al., 2004).
Rehabilitative Training	• Interventions after spinal cord injury include weight-supported treadmill training, upper extremity exercise, robotic or manually assisted training, or functional electrical stimulation.	• **In rats**: weight supported treadmill training accelerates functional recovery, reduces muscle atrophy (Singh et al., 2011) and can restore normal pattern of hindlimb movements (Van Meeteren et al., 2003) after spinal cord injury. • **In humans:** Locomotor training enhances the ability of humans to walk on a treadmill, particularly when the body weight is being supported (Engesser-Cesar et al., 2005). Training humans to step and stand after incomplete spinal cord injury can stimulate independent walking (Dobkin et al., 2006; Wolpaw, 2006). Treadmill training combined with functional electrical stimulation improved the quality of stepping in a patient with an incomplete spinal cord injury (Herman et al., 2002).

Inflammatory and astrocytic response to CNS injury

Microglia

Pio del Rio-Hortega first recognised microglia as a separate glial entity (Del Rio-Hortega, 1932). They originate from neuroectodermal matrix cells and establish themselves in the brain during the embryonic stage (Ginhoux et al., 2010). The microglial plasma membrane contains a large variety of receptor and adhesion molecules. They express receptors that are also found on macrophages on non-neuronal tissues, which underscores their close relationship to the myelomonocytic cell lineage. They are known as the macrophages of the brain parenchyma. The major histocompatibility complex (MHC) is expressed in the surface of microglia, as well as endothelial cells and perivascular macrophages (Hayes et al., 1987; Streit et al., 1989a). In addition to receptors such as Fcɣ and complement receptors, macrophages express cell adhesion molecules including members of the integrin superfamily of adhesion molecules such as lymphocyte function antigen, CD4 antigen and leucocyte common antigen (Akiyama and McGeer, 1990; Perry and Gordon, 1987) constitutively in normal brain.

Morphological changes associated with microglial activation

In non-pathological conditions, microglia are in the resting state. They have an elongated soma bearing two or more processes extending from both poles of the cells (Fig. 4A). From these primary processes, a variable number of secondary braches emanate (Kershman, 1939). In the grey matter they display stellate morphology, while in the white matter they are orientated parallel to the nerve fibres. They can cover territories of up to 40 micrometres in diameter (Compston et al., 1997). They occupy non-overlapping areas and their constantly moving processes actively perform surveillance of their microenvironment (Nimmerjahn et al., 2005; Ransohoff and Perry, 2009).

In pathological conditions microglia respond in a stepwise manner and can transform rapidly from a resting to an activated state. This is characterised morphologically by an increase in cell body size, a thickening of proximal processes and decrease in the ramification of distal branches (Fig. 4B) (Del Rio-Hortega, 1932). Microglia also show membrane ruffling which is consistent with motile exploratory behaviour (Raivich et al., 1999). Microglial also proliferate in

many pathological situations. If there is no cellular debris to phagocytose microglia revert back to a resting state, characterised by decrease in the number of microglia, and a territorial, non-overlapping, distribution of microglia with a ramified morphology (Del Rio-Hortega, 1932). However, in the presence of neuronal cell death there are further changes in microglia. Microglia lose their processes, become amoeboid in shape and phagocytic to remove neuronal debris (Fig. 4C) (Del Rio-Hortega, 1932). In addition, when it is required to remove large structures such as pyramidal neurons or degenerating motor neurons, microglial clusters are formed. Microglial clusters consist of three to twenty microglial phagocytes (Moller et al., 1996; Streit and Kreutzberg, 1988), which are 60-100 um in diameter. Bystander microglial activation gradually decreases the further away they are from the microglial cluster (Raivich et al., 1999).

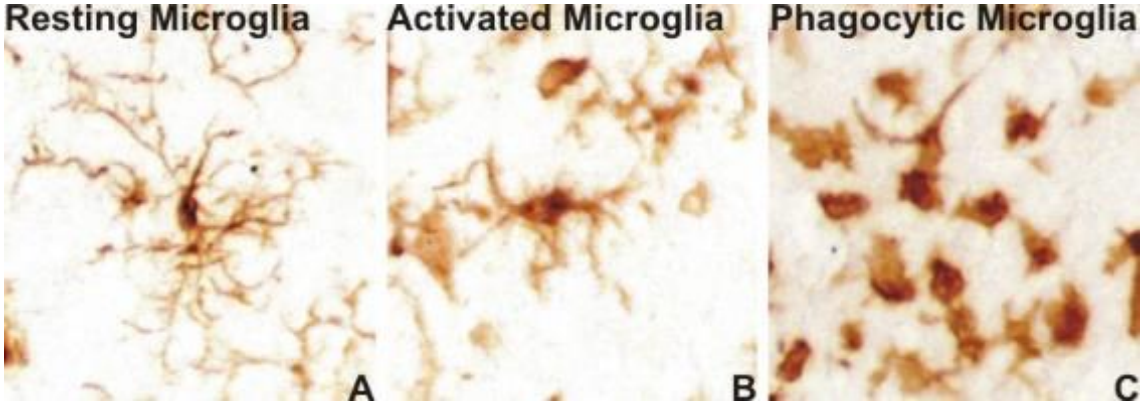

Figure 4: Microglia have different morphology according to their activation states. Micrographs show microglia in the motor cortex of rats stained for IBA1. A: Resting microglia have a ramified morphology. B: Microglia that are activated have a larger cell body with fewer but thicker branches. C: Phagocytic microglia lose their processes and have a round/amoeboid shape.

Molecular changes during microglial activation

On the molecular level, microglial activation proceeds through a series of steps in which their expression of molecules for cell adhesion, cytoskeletal organisation, and antigen presentation are altered summarised in Fig. 5.

In rodents, twenty-four hours following injury to axons of the peripheral nervous system, microglia around cell bodies of injured motor neurons are in a state of alert. They increase the expression of molecules with immune functions including IgG and thrombospondin (Kloss et al., 1999; Moller et al., 1996; Raivich et al.,

1998a). There is an increase in expression of ICAM1, and αMβ2 and αLβ2 integrins (Hynes and Lander, 1992), which mediate the adhesion of microglia to other microglia or infiltrating white blood cells including macrophages, granulocytes or lymphocytes (Fig 5: alert).

Microglia home-in on and adhere to damaged structures such as neurons or degenerating neurite terminals (Fig 5: homing). In addition, microglia upregulate α5β1 and α6β1 integrins in mice, and in rats, microglia increase the expression of α4β1 and αLβ2 integrins (Hailer et al., 1997; Kloss et al., 1999; Moneta et al., 1993). To enhance posttraumatic mobility cytoskeletal proteins such as vimentin are also expressed (Graeber et al., 1988b; Raivich et al., 1993). Markers of the alert state, such as ICAM1, and αMβ2 are now down regulated (Raivich et al., 1998a; Werner et al., 1998). Receptors for microglial mitogens such as macrophage colony stimulating factor (M-CSF) and granulocyte macrophage colony stimulating factor (GM-CSF) are increased (Raivich et al., 1991a; Raivich et al., 1998a). This coincides with the proliferation of microglia (Graeber et al., 1988c; Kloss et al., 1999; Moneta et al., 1993). Microglia proliferation around the cell bodies of facial motor neurons is maximal around three days following facial nerve injury (Raivich et al., 1994) or around hippocampal neurons following injury to the entorhinal cortex (Gall et al., 1979). By this time, microglia express major histocompatibility complex class 1 molecules (MHC1) (Raivich et al., 1993; Streit et al., 1989b), and immunoaccessory glycoproteins such as B7.2 (Bohatschek et al., 1998).

Microglial transform into phagocytic cells in the presence of neuronal cell death (Fig 5: phagocytosis). They remove neuronal debris (Graeber et al., 1989; Moller et al., 1996), disconnected axons and myelin in Wallerian degeneration, and myelin debris in demyelinating diseases including multiple sclerosis (Bauer et al., 1995; McGeer et al., 1993; Trapp et al., 1998). Phagocytic microglia now more strongly express most activation markers including the adhesion molecules α5β1, α6β1 and αMβ2 integrins, thrombospondin and ICAM1 (Kloss et al., 1999; Werner et al., 1998). These molecules may mediate the adhesion to and internalisation of diverse components of the cellular debris. Molecules with an immune function are upregulated with a strong increase in FC-gamma receptors,

B7 and MHC class I (Bohatschek et al., 1999; Desimone et al., 1995). In addition, antigen presenting complexes MHC I and/or MHC II (Butter et al., 1991; Kosel et al., 1997; Schmitt et al., 1998) and co-stimulatory molecules like B7.2, ICAM and αXbeta2 integrin are also up regulated (Bohatschek et al., 1998; Giulian et al., 1986). In the presence of specific antigens, these co-stimulatory molecules are potent stimuli for the activation of T-cells (Bretsche and Cohn, 1970; Robey and Allison, 1995) (Fig 5: T-cells).

Around areas of phagocytosis, adjacent microglia increase the expression of MHCI, B7.2, α4β1 and αMβ2 integrin (Bohatschek et al., 1998; Kloss et al., 1999; Raivich et al., 1998b) (Fig 5: bystander activation). These activated microglia are arranged concentrically with phagocytic cells residing in the centre (Raivich et al., 1999). A similar pattern is observed when lymphocytes infiltrate into the CNS around injured neurons; lymphocytes aggregate around phagocytic microglial clusters (Raivich et al., 1998b).

A graded microglial response is also evident during an immune response provoked by viral, bacteria, or parasite infection, autoimmune-mediated inflammation (multiple sclerosis, encephalomyelitis), or in graft versus host disease. In contrast to non-immune mediated pathologies there is a strong increase in MHC II and the inducible nitric oxide synthase (iNOS). Both changes appear to be mediated by infiltrated lymphocytes which produce a large number of microglia activating cytokines such as interferon gamma which is a potent inducer of MHC II and iNOS in vitro and in vivo (Schluter et al., 1998; Wong et al., 1984). Overall, the induction of MHC II is critical for antigen presentation to the CD4 positive T helper/inducer cells. In the case of iNOs the enzyme is responsible for the production of nitric oxide which can react with superoxide to produce peroxynitrite (van der Veen et al., 1997). Peroxynitrite is an extremely aggressive oxidant which causes lipid, protein, and DNA damage.

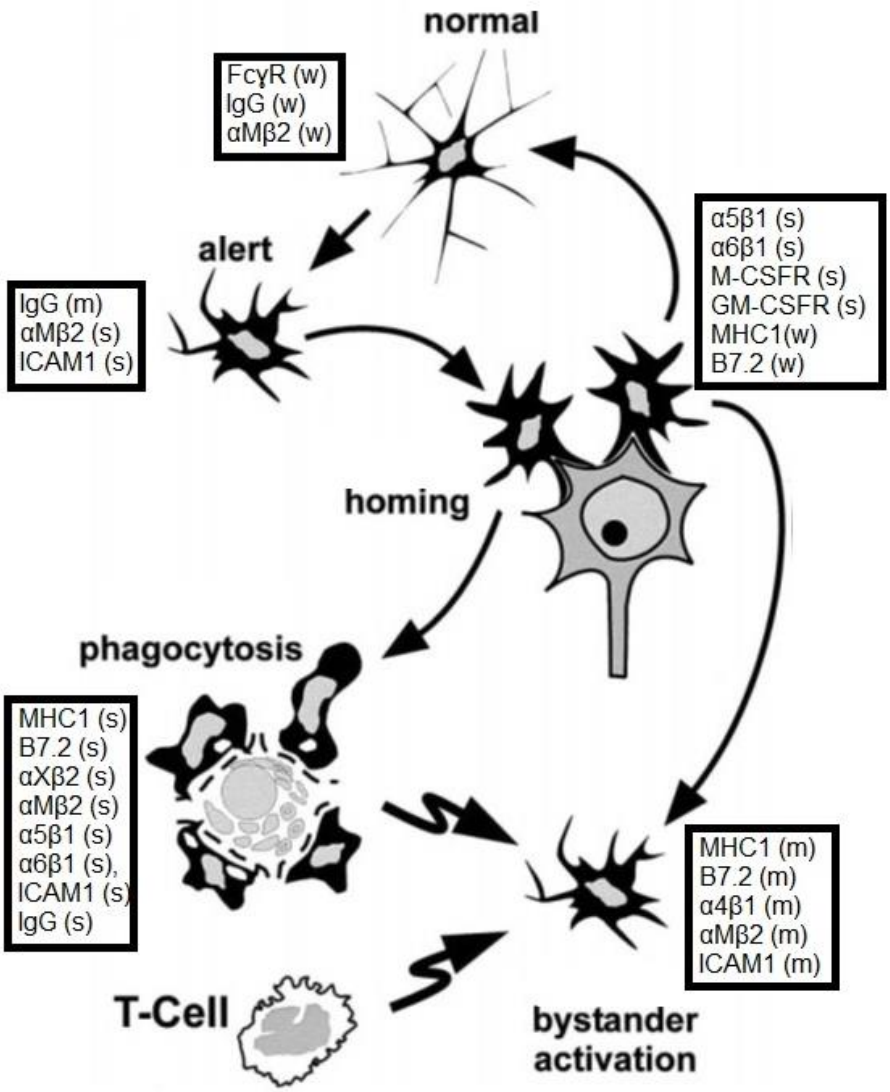

Figure 5: Stages of microglial activation. Diagram shows the different morphologies microglia acquire in response to CNS injury. From a ramified morphology (normal) they become activated and lose their ramifications (alert), they home-in on the injure neuron (homing), and in the presence of cell death they become amoeboid and remove debris (phagocytosis). They can cause neighbouring microglia to become activated (bystander activation) and can communicate with T-cells. Each of the boxes lists the different molecules which microglia up regulate at each stage of activation. Edited from Raivich et al., (1999).

Classical vs Alternative microglial activation

Microglial activation can also be defined by the pattern of pro-inflammatory or anti-inflammatory and neurotrophic factors they secrete. Like peripheral macrophages, microglia can shift from a pro-inflammatory to a protective state, changes which are known as ‘classical’ activation or ‘alternative’ activation, respectively.

Microglia have membrane and cytosolic receptors, called pattern recognition receptors (PRRs), which include toll-like receptors (TLRs), nucleotide-binding oligomerization domain (NOD) proteins, and non-TLR (C-type lectin receptors). Cellular defence is initiated when these receptors interact with pathogen-associated molecular patterns (PAMS) or with damage-associated molecular patterns (DAMPS) (Colton, 2009; Han and Ulevitch, 2005; Rubartelli and Lotze, 2007). Downstream signalling culminates in the induction of genes that trigger the expression of reactive oxygen species, pro-inflammatory cytokines, such as tumour necrosis factor alpha (TNF-α), interleukin (IL)-1β and IL-12 and expression of inducible nitric oxide synthase, which are necessary for defence against pathogens but in the process cause tissue damage (Boche et al., 2013). The reinforcement of this pattern of expression by surrounding cells leads to the classical activation. In particular, it has been found that interferon gamma (IFN-ɣ), which is known to be secreted by T-helper cells type 1 in the periphery and microglia or astrocytes in the CNS, induces/maintains the toxic state of microglia (Merson et al., 2010).

Macrophages can change their activation phenotype from one that is pro-inflammatory to one that supports repair and tissue reconstruction. The latter phenotype has been termed alternative activation. Anti-inflammatory cytokines, including IL-4, IL-3, IL-10 and TGF-β induce alternative activation by suppressing macrophage pro-inflammatory gene expression (Bogdan et al., 1991; Hamilton et al., 1999; Martinez et al., 2008; Mills et al., 2000). Like macrophages, microglia can also become alternatively activated. In vitro, microglia stimulated with LPS, expressed lower levels of NOS, IL-2, IL-1β, IL-6, and TNF-α when treated with anti-inflammatory IL-4 or IL-3 (Colton et al., 2006; Kitamura et al., 2000; Ledeboer et al., 2000; Lee et al., 2002a), and showed increased expression of

anti-inflammatory cytokines IL-10, TGF-β and growth factors, including insulin growth factor-1 and NGF (Kitamura et al., 2000; van Rossum et al., 2008).

Phagocytosis of neurons

Microglia are the professional phagocytes of the brain and are able to engulf whole neurons within hours (Fuhrmann et al., 2010; Neher et al., 2011). Phagocytosis of dead and dying neurons and neuronal debris is beneficial in part because it reduces inflammation (Neumann et al., 2009; Sierra et al., 2013). However, microglia can also phagocytose live neurons causing death of the engulfed cells (Fricker et al., 2012a; Fricker et al., 2012b; Neher et al., 2011; Neher et al., 2013; Neniskyte et al., 2011; Neniskyte and Brown, 2013).

Phagocytosis begins with the recognition of pro-phagocytosis signals on the surface of target cells to be phagocytosed (e.g. phosphatidylserine, calreticulin; de-sialylated glycoproteins) (Neumann et al., 2009; Sierra et al., 2013). Such signals can be picked up by opsonins in the extracellular environment such as, Milk fat globule EGF factor 8, Annexin A1, tubby, galectin 3, growth arrest specific protein 6 or protein S, and components of complement C1q, C3, or C3b. Opsonins aid recognition by receptors on phagocytes, including vitronectin receptors – alphaVbeta3 or alphaVbeta5, MER receptor tyrosine kinase (MERTK), low density lipoprotein receptor related protein, and αMβ2. This induces signalling cascades and remodelling of the actin cytoskeleton, which culminate in the engulfment and digestion of neurons through the fusion of phagosomes with lysosomes (Fu et al., 2014; Hochreiter-Hufford and Ravichandran, 2013).

Astrocytes

Astrocytes exist in two typical forms: stellar fibrillary astrocytes and protoplasmic. Fibrillary astrocytes are normally found in the white matter, with long slender processes which stain for glial fibrillary acid protein (GFAP), a typical astrocyte cytoskeletal protein (Bignami et al., 1972). Protoplasmic astrocytes are located in the grey matter and exhibit numerous short and highly ramified processes with many membranous extensions. In non-pathological conditions protoplasmic astrocytes cannot be stained for GFAP, but can be visualised by staining for S100b or endothelial NOS (eNOS). Nonetheless, it is difficult to stain the entire

cellular contour of protoplasmic astrocytes, as S100b or endothelial NOS (eNOS) only stain the cell body and the main processes (Cammer and Tansey, 1988; Didier et al., 1986; Gabbott and Bacon, 1996).

Astrocytes have various roles in the nervous system. They provide physical support to neighbouring neurons, meninges and vasculature, they give nutrients to the highly energy consuming neurons, their dendrites and synapses, they maintain ionic balance in the extracellular space by removing water and excitotoxic amino acids (Nedergaard et al., 2003; Stobart and Anderson, 2013; Tsacopoulos and Magistretti, 1996). In addition, astrocyte induce tight junctions on endothelial cells (Janzer, 1993; Pekny et al., 1998; Taocheng et al., 1987), the ramified phenotype in microglia and blood derived monocytes (Kloss et al., 1997; Schmidtmayer et al., 1994). They are a source for numerous trophic factors (NGF, CNTF, PDGF, IGF-1, TGFa, BDNF, bFGF) for adjacent neurons and oligodendrocytes particularly following injury (Eddleston and Mucke, 1993; Hermanson et al., 1995; Ridet et al., 1997).

Astrocyte activation following neuronal injury

Following injury to the CNS, astrocytes undergo a series of changes that lead to their activation. Protoplasmic astrocytes around motor neurons increase the production of GFAP within 24 hours after injury to peripheral nerves (Tetzlaff et al., 1988b). By two to three days after injury there are numerous GFAP-positive fibrillary astrocytes around the cell body of the injured neuron (Graeber and Kreutzberg, 1986). There is an early appearance of GFAP-positive astrocytes with a velate morphology in the brains of mice following ischaemic, traumatic or infective brain injuries (Raivich et al., 1999). This early activation is controlled by cytokines. IL-6-deficient mice have a reduced presence of fibrillary astrocytes (Klein et al., 1997b), while TGFβ1 deficient mice have increased numbers of GFAP-positive fibrillary astrocytes and protoplasmic astrocytes with a velate morphology both of which are positive for the CD44 integrin (Jones et al., 1998; Makwana et al., 2007).

Reactive fibrillary astrocytes create a physical barrier between damaged and healthy cells. The scars are composed of a dense network of hypertrophic astrocytes with thick, interdigitating processes and associated extracellular

matrix. They inhibit neurite outgrowth, a phenomenon attributed to both molecules on the cell surface of reactive astrocytes and components of the extracellular matrix including, chondroitin sulphate proteoglycans, collagen IV and tenascin (Brodkey et al., 1995; Giftochristos and David, 1988; Laywell et al., 1992; Lips et al., 1995; McKeon et al., 1991; Stichel et al., 1999).

Reactive astrocytes additionally synthesise collagens and proteoglycans which also impede neurite growth (Fidler et al., 1999; Ridet et al., 1997; Smiththomas et al., 1994). Astrocytes might promote remodelling of extracellular matrix components and influence scar architecture by producing matrix metalloproteases and their inhibitors (Ridet et al., 1997; Sivron and Schwartz, 1995). They express the structural protein vimentin (Eng et al., 2000). Following brain injury, the expression of copper-zinc superoxide dismutase (SOD-1), glutathione peroxidase, and metallothionein is also increased in reactive astrocytes (Campagne et al., 2000; Liu et al., 1993; Neal et al., 1996; Takizawa et al., 1994). Similarly, astrocytes express the inducible form of haemoxygenase in response to brain insults which might be important in preventing metal catalysed free radical production (Geddes et al., 1996; Takeda et al., 1996).

Astrocytes are players in innate immunity. Astrocytes intercommunicate with microglial through cytokines and growth factors. Specifically it has been found that astrocytes regulate microglial proliferation via M-CSF and GM-CSF production (Giulian and Ingeman, 1988; Malipiero et al., 1990; Sawada et al., 1990), induce a ramified phenotype in microglia (Kloss et al., 1997; Lee et al., 1994), reduce the production of nitric oxide by transforming growth factor beta (TGF-β) (Vincent (Vincent et al., 1997). Likewise, microglia regulate astrocyte proliferation trough the production of IL-1 (Giulian and Lachman, 1985; Giulian et al., 1986) and stimulate astrocytes to make tenascin via the production of Transforming growth factor beta (TGF-β) and basic fibroblast growth factor (bFGF) (Smith and Hale, 1997). Activated astrocytes can also express TNF, IL-6, IFNβ, TGF-β and chemokines (CCL2, CCL5, CCL20, CXCL8 and CXCL10) (Farina et al., 2005; Jack et al., 2005; Park et al., 2006). Finally, reactive astrocytes can produce neurotrophic factors, notably NGF, bFGF, and BDNF

which can stimulate neurite outgrowth (Mocchetti and Wrathall, 1995; Schwartz and Nishiyama, 1994; Strauss et al., 1994; Tokita et al., 2001).

Leukocyte recruitment into the injured brain

The extent of leukocyte recruitment to the brain is dependent on the severity of injury (Raivich et al., 1999). In the normal brain, few white blood cells are present. Cells of the monocyte lineage enter the brain to give rise to perivascular brain macrophages (Hickey and Kimura, 1988). In addition, cells of the monocyte lineage give rise to a small percentage of microglia in the adult brain. Mice that have undergone conjoined surgery to share the same blood circulation, have less than 5% of microglia of donor origin (Ginhoux et al., 2010). Furthermore, T-cells can enter the brain when they are activated (Hickey et al., 1991; Wekerle et al., 1986). Also, work on Prion disease suggests that B-cells may also go into the brain. Making mice deficient of B-cells abolishes the spread of prions from the periphery to the CNS (Klein et al., 1997a).

Following mild or indirect injury, T-cells are recruited to the affected brain region. T-cells invade the facial motor nucleus one day after facial nerve injury (Raivich et al., 1998b). Similarly, in rats with experimental autoimmune encephalomyelitis, T-cells can be found in the cryo-injured cerebral cortex (Phillips et al., 1997). In the presence of cell death numerous T-cells are recruited and accumulate around phagocytic microglia. The T-cells express CD44, ICAM1 and αLβ2, which are proteins upregulated when T-cells are activated. In addition, the phagocytic microglia are positive for MHC1, B7.2 and αXβ2, making them efficient at antigen presentation to the activated T-cells (Engelhardt et al., 1998; Werner et al., 1998).

Direct trauma to the brain or spinal cord is not only associated with the extravasation of T-cells, but also with an abundance of macrophages and neutrophil granulocytes (Carlson et al., 1998; Holmin et al., 1998; Popovich et al., 1997). The entry of activated neutrophils may play a part in causing secondary tissue damage in the brain injured by hypoxia/ischemia. Reducing the number of recruited neutrophils to the injured brain by inhibition of neutrophil chemoattractants (Bell et al., 1994; Garcia et al., 1995) or transgenic deletion of endothelial adhesion molecules ICAM1 and P-selectin (Connolly et al., 1996; Kurkowska-Jastrzebska et al., 1999), protects the brain from tissue damage.

Similarly, macrophages contribute to secondary axonal degeneration and tissue damage. When rats with spinal cord injuries received intravenous injections of liposome-encapsulated clodronate to deplete peripheral macrophages, a reduction of peripheral macrophages at the site of injury was associated with decreased cavitation, enhanced axonal sprouting and improved hindlimb usage (Popovich et al., 1999).

Cytokine expression and function in the injured CNS

Pro-inflammatory and anti-inflammatory cytokines are expressed in the injured CNS in a graded fashion (Raivich et al., 1999). In the normal adult brain M-CSF and TGFβ-1 are present in moderate amounts (Jones et al., 1998; Kiefer et al., 1993; Raivich et al., 1998a; Streit et al., 1998). Mild or indirect trauma leads to the induction of IL-6 and an increase expression of TGFβ-1 (Kiefer et al., 1993; Klein et al., 1997b; Streit et al., 1998). Direct brain injury, ischaemia, convulsion and Alzheimer's disease typically lead to the additional production of IL1-β and TNF-α. Infectious inflammation due to viral and bacterial meningitis and encephalitis, HIV, malaria, and autoimmune disease including multiple sclerosis also cause the additional synthesis of IFN-ɣ (Frei et al., 1988; Gallo et al., 1989; Merrill et al., 1992).

Macrophage colony stimulating factor (M-CSF)

M-CSF is involved in the proliferation and activation of microglia (Roth and Stanley, 1992). Microglial proliferation in the facial motor nucleus is severely reduced in mutant mice lacking biologically active M-CSF, which have undergone facial nerve axotomy (Raivich et al., 1994; Wiktor-Jedrzejczak et al., 1990). These mice show little expression of the markers of microglial activation, αMβ2 and M-CSFR (Raivich et al., 1996).

The effect of M-CSF on neuronal survival and regeneration is dependent on the severity of injury. Axonal regeneration following facial nerve axotomy is not affected in mice with a mutation in the M-CSF gene, even though the microglial reaction and early lymphocyte recruitment is muted. However, in severe forms of damage M-CSF plays a role in recovery. The absence of M-CSF enhances neuronal cell death in the brain of mice that have undergone hypoxia ischemia. But when astroglia secreting M-CSF were transplanted into the brain, the

microglia response was restored and there was an enhancement of neuronal survival (Berezovskaya et al., 1995).

Tumour Necrosis Factor-alpha (TNF-α)

TNF-α, a proinflammatory cytokine, acts on a variety of cells including neurons, oligodendrocytes, astrocytes and microglia. There is little expression of TNF-α in the early phase to facial nerve injury (Kiefer et al., 1993; McClellan, 1994), but the expression is pronounced following direct brain trauma, ischaemia, infection or excitotoxic injury (Bruce et al., 1996; Seilhean et al., 1997; Uno et al., 1997; Yang et al., 1993).

TNF-α plays a toxic and protective role in the CNS. Neurons and glia express two TNF receptors, TNFR1 and TNFR2. In the mouse facial axotomy model, deletion of the TNFR1 reduces the cytotoxic potential of macrophages by limiting their iNOS production. The absence of TNFR2 inhibits the expression of endothelial ICAM 1, and thus reduces the neurovascular response in infection. The absence of both receptors reduces both the numbers of microglial clusters found in the facial nucleus during neuronal cell death and the associated expression of markers of the phagocytic phenotype, including MHC I, B7.2 and thrombospondin (Raivich et al., 2002). However, the absence of both TNF receptors exacerbated neuronal damage following focal cerebral ischaemia or epileptic seizures suggesting that TNF may be neuroprotective (Bruce et al., 1996). Neuroprotection may be mediated by the stimulation of TNFR2. In vitro, neurons stimulated with TNF that express TNFR2-only, are protected against glutamate mediated excitotoxic insult (Dolga et al., 2008). In vivo, mice lacking neuronal TNFR1 that underwent retinal ischemia exhibited a strong reduction in neuronal cell death, while lack of TNFR2 led to an enhancement in neuronal cell death in three retinal layers: the outer nuclear layer, inner nuclear layer, and ganglion cell layer (Fontaine et al., 2002).

Interleukin 1

IL-1 is strongly upregulated in severe brain injury (Wang et al., 1997). IL-1 family consists of three members, IL-1 alpha, IL beta, IL receptor antagonist (IL1ra) for which there are two receptors IL-1R1 and IL-1R2 (Alheim and Bartfai, 1998).

Although, astrocytes, invading immune cells, vascular cells and probably neurons can produce IL-1, it is activated microglia that are the first to express IL-1 (Gibson et al., 2004) and are the major source of the three members of the IL-1 family (Eriksson et al., 1998; Schluter et al., 1997; Sheng et al., 1997; Zhang et al., 1998). Inhibiting the activity of IL1 is associated with a reduction in neuronal cell death, microglial activation and leucocyte recruitment following focal or global ischemia, excitotoxic or traumatic injury to the CNS (Panegyres and Hughes, 1998; Relton and Rothwell, 1992; Toulmond and Rothwell, 1995; Yang et al., 1998). Most neuronal effects are apparently due to the IL1β isoform (Alheim and Bartfai, 1998; Horai et al., 1998; Shibayama et al., 1996). Interleukin 1 beta but not alpha activity requires the presence of IL1 converting enzyme. Mice deficient of this enzyme have reduced neurological damage in cerebral ischaemia (Loddick et al., 1997).

Interleukin 6

Neurons and astrocytes but not microglia express IL-6 receptors and the expression pattern remains constant in the normal and injured brain (Klein et al., 1997b). IL-6 is markedly expressed by endothelial cells, microglia and astrocytes following spinal cord injury, ischaemia, infection, neurodegeneration (Alzheimer, Parkinson), autoimmune disease, and following indirect injury in the facial nerve axotomy model (Hopkins and Rothwell, 1995; Raivich et al., 1999; Stammers et al., 2012). A variety of cells are affected when IL-6 is not expressed in the injured CNS. IL-6-deficient mice that have sustained facial nerve injury, show few astrocytes expressing GFAP in the facial nucleus and lymphocyte recruitment is limited (Raivich et al., 1999). In addition, injured neurons respond by a late and strong increase in galanin. IL-6 has indirect effects on microglial proliferation, as there were fewer microglia in IL-6 deficient mice than controls (Klein et al., 1997b)

Interferon gamma (IFNɣ)

Interferon gamma is a critical regulator of T-cell mediated inflammation. It induces the production of cytotoxic oxygen radicals, phagocytosis and molecules involved in the presentation of antigen such as MHC II predominantly in microglia (Suzumura et al., 1987). Genetic ablation of IFNɣ or its receptor, causes

inefficient upregulation of iNOS, TNF alpha or MHC II, and compromises the ability to fight neuronal infection (Deckert-Schluter et al., 1996; Geiger et al., 1997; Hooper et al., 1998; Nansen et al., 1998; Schluter et al., 1998).

Transforming growth factor beta 1 (TGF-β1)

Transforming growth factor beta 1 is an anti-inflammatory cytokine with potent neurotrophic properties. The expression of receptors for TGF-β1 is restricted to neurons and is upregulated in the facial nucleus following facial nerve axotomy (Jones et al., 1998; Unsicker et al., 1996). It is present at low levels in the normal CNS, but the expression is strongly upregulated in almost all forms of brain pathology (Kiefer et al., 1993). TGF-β1-deficient animals exhibit a severe decrease in microglial cell density, their ability to proliferate in the axotomised facial nucleus, diminished expression of activation markers, and a striking reduction of their normal ramified morphology. In addition, these mice show an increase in astrocyte activation following facial axotomy (Jones et al., 1998).

Intrinsic ability for CNS neurons to regenerate

Although inhibitory and trophic molecules at the site of injured CNS are clearly important, the success of axonal regeneration is also determined by the intrinsic ability of neuronal cell bodies to mount an appropriate response to axonal injury (Anderson et al., 1998). Neurons whose axons extend to the PNS, display a hypertrophic cell body following axonal injury. However neurons with axons confined to CNS, such as the rubrospinal neurons (Kwon et al., 2002) and corticospinal neurons, atrophy in response to injury, showing a decrease in cell body volume and number of dendrites, and low levels of protein synthesis (Lieberman, 1971).

Neurons projecting axons into the PNS also mount a strong molecular response at the cell body, upregulating growth-related molecules that include transcription factors, cytoskeletal proteins, and adhesion molecules. In contrast, neurons whose axons are confined to the CNS mount a weak, transient or incomplete response to axotomy, or none at all (Anderson et al., 1998). The strong neuronal cell body response seen after peripheral axotomy to motor, autonomic and dorsal DRG neurons is associated with vigorous axonal regeneration. However, the feeble or absent cell body response following CNS lesions to Purkinje cells and

corticospinal (CS) neurons is not normally accompanied by axonal regeneration. Some CNS neurons such as rubrospinal and thalamic reticular neurons and retinal ganglion cells mount a transient cell body response and this may allow them an opportunity to regenerate axons if a suitable environment is provided (Anderson et al., 1998).

Correlation between the cell body axotomy response and axonal regeneration into peripheral nerve grafts

Implanting peripheral nerve grafts into the rodent CNS promotes axonal regeneration (David and Aguayo, 1985; Morrow et al., 1993; Richardson et al., 1980). This effect however, is not common to all injured CNS neurons but it appears to be differential; with implants in the thalamus promoting the regeneration of axons of thalamic reticular neurons but not dorsal thalamic neurons, and cerebellar implants promoting axonal regeneration of deep cerebellar neurons (DCN) but not of Purkinje neurons (Anderson et al., 1998; Anderson and Lieberman, 1999).

Interestingly, neurons that regenerate their axons into peripheral nerve grafts show a transient upregulation of regeneration associated molecules (GAP-43, CAP-23, SCG-10) following injury, which is prolonged in response to the graft. However, neurons which do not regenerate into peripheral nerve grafts do not mount such a response (Campbell et al., 1991; Chaisuksunt et al., 2000; Mason et al., 2002; Vaudano et al., 1995). Thus, the regenerative potential of neurons may be determined by their intrinsic ability to upregulate growth related molecules in response to axotomy.

In addition, peripheral nerve graft experiments provide evidence that the axotomy response mounted by injured CNS neurons may be increased by providing regenerating axons with a more pro-regenerative environment. For example, delivery of chondroitinase to the spinal cord resulted in GAP-43 upregulation in DRG neurons after dorsal rhizotomy (Bradbury et al., 2002), and delivery of an anti-Nogo antibody to the cerebellum led to the upregulation of c-jun in Purkinje cells (Zagrebelsky et al., 1998). However, corticospinal neurons do not mount an axotomy response nor regenerate their axons following spinal cord injury or

pyramidotomy, even when the injured axons are exposed to neurotrophin-producing peripheral nerve grafts (Richardson et al., 1980).

This suggests that corticospinal neurons might be intrinsically unable to mount an axotomy response. However, corticospinal neurons have, in fact, been shown to mount a significant response to axotomy if injured very proximally (intracortical lesion); upregulating most of the aforementioned growth associated molecules (Mason et al., 2003; Tetzlaff et al., 1991). Indeed, they might even extend regenerating axons into peripheral nerve grafts in the cortex (Benfey and Aguayo, 1982) This indicates that although the ability of corticospinal neurons to regenerate their axons may be limited by their lack of an axotomy response after distal axotomy, they are capable of mounting a similar response as neurons and successfully regenerating, given a sufficiently strong stimulus. The most likely explanation of the requirement for a very proximal axotomy is the need to eliminate axon collaterals with intact synapses, which may suppress the response to injury of the main axon.

Neuroinflammation and the axotomy response

There is evidence that the neuronal cell body response to axotomy is connected to the activation of inflammatory cells around injured neurons. Following peripheral nerve injury there is a vigorous axotomy response, and microglia in the vicinity of motor neurons become activated, proliferate and migrate towards the cell bodies of axotomised neurons (Kreutzberg, 1996; Svensson et al., 1994). Similarly, macrophages surrounding peripherally axotomised DRG neurons also become activated (Fenzi et al., 2001; Hu and McLachlan, 2003; Lu and Richardson, 1993) and insinuate themselves between the neurons and the satellite cells. Such inflammatory changes may be explained by the fact that motor, DRG and autonomic neurons upregulate a variety of inflammation-related genes following peripheral nerve injury (Boeshore et al., 2004; Costigan et al., 2002; Raivich et al., 1999).

In contrast, axonal injury at the CNS is associated with varying levels of microglial activation around the injured neurons. Corticospinal tract injury in the spinal cord results in no increase in microglia number or activation around the injured pyramidal neurons (Leong et al., 1995), whereas following rubrospinal tract injury

microglia activation in the red nucleus has been reported to be absent (Barron et al., 1990), minimal and transient (Streit et al., 2000), or noticeable (Tseng et al., 1996; Xu et al., 1998). However, the levels of microglial activation even in the latter case are modest in comparison to those that may be observed around motor neurons following facial nerve injury, for example.

Correlation between the neuroinflammatory response and axonal regeneration into peripheral nerve grafts

Interestingly, peripheral nerve graft experiments have demonstrated that the extent of perineuronal microglial activation correlates well with axonal regeneration. Shokouhi et al. (2010) demonstrated that axonal growth into peripheral nerve implants provokes a substantial increase in perineuronal neuroinflammation, which is most obvious around the highly regenerative TRN neurons. Increased microglial activity is also found around rubrospinal neurons which regenerate into peripheral nerve grafts in the spinal cord (Harvey et al., 2005; Richardson et al., 1984).

In contrast, corticospinal neurons do not regenerate axons into peripheral nerve grafts (Richardson et al., 1982) and no microglia activation at the motor cortex can be observed (Shokouhi et al., 2010). Similarly, little microglia activation can be found around the regeneration competent TRN and rubrospinal neurons under conditions where axonal regeneration does not occur (i.e. following axotomy alone or after insertion of freeze-killed peripheral nerve grafts). Thus, there is little microglial activation around intrinsic CNS neurons in the absence of axonal regeneration (Shokouhi et al., 2010). Interestingly, this pattern of perineuronal microglial activation is in keeping with that of the cell body response of intrinsic CNS neurons in peripheral nerve graft experiments (Mason et al., 2003). Figure 6 summarises the characteristics demonstrated by neurons that can and cannot regenerate into the peripheral nerve graft.

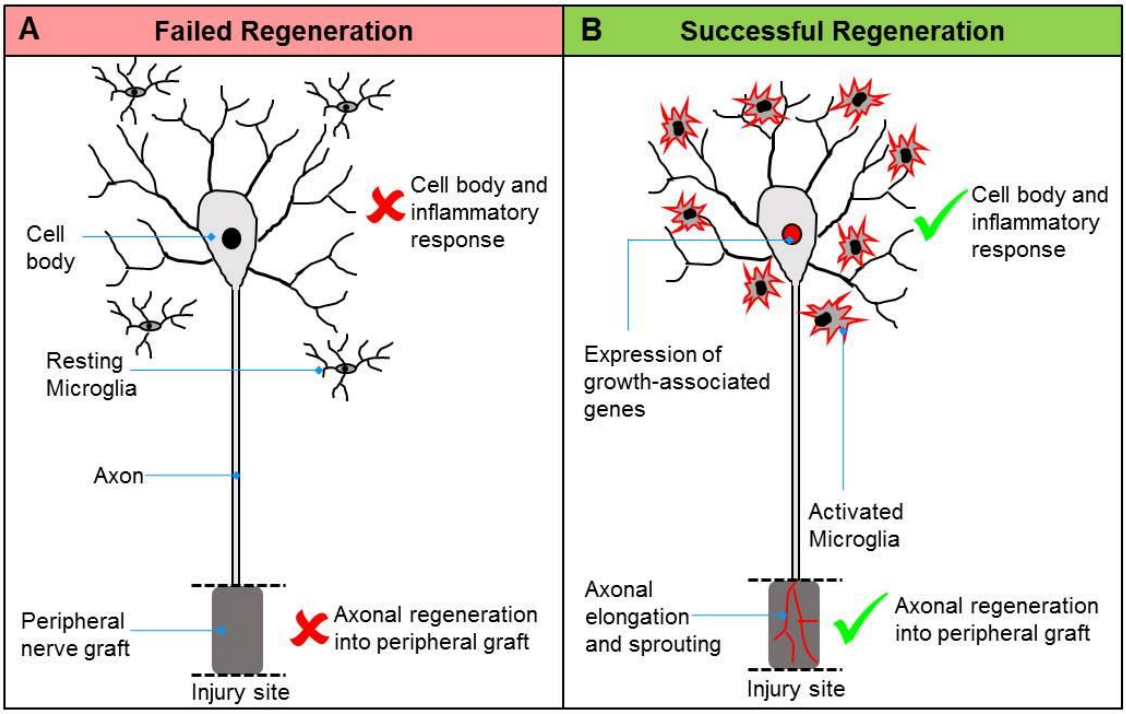

Figure 6: Factors determining CNS regeneration into a peripheral nerve transplant. **A:** Diagram indicates that injured neurons that fail to regenerate into a peripheral nerve graft do not show a change in the cell body and perineuronal microglia remains ramified. **B:** Neurons that extend their axons into the peripheral nerve graft demonstrate changes in the cell body, characterised by an increase in the expression of growth related genes. Additionally, it is evident that microglia surrounding the cell body of the injured neuron become activated.

Neuroinflammation, neuronal axotomy response and axonal regeneration

Stimulating the neuronal cell body response can dramatically enhance axonal regeneration (Chong et al., 1994; Chong et al., 1996; Leon et al., 2000; Neumann and Woolf, 1999; Richardson and Issa, 1984). For example, while dorsal root injury has little effect on the expression of growth associated molecules by DRG neurons and results in weak axonal regeneration into the CNS (Chong et al., 1996), a conditioning lesion to the corresponding peripheral nerve provokes a strong inflammatory and neuronal cell body response that enhances axonal regeneration in the dorsal root (Richardson and Verge, 1987).

Interestingly, work on DRG neurons and retinal ganglion cells (RGCs) demonstrates that simply provoking an inflammatory response around the cell bodies of axotomised neurons is enough to enhance the regeneration of their axons. Injection of Corynebacterium parvum into DRG prior to dorsal root injury stimulates the upregulation of growth associated molecules in the cell bodies of injured neurons (Lu and Richardson, 1995) and dramatically increases axonal regeneration (Lu and Richardson, 1991).

Similarly, inflammation in the retina, following lens injury or injection of zymosan into the vitreous body of the eye, causes RGCs to upregulate growth associated molecules and enhances regeneration of axons after optic nerve injury (Leon et al., 2000). This positive effect of perineuronal inflammation on CNS axonal regeneration appears to be mediated by activated-macrophages which produce neurotrophic molecules, termed macrophage derived factors (MDFs). Identified MDFs include BDNF (Zhi et al., 2005), GDNF (Yan et al., 1999), platelet-derived growth factor (PDGF) (Mekada et al., 1998), IL-6 (Schuettauf et al., 2005), basic fibroblast growth factor (FGF-2) (Rappolee and Werb, 1992), and oncomodulin, a novel 14-kDa molecular weight factor which requires elevated cAMP to promote axon growth (Leon et al., 2000; Yin et al., 2000).

Neuroinflammation and corticospinal tract regeneration

Like peripheral macrophages, activated microglia are potent producers of neurotrophic factors and cell adhesion molecules that can exert survival and regenerative effects on neurons; these include: BDNF (Bouhy et al., 2006), IGF1 (Lalancette-Hebert et al., 2007), TGFb1 (Makwana et al., 2007) and osteopontin

(Schroeter et al., 2006). Thus it has been hypothesized that activating microglia in the rodent motor cortex might induce the characteristically quiescent corticospinal neurons to regenerate following spinal cord injury.

To test this, Hossain-Ibrahim et al. (2006) applied lipopolysaccharide (LPS) to the pial surface of the rat motor cortex, producing a gradient of inflammation through all cortical layers, characterized by the presence of activated amoeboid microglia and macrophages. This inflammatory response was found to stimulate corticospinal neurons to upregulate the expression of growth associated genes ATF3, GAP-43, c-Jun and SCG10. However, LPS treatment was unable to enhance of corticospinal tract (CST) regeneration in animals with a concomitant spinal cord injury (Hossain-Ibrahim et al., 2006).

The challenges of promoting corticospinal tract regeneration through perineuronal inflammation

The failure of LPS application to enhance CST regeneration may be explained by the following possibilities: a) LPS is not a potent enough inflammogen or may induce the wrong type of inflammation b) insufficient inflammation is achieved in the corticospinal neuron layer because of the superficial application of LPS; c) the inflammatory effect of LPS is too transient.

Although LPS is a potent inflammatory agent , it is interesting to note that injecting it to the vitreous body is not a sufficient stimulus to enhance retinal ganglion cell axonal regeneration after optic nerve injury (Leon et al., 2000). Thus, LPS might be less potent than zymosan which, as described earlier, does stimulate regeneration of RGC (Leon et al., 2000).

Application of LPS to the pial surface of rat cortex might limit the level of inflammation at the deeply located cortical layer V, which contains corticospinal neurons. However, Hossain-Ibrahim et al. (2006) report that injection of LPS directly into deep motor cortex did not result in neither a detectably greater inflammatory response nor greater upregulation of growth-associated proteins in layer V.

Finally, the transient effect of LPS treatment might suggest that methods to deliver LPS chronically to the motor cortex would be more suitable to promote CST regeneration. However, microglia when activated express a number of

potentially cytotoxic molecules such as TNF, IL-1beta, NO, oxygen radicals and components of the complement cascade (Raivich et al., 1999). Thus, unlike pial application (Hossain-Ibrahim et al., 2006), chronic infusion of LPS has been shown to produce neurotoxic focal necrosis at the infusion site (Szczepanik et al., 1996), which would be counterproductive to regeneration. Thus it remains to be seen whether other approaches to inducing cortical inflammation would promote a stronger and longer-lasting expression of growth-associated proteins, with the effect of stimulating CST axon regeneration and without causing neurotoxicity.

Inflammation to model neurotoxicity

Increasing inflammation in the brain to toxic levels could be detrimental. Perinatal brain damage is a major cause of motor (e.g. cerebral palsy), cognitive, behavioural, attentional or socialisation deficits (Becher et al., 2004; Kubota et al., 2002). The neuropathological correlate that accounts for most brain damage in the immature brain is injury to the cerebral and periventricular white matter, known as periventricular leukomalacia (PVL) (Volpe, 2009). PVL is followed by neuronal and axonal damage in the cerebral cortex, basal ganglia, brainstem and cerebellum (Inder et al., 1999). The main factors initiating perinatal brain damage include, hypoxia, ischemia, infection and/or inflammation (Bell and Hallenbeck, 2002; Dammann and Leviton, 1997; Pleasure et al., 2006; Volpe, 2009).

Microglial activation and white matter damage

The normal immature brain contains clusters of amoeboid microglia within the supraventricular corpus callosum and are known as the fountains of microglia (Del Rio-Hortega, 1932). They appear in the 2nd gestational trimester in humans (Monier et al., 2007; Rezaie and Male, 1999), and in mice and rats from a week before to 10 days after birth (Brockhaus et al., 1996; Hirasawa et al., 2005; Hurley et al., 1999; Leong and Ling, 1992). In mice, phagocytic microglia in the white matter are highly activated, as they show strong expression of activation markers α5, α6, αM, αX, and β2 integrins, B7.2, IGF-1 and M-CSF. In addition, microglial activation in the white matter is transient; highest at 0 days after birth and disappearing at day 10 in mice (Hristova et al., 2010).

The presence of activated phagocytic microglia in the vicinity of vulnerable white matter could play an important role in initiating axonal damage in the immature

brain. Following hypoxia/ischaemia, rats demonstrated significant death of pre-oligodendrocytes within the pericallosal white mater. This coincided with abundant microglial activation. Rats that received intraperitoneal injections of minocycline to decrease microglial activation, showed less white matter damage (Lechpammer et al., 2008). In addition, microglial activation and astrocyte cell death are observed in the mouse model of excitotoxic white matter damage (Tahraoui et al., 2001). Furthermore, maternal intrauterine infection and perinatal foetal inflammation (both systemic and affecting the CNS) is correlated with the development of PVL and subsequent cerebral palsy (Leviton and Paneth, 1990; Saliba and Marret, 2001; Svigos, 2001; Yoon et al., 1997a)

Inflammation may mediate white matter damage through the production of toxic factors. Necrosis of oligodendrocyte precursors and axonal damage is associated with the presence of pro-inflammatory cytokines, such as IL-1β, IL-6 and TNF-α, in foetal plasma (Gomez et al., 1998), cerebrospinal fluid and spinal cord blood (Romero et al., 1990). Activated microglia, peripheral macrophages and hypertrophic astrocytes can produce the pro-inflammatory cytokines (Kadhim et al., 2001; Yoon et al., 1997b). The release of these cytokines may cause brain damage by exacerbating the production of cytotoxic inflammatory cytokines (TNF-α and IL-6) and free radicals such as superoxide and NO by microglia (Hu et al., 1995).

Models of white matter damage

Infectious and inflammatory models used to investigate the development of white matter damage include intrauterine and intrauterine administration of LPS, the direct delivery of LPS into the subcortical white matter, intravenous injection of LPS into the foetus, or intraperitoneal injection into the mother or the pup (Wang et al., 2006).

Intracerebral administration of LPS in rodents induces the expression of TNF-α, IL-1b and iNOS by microglia/macrophages, reduces myelination and oligodendroglial numbers, and causes astrogliosis and cystic lesions in the white matter. Ventricular dilatation as well as some neuropathological changes in grey matter have been found (Cai et al., 2003; Coumans et al., 2003; Lehnardt et al., 2002; Pang et al., 2003).

Intrauterine injection of LPS was associated with cell death in the brain of foetal rats (Bell and Hallenbeck, 2002). There was increased expression of TNF-α and IFN-ɣ increased, whereas IL-6 and IL-10 levels declined following LPS exposure (Bell et al., 2004). However, there were no differences between LPS-injected and control rats in their ability to carry out motor tasks in adult animals (Poggi et al., 2005).

Intravenous injections of LPS into the sheep foetus was associated with the presence of IL-6 in foetal plasma. Analysis of the brains of sheep exposed to LPS showed gliosis, subcortical and white matter damage, as well as a reduction in the size of corticospinal tracts in the brainstem (Duncan et al., 2002). In addition, sheep injected with LPS had increased microglial activation in the white matter, astrocyte damage and loss of oligodendrocytes (Peebles et al., 2003).

Intraperitoneal injection of LPS into the mothers is associated with increased foetal mortality (Silver et al., 1995). There is a higher concentration of IL-1 β, TNF-α and IL-6 in the placenta and of TNF-α in the amniotic fluid in rats injected with LPS than those injected with PBS (Urakubo et al., 2001). LPS also increases the expression of IL-1β and TNF-α, and causes astrogliosis and hypomyelination in the foetal brain (Cai et al., 2000).

Intraperitoneal injection of LPS into neonatal mouse pups initiates an acute inflammatory response, both systemically as well as centrally. Systemically, there is a marked increase in IL-1β and IL-6 protein. Centrally, there is increased expression of IL-1β and microglial activation. Neonatal rats injected Intraperitoneally with LPS can show impaired memory function in adulthood (Wang et al., 2006).

Despite the associations between LPS-induced inflammation and damage to subcortical white matter, there is, as yet, no direct experimental model available that specifically induces white matter damage. In addition, the aforementioned models are limited by the fact that LPS-mediated inflammation is only transient and multiple injections are often required. A model which affects white matter specifically through a more targeted chronic stimulation of resident fountains of microglia may overcome these limitations.

Poly I:C and GMCSF to promote corticospinal tract regeneration

Microglial activation may play a role in promoting axonal regeneration but may also cause neurotoxic effect. Polyinosinic:polycytidylic acid (Poly I:C) and granulocyte-macrophage colony stimulating factor (GM-CSF) are two agents known to produce inflammation. The effect of producing perineuronal inflammation on axonal regeneration and degeneration using these substances has not yet been determined.

Poly I:C

Poly I:C is a synthetic double-stranded RNA, injections which has been shown to mimic the effects of systemic viral infection (Cunningham et al., 2007). Microglia, astrocytes, and even neurons can recognise Poly I:C via cell surface or endosomal TLR3 (Bsibsi et al., 2002; Bsibsi et al., 2003; Cameron et al., 2007; Jack et al., 2005; Kim et al., 2008), cytoplasmic MDA-5 (melanoma differentiation-associated protein 5) (Yoneyama and Fujita, 2010) and/or cytoplasmic retinoic acid inducible gene (RIG-I) I receptors (Peltier et al., 2010). Poly I:C binding to these receptors induces activation of IFN-regulatory factor 3, NF-κB and PI3K signalling pathways (Cameron et al., 2007; Deleidi et al., 2010; Patro et al., 2010).

In vitro studies have shown that Poly I:C stimulates microglia and astrocytes to produce cytokines IL-6, TNF-α IFN- β and nitric oxide (Furie and Randolph, 1995; Matsui et al., 2013; Wahl et al., 1996). In vivo, intra-ventricular administration of Poly I:C also results in the expression of IL-1β and NO (Melton et al., 2003), whilst intraperitoneal Poly I:C in mice provokes a global upregulation of a range of chemokines, including CXL1 and 2 and CCL2 and 4 (Bajetto et al., 2001; Bell et al., 1996; Hausmann et al., 1998).

Inflammatory and glial response to Poly I:C in the CNS

Infusion of Poly I:C into the brain of rats was associated with an increase in the number of reactive microglia and phagocytic microglia in the hippocampus (Patro et al., 2010). Similarly, microglial and astocyte activation was evident in the substantia nigra and striatum following intranigral injection of Poly I:C (Deleidi et al., 2010). After intra-ventricular injections of Poly I:C , gliosis is seen in the mouse cerebral cortex (Town et al., 2006). Poly I:C-mediated neuroinflammation is

associated with neuronal damage. In rats, prolonged intraventricular Poly I:C administration is associated with neuronal cell loss in the septal nucleus, hippocampus, cortex and thalamus (Melton et al., 2003). Systemic Poly I:C aggravates neurodegeneration in hippocampus in a mouse model of prion disease (Field et al., 2010). Intra-nigral injections of Poly I:C are associated with dopaminergic neuronal degeneration (Patro et al., 2010). In addition to the toxic effects exerted on neurons, Poly I:C causes oligodendrocyte precursor cell death in vitro (Steelman and Li, 2011).

Neurite collapse

Poly I:C produces a strong and long-lasting inhibition of neurite growth from DRG neurons in vitro (Cameron et al., 2007). Toll like 3 receptors are found in cell bodies, axons and growth cones of growing neurons. The absence of these receptors abolishes the effects of Poly I:C on neurite outgrowth. In vivo, intrathecal injections of Poly I:C in neonatal mice resulted in fewer axons exiting the dorsal root ganglia and the animals displayed sensory motor deficits (Cameron et al., 2007). Similarly, axonal outgrowth from cerebellar granule cells in vitro is also decreased by Poly I:C exposure. This effect appears to be mediated via the epidermal growth factor (EGF) receptor (ErbB) pathway as the inhibitory effect of Poly I:C effect was eliminated when ErbB1 was knocked out from neurons or ErbB1 kinase activity was blocked (Leinster et al., 2013).

GMC-SF

GM-CSF is a cytokine belonging to the family of colony stimulating factors (CSF). Colony stimulating factors are crucial for survival, proliferation, differentiation, maturation and functional activation of haematopoietic cells (Metcalf, 2008).

GM-CSF receptor activation

GM-CSF is involved in the generation of granulocytes, macrophages, and dendritic cells from hematopoietic cells (Metcalf, 1989). It is a 24 kDa glycoprotein protein that exerts its effects by activating the GM-CSF receptor (GM-CSFR) (Rozwarski et al., 1996). The GM-CSFR is a heterodimer consisting of the transmembrane glycoproteins α-subunit and β-subunit. The α-subunit is responsible for ligand ligation and is specific for GM-CSF, while the β-subunit is required for signal transduction and is shared with IL-3 and IL-5 receptors (Chiba

et al., 1990). Two GM-CSFRβ-subunits need to be in close proximity for the phosphorylation of the downstream receptor-associated Janus Kinase-2 (JAK2) kinase to occur. The activation of JAK2 leads the activation of subsequent signalling pathways (Quelle et al., 1994) including the Jak/signal transducer and activator of transcription (STAT), Ras/mitogen activated protein kinase (MAPK), phosphatidylinositol 3 (PI-3) kinase, nuclear factor kappa-light-chain-enhancer of activated B cells (NF-κB) pathways. Activation of the JAK/STAT induces cell differentiation. JAK/STAT and the PI3K pathways can also lead to apoptosis inhibition and cell survival. While, Ras/MAPK and NFκB pathways are responsible for GM-CSF induced proliferation and inflammation (de Groot et al., 1998).

Expression and effects of GM-CSF

Following stimulation with cytokines, antigens, microbial products or inflammatory agents (IL-1, TNFα or LPS) a number of cells strongly upregulate GM-CSF expression; these include cells of the adaptive system (T-cells and B-cells), innate immune cells (natural killer cells, macrophages, neutrophils, mast cells eosinophils), constitutive immunity (Paneth's cells, Pneumocyte II cells, endothelial cells, mesenchymal stromal cells, osteoblasts, chondrocytes and smooth muscle) (Conti and Gessani, 2008; Fukuzawa et al., 2003; Sallerfors, 1994), and cells of the nervous system (astrocytes) (Aloisi et al., 1992b).

GM-CSF has roles in the proliferation and survival of macrophage and granulocyte precursors (Verdrengh and Tarkowski, 1998). It promotes chemotaxis (Cheng et al., 2001; Gomez-Cambronero et al., 2003; Khajah et al., 2011), the release of oxygen radicals and phagocytosis by neutrophils (Bourgoin et al., 1992; Corey and Rosoff, 1989; Kumaratilake et al., 1996). Similarly, GM-CSF promotes a phagocytic phenotype in monocytes.

When monocytes isolated from human peripheral blood were grown in serum containing GM-CSF, they increased in size and granularity, had increased phagocytic activity, and expressed various adhesion molecules, CD14 and major histocompatibility complex (MHC) class II.

Deletion of the GM-CSF gene results in mice having abnormalities in the lungs, such as an extensive presence of lymphocytes in the peribronchovascular interstitium and large intra-alveolar phagocytic macrophages. Mice are also vulnerable to lung infections caused by bacterial or fungal organisms (Stanley et al., 1994). However, mouse development and haematopoiesis is normal. On the other hand the global over-expression of GM-CSF protein by transgenic mice is associated with effects in peripheral tissues as well as in the nervous system. GM-CSF over-expressing mice develop blindness resulting from the increased presence of macrophages in the eye and retinal damage. They also show signs of generalised muscle wasting with hind limb weakness or paralysis associated with increased presence of macrophages in skeletal muscle. In addition, there is accumulation of large numbers of macrophages and neutrophils in the peritoneal and pleural cavities (Lang et al., 1987; Metcalf and Moore, 1988).

GM-CSF has potent effects on microglia in vitro. It promotes ameboid morphology, phagocytosis (Giulian and Ingeman, 1988), antigen presentation (Fischer et al., 1993) activation marker expression and proliferation (Giulian and Ingeman, 1988; Kloss et al., 1997). In vivo, similar effects on microglial morphology, phagocytosis and proliferation have been observed (Giulian and Ingeman, 1988; Mangano et al., 2011; Mausberg et al., 2009; Schermer and Humpel, 2002). In addition, GM-CSF can stimulate the production of IL-6 and TNF-α by microglia (Reddy et al., 2009).

As well as having effects on immune cells, GM-CSF has been shown to act on cells of the nervous system such as astrocytes and neurons. It promotes astrocyte proliferation and activation in vitro and in vivo (Guillemin et al., 1996; Mangano et al., 2011; Reddy et al., 2009). GM-CSF receptors are also found in neurons (Schaebitz et al., 2008). In vitro, GM-CSF protects neurons from nitric oxide-induced cell death (Schaebitz et al., 2008). In vivo, GM-CSF is neuroprotective in models of stroke and spinal cord injury, probably through the stimulating the production of neurotrophins by microglia (Bouhy et al., 2006; Ha et al., 2005; Huang et al., 2009; Kong et al., 2009; Schaebitz et al., 2008).

Aims

In contrast to the PNS, the CNS displays limited axonal regeneration after injury, which is associated with a lack of perineuronal inflammation. Stimulation of microglia around the cell bodies of injured neurons has been demonstrated to promote CNS regeneration. However, it is well known that microglial activation can impair neuronal survival and cause CNS degeneration by the production of cytotoxic molecules. The current project used Poly I:C and GM-CSF to stimulate microglial activation around the cell bodies of injured neurons in the aim of boosting axonal growth following injury. In addition, the study also wanted to evaluate the possible toxic effects associated with Poly I:C and GM-CSF mediated microglial activation in the CNS.

Poly I:C was used to investigate the effects of acute inflammation in the rat CNS. The primary aim here was to stablish a safe dose of Poly I:C and to characterize the inflammatory response generated by Poly I:C in the rat motor cortex. It was also investigated whether Poly I:C injected into motor cortex will improve the regeneration of corticospinal tract axons. In addition, to determine the effect of perineuronal Poly I:C on peripheral nerve regeneration, Poly I:C was injected near the facial nucleus of rats with facial nerve injuries.

GM-CSF was used to investigate the effects of chronic inflammation in the normal and injured rodent CNS. For the prolonged expression of GM-CSF in the CNS, a non-integrating lentivirus encoding for GM-CSF and for the marker enhanced Green Fluorescent Protein was created. As a next step the transfection levels over time, microglial activation and other parameters of the inflammatory response, and effects on cell survival and toxic side effects were evaluated in the adult rat CNS.

The effect of GM-CSF-virus in mice was also studied. Mice are particularly interesting due to the availability of the many well characterized strain backgrounds and genetically modified mouse lines. The responses of one inbred

and six outbred mouse strains to GM-CSF-virus were characterised. To further characterize possible detrimental effects prolonged inflammation may cause the FVB mouse stain was used to model potential neurotoxic effects following fetal delivery of GM-CSF.

Finally, potential neuroprotective or regenerative effects of GM-CSF were studied in rats. The principal aim of the project was to define the specific effects delivering GM-CSF-virus around the neuronal cell body of injured corticospinal neurons would have on axonal regeneration and functional recovery after corticospinal tract injury.

CHAPTER TWO

Materials and Methods

Materials

The following materials were used for the production of replication deficient and integration deficient lentivirus.

Molecular cloning

1kb Plus DNA ladder	Invitrogen
Restriction enzymes	New England Biolabs
T4 DNA ligase	Promega
T4 DNA ligase buffer	Promega
Ethidium bromide	Sigma-Aldrich
QIAquick gel extraction kit	Qiagen
Qiagen Spin Miniprep kit	Qiagen
Qiagen Plasmid Maxiprep	Qiagen
Agarose	Invitrogen
Agar	MERCK
Ampicillin	Stratagene

Solutions

TAE	40mM Tris-acetate and 5mM EDTA from (Sigma-Aldrich)
Orange G- DNA loading dye	10% glycerol, 0.1% Orange G (Sigma-Aldrich)
LB broth	1% bactotryptone, 0.5% yeast extract, 1% NaCl: (Sigma-Aldrich)
S.O.C. medium	For 250mLs: 5g Tryptone Peptone, 1.25g Yeast extract, 0.15g NaCl, 0.05g KCl, 0.51g MgCl2, 2.5mLs $MgSO_4$. Autoclave. Add 10mLs 20% glucose after autoclaving. (Sigma-Aldrich)

LB (Luria-Bertani) Broth	10g NaCl, 5g Yeast extract, 10g tryptone peptone for 1L. (Sigma-Aldrich). Autoclave. Add 100µg/ml ampicillin when cool.
LB (Luria-Bertani) Agar	For 1L: 10g NaCl, 5g Yeast extract, 10g tryptone peptone, 15g bacto agar. Autoclave. Add 100µg/ml ampicillin when cool.

Methods

Production of replication and integration deficient lentivirus

The current study used a HIV-1 based, replication-deficient, non-integrating lentivirus encoding for GM-CSF and enhanced Green Fluorescent Protein (eGFP). As a control to the GM-CSF-virus, a lentivirus carrying eGFP-only was used.

Cloning GM-CSF lentiviral plasmid

To create the GM-CSF lentiviral plasmid (Fig. 1B), GM-CSF cDNA (0.5kB), kindly provided by Dr. C-O Yun, Yonsei University College of Medicine, Korea, and the Xiap-derived Internal Ribosome Entry Site (IRES) element was inserted between the Spleen Focus-Forming Virus (SFFV) promoter and eGFP-gene encoded in the eGFP-plasmid (Fig. 1B) (Yanez-Munoz et al., 2006).

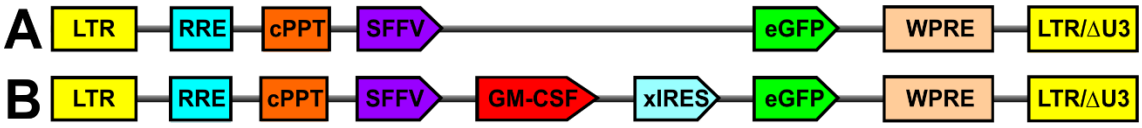

Figure 1: Schematic representation of the lentiviral plasmid constructs used in the study**.** A) The eGFP lentiviral plasmid (eGFP-virus). The lentiviral plasmid carries Spleen Focus-Forming Virus promoter (SFFV), driving the expression of eGFP. The promoter is preceded by long terminal repeats (LTRs), a rev Response Element (RRE) and a central PolyPurine Tract (cPPT) and followed by the Woodchuck Hepatitis Post-transcriptional Regulatory (WPRE) element to stabilize the eGFP mRNA. In this study this plasmid was used as a control to the current GM-CSF virus. B) The GM-CSF lentiviral plasmid was cloned by inserting the murine GM-CSF gene and the xiap derived Internal Ribosome Entry Site (xIRES), between the SFFV promoter and eGFP of the eGFP plasmid. SFFV directs the expression of GM-CSF and xIRES permits bicistronic expression of eGFP (GM-CSF/eGFP).

Cloning strategy

As seen in figure two, the creation of the GMCSF/eGFP lentiviral plasmid required four cloning steps (Fig. 2A-D):

A. The 220 base pair long xIRES was cloned from its parental DNA plasmid pMA-xIRES into pSL301 plasmid (3.2Kb- Invitrogen) using KpnI and SacI enzymes (pSL-xIRES) (Fig.2A).
B. Similarly, from the pGL3-GM-CSF plasmid, GM-CSF (854bp) was inserted to pSL301 using XhoI and NheI (pSL-GMCSF) (Fig. 2B).
C. GMCSF from pSL-GMCSF was inserted into pSL-xIRES using BglI and KpnI enzymes, resulting with pSL-GMCSF/xIRES (Fig. 2C).
D. Finally, GMCSF/xIRES insert was placed between the SFFV and eGFP genes, of the eGFP-only plasmid, by digesting pSL-GMCSF/xIRES with BclI enzyme and the eGFP-only plasmid with BamHI (Fig. 2D)

The cloning of the plasmid required the following steps: plasmid digestion with restriction enzymes, analysis of plasmid derived fragment using gel electrophoresis, purification of DNA fragments from gel fragments, ligation of restricted bands, and plasmid replication using bacteria. *Cloning of the viral plasmid was carried out by me, Francia Carolina Acosta-Saltos, under the supervision of Dr Roman Gonitel.*

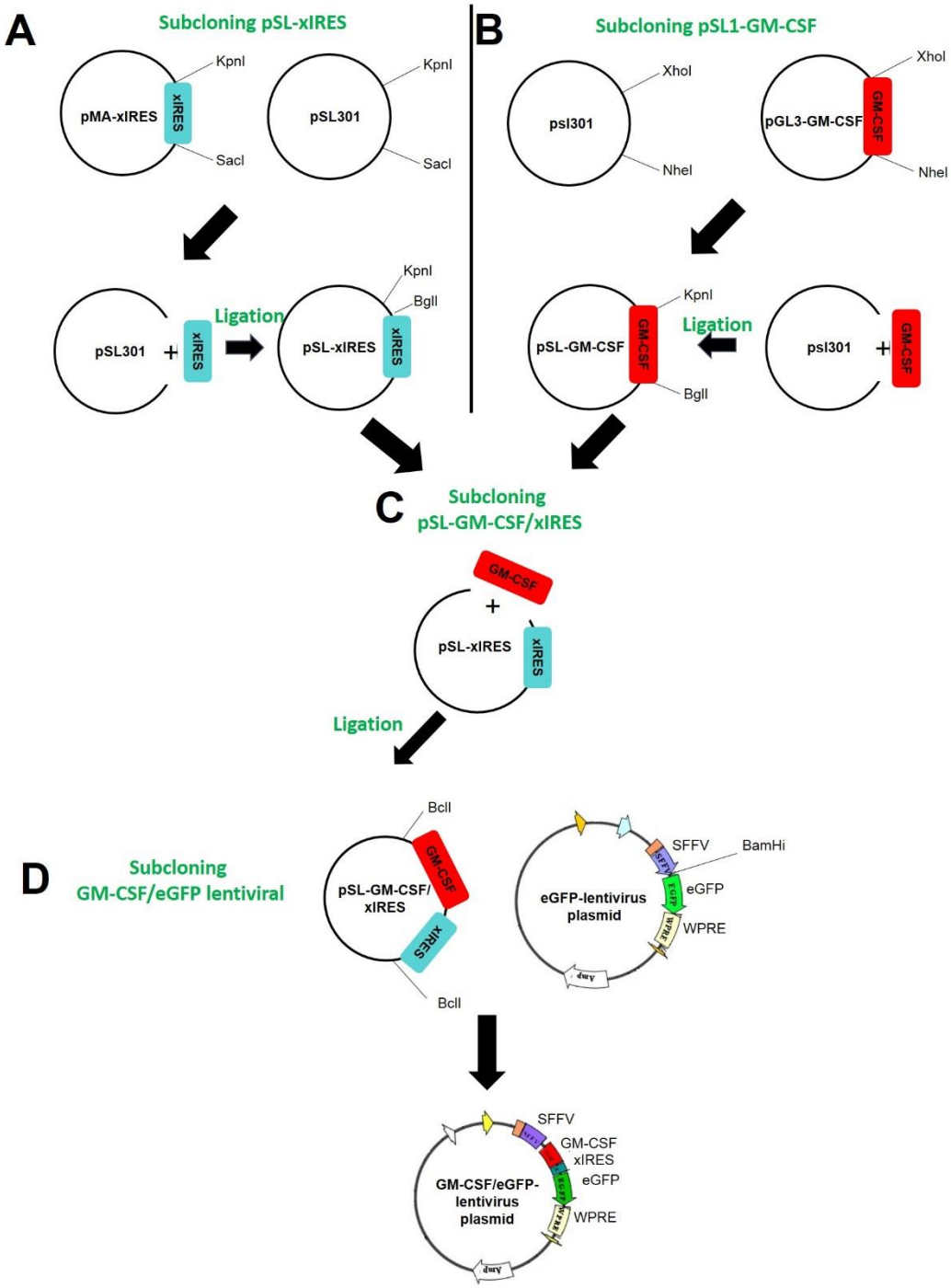

Figure 2: Cloning strategy. Diagram represents the four steps required for the production of GM-CSF/eGFP-lentivirus plasmid.

Molecular Cloning

RESTRICTION ENZYME DIGESTION OF PLASMID DNA

Restriction digest reactions were typically a final volume of 30ul. Reactions contained 1ug-2ug of plasmid DNA, 1.5ul of one or two restriction enzymes (New England Biolabs), 1x buffer and 1x BSA (0.1mg/mL) (supplied with restriction enzymes: New England Biolabs). The reactions lasted for 1-2 hours and were carried at the temperature recommended by the manufacture.

ISOLATION AND PURIFICATION OF DNA FRAGMENTS BY ELECTROPHORESIS

DNA fragments were resolved by electrophoresis through 1% agarose gels in 1xTAE buffer. Gels were prepared by boiling 1xTAE (40mM Tris-acetate and 5mM EDTA from Sigma-Aldrich), dissolving agarose (Invitrogen), adding ethidium bromide (0.5g/ml- Sigma-Aldrich) before the being allowed to set in an appropriate gel tray. DNA samples were loaded with Orange G loading dye (10% glycerol, 0.1% Orange G- Sigma-Aldrich) along with 1kb Plus DNA ladder (Invitrogen). Gels were electrophoresed at 100-150V and visualised by exposure to ultraviolet light using UviDoc gel documentation system.

Following electrophoresis, DNA fragments were extracted from agarose gel using a clean scalpel blade under ultraviolet light. DNA was purified using QiAquick gel extraction kit (Qiagen) gel extraction kit as recommended by the manufacture.

DNA LIGATION

Digested plasmid backbone was ligated to insert DNA in a 1:1 or 1:4 molar ratio using T4 DNA ligase (Promega) and 1X T4 DNA ligase buffer (Promega) in a final volume of 20µl. Ligation of sticky ends was performed for 1 hour at room 37°C. Ligation products were transformed into competent chemically competent Stbl3 *E. coli* (Invitrogen).

BACTERIAL MANIPULATION

GROWTH AND MAINTENANCE OF E. COLI

Chemically competent Stbl3 *E. coli* were grown at 37°C in LB broth (1% bactotryptone, 0.5% yeast extract, 1% NaCl: Sigma-Aldrich) while shaking at 250rpm or streaked out on solid LB agar plates (1.5% agar dissolved in LB by

heating). For antibiotic selection, 100µg/mL ampicillin was added into LB broth or agar.

TRANSFORMATION OF BACTERIAL CELLS

For every transformation, Stbl3TM E.coli were thawed slowly in ice. In a 50ul vial of bacteria, 10pg-100ng of DNA was added and gently mixed. The mixture was left to incubate for 30 minutes in ice. Bacteria were then heat shocked for 45 seconds at 42°C and placed immediately in ice for 2 minutes. 250ul of preheated S.O.C. medium was added to cells and placed in a shaking incubator at 250rpm for 1 hour at 37°C. The bacteria were plated out on agar LB plate with ampicillin (50ug/mL).

PLASMID DNA PREPARATION

Colonies were picked from agar plates using a 20ul pipette tip. *E. coli* containing plasmids of interest were subsequently grown overnight in 5mL (small-scale), 100mL or 500mL (large-scale) LB broth at 37°C in a shaking incubator. DNA plasmids were extracted by alkaline lysis using Qiagen Spin Miniprep kit (≤ 20uL plasmid DNA), Qiagen Plasmid Maxiprep (≤500µg) as instructed by the manufacturer.

Plasmid DNA concentration was quantified by measuring the absorbance of light with a wavelength of 260nm using a NanoDrop ND-100 spectrophotometer with a 0.2mm path length.

ANALYTICAL DIGESTS

To find out the presence of and orientation of the inserts, analytical digests on the various plasmids was carried out.

Following restriction reaction of pSL 301 variants with SacI and MfeI enzymes, it was confirmed that pSL-xIRES (Fig. 3A lane 3) contained xIRes insert (292bp), pSL-GMCSF (Fig. 3A lane 4) had GM-CSF insert present (584bp), and pSL-GMCSF/xIRES plasmids (Fig. 3A lane5) had both GM-CSF and xIRES present (754bp).

Lentiviral plasmids digested with EcoR1 and Nhe1 enzymes confirmed that GM-CSF and xIRES are present and in the right orientation (Fig. 3B). Three digestion products were found: lentiviral plasmid backbone (7.15 kb),

GMCSF/xIRES/eGFP/WPRE (2.71 kb) and SFFV promoter (486 bp) (Fig. 3B lane two).

Cloned plasmids were sequenced at the Wolfson Institute of Biomedical Research, UCL. Sequencing confirmed that GM-CSF and xIRES were present in the lentiviral vector and in the right orientation.

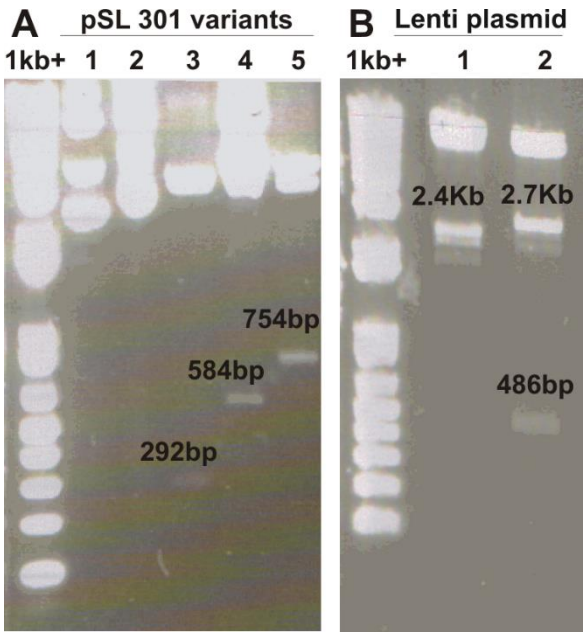

Figure 3: Analytical digests of pSL301 and lentiviral plasmids cloned in this study. A) Lane 4, 5 and 6 show the reaction products of pSL-xIRES (3.4kb), pSL-GMCSF (4.1 kb), pSL-GMCSF/xIRES plasmids after SacI and MfeI digestion. The xIRes (292bp) (line 4), GMCSF (584bp) (line 5) and GMCSF+xIRES (754) (line 6) are evident after digestion of pSL301 variants. Lane 1, 2 and 3 demonstrate the 1kb+ ladder, undigested pSL-xIRES and pSL-GMCSF, respectively. B) eGFP-only (9.7 kb) and GMCSF/eGFP (10.3 kb) lentiviral plasmids where digested with EcoR1 and Nhe1 enzymes. The GMCSF/eGFP lentiviral plasmid (lane 2) shows three digestion products: lentiviral plasmid backbone (7.15 kb), GMCSF/xIRES/eGFP/WPRE (2.71 kb) and SFFV promoter (486 bp). The reaction products of eGFP-only plasmid (lane 3) are the lentiviral backbone (7.25kb) and SFFV/eGFP/WPRE genes (2.4kb), confirming the presence of GMCSF and xIREs genes in the GMCSF/eGFP lentiviral plasmid.

Cell culture and virus preparation

PROPAGATION AND STORAGE OF MAMMALIAN CELL LINES

Adherent cells, Human Embryonic Kidney 293 (HEK-293T) cells and murine BV-2 cells, kindly provided by Dr Jennifer Pocock, Institute of Neurology ULC, were maintained in Dulbecco's Modified Eagle Medium (DMEM- Invitrogen) containing

GlutaMAX supplemented with 10% foetal calf serum (FCS- Invitrogen) and 1% penicillin/streptomycin (hereafter referred to as 'complete DMEM'). All cells were incubated at 37°C and a 5% CO_2 atmosphere.

LENTIVIRUS PREPARATION

To produce non-integrating lentiviral vector, 1.2 x 10^7 HEK293T cells were seeded in 175cm^2 flasks (Sigma-Aldrich) one day before transfection to reach >90% confluence. For each flask, 50µg vector plasmid (Fig. 4 A or B) , 32.5µg non-integrating virus packaging plasmid pCMV-dR8.74 D64V, and 17.5µg vesicular stomatitis virus envelope plasmid pMDG2 was added to 5ml Optimem and 0.22µm filtered. 1µl PEI was added to 5ml Optimem and also 0.22µm filtered. The two mixtures were combined and allowed to complex for 20min. Cells were washed with PBS, overlaid with the complex, and incubated at 37°C 5% CO2 for 4 hours. The complex was removed and replaced with complete DMEM 24 hours later, the medium was replaced 48 and 72 hours after transfection, the medium was removed, 0.22µm filtered, and centrifuged at 98,000*g* for 2 hours. Virus pellets were re-suspended in Optimem and aliquots were stored at -80°C.23.

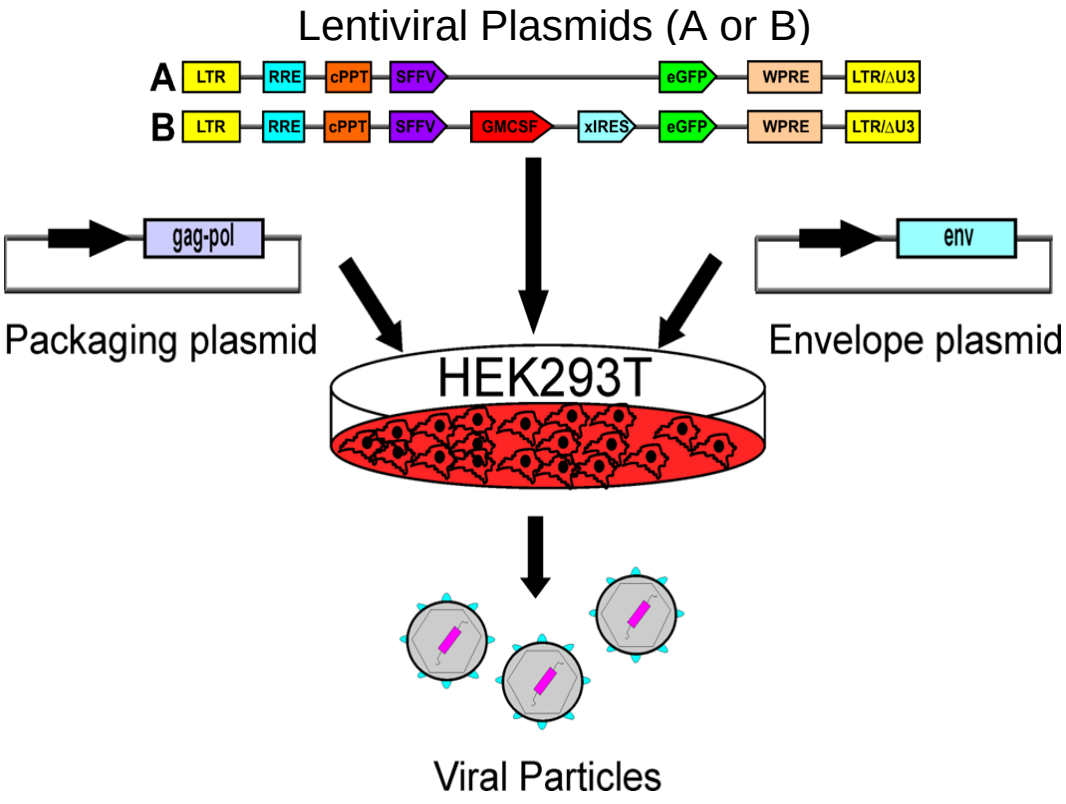

Figure 4: Lentivirus production. Non-integrating lentiviral particles were produced by transient transfection of HEK293T cells with three plasmids: Lentiviral genome plasmid (A or B), the integrase deficient Gag-pol packaging plasmid and an envelope plasmid expressing vesicular stomatitis virus G protein (VSVG), which pseudotypes the virus to predominantly transduce neurons in vivo, as described by Rahim et al., (2009).

FLOW CYTOMETRY

To calculate the titre of eGFP-lentivirus and GM-CSF/eGFP-lentivirus, 10^5 HEK-293Tcells were seeded in a 24 well plate, in a final volume of 300µL and were left overnight. The next day the cells were treated with 2ul, 0.4ul, 0.08ul, 0.016ul of eGFP-lentivirus or GM-CSF/eGFP-lentivirus. As a negative control, cells were treated with vehicle medium (DMEM). Two days following transduction, the cells were harvested, washed with PBS and pelleted in a FACS tube by centrifugation at 1500rpm for five minutes. The samples were then re-suspended in 200µL of PBS and were then analysed by flow cytometry using a CyAn ADP flow cytometry analyser and FlowJo software. Figure 4 and 5 show an example of the results obtained from flow cytometry after the cells transduced with increasing concentrations of eGFP-lentivirus (Fig. 5) or GM-CSF/eGFP-lentivirus (Fig. 6) were analysed. The histograms represent the correlation between side scatter (Y-axis) and eGFP fluorescence (X-axis).

VIRAL TITRE CALCULATION

Using the flow-cytometry histograms obtained from the above section, a region of the histogram was gated to pick up viable cells expressing eGFP, which are most likely infected with one viral particle. Only samples that had between 2% and 5% of eGFP-fluorescent cells within the gated area were used to quantify the titre. A typical example might be 10^5 cells transduced with 0.016ul eGFP-virus resulting in 2.89% of green fluorescent cells (Fig. 5) or 10^5 cells transduced with 0.08ul GM-CSF-virus resulting in 4.67% of green fluorescent cells (Fig. 6).

Subsequently, the titre of the vector can be calculated by using the following formula:

$$\frac{Number\ of\ transduced\ cells}{Volume\ of\ virus\ used\ to\ transduce\ cells} = \text{viral titre}$$

For example, the following calculation was carried out to determine the titre of eGFP-virus (Fig. 5):

$$\frac{(2.89/100) \times 10^5}{0.016ul} = 180625 \text{ TU/ul}$$

*10^5= the number of cells seeded in in one well

To calculate titre in TU/ml:

$$180625 \text{ TU/ul} \times 1000 = 1.8 \times 10^8$$

Additionally, the following calculation was carried out to determine the titre of GM-CSF-virus (Fig. 6):

$$\frac{(4.67/100) \times 10^5}{0.08ul} = 58375 \text{ TU/ul}$$

To calculate titre in TU/ml:

$$58375 \text{ TU/ul} \times 1000 = 5.84 \times 10^7$$

INTENSITY OF FLOURESCENCE

Flow cytometry histograms (Fig. 5 & 6) were also used to determine the intensity of fluorescence of cells infected with eGFP-only (Fig 5) or GM-CSF/eGFP-lentivirus (Fig. 6) at 0µl, 0.032µl, 0.016µl, 0.08µl, 0.4µl and 2µl. The median fluorescent intensity of cells within the gated area was measured using FlowJo software.

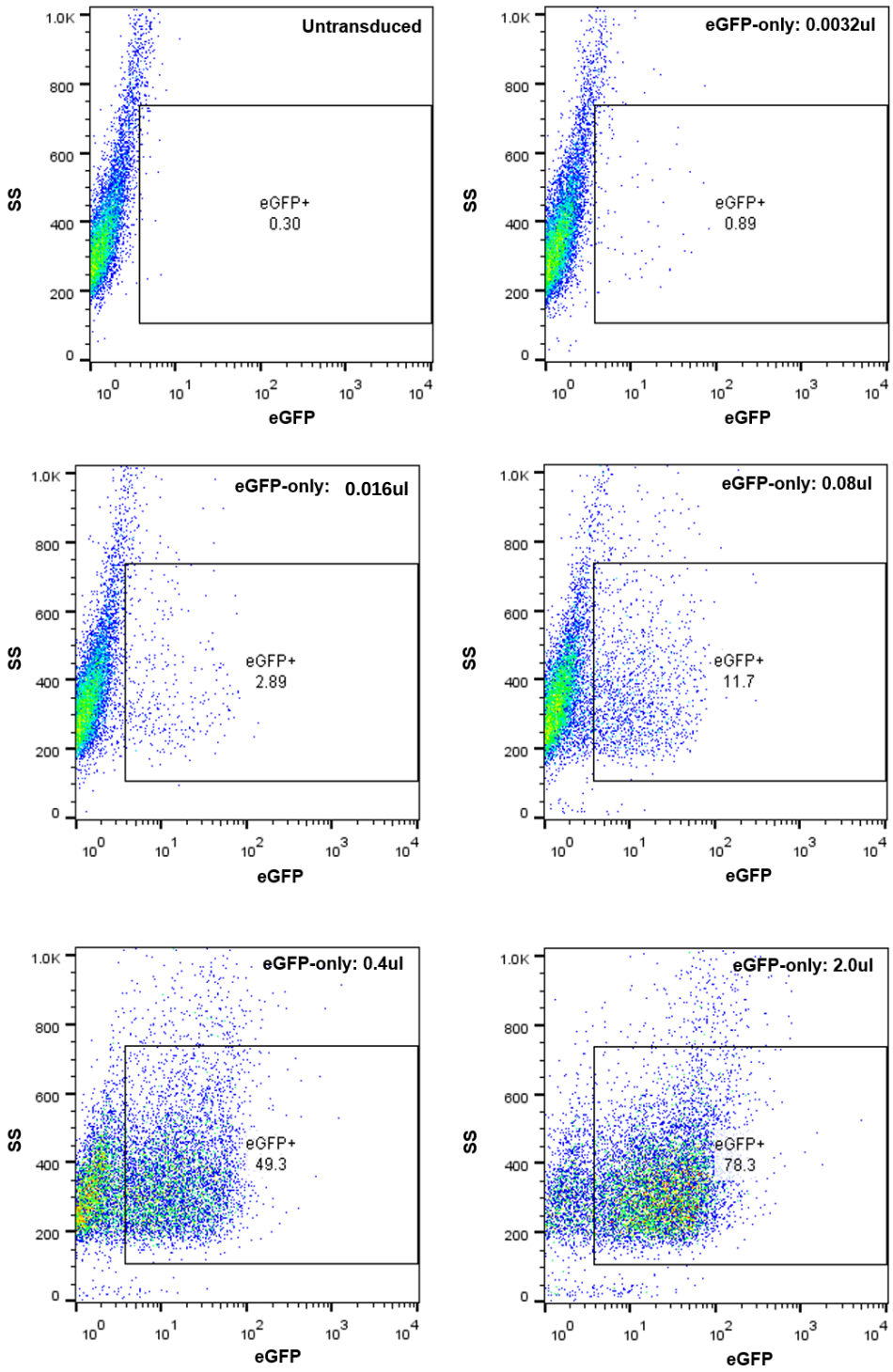

Figure 5: eGFP-expression from HEK293T cells infected with eGFP-only lentivirus. eGFP-expression was determined by flow cytometry 2 days following transfection of HEK293T cells with 0µl (untransduced), 0.032µl, 0.016µl, 0.08µl, 0.4µl and 2µl of eGFP-lentivirus. The proportion of HEK293T cells expressing eGFP is given as a percentage within the gated area.

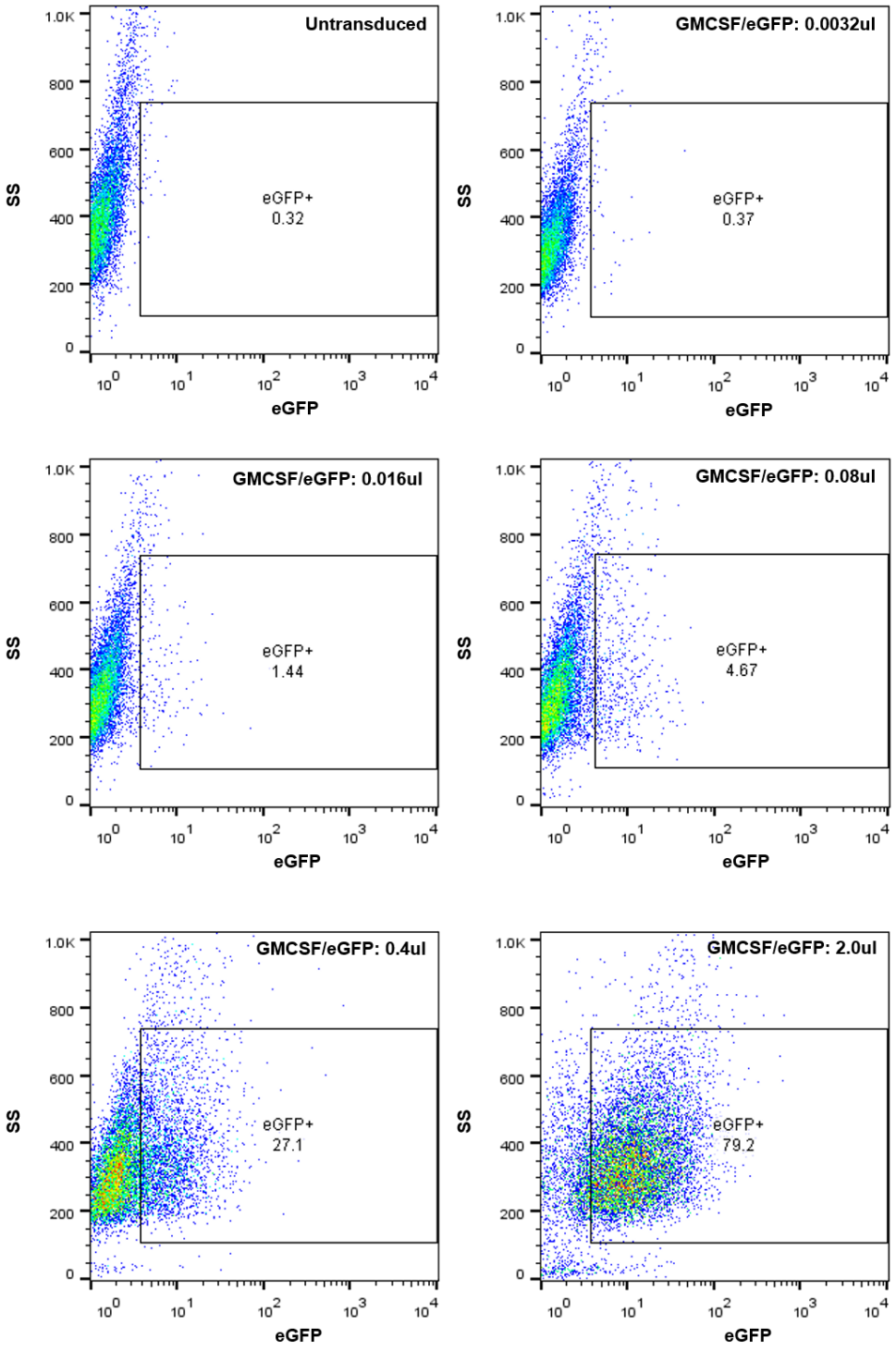

Figure 6: eGFP-expression from HEK293T cells infected with GM-CSF/eGFP lentivirus. eGFP-expression was determined by flow cytometry 2 days following transfection of HEK293T cells with 0µl (untransduced), 0.032µl, 0.016µl, 0.08µl, 0.4µl and 2µl of GM-CSF/eGFP-lentivirus. The proportion of HEK293T cells expressing eGFP is given as a percentage within the gated area.

Lentivirus was produced by me or Dr Roman Gonitel.

In vitro assay

GM-CSF/EGFP-lentivirus bioactivity assay

0.3 X 10^6 HEK293T cells were seeded to a 6 well plate. Once confluent, cells were treated with medium or increasing titres of GM-CSF/eGFP-lentivirus or eGFP-lentivirus (10^2 to 10^5 TU/ml). Supernatant from transfected HEK293T cells, obtained 24 hours after infection was used to treat 10^5 BV2 microglial cells. BV2 cells were seeded in a 96 well plate 24hrs before treatment. BV2 cells were maintained for 24hr in: a) GM-CSF-lentivirus conditioned medium b) eGFP-lentivirus conditioned medium or c) medium with GMCSF recombinant peptide (Gibco) at concentrations from 1 to 100 ng/ml.

BV2 cell proliferation was measured using 3(4,5-dimethythiazol-2-yl)-25-diphenyltetrazolium bromide (MTT) assay kit (Sigma-Aldrich). Briefly, 20ul of MTT was added per well and placed to incubate for 4 hours to allow the formation of formazan crystals. Medium was carefully removed and 200ul of sterile PBS was added. The formazan crystals were then dissolved in MTT solubilisation solution provided with the kit. Light absorbance was measured using 595 nm wavelength FLUOstar OPTIMA (BMG Labtech, Offenburg, Germany). *This assay was performed by me.*

In vivo experiments

Surgical procedures

All surgical procedures were approved by the UK Home Office and the University College London local ethics committee. Experiments used adult female Sprague Dawley rats, outbred and inbred mice. Animals had access to adequate food and water ad libitum.

Anaesthesia was induced with a mixture of 4% Isoflurane and oxygen and then maintained with 1.5% Isoflurane and oxygen. All animals received 0.1ml of intra-peritoneal amoxicillin at the end of surgery whilst still under anaesthetic and all wounds were closed with skin clips or sutures.

RAT

STEREOTACTIC MOTOR CORTEX INJECTIONS

Adult female Sprague-Dawley rats (275-300g) (Charles Rivers) were anaesthetised with isofluorane. To expose the surface of the motor cortex, a scalp incision 1mm lateral to the midline, followed by craniotomy was performed. Subsequently, rats were placed in a stereotaxic frame (World Precision Instruments). Using a 10µl Hamilton syringe (Hamilton Company) attached to a micromanipulation pump (World Precision Instruments), 2ul of experimental substance was delivered into the motor cortex at a rate of 0.4µl/min. Injections were completely withdrawn after 5 minutes. The scalp incision was closed with Michel clips (Vet Tech). Substances were delivered into the motor cortex at four different sites. When anterograde tracing of the corticospinal tract was required, biotinylated dextran amine (BDA), was injected into the motor cortex at five different sites (Table 1).

Poly I:C project

Dose response: Animals received injections of Poly I:C (Sigma-Aldwich) at either 5.6mg/ml, 1.0mg/ml or 0.1mg/ml and a control injection of PBS to the contralateral motor cortex described above. The animals were allowed to survive for 3 days. *Surgery was performed by Prof. Patrick Anderson.*

Time course: Poly I:C 1.0mg/ml injections into the left motor cortex, with a control injection of PBS contralateral hemisphere. Rats survived up to 3 days, 7 days and 14 days following injection. *Surgery was performed by Prof. Patrick Anderson.*

GM-CSF project

Dose response: Animals received injections of eGFP-virus at 10^8 or GM-CSF/eGFP-virus at concentrations from 10^3 TU/ml to 10^7 TU/ml. GM-CSF-virus dilutions were carried out using eGFP-virus at 10^8. The animals were allowed to survive for 14 days. *Surgery was performed by Prof. Patrick Anderson, Dr Roman Gonitel and me.*

Time course: eGFP-virus (10^8 TU/ml) or GM-CSF/eGFP (10^7 TU/ml) injections into the motor cortex. Rats survived up to 3 days, 7 days, 14 and 28 days following

injection. *Surgery was performed by Prof. Patrick Anderson, Dr Roman Gonitel and me.*

Table 1: Co-ordinates for injections into the rat motor cortex. The coordinates are given as three-dimensional (x, y and z) distances (in mm) relative from the bregma. The x plane represents the medial-to-lateral (left-to-right) distance from bregma, the y plane represents the rostral-to-caudal (front-to-back) distance from bregma and the z plane represents the dorsal-to-ventral (up-and-down) distance from bregma.

Rat	Caudal	Lateral	Ventral
Motor Cortex injection	0.0mm	3mm	1.8mm
	0.5mm	2mm	1.6mm
	1.0mm	2mm	1.6mm
	1.5mm	2mm	1.6mm
Additional injection for BDA	2.5mm	2mm	1.6mm

RETROGRADE FLUOROGOLD (FG) CORTICOSPINAL NEURON LABELLING.

Under continuing anaesthetic and with the rodent neck supported in flexion, the cervical spine was exposed by incising through skin and soft tissue along the midline. A laminectomy was performed to expose the dura and spinal cord. A bilateral incision was made through the corticospinal tract at C4 level with microscissors, and a small piece of Gelfoam (Johnson and Johnson, Skipton, UK) impregnated with 2µl of 2% Fluorogold (Molecular Probes) in distilled water was inserted into the incision. In addition to Fluorogold retrograde labelling:

Poly I:C project: rats received Poly I:C 1.0mg/ml injections into the left motor cortex and a PBS injection into the right motor cortex as described previously. *Surgery was performed by Prof. Patrick Anderson.*

GM-CSF project: rats received GM-CSF/eGFP-virus injection into the left or eGFP-virus injection into the right motor cortex as described previously. *Surgery was performed by Prof. Patrick Anderson and Dr Roman Gonitel.*

The animals injected with the Poly I:C project were allowed to survive for 7 days and those of the GM-CSF project survived 14 days.

CORTICOSPINAL TRACT INJURY

Anesthetised adult female Sprague-Dawley rats (275-300g) were injected into the motor cortex with experimental substances and BDA (10mg/ml) anterograde tracer. They also underwent a contralateral dorsal corticospinal tract injury (Fig. 7).

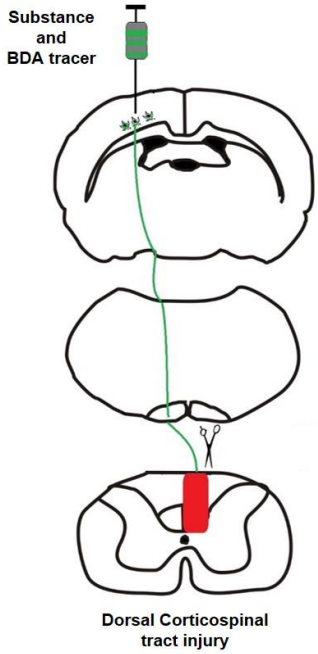

Figure 7: Surgical procedure. Rats were injected with experimental substances and anterograde tracer into the motor cortex. They endured a dorsal corticospinal tract injury contralateral to the injected motor cortex (in red). Edited from Hutson et al., (2012).

Experimental substances and anterograde tracer injection

In the Poly I:C and GM-CSF experiments injections to the left motor cortex were carried out the as previously described.

- *Poly I:C experiments:* Rats were injected into the motor cortex with PBS/BDA or Poly I:C/BDA (1mg/ml).
- *GM-CSF experiments:* Rats were injected into the motor cortex with GM-CSF-lentivirus (10^4, $10^{5.5}$, 10^7 TU/ml) mixed in eGFP-lentivirus (10^8 TU/ml) or eGFP-lentivirus (10^8 TU/ml). Rats were injected with BDA 14 days prior to sacrifice. In addition, animals were injected intravenously with Fluorospheres via the tails 24h before sacrifice at 1ul/g.

Dorsal corticospinal tract injury

Following motor cortex injection, with the rat neck supported in flexion, the cervical spine was exposed by incising through skin and soft tissue along the midline. At cervical segment 4, a laminectomy was performed to expose the dura and spinal cord. A dorsal incision was made to the corticospinal tract, contralateral to the motor cortex injection. Time line of surgical procedures are presented in figure 8.

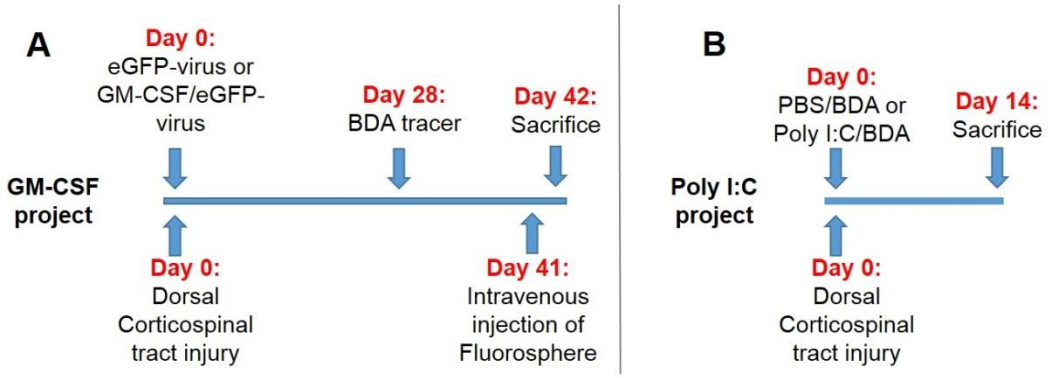

Figure 8: Experimental time line of GM-CSF (A) and Poly I:C (B) corticospinal tract injury projects.

Post-surgery care included an injection of 1 ml of Clamoxyl antibiotic and an analgesic regimen. A dose of 0.1 mg/kg of vetergesic was injected subcutaneously pre-surgery on the first day and a follow up injection was given 7 hours after surgery. Maintenance vetergesic administration was provided orally via cherry gelatine to be eaten ad libitum.

Corticospinal tract injury experiment contributions: For the Poly I:C project, surgery was performed by Prof. Patrick Anderson. The surgery for the GM-CSF project was carried out for two separate purposes: histological or behavioural assessments. Surgery for histological assessments was carried out by Prof. Patrick Anderson, Dr Roman Gonitel and me. Surgery for behavioural assessments was performed by Patrick Anderson and me.

FACIAL NERVE INJURY

Adult female Sprague-Dawley rats (275-300g) received a unilateral right craniotomy and then one injection of either 1µl of Poly I:C 1.0mg/ml or 1µl of PBS

near the right facial nucleus at the following coordinate from bregma; 2mm lateral, 10.8mm posterior, 8.5mm deep.

Right facial nerve axotomy was performed by making a 1cm skin incision posterior to the right ear at the level of the mastoid process. Superficial muscles were bluntly dissected to expose the facial nerve. The facial nerve was transected completely with microscissors at the stylomastoid foramen and included the retro-auricular branch. The skin was closed with wound clips (Autoclip, USA). Two days prior to sacrifice (28 days), a piece of Gelfoam (Johnson and Johnson, Skipton, UK) impregnated with 30µl of Fluorogold (Fluorochrome, Denver, USA) diluted to 2% with distilled water was inserted under the left and right whisker pads. The animals were allowed to survive for 30 days (Fig. 9). *Surgeries were performed by Prof. Patrick Anderson and me.*

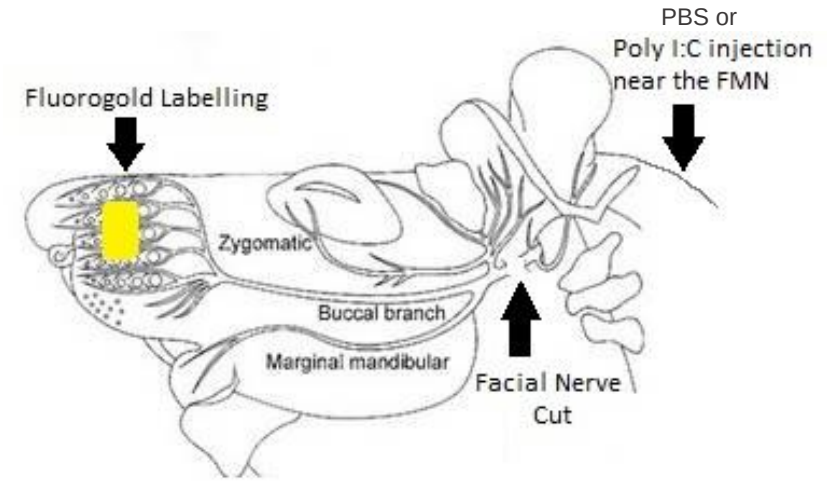

Figure 9: Facial nerve axotomy model and retrograde tracing of the facial nerve. Rats were injected with Poly I:C or PBS near the facial motor nucleus (FMN) and subsequently received a facial nerve axotomy. At 28 days post injury fluorogold was inserted into the whisker pad. Rats were sacrificed at 30 days post facial nerve injury. Picture edited from Peeva et al., (2006).

MOUSE

Adult females (6-8 weeks) of one outbred and six inbred mouse strains were used, including outbred strain CD1 and inbred strains- 129S2/Sv, FVB/N, SJL, Balb/C, C3H/N, C57/BL6 (Charles Rivers).

MOTOR CORTEX INJECTION:

CD1 mice had a scalp incision at 0.5mm lateral to the midline and craniotomy was performed to expose the surface of the motor cortex. Mice were placed in the stereotaxic frame. Using a 10µl Hamilton syringe attached to a micromanipulation pump, 0.5ul of eGFP-virus (10^7 TU/ml) or GM-CSF/eGFP-virus (10^7 TU/ml) was delivered into the motor cortex at a rate of 0.1µl/min. Injections were completely withdrawn after 2 minutes. The scalp incision was closed with Michel clips (Vet Tech). Mice received three virus injections: 1.0mm lateral and 0.5 rostral, 1mm caudal, or 1.5mm caudal to the bregma. All injections were 0.5mm deep into the motor cortex. Mice were allowed to survive for 3, 7, 14 or 28 days after injection. *Surgeries were performed by Dr Roman Gonitel and me.*

CORPUS STRIATUM INJECTION

eGFP-virus (10^7 TU/ml) or GM-CSF/eGFP-virus (10^7 TU/ml) was injected into the corpus striatum of CD1, 129S2/Sv, FVB/N, SJL, Balb/C, C3H/N, or C57/BL6. Mice had a scalp incision at 1mm lateral to the midline and craniotomy was performed to expose the surface of the brain. Mice were then placed in the stereotaxic frame. Using a 10µl Hamilton syringe attached to a micromanipulation pump, 2.5µl of the virus was injected at 0.5 µl/ml. Mice received one injection: 0.5mm rostral and 1.8mm lateral to bregma. The needle was inserted 3mm deep. All mice survived 14d post-surgery. *Surgeries were performed by me.*

INTRAVENTRICULAR INJECTIONS IN FOETAL FVB MICE

Pregnant female FVB mice at gestational day 14 were anaesthetised. To access the uterus a full-depth midline laparotomy was performed. A 34-gauge needle (Hamilton) was used to deliver 5 µl of eGFP-only vector (10^8 TU/ml) or mixed with GM-CSF/eGFP (10^7 TU/ml) into the lateral ventricle located on the left or right side of the foetal brain. GM-CSF/eGFP or eGFP-only pups were taken at postnatal day 0, 7, and 14. *Surgeries were performed by Dr Simon Waddington and me.*

RAT BEHAVIOURAL ASSESSMENT

FOREPAW REACHING AND REARING ASSESSMENT

The behaviour of rats with right dorsal corticospinal tract injury at cervical level 4 and with injections of eGFP-virus or GM-CSF/eGFP-virus (10^4 TU/ml, $10^{5.5}$ TU/ml or 10^7 TU/mL) into the left motor cortex was examined. Rats were tested at 2 time points prior to injury, and from 3 days to 42 days following injury, in 3 to 4 day intervals. Behaviour was recorded using a Canon digital video camera (VIXIA HF S10, Canon, UK). *Behaviour was recorded by me and Lucas Topham.* Behavioural analysis was carried out blindly using video recordings. *Behaviour was assessed by Lucas Topham and Dr Alejandro Acosta Saltos and me*.

Forepaw reaching assessment

In order to ensure consistent participation from female Sprague-Dawley rats (275-300g), all rats went through a two week training session before baseline function was assessed. Before training, rats were habituated to the reaching cage in groups of four cage-mates for two days. The cage had a vertical slit (8 cm x 1.5 cm) in the middle of cage with a rectangular platform (3 cm x 4 cm) protruding at the bottom of the slit. During training, Cheerios were broken into thirds to provide food motivation and were given to the rats using a set of forceps. To encourage reaching through the slit, with either the right or left forepaw, the Cheerio was held to the left or right of the slit in the cage. Once the rat demonstrated an ability to perform 25 reaches with each forepaws, the rat was considered trained. During testing, rats were required to reach 25 times with each forepaw for a total of 50 reaches per behavioural testing session.

Sub-movement scoring

Rats were evaluated on the function of their proximal and distal muscles, such as shoulder, arm and lower arm muscles (Whishaw and Pellis, 1990). Ability to perform a certain movement was scored on a scale of 1-3 (1-attempted but with no use, 2-partial use, or 3-complete use). Proximal shoulder movements included abduction, adduction and flexion; the elbow was used as a landmark to evaluate these movements. Upper arm movement studied was biceps flexion. Distal, lower arm movements included wrist flexion and extension, and paw opening and closure.

Eating Success

This was a quantitative measure. The number of times a rat carried out a successful eating movement were counted. A successful eating consisted of a sequence of lifting paw from floor, exiting the slit, covering the food, grasping the food, withdrawing food, and transporting it to mouth to eat the pellet.

REARING TEST

The rearing test was carried out in parallel to the reaching assessment. The rearing test assesses the ability of the rat to use the forelimb for weight bearing during exploration of a cylinder. Rats were placed in a transparent vertical Plexyglas cylinder (30 cm height and 20 cm diameter) (Gharbawie and Whishaw, 2003) with two mirrors (30 cm x 30 cm) placed at 90˚ behind the cylinder, so that a 360˚ view of the rat was available. Using video recordings, the experimenter counted the number of times the left paw (uninjured), right paw (uninjured) or both paws were used during pushing off from the floor, rearing and landing.

WHISKER MOTOR ASSESSMENT

Rats with facial nerve injury, which were injected with Poly I:C or PBS into the hindbrain, were assessed for whisker movement from day 7 to 28. Whisker movement was scored in 0.5 increments, on a scale of 0.0 (no movement) to 3.0 (normal movement as on the operated side) (Raivich et al., 2004). *Behaviour was assessed by me and Dr Alejandro Acosta Saltos.*

Rodent perfusion

Adult rat perfusion: Rats were terminally anaesthetised with an overdose of Halothane. The paw withdrawal reflex was used as an indication of sufficient anaesthesia. Rats were then perfused through the heart with 300mls of PBS followed by 300mls of 2% paraformaldehyde in PBS. During perfusion, 3ml of blood from rats injected with Fluorospheres was taken. Blood was added to 15ml tubes containing heparin (0.5-2.0 IU/ml-Sigma-Aldrich) to prevent coagulation. Following perfusion, the brains and spinal cords of rats were dissected out, as well as livers and spleen of those injected with Fluorospheres.

Adult mouse perfusion: Mice were terminally anaesthetised by means of a 16.6ul/g of body weight, intraperitoneal injection of 2,2,2,tribromoethanol (Avertin). The paw withdrawal reflex was used as an indication of sufficient

anaesthesia. Transcranial perfusions were carried out using PBS at a rate of 0.02l/min for 5 minutes, which was followed by 10 minutes with 2% PFA solution at the same rate. Brains were subsequently dissected.

Neonatal mouse perfusion: Neonate mice at post natal day 0 to 3 were killed by placing them in ice for 5 minutes. Neonate mice at postnatal day 7 were killed by intraperitoneal injection of pentobarbitone. Mice were perfused intracardially for 2.5 min (8 mL/min) with PBS followed by 2.5 mutes with 4% FA/PBS. The brains were dissected.

Perfusions and dissections were performed by me or Prof. Patrick Anderson.

Cryoprotection

Adult mice and rat tissue: tissue was post fixed by rotating (8 rpm) immersion for 1 hour in 2% PFA/PBS before being cryoprotected in 30% sucrose in 0.1 M PBS buffer for 48 hours. Subsequently, tissue was embedded in OCT and frozen with dry ice. All tissue samples were stored at -80˚C prior to use.

Neonate mice: brains were post-fixed for 1h by rotating (8 rpm) immersions in 4% FA/PBS at 4˚C and then cryoprotected for 24h in 30% sucrose in 0.1 M PBS buffer.

Cryostat sectioning

A cryostat (Leica, Germany) with the chamber set at -20˚C was used for tissue sectioning. Tissue was collected on warm, 0.5% gelatine coated slides (MECK), refrozen in dry ice and stored at –80˚C.

Forebrains and hindbrains: Adult rat, adult mouse and neonate mouse forebrains, as well as rat hindbrains were cut in the coronal plane. Sections were 30um in thickness for adult rodents and 40um for neonate mice. Symmetry between the two hemispheres was checked regularly using a light microscope.

Spinal cord: Rat spinal cords taken from cervical segment 1 to 8. They were suspended in a well of OCT and frozen with dry ice. Subsequently, transverse and horizontal sections of the spinal cord were taken. Sections were 40µm thick.

Spleen: Coronal sections through the spleen were cut at 20um thickness.

Cryostat sectioning was carried out by me or a BSc/MSc student.

Light-microscopic immunohistochemistry and fluorescence-labelling

General staining protocol

All phosphate buffer (PB) and phosphate buffer /bovine serum albumin (PB/BSA) solutions had a pH of 7.4.

A. Tissue preparation for antigen presentation and primary antibody incubation: 1) Frozen sections were rehydrated in distilled water and spread onto the slide. 2) Dry sections were fixed for 5 min in 4% formaldehyde (FA) in 0.1M phosphate buffer (PB). 3) They were then placed in 0.1M PB, washed in acetone (50%, 2 min; 100%, 2 min; 50%, 2 min) to remove tissue fat, 4) transferred to PB (2min), moved to 0.1% bovine serum albumin (BSA: Sigma-Aldrich) in 0.1M PB (PB/BSA). 5) Subsequently, washed sections were incubated in goat serum (5%, 30 min) (Vector). 6) Serum was removed from sections and a primary antibody was added and left to incubate over night at 4˚C. A list of primary anti-bodies used in this project is listed in Table 2.

These steps were followed by two different tissue staining processes:

B. Light microscopic immunohistochemistry: 1) Sections were washed by dipping the slide sequentially in 1% PB/BSA, 0.1M PB, 0.1M PB and 1% PB/BSA. 2) Then sections were incubated with biotinylated secondary anti-rabbit antibody for 1hr (table 2). 3)This was followed by 1 hour incubation with Avidin Biotinylated horse radish peroxide Complex or ABC (ABC kit, Vector; 1:200) and 5) staining with diaminobenzidine (DAB) (Sigma) and hydrogen peroxide (Sigma). The reaction mixture contains 0.5 g/l DAB, 1:3000 dilution of 30% H_20_2 in PBS (pH7.4). The reaction was allowed to run for a maximum of 5 minutes. 6) To stop the reaction, sections were transferred to 10mM PB, washed with distilled water and dehydrated with increasing concentrations of alcohols and xylene. 7) Sections were mounted on a glass cover slip using DePex mounting medium (BDH,UK). Figure 10 demonstrates the main steps in the immunohistochemical process.

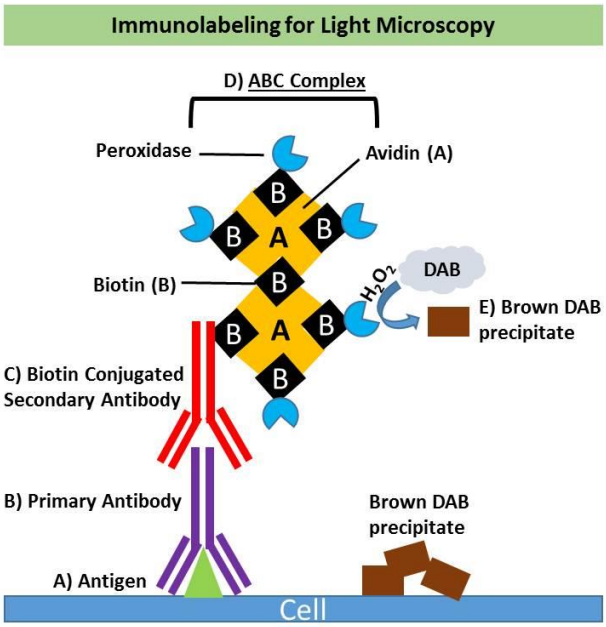

Figure 10: A diagram showing the steps of the immunolabelling process used for light microscopy. A) Antigen presentation. B) Primary antibody incubation. C) Secondary antibody incubation. D) ABC complex exposure. E) DAB staining.

C. Fluorescent labelling: 1) Sections were sequentially washed in 0.1 MPB, 0.1 MPB, PB/BSA and PB/BSA. 2) Subsequently, sections were incubated with fluorescent secondary antibody, 3) rinsed (PB/BSA, PB/BSA, 0.1M PB, 0.1M PB), 4) dried and covered with Vectashield mounting medium with DAPI or without DAPI (Vector). Secondary antibodies fluoresced green (Alexa 488) or red (Cy3). Figure 11 demonstrates the main steps in the process of fluorescent labelling.

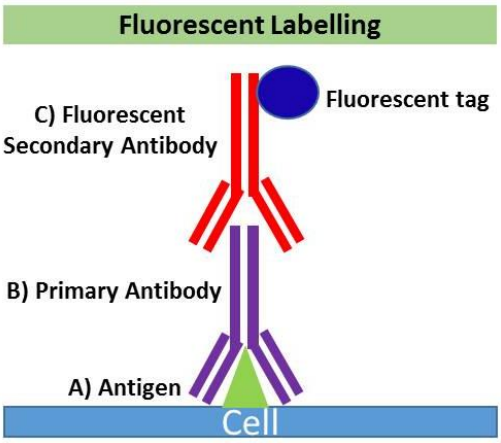

Figure 11: A diagram showing the steps of the fluorescent labelling process. A) Antigen presentation. B) Primary antibody incubation. C) Incubation of secondary antibody conjugated with a fluorescent tag.

Double-fluorescent labelling

This process can be divided into two parts: the first is the presentation of the antigen and biotin conjugate (Fig.12A1, A2, & B1), while the second is the visualisation of both of them (Fig.12A3, & B2, B3).

Part 1: Presentation of biotin conjugate and antigen

Three different double labelling procedures were carried out in this project. Below is the description of part 1 of each.

1) TUNEL/IBA1/eGFP: TUNEL assay relies on terminal Deoxynucleotidyl Transferase (TdT-Roche) to mediate the addition of dUTP-biotin to the ends of DNA fragments.

   Forebrain sections that had been shown to contain eGFP-positive cells were spread on to the slide and fixed in PFA, then incubated for 15 minutes in 3% hydrogen peroxide in methanol. Next, they were washed sequentially in acetone, 0.1PBS (2mins) and PB/BSA (2mins). TdT solution (1ul TdT (400U/ul-from stock; Roche), 1.5ul dUTP, 100ul cacodylate buffer and 8975 ul H_2O) was pipetted on to sections which were then incubated at 37˚C for 2 hours. Sections were then moved into TUNEL stop solution (1753.2mg NaCl in 100ml ddH_2O and 882.3mg Sodium Citrate in 100ml of ddH_2O) for 10 minutes. Sections were washed with 0.1M PB before incubating them with goat serum for 30 mins. After that

antibody to IBA1 was added and the sections were left to incubate at 4˚C overnight. *Continue to Part 2: visualisation of biotin conjugate and antigen.*

Endogenous peroxidase (EP)/IBA1/eGFP stain: Forebrain sections containing eGFP-positive cells were treated using *the tissue preparation for antigen presentation* protocol previously described (A: steps 1-5). Subsequently, sections were incubated with antibody to IBA1 overnight. The next day sections were washed sequentially in PB/BSA, 0.1M PB, 0.1M PB and PB/BSA. Then sections were incubated with 0.1% biotinylated tyramide (NEN, Cologne, Germany, in 0.1M PBS) in 0.01% hydrogen peroxide for 10 minutes. *Continue to Part 2: visualisation of biotin conjugate and antigen.*

GFAP/BDA labelling: Spinal cord sections containing the corticospinal tract were treated using *the tissue preparation for antigen presentation* protocol previously described (A: steps 1-5). Subsequently, sections were incubated with antibody to GFAP overnight. *Continue to Part 2: visualisation of biotin conjugate and antigen.*

Part 2: Visualisation of biotin conjugate and antigen

Sections are washed sequentially in 0.1 MPB, 0.1 MPB, PB/BSA and PB/BSA. The sections are then incubated with ABC for 1 hour, then washed with 0.1M PB, 0.1 MPB, PB/BSA and PB/BSA. Sections are then incubated with fluorescent secondary antibody: anti-rabbit Cy3 was used to bind to IBA1-antibody or anti-rabbit Alexa Fluor 488 to bind to GFAP-antibody. To remove excess secondary antibody, sections were washed sequentially in PB/BSA, PB/BSA, 0.1M PB and 0.1M PB. To visualise the biotin conjugate, sections were incubated with avidin-AMCA or avidin-Texas red for 1 hour. After that, sections were washed four times with 10mM PB. A cover slip was mounted using vectashield. Figure 12 demonstrates the main steps in the process of double-fluorescent labelling.

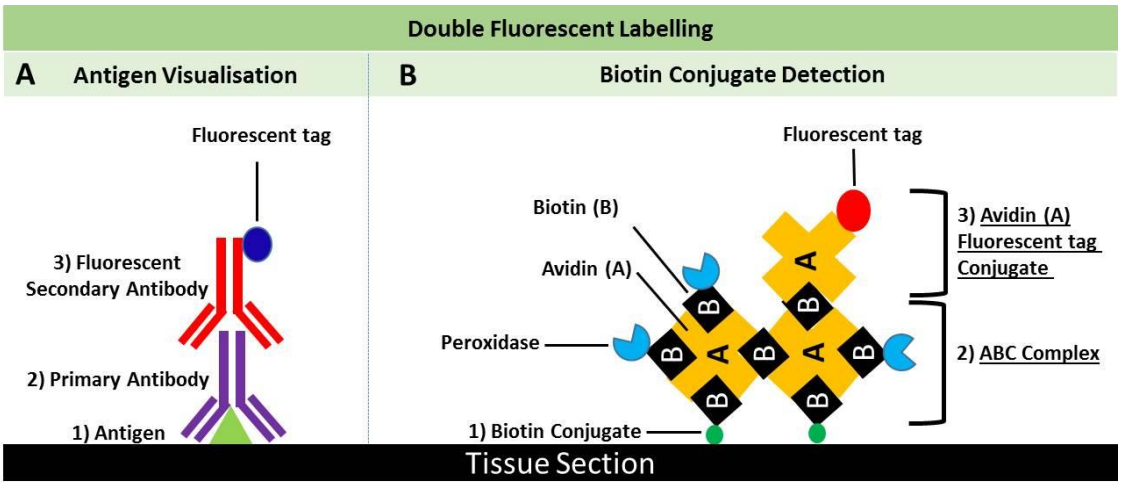

Figure 12: A diagram showing the steps of the process of double fluorescent labelling. A: 1) Antigen presentation. 2) Primary antibody incubation. 3) Incubation of secondary antibody conjugated with fluorescent tag. B: 1) Biotin conjugate presentation. 2) Incubation with ABC complex. 3) Incubation with avidin-fluorescent tag conjugate.

Other stains

BDA tracer detection: To detect corticospinal axons in injured rats, spinal cord and hindbrain sections were rehydrated and spread sections onto slides. Sections were dried and then fixed for 5 min in 4% FA/PB. Then they were placed in 0.1M PB, 50% acetone, 100% acetone and then 50% acetone before being transferred to PB and then moved to PB/BSA. Sections were then incubated with ABC peroxidase complex for 1 hour at room temperature and stained with DAB and H_2O_2. The reaction was enhanced by adding cobalt/nickel to the DAB mixture.

Endogenous peroxidase (EP) stain: For granulocyte visualisation sections were prepared as described in A, but omitting the step 5 and 6. Next, sections were incubated with 0.1% biotinylated tyramide (in 0.1M PBS) in 0.01% hydrogen peroxide for 10 minutes. Sections were then incubated with ABC peroxidase complex for 1 hour at room temperature. Sections were then stained with DAB and H_2O_2.

Blood samples: Blood samples taken from rats were spread onto a slide. Slides were left to dry and then mounted under a glass cover slip using vectashield with DAPI, to visualise cellular nuclei.

Spleen and livers: Sections were thawed and left to dry on glass slides. Sections were mounted under a glass cover slip using vectashield with DAPI, to visualise cellular nuclei.

Table 2: Summary of antibodies and avidin conjugates used.

		Dilution	Source
Primary Antibody	ATF3 (Rabbit polyclonal)	1:100	Santacruz Biotechnology
	c-Jun (Rabbit polyclonal)	1:200	Santacruz Biotechnology
	eGFP (Rabbit polyclonal)	1:500	Millipore, CA
	GFAP (Rabbit polyclonal)	1:6000	Dako, UK
	IBA1 (Rabbit polyclonal)	1:3000	Wako, Germany
	TCR (Rabbit polyclonal)	1:1000	Abcam, UK
Secondary Antibody	Anti-rabbit IgG-Cy3 produced in donkey	1:200	Jackson, UK
	Anti-rabbit IgG-Alexa flour 488 produced in goat	1:600	Life technologies
	Anti-rabbit IgG biotinylated secondary antibody made in goat	1:100	Vector, UK
Avidin conjugates	Avidin TEXAS red conjugate	1:1000	Jackson, UK
	Avidin AMCA conjugate	1:200	Jackson, UK

Stains were carried out by me and a BSc/MSc student.

Cellular and axonal quantifications

For cell and axonal quantifications a Nikon Eclipse E600 fluorescent/light microscope was used.

Rat motor cortex cell counts:

Light microscopy

Coronal sections through the PBS and Poly I:C injection site in the motor cortex were cut in the rostro-caudal direction at 30um thickness. Sections were immunostained for IBA1, GFAP, TCR, endogenous peroxidase, c-Jun or ATF3 to visualise, microglia, astrocytes, T-cells, granulocytes, c-Jun-positive or ATF3-positive nuclei, respectively. Cells or nuclei were counted, using four fields of a x40 objective, at the injection site, 0.5mm, 1mm, or 2 mm lateral to it. Four tissue samples were quantified per animal per stain. The mean counts of the four visual fields were calculated per location, i.e. at the injection site or lateral to it (Fig, 13). Then the mean per animal and then the mean of the experimental condition were calculated.

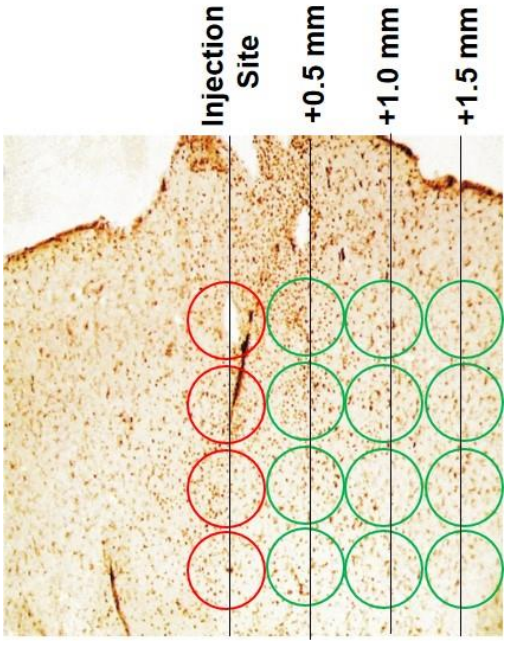

Figure 13: Cell quantifications in the motor cortex along the injection site (red circles) or lateral (+) to it (green circles). Quantifications were carried out at x40 objective lens. Not drawn to scale.

Fluorescent microscopy

Coronal sections through the eGFP-virus or GM-CSF-virus injection site in the motor cortex were cut in the rostro-caudal direction at 30um thickness. Sections containing eGFP-positive cells were fluorescently labelled with Cy3 and/or avidin-Amca for IBA1, GFAP, TCR, endogenous peroxidase, c-Jun or ATF3 to visualise, microglia, astrocytes, granulocytes, T-cells, c-Jun-positive or ATF3-positive nuclei, respectively. If visualisation of nuclei was required sections were additionally labelled with DAPI. Counts were performed on a fluorescent microscope using 340-380 filter for u.v. (DAPI or avidin-AMCA), 450-490 filter for green (eGFP), 510-560 filter for red (Cy3). Cells or nuclei were counted, using four fields of a x40 objective, at the injection site. Four tissue samples were quantified per animal per stain. The mean counts of the four visual fields were calculated at the injection site. The mean per animal and then the mean per experimental condition were subsequently calculated.

Rat pyramidal and corticospinal tract cell and axon counts

Cell counts

Light microscopy

Pyramids: Coronal sections trough the pyramids of rats injected with eGFP-virus or GM-CSF/eGFP-virus into the motor cortex were cut in a caudo-rostral direction at a 30um thickness. Sections through the pyramids were stained for microglia or astrocytes. Using one field at x40 objective lens, cells within the pyramids were counted. For every stain, three tissue samples five consecutive sections apart were quantified per animal. Mean cellular counts of the left or right pyramids were calculated per animal per experimental group.

Corticospinal tract: Spinal cords were dissected from cervical segment 1 to 8. Longitudinal horizontal sections through the spinal cords of animals injected with eGFP-virus or GM-CSF/eGFP-virus into the motor cortex were cut in an anterior-posterior direction at a 30um thickness. Sections through the spinal cord were stained for microglia or astrocytes. For every stain, three sections through the corticospinal tract, around 10 consecutive sections apart were quantified per animal. Using 13 fields of a x40 objective lens, cells within the left and right corticospinal tracts were counted caudal to cervical segment 1. The mean

number of cells counted per field calculated. Then the mean number of cells per animal and per experimental condition was calculated.

Axon counts

PYRAMIDS AND PYRAMIDAL DECUSSATION

Light microscopy

Pyramidal decussation: Coronal sections trough the pyramidal decussation of rats with corticospinal tract injury and injected with eGFP-virus or GM-CSF/eGFP-virus and BDA, 14 days prior to sacrifice, were cut in a caudo-rostral direction at a 30um thickness. Sections through the pyramidal decussation were stained for BDA. Using x40 objective lens, BDA-positive axons within the whole of the pyramidal decussation were counted. Four tissue samples five consecutive sections apart were quantified per animal. Mean BDA-positive axons counts in the pyramids per field were calculated, then per animal and subsequently per experimental group.

Fluorescent labelling

Pyramids: Coronal sections trough the pyramids of rats with corticospinal tract injury and injected with PBS/BDA or Poly I:C/BDA were cut in a caudo-rostral direction at a 30um thickness. Sections through the ipsilateral pyramid were stained for BDA using fluorescent avidin-Texas red. Using x40 objective lens, BDA-positive axons within the whole of the pyramidal were counted. Four tissue samples five consecutive sections apart were quantified per animal. The total BDA-positive axons counts in the pyramids were calculated per animal.

CORTICOSPINAL TRACT

Light microscopy

Corticospinal tract: Spinal cords were dissected from cervical segment 1 to 8. Longitudinal horizontal sections through the spinal cords of animals with corticospinal tract injury and injected with eGFP-virus or GM-CSF/eGFP-virus into the motor cortex were collected. Sections were cut in an anterior-posterior direction at a 30um thickness. Sections through the spinal cord were stained for BDA.

Fluorescent labelling

Corticospinal tract: Spinal cords were dissected from cervical segment 1 to 8. Longitudinal horizontal sections through the spinal cords of animals with corticospinal tract injury and injected with PBS/BDA or Poly I:C/BDA into the motor cortex were collected. Sections were cut in an anterior-posterior direction at a 30um thickness. Sections through the spinal cord were fluorescently stained to visualise BDA using avidin-Texas red, GFAP-positive astrocytes using Alexa flour 488 and nuclei using DAPI.

For corticospinal tracts analysed using both light and fluorescent microscopy, six sections through the corticospinal tract, around 10 consecutive sections apart were quantified per animal. Using a x40 objective lens BDA-labelled axons and retraction bulbs in the spinal cord, crossing a line on a microscope graticule grid every 0.5mm from 4.5mm above (rostral) to 4.5mm below (caudal) to the injury site were counted. The middle of the lesion site was taken as point zero. Corticospinal tract axon or retraction bulb counts were normalised for the success of anterograde labelling in each animal by comparison with the corresponding count of labelled axons in the pyramidal decussation or spinal axon counts, respectively.

Adult mouse striatum cell scoring or counts

Light microscopy

Coronal sections through the eGFP-virus or GM-CSF-virus injection site in the striatum were cut in the rostro-caudal direction at 30um thickness. Sections were immunostained for IBA1, GFAP, CD3, endogenous peroxidase and eGFP to visualise microglia, astrocytes, T-cells, granulocytes and eGFP-expressing cells. The injection site was evaluated using four fields of a x40 objective lens (Fig. 14). The injection site was given a score from 0-3 for granulocyte density, local reactive microglial density, spread of reactive microglia, phagocytic microglial density, amount of necrosis, and astrocyte activation. Alternatively, microglia, astrocytes, T-cells and eGFP-positive cells were counted along the injection site. Five tissue samples were quantified per animal per stain. The mean counts of the four visual fields were calculated. This mean was used to calculate a mean per animal and then a mean per experimental condition.

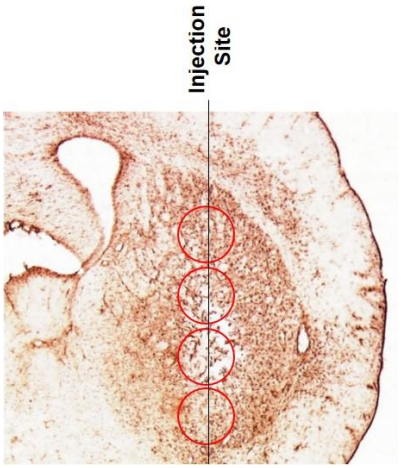

Figure 14: Cell quantifications in the striatum along the injection site (red circles). Quantifications were carried out at x40 objective lens. Not drawn to scale.

Neonate brain scoring

Light microscopy

Coronal sections through the hippocampus or lateral ventricles of neonate mice injected with eGFP-virus or GM-CSF-virus injections were cut in the rostro-caudal direction at 30um thickness. Four sections were collected per animal: two through the hippocampus or two through the lateral ventricle. Sections were immunostained for IBA1 or eGFP, to visualise, microglia or eGFP-expressing cells. Using two fields of a x40 times objective the amount of microglial activation or eGFP-expression was scored for each different area of the brain; cortex, white matter, septum, striatum, hippocampus, ventricular epithelium, choroid plexus and meninges. A score was given for each area of 0 to 3 for the level of microglial activation (0 being no cells transduced or no activated microglia and 3 being the majority of cells transduced and lots of activated or phagocytic microglia). Mean scores of the two visual fields were calculated per location. This mean was used to calculate a mean per slide, per animal and then an mean per experimental condition.

Cellular quantifications were performed by me or a BSc/MSc student

Fluorescent and light microscopy image acquisition

A Sony 3CCD colour video camera (AVT-Horn, Aachen, Germany) was used to obtain 8-bit digital images of the antibody stained sections. Digital micrographs of fluorescently labelled sections were taken using Leica TCS SP2 confocal laser microscope with x20 or x40 objective for illustrations. The software used was Application Suite 2.6.0.7266 (Leica). Images were further edited using Optimas 6.2 software (Bothwell, WA).

Image acquisitions were performed by me.

Statistical analysis

When two groups were compared a two-tailed, unpaired Student's t-test. When more than two groups were evaluated, statistical analysis was done using repeated measures ANOVA or one-way ANOVA followed by post-hoc Tukey or Bonferroni corrected test.

Statistical analyses were performed by Prof Gennadij Raivich or myself.

CHAPTER THREE

Perineuronal Poly I:C can be protective and proregenerative in the injured central and peripheral nervous system

Introduction

Peripheral nervous system (PNS) axons, such as those of the facial nerve, regenerate spontaneously after injury, a process that is accompanied by an inflammatory response around the neuronal cell bodies. Central nervous system (CNS) axons such as the corticospinal tract, however, lack both this spontaneous regenerative capacity and the accompanying perineuronal inflammation. However, when inflammation is experimentally induced around the cell bodies of neurons that project into the CNS there is an increase in axonal regeneration following injury. Activating macrophages in the dorsal root ganglion (DRG) via injection of Corynebacterium increases regeneration following dorsal rhizotomy (central axotomy) (Lu and Richardson, 1991). Similarly, injection of zymosan or injury to lens in the eye produces greater retinal ganglion cell (RGC) survival and more vigorous axonal regeneration following optic nerve crush (Leon et al., 2000).

Polyinosinic:polycytidylic acid (Poly I:C), is a synthetic double stranded RNA which stimulates innate immunity through Toll-Like Receptor 3 (TLR3) in macrophages, dendritic cells, microglia and astrocytes (Alexopoulou et al., 2001; Town et al., 2006). Activation of TLR3 signalling has been suggested to induce the strongest pro-inflammatory response in human microglia promoting the secretion of high levels of IL-12, TNF-α, IL-6, CXCL-10, and IL-10, and the expression of IFN-ɣ (Field et al., 2010; Jack et al., 2005). In vivo delivery of Poly I:C is associated with the expression of ionised calcium-binding adaptor molecule-1 (IBA1) in microglia (Patro et al., 2010). Like microglia, primary astrocyte cultures treated with Poly I:C induces a strong proinflammatory response (increased expression of inflammatory cytokines) (Bsibsi et al., 2002; Bsibsi et al., 2006; Carpentier et al., 2005; Farina et al., 2005; Scumpia et al., 2005) and the increased expression of glial fibrillary acidic protein (GFAP)

(Brahmachari et al., 2006). Poly I:C can also interact with Retinoic acid Inducible Gene-1 (RIG-1) receptor which is expressed in neurons (Peltier et al., 2010).

In addition to the immune role, Poly I:C intraventricular injections in to the rat CNS has been associated with decreased motor activity (Patro et al., 2010). Intranigral injections trigger nigrostriatal dopaminergic degeneration which is associated with the cytoplasmic mislocalization of neuronal TDP-43, a change normally observed following peripheral nerve axotomy of motor neurons (Moisse et al., 2009). Furthermore, there is evidence that Poly I:C may be inhibitory to regeneration in vitro. It produces a strong and long-lasting inhibition of neurite growth by hippocampal neurons and DRG neurons, probably by acting on TLR3 expressed on neuronal growth cones (Cameron et al., 2007). However, whether its effect on stimulating microglia around the neuronal cell body may overcome its direct effects on the growth cones of axotomised neurons has not been studied. I therefore decided to stimulate microglia in vivo around injured corticospinal neurons, whose axons do not normally regenerate, and facial motor neurons, whose axon regenerate vigorously after injury.

This chapter is divided into three parts: Part 1 explains the preliminary work undertaken to find the concentration of Poly I:C required for optimal microglial activation. Part 2 evaluates the time-dependent effects of Poly I:C on inflammation. Finally, Part 3 demonstrates the effect of Poly I:C on the regeneration of corticospinal and facial motor neuron axons.

Results

Part 1: Titration of Poly I:C

Poly I:C produces a dose dependent and widespread activation of microglia in rat motor cortex

Microglia, the macrophages of the brain, become activated in response to injury. They undergo a sequence of changes in response to neuronal injury. These can be divided into stages: resting microglia (Stage 0), state of alert (Stage 1), homing and adhesion (Stage 2), phagocytosis in the presence of neuronal cell death (Stage 3a), and bystander activation of surrounding non-phagocytic microglia

(Stage 3b) (Raivich et al., 1999). The first step in this study was to evaluate the effects of Poly I:C on the normally dormant cortical microglia.

Rats received injections into the left motor cortex of one of three different concentrations of Poly I:C: 0.1 mg/ml (n=3), 1 mg/ml (n=3) or 5.6 mg/ml (n=3). As an internal control, PBS was injected in the contralateral motor cortex of each animal. To analyse effects on microglia, coronal sections through the motor cortex were immunostained for IBA1, a calcium-binding protein specifically expressed by mononuclear phagocytes (Imai et al., 1996) that is upregulated in activated macrophages and microglia (Ito et al., 1998).

Three days following injection, coronal sections through the Poly I:C-injected motor cortex (Fig. 1B, D & F) demonstrated a higher level of IBA1 immunoreactivity and microglial density than the PBS injected cortex (Fig. 1A, C & E). This effect was found at the injection site and 2mm beyond. Following Poly I:C injection, microglial morphology changed from the ramified form, typical of the quiescent/resting state (Fig. 1A-insert), to the alert/activated type as evident by their proximal processes becoming shorter and thicker (Fig. 1B-insert) and to the phagocytic state with a rounded amoeboid shape and loss of ramification of their distal processes (Fig. 1F-insert). These effects were dose-dependent; microglial morphology at the injection site was largely resting at 0.1 mg/ml Poly I:C concentration, activated at 1mg/ml and phagocytic at 5.6 mg/ml. Additionally, some necrosis could be observed in the motor cortex of animals treated with the 5.6mg/ml Poly I:C (not shown in figure), but this was absent in animals treated with 1mg/ml, despite the presence of microglial activation. Microglia in the PBS-injected motor cortex were mainly in the ramified, resting state (Fig. 1A, C & E inserts), with a few phagocytic microglia/macrophages directly at the site of injection.

To quantify the level and spread of microglial activation following Poly I:C treatment, microglia were counted in layers II to V of the motor cortex at the injection site and 0.5mm, 1mm, and 2mm lateral to it (Fig. 2). The motor cortex was evaluated using x40 objective lens.

The effect of Poly I:C on microglial numbers was dose-dependent, and greatest close to the injection site. In comparison to the PBS side (Fig. 2A-D blue bars), cortex injected with 1mg/ml (Fig. 1C & D; Fig. 2A-D-middle red bars) showed significantly higher numbers of microglia per field up to 1mm away from the injection site ($p<0.004$, in a paired student t-test; post hoc to a mixed measures ANOVA, Bonferroni corrected). Although higher numbers of microglia were also found in animals treated with 5.6mg/ml Poly I:C (Fig. 1E & F; Fig. 2-right red bars) and 0.1mg/ml Poly I:C (Fig. 1E & F; Fig. 2-left red bars) this did not reach statistical significance compared to PBS-injected cortex.

After averaging across all the distances (Fig. 2E), a dose response emerged. Rats injected with 5.6 mg/ml Poly I:C (Fig. 1F; Fig. 2E-right red bar) had 162±18 (M±SEM) microglia per visual field, which was significantly higher than 55±19 microglia sampled following 0.1 mg/ml Poly I:C (Fig. 1B; Fig. 2E-left red bar) ($p<0.02$: post hoc comparison after a mixed measures ANOVA: Bonferroni corrected). The PBS-injected motor cortex had 53±3 IBA1-positive microglia contralateral to an injection of 5.6mg/ml Poly I:C (Fig. 1E; Fig. 2E-blue right bar), which was mildly elevated compared to 31±3 microglia found contralateral to injections of 0.1mg/ml Poly I:C (Fig. 1A; Fig. 2E-blue left bar) ($p<0.02$: post hoc comparison after a mixed measures ANOVA: Bonferroni corrected). This shows that Poly I:C at 5.6mg/ml acted diffusely; having an effect on microglia even in the contralateral motor cortex.

Figure 1: Poly I:C produces microglial activation in rat motor cortex in a dose-dependent manner. Coronal brain sections of IBA1-immunostained rat motor cortex through the PBS injection sites (A,C,E) and Poly I:C injection sites (B,D,F) and at concentrations 0.1mg/ml (B), 1.0mg/ml (D), or 5.6mg/ml (F). Enhanced IBA1 immunoreactivity is present in the Poly I:C-injected cortex compared to the contralateral PBS-injected side. Inserts show at higher magnification the morphological changes in microglia from resting (B), to reactive (D) to phagocytic states (F). Only resting (A) or reactive (C-E) microglia were found in PBS-injected cortex.

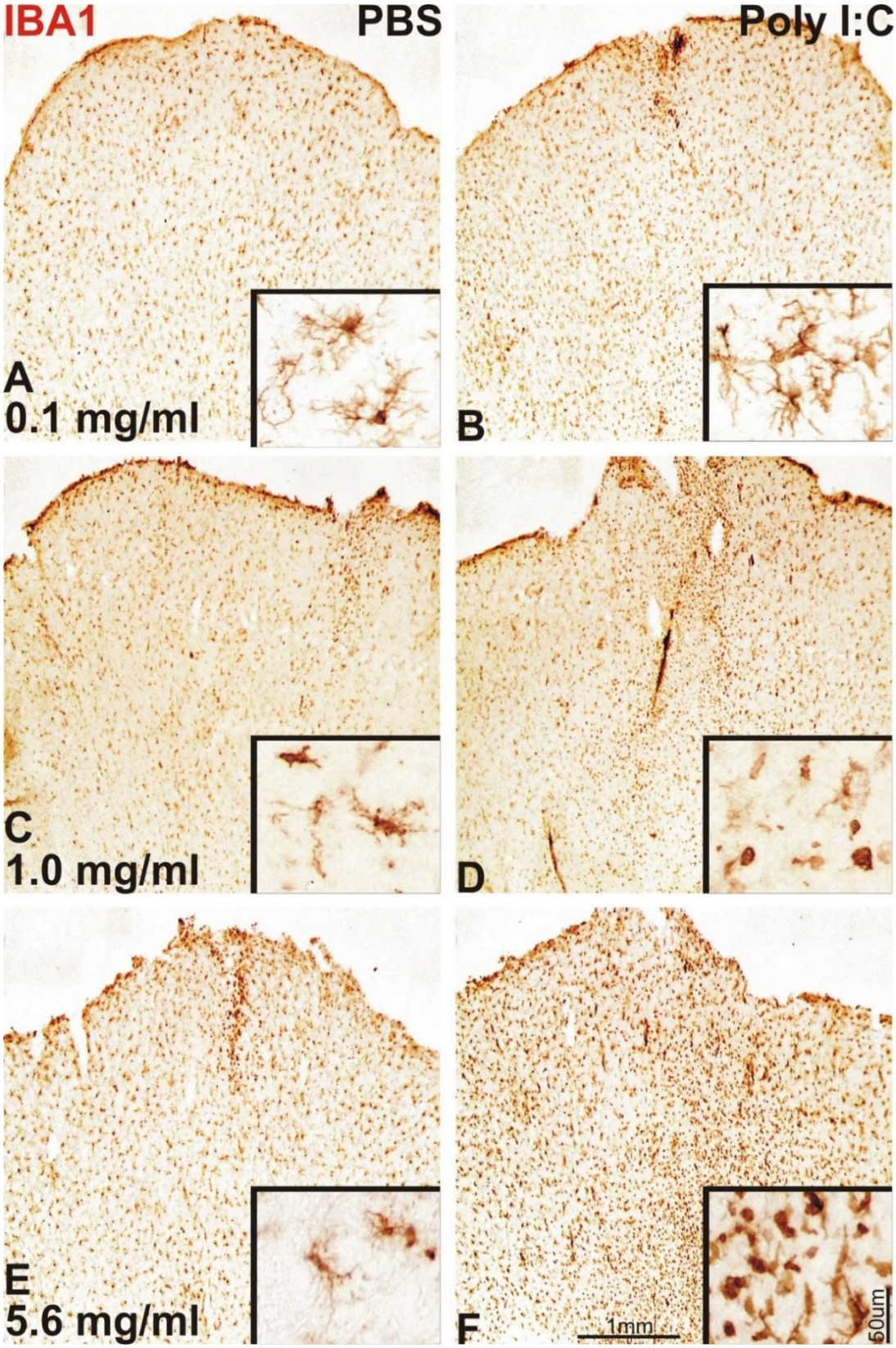
IBA1
PBS
Poly I:C
A
0.1 mg/ml
B
C
1.0 mg/ml
D
E
5.6 mg/ml
F
1mm
50um

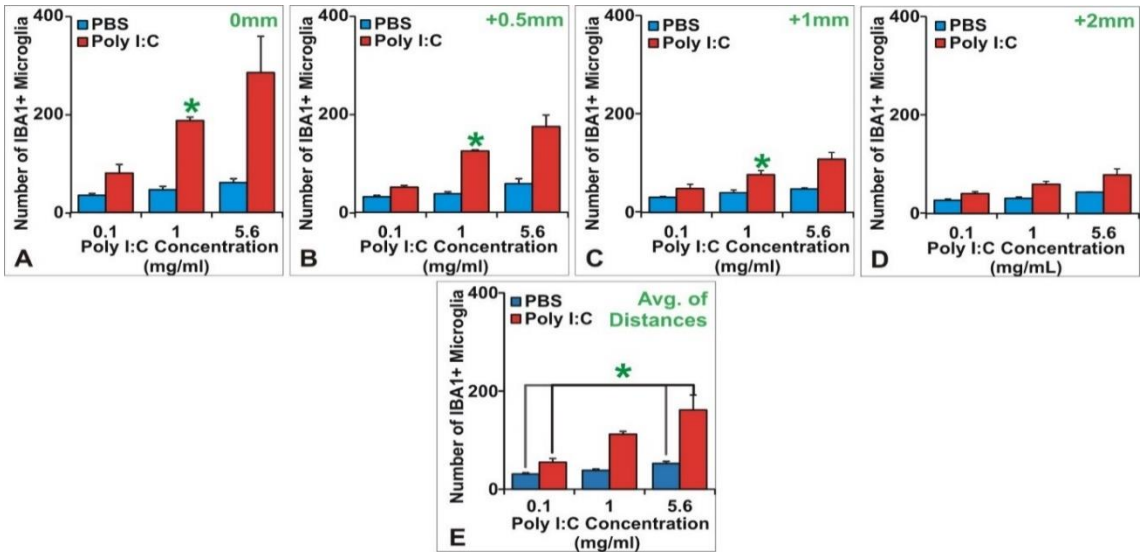

Figure 2: Poly I:C injection into motor cortex increases microglial density in a dose-dependent manner. Graphical representation of microglial numbers at varying distances away from the Poly I:C (red bars) and PBS (blue bars) injection sites, n=3 for each concentration. **A-D** Histograms show mean number of Iba1 positive (+) microglia at (A) 0mm (injection site), (B) 0.5mm, (C) 1mm and (D) 2mm (+) lateral from the injection site. **E:** Average microglia number across all distances (0mm to 2mm). (*) denotes statistical significance following Bonferroni corrected post hoc comparisons to a mixed measures ANOVA. Bars and error bars represent, mean and standard error of the mean (SEM).

Poly I:C produces astrocyte activation in the rat motor cortex

Protoplasmic astrocytes that reside in the grey matter become activated in response to injury or inflammation resulting in an increased expression of GFAP (Raivich et al., 1999; Tetzlaff et al., 1988a) and a change in morphology so that they become more fibrous with characteristically long extended processes (Graeber and Kreutzberg, 1986; Graeber et al., 1989; Kreutzberg et al., 1989; Raivich et al., 1999). Here we characterised the effect of increasing doses of Poly I:C on astrocytes in the rat motor cortex.

Three days following injection of Poly I:C into the motor cortex (Fig. 3B, D &F), GFAP immunoreactivity was higher than in the PBS-injected side (Fig. 3A, C & E). The increase in astrocyte reactivity was widespread, being evident more than 3mm away from the injection site. High magnification images of Poly I:C-injected cortex showed that GFAP was more strongly expressed in the cell bodies of astrocytes than was the case in the PBS-injected cortex (Fig. 3-inserts). Additionally, the cell processes appeared longer in the Poly I:C-injected animals than the PBS.

The number of GFAP-positive astrocytes at the injection sites and 2mm lateral to it, counted using a x40 objective magnification, was greater following injection of Poly I:C at 0.1, 1 and 5.6 mg/ml (Fig. 4A-D red bars) than in the contralateral, PBS-injected cortex (Fig. 4A-D blue bars). However, this increase was not significant ($p>0.004$ post hoc comparison after a mixed measures ANOVA: Bonferroni corrected).

Averaging across all the distances from the injection site (Fig. 4E), Poly I:C significantly increased the number of astrocytes in the motor cortex. 1mg/ml Poly I:C-injected cortex had 43±3 GFAP-positive astrocytes per field and 5.6mg/ml had 40±3 astrocytes; both concentrations were significantly higher than the 23±3 astrocytes seen following 0.1mg/ml ($p<0.02$: post hoc comparison after a mixed measures ANOVA: Bonferroni corrected). The number of astrocytes in the PBS-injected motor cortex (blue bars), did not significantly increase when rats received a contralateral injection of Poly I:C at 5.6mg/ml, 1mg/ml or 0.1mg/ml doses ($p>0.02$: post hoc comparison after a mixed measures ANOVA: Bonferroni corrected).

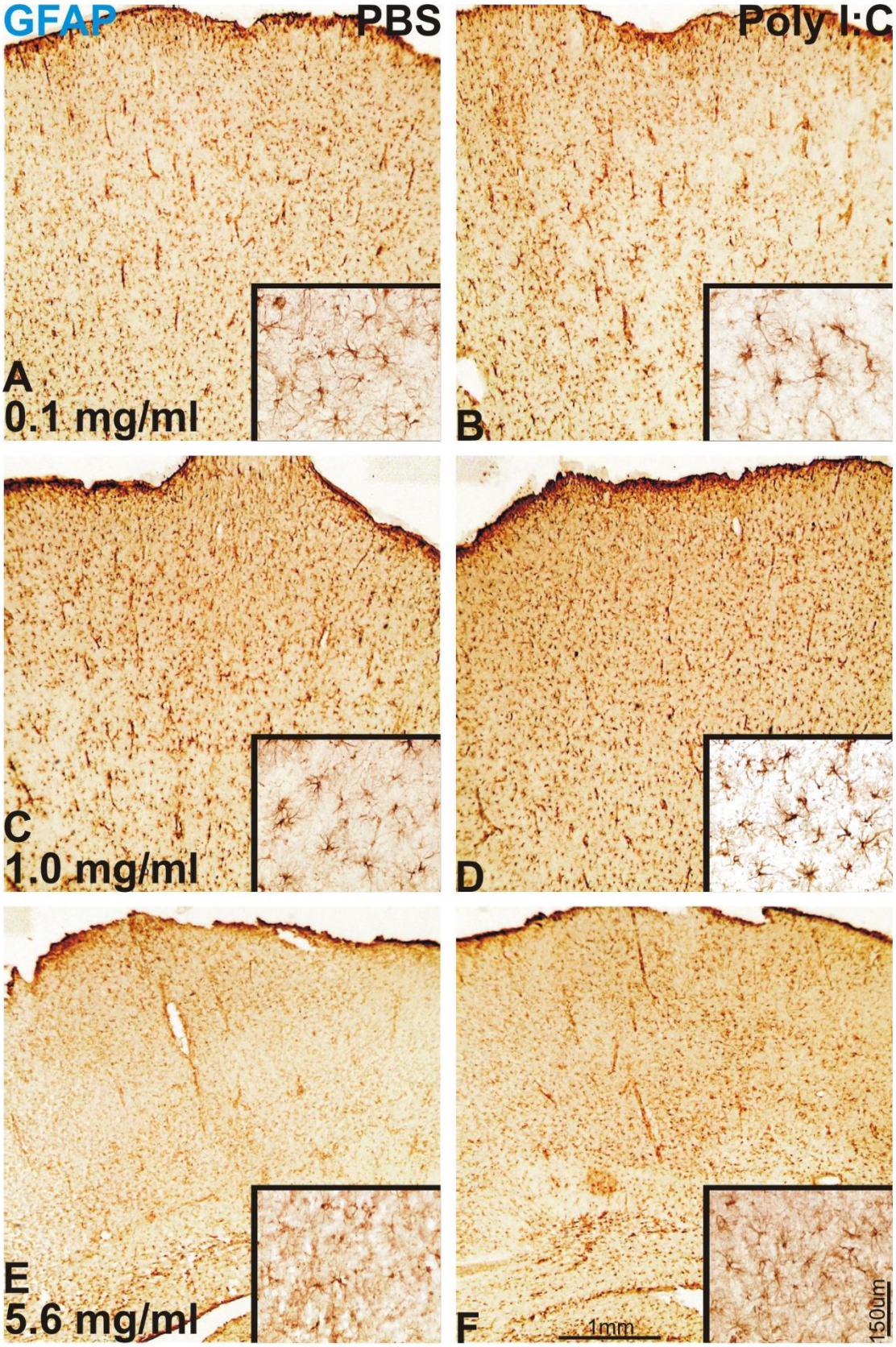

Figure 3: Poly I:C increases GFAP immunoreactivity in rat motor cortex. Rats were injected with poly I:C in one hemisphere and PBS in the contralateral hemisphere. Coronal sections through the PBS-injected (A,C,E) and Poly I:C-injected (B,D,F) motor cortex at doses of 0.1mg/ml Poly I:C (B), 1.0mg/ml Poly I:C (D) and 5.6 mg/ml (F). Inserts show astrocytes with greater GFAP+ expression in their cell bodies following Poly I:C rather than PBS injection.

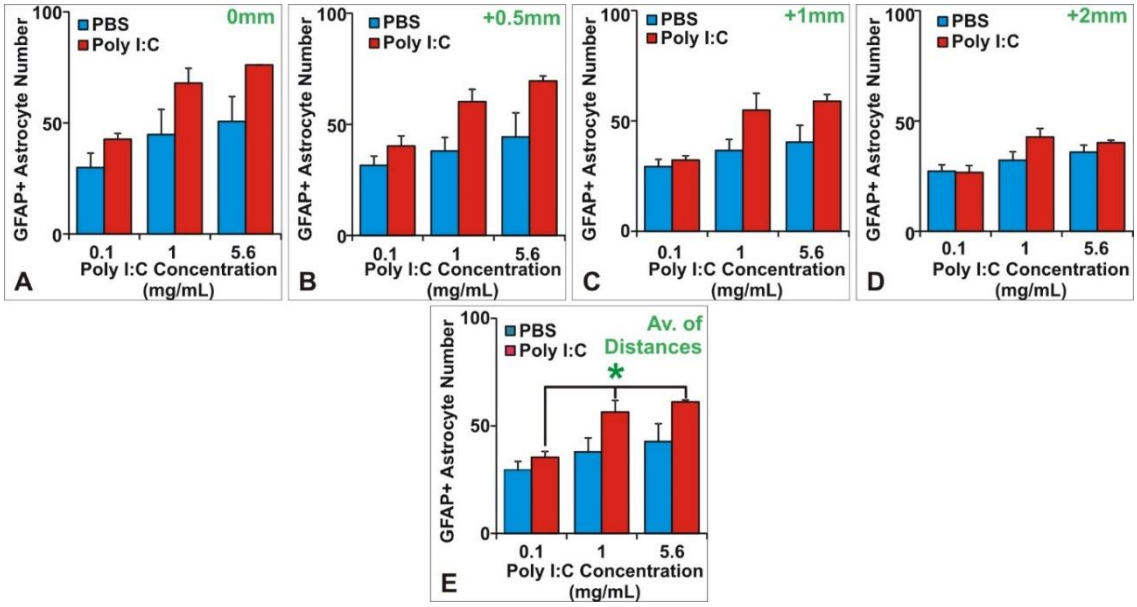

Figure 4: Poly I:C injection into motor cortex increases astrocyte density in a dose-dependent manner. Graphical representation of astrocyte numbers at varying distances away from the Poly I:C (red bars) and PBS (blue bars) injection sites, n=3 for each concentration. A-D Histograms show mean number of astrocytes at (A) 0mm (injection site), (B) 0.5mm, (C) 1mm and (D) 2mm (+) lateral to the injection site. E: Average astrocyte number across all distances (0mm to 2mm). (*) denotes statistical significance following Bonferroni corrected post hoc comparisons to a mixed measures ANOVA. Bars and error bars represent, mean and standard error of the mean (SEM).

Part 2: Time Course

Microglia activation persists up to 14 days following Poly I:C injection into motor cortex

The overall aim of the project was to determine if Poly I:C-mediated perineuronal inflammation is pro-regenerative. Here we examined the timing of microglial activation following cortical injections of Poly I:C. A dose of 1mg/ml was chosen, as it causes microglial activation without tissue damage, as shown in the previous section. Rats were injected with 1mg/ml Poly I:C in the right motor cortex and with PBS on the contralateral side, and were allowed to survive 3 (n=3), 7 (n=3), or 14 (n=4) days following injections.

Compared to PBS-injected cortices (Fig. 5-right column), the Poly I:C- injected (Fig. 5-left column) cortices demonstrated higher levels of IBA1-positive microglia at days 3 (Fig. 5A-B), 7 (Fig. 5C-D) and 14 (Fig. 5E-F). However, Poly I:C-treated cortices showed a gradual decrease in IBA1 immunoreactivity from day 3 to 14 (Fig. 5-left column). High magnification images at day 3 revealed that microglia

in the Poly I:C-injected cortices had a phagocytic morphology (Fig. 5B-inserts) whereas by day 7 the microglia had a reactive morphology(Fig. 5D-inserts). On the other hand, by day 14 after Poly I:C injection (Fig. 5F-inserts) microglia returned to a more resting type, but retained a higher IBA1 immunoreactivity. The PBS-treated cortices had resting microglia at all time-points.

Using a x40 objective the number of IBA1-positive microglia were counted in four fields down the PBS (Fig. 6A-blue bars) and Poly I:C (Fig. 6A-purple bars) injection sites. In the Poly I:C-injected motor cortex there was a peak in the number of activated microglia per field at day 3 (149±23 microglia per field) which was significantly higher than the numbers counted at day 7 (73±3) and day 14 (46±2) ($p<0.05$; post hoc comparison to a mixed measures ANOVA). However, in the PBS injected cortex microglial numbers remained constant across all time points; at day 3 there were 28±3 microglia per field, at day 7 there were 25±2 and at day 14 post injection 28±2 were found ($p<0.05$; post hoc comparison to a mixed measures ANOVA). Compared to PBS, Poly I:C injections resulted in significantly higher number of IBA1-positive microglia at all time-points. Inflammation remained up to 14 days following Poly I:C injection (the maximum time examined), as almost twice the number of activated microglia were still present at day 14 compared with the contralateral side ($p<0.01$; Bonferroni corrected post hoc comparison following a repeated measures ANOVA).

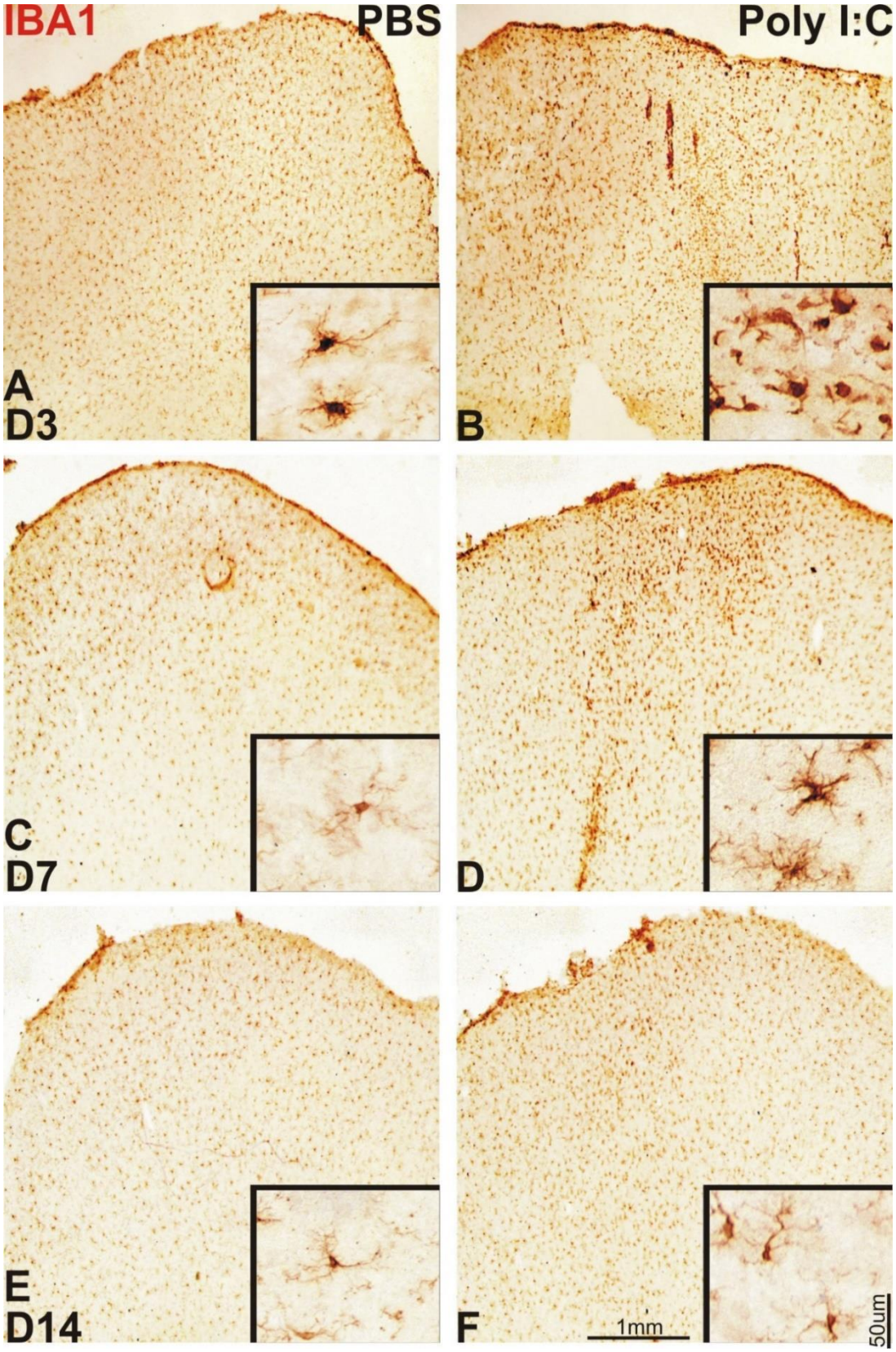

Figure 5: Inflammation persists up to two weeks following Poly I:C injection to the motor cortex. Coronal sections immunostained for IBA1 at 3 days (A-B), 7 days (C-D) and 14 days (E-F) after PBS (A,C,E) and Poly I:C (B,D,F) injections to the motor cortex. Poly I:C-treated cortex showed greater IBA1 intensity than PBS-treated cortex at day 3 (A-B), 7 (C-D) and 14 (E-F); this difference peaks at day 3. (Inserts show reactive microglia gradually returning to the resting state following Poly I:C injections whereas microglia were in the resting state at all time-points following PBS iniections.

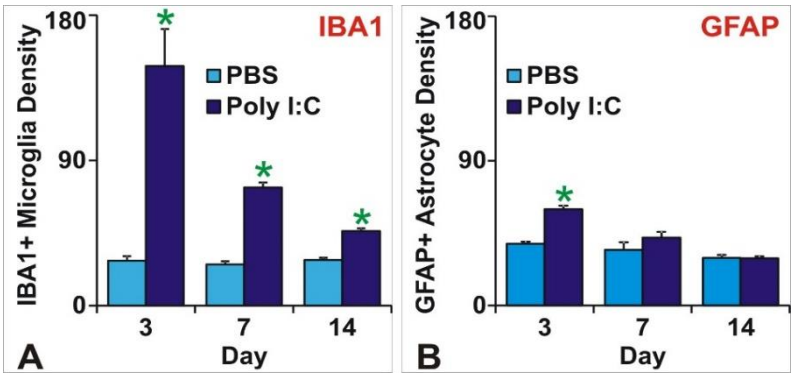

Figure 6: Quantitation of microglia and astrocyte numbers following PBS or Poly I:C injections into the rat motor cortex. **A-B:** Histograms representing the number of microglia per field (A) or astrocytes per field (B) at 3 (n=3), 7 (n=3) and 14 (n=4) days post injection. (*) $p<0.01$ in a Bonferroni corrected post hoc comparison following a mixed measures ANOVA. Bars and error bars represent the mean and standard error of the mean (SEM).

Poly I:C-induced astrocyte activation is transient

To evaluated how long astrocyte activation was maintained following Poly I:C injections, sections through the rat motor cortex were collected at 3 (n=3), 7 (n=3) and 14 (n=4) days after injection of Poly I:C (1mg/ml) into the right motor cortex and PBS into the contralateral cortex. Coronal brain sections were subsequently immunostained for the astrocyte marker GFAP.

The Poly I:C-injected cortices were always more strongly GFAP-immunoreactive than the contralateral PBS-injected cortices. There was a strong increase in GFAP reactivity following Poly I:C injections at day 3 (Fig. 7A-B & inserts), and moderate at day 7 (Fig. 7C-D & inserts) and 14 (Fig. 7E-F & inserts). At high magnification it could be seen that astrocytes had darkly stained cell bodies and elongated processes at 3 days (Fig. 7B-insert) post Poly I:C delivery; thereafter GFAP intensity at the cell body and the size of the processes appeared to decrease (Fig. 7F-inserts). GFAP immunoreactivity of astrocytes remained broadly similar at days 3-14 post injection.

The number of GFAP positive astrocytes per field using a 40x objective were quantified at the Poly I:C and PBS (control) injection sites. The number of GFAP positive astrocytes per field significantly decreased from days 3 to 14 ($p<0.05$; post hoc comparison to a mixed measures ANOVA) in Poly I:C-injected cortices (Fig. 6B-purple bars). Similarly, a time dependent decrease in astrocyte number

per field was seen in the PBS-injected cortices ($p<0.05$; post hoc comparison to a mixed measures ANOVA) (Fig.6B-blue bars).

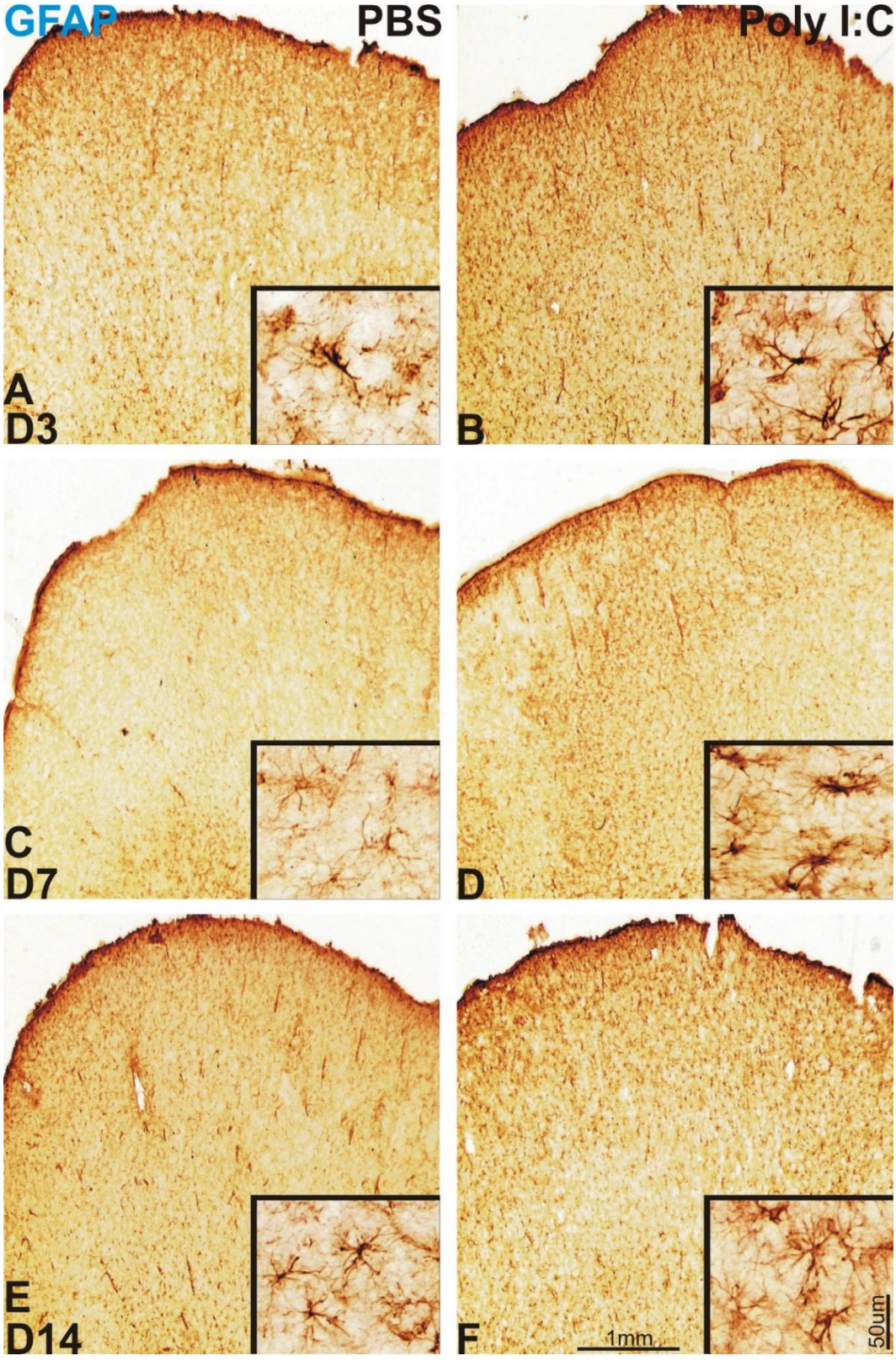

Figure 7: Astrocytes were temporarily activated following Poly I:C delivery to the motor cortex. Coronal sections stained for GFAP 3 days (A-B: D3), 7 days(C-D: D7) or 14 days (E-F: D14) after injection of PBS (left column) or Poly I:C (right column) into the motor cortex. Notice that in comparison to PBS, there is strong GFAP expression following Poly I:C at day 3 (B) and moderate at day 7 (D) and 14 (F). (A-B) Inserts demonstrate astrocytes at day 3 (A-B) with highly stained cell bodies and extended processes, at day 7 (C-D) and 14 (E-F) the intensity and sizes of processes decreases.

Unlike the persistent microglia activation found following Poly I:C delivery, astrocyte activation was transient. At day 3 Poly I:C had 60±2 GFAP-positive astrocytes per field, which was higher than the 39±1 astrocytes found in the PBS-injected motor cortex ($p<0.01$; post hoc to a mixed measure ANOVA). Comparisons between PBS-injected and Poly I:C-injected cortices were not significant at days 7 and 14 (Fig. 6B).

T-cells are recruited to the motor cortex by three days post Poly I:C treatment

To further characterise the inflammatory response to Poly I:C, coronal brain sections of rats injected with Poly I:C (1mg/ml) and PBS to the right and left hemispheres respectively, were collected at 3 (n=3), 7 (n=3) and 14 (n=4) days post injection. Sections were stained for endogenous peroxidase to identify granulocytes or T-cell receptor antibody (TCR) to identify T-cells. Granulocytes or T-cells were counted in four fields using x40 objective, starting near the surface of the cortex and passing progressively deeper. No granulocytes were observed at any time points studied following PBS-injection or Poly I:C-injection.

When sections were evaluated for the presence of T-cells, the Poly I:C-injected cortex had 7±2 T-cells per field at day 3 (Fig. 8B & C), which was significantly higher than 1±0.1 T-cells found in the PBS-treated cortices (Fig. 8A) ($p=0.02$, post hoc comparison following a mixed measures ANOVA; Bonferroni corrected). All other comparisons were not significant. The Poly I:C-injected cortices (Fig. 8C-purple bars) showed a peak in T-cell recruitment that sharply decline by day 7 and 14 ($p<0.05$; post hoc comparison to a mixed measures ANOVA). While the PBS-injected cortices (Fig. 9C-blue bars) had some T-cell influx at day 3, T-cells were absent at subsequent time points.

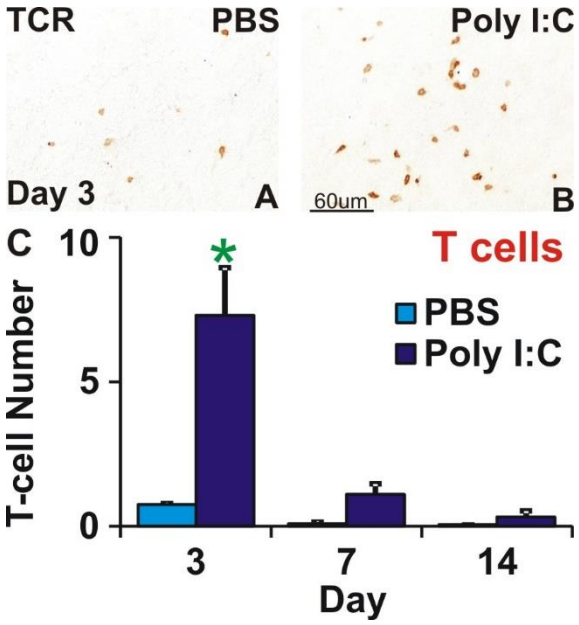

Figure 8: Poly I:C delivery to the rat motor cortex is associated with transient T-cell recruitment. **A-B:** Coronal brain sections through the motor cortex of rats 3 days post PBS (A) and Poly I:C (1mg/ml) (B) injections, stained for T-cells using T-cell receptor antibody. **C:** Histogram representing the mean number of T-cells quantified per field using a x40 objective, at 3 (n=3), 7 (n=3) and 14 (n=4) days following PBS injection to the left cortex (blue bars) and Poly I:C injection to the right cortex (purple bars). The Poly I:C-injected cortex has significantly higher T-cells per field at day 3 than the PBS-injected cortex. (*) $p<0.02$ in a post hoc comparison to a mixed measures ANOVA; Bonferroni corrected. Bars and error bars represent mean and standard error of the mean (SEM), respectively.

Poly I:C-induced inflammation does not cause death of corticospinal neurons

In vitro and in vivo models have shown that Poly I:C can be toxic when applied to neuronal cultures or brain. To find out whether Poly I:C at 1mg/ml was associated with neuronal death four rats received PBS and Poly I:C (1mg/ml) injections to the left and right motor cortex, respectively. Corticospinal (CST) neurons were retrogradely labelled with fluorogold from the fourth cervical segment of the spinal cord. Sections through the motor cortex containing fluorogold-labelled corticospinal neurons were fluorescently labelled for IBA1 antibody to visualise microglia. Rats survived for seven days post-surgery.

Quantification of fluorogold-positive CST neurons in layer V of the motor cortex and neighbouring IBA1-positive microglia were carried out using a x20 objective. The Poly I:C treated group (Fig.9-red bar) had 178±15 IBA1 positive microglia per visual field, which was significantly higher than 109±11 found in the PBS group (Fig.9- yellow bar) (paired samples student t-test; $p<0.05$). However, no

difference between Poly I:C-injected (110.3±7.3) (Fig. 11-red bar) and PBS-injected (96.3±9.3) cortices in the number of fluorogold labelled CST neurons per field (Fig. 11-red bar: paired samples student t-test; p>0.05).

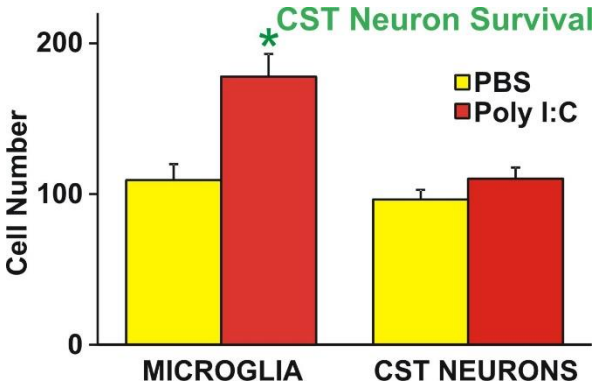

Figure 9: Poly I:C-mediated inflammation does not cause neuronal cell death. Histogram showing the mean number of IBA1-positive microglia and fluorogold-positive corticospinal tract neurons (CST) counted per field following injection of PBS (yellow bars) and Poly I:C (red bars) into the motor cortex. Rats (n=4) survived 7 days post-surgery. Notice that Poly I:C and PBS have similar number of CST neurons even though there is greater microglia density in the Poly I:C-injected cortex (*) p<0.05 significance following a paired samples T-test. Bars and error bars represent the mean and standard error of the mean (SEM), respectively.

Part 3: Regeneration experiments

Spinal Cord Injury

Poly I:C has a protective effect on the corticospinal tract following injury

Since Poly I:C at 1mg/ml causes microglial activation with no significant cytotoxicity, we tested its effects on the regeneration of corticospinal axons in injured cervical spinal cord. Rats were injected with a mixture of BDA (biotinylated dextran amine) and Poly I:C (Poly I:C/BDA: n=4) or BDA and PBS (PBS/BDA: n=3) into the motor cortex contralateral to a unilateral transection of the dorsolateral spinal cord, which injured the dorsal and lateral corticospinal tract (CST) at C4. The animals were allowed to survive 14 days after surgery. Axons in the pyramids and in the cervical spinal cord were visualised by fluorescent labelling of BDA.

BDA-positive CST axons in transverse sections of the pyramids were counted using two fields of a x40 objective. The Poly I:C-injected group had 252±32 BDA-labelled axons per field (Fig. 10-blue bar), which was not significantly different

from the PBS-injected group that had 288±32 per field (Fig. 10-grey bar) (unpaired student t-test; p>0.05). This result shows that there was similar success in the anterograde labelling of the CST in Poly I:C-injected and PBS-injected groups.

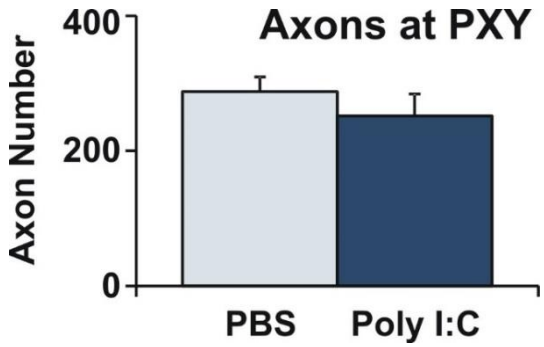

Figure 10: CST axonal density at the pyramids is the same following PBS or Poly I:C injections into the motor cortex. Histogram representing the mean number of BDA positive axons per visual field in the pyramids (PXY) of rats injected with PBS (n=3; grey bars) or Poly I:C (n=4; blue bars). Cortical injections were contralateral to a C4 corticospinal tract injury. There was no difference between PBS and Poly I:C groups: p>0.05 unpaired student t-test.

Longitudinal horizontal sections through the spinal cord were stained for astrocytes (GFAP; Fig. 11A&B in green) to visualise the injury site, and BDA to visualize CST axons (Fig. 11A&B in red). In the corticospinal tract of both Poly I:C (Fig. 11B) and PBS (Fig. 11A) injected groups, there was evidence of successful BDA axonal labelling rostral to the injury site. Axons can be seen to reach the injury site in both Poly I:C and PBS groups, with an apparent higher density of BDA axons in the Poly I:C injected group than PBS.

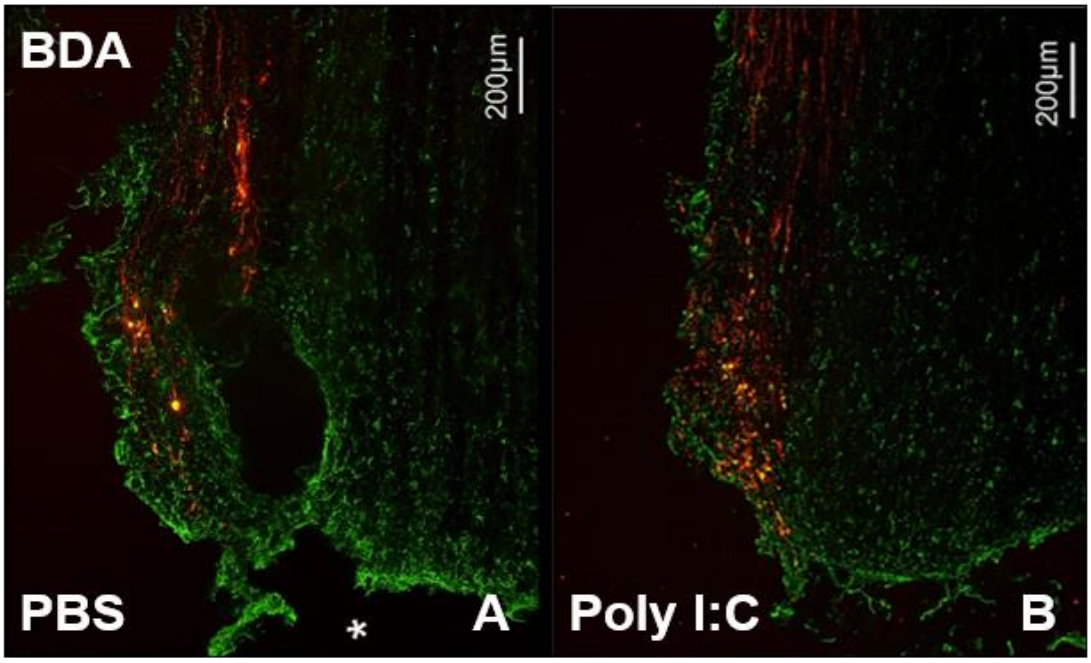

Figure 11: The effect of Poly I:C on corticospinal axons after injury. **A-B:** Micrographs show longitudinal horizontal sections through the spinal cord of rats with a right C4 corticospinal tract injury, which received a PBS/BDA (A) or Poly I:C/BDA (B) injection to the motor cortex, contralateral to the injury site. The absence of astrocytes (green) permit identification of the injury site (*) at the bottom of each image and BDA (red) show axons of the corticospinal tract.

The number of BDA-labelled axons and retraction bulbs, were quantified at the corticospinal tract injury site (0mm), rostrally (-4.5mm to -0.5mm), and caudally (0.5mm to 4.5mm) to it using a x40 objective (Fig. 12). Corticospinal tract axonal counts in the spinal cord were normalised for the success of anterograde labelling in each studied animal with their corresponding count of labelled axons in the pyramid. Higher numbers of BDA-positive axons were found in the spinal cord of Poly I:C-injected rats (Fig. 12- pink bars) compared to PBS-injected controls (Fig. 12- blue bars) at the majority of distances rostral to the injury site. However, this effect was not significant for any individual distance from the injury site ($p<0.05$; in an unpaired student T-test). No axons were found in the dorsal corticospinal tract caudal to the injury site in both groups.

However, there was an overall effect of Poly I:C treatment independent of distance from the injury site. The average number of axons at all distances rostral to the injury site was over 30% greater in the Poly I:C-treated group (Fig. 12- insert pink bars) compared to PBS-treated controls (Fig. 12- insert blue bars)

(p<0.05; in an unpaired student T-test). This suggest that cortical injections of Poly I:C preserves a higher number of axons in the dorsal corticospinal tract within the cervical spinal cord after spinal cord injury.

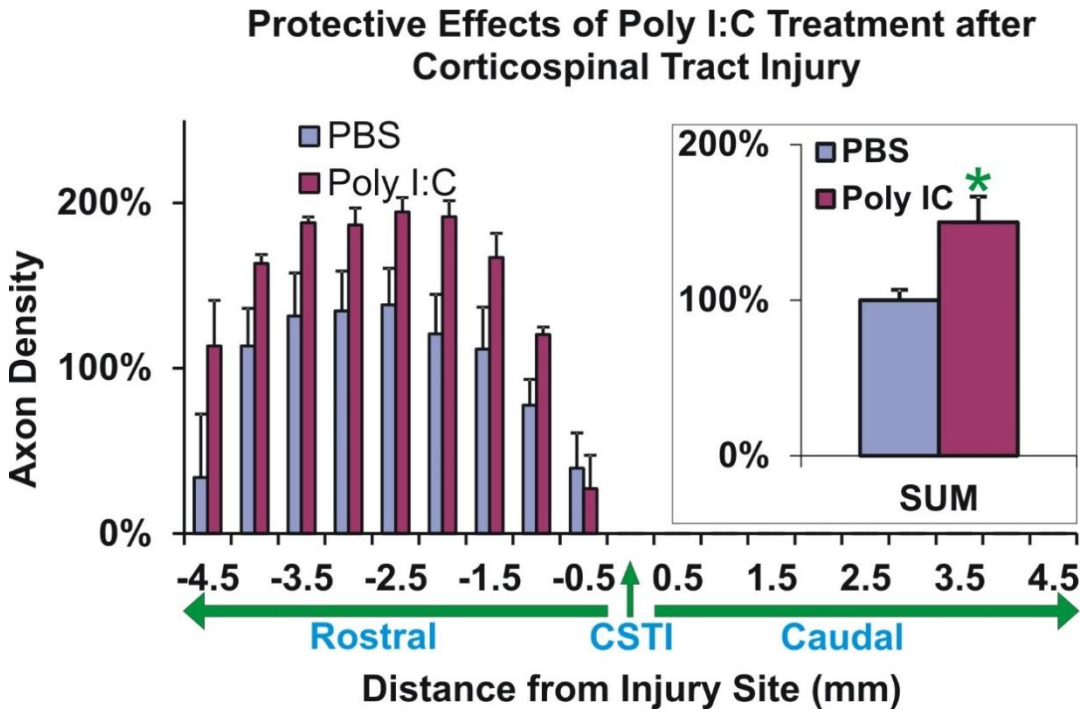

Figure 12: Poly I:C injection to the motor cortex has a protective effect on CST axons following injury. Histogram showing the axonal density rostral (-0.5 to -4.5 mm) and caudal (0.5 to 4.5 mm) to the corticospinal tract injury site (CSTI). Blue bars represent PBS-injected animals and pink bars represent Poly I:C-injected animals. **Insert:** Histogram showing the axonal density after averaging (SUM) the counts for all distances rostral to the injury site. (*) p<0.05 significance in an unpaired student T-test. Bars represent the percentage of the ratio between the mean numbers of axons in the spinal cord to those in the pyramid. Error bars show the standard error of the mean (SEM).

To further evaluate the axonal response, axonal retraction bulbs which are characterised by the accumulation of BDA positivity in the axonal stumps were analysed. Retraction bulbs were found rostral to the injury site in both PBS-treated (Fig.13A) or Poly I:C-treated (Fig.13B) groups. Quantification normalised with spinal axon counts, demonstrated that there was a similar number of bulbs at every distance rostral to the injury site in both Poly I:C (Fig.13-pink bars) and PBS groups (Fig.13-blue bars) (p<0.05; in an unpaired student T-test). In addition, irrespective of distance from injury site, the average number of bulbs

found in the Poly I:C (Fig. 13-insert pink bars)-treated animals was not different from PBS-treated animals (Fig. 13-insert blue bars) ($p<0.05$; in an unpaired student T-test).

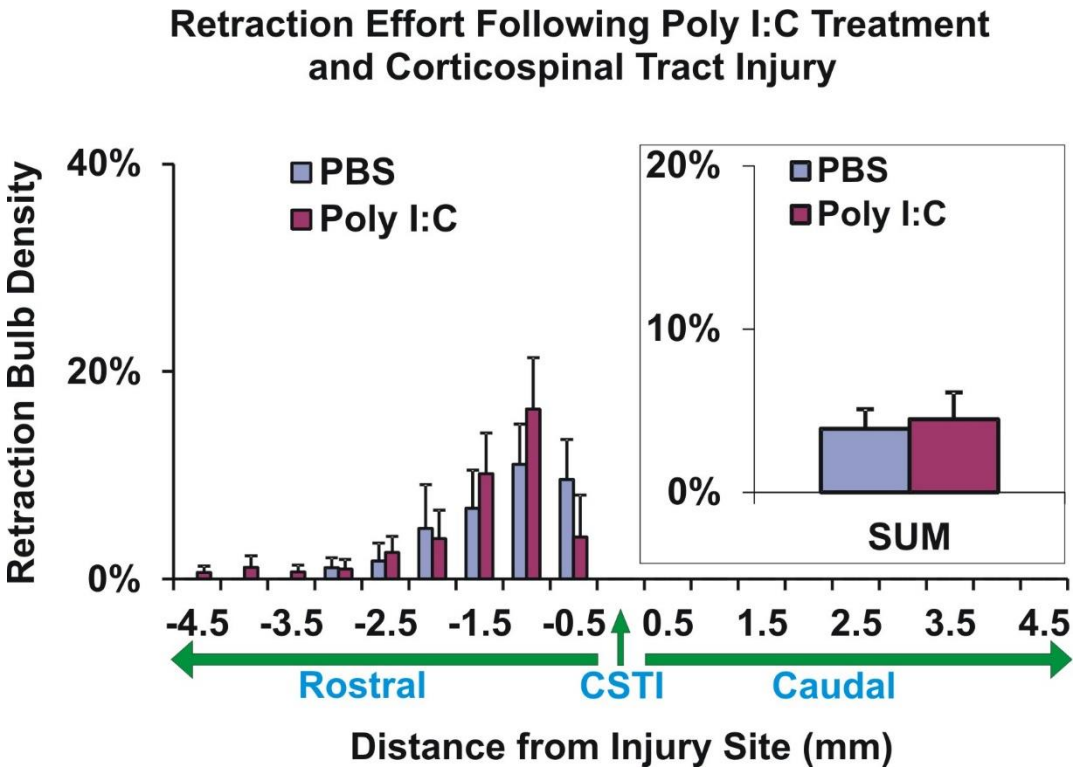

Figure 13: Poly I:C treatment into the motor cortex does not affect axonal retraction in the injured corticospinal tract. Histogram represent the retraction bulb density, rostral (-0.5 to -4.5 mm) and caudal (0.5 to 4.5 mm) to the corticospinal tract injury site (CSTI), following PBS (blue bars) or Poly I:C (pink bars) cortical injections. **Insert:** Histogram shows the retraction bulb density after averaging (SUM) the counts at all the distances rostral to the injury site. Bars represent the number of retraction bulbs as a percentage of the number of axons in the spinal cord. Error bars show the standard error of the mean (SEM).

Facial Nerve Axotomy

Poly I:C Accelerates Behavioural Improvement Following Rat Facial Nerve Axotomy.

To further evaluate any effects that Poly I:C may have on axonal regeneration, the facial nerve axotomy model was used. Rats injected into the hindbrain with PBS (n=5) or Poly I:C (n=5) underwent an ipsilateral facial nerve axotomy. Their whisker movement was assessed, from day 7 to 28 post injury. Movement was compared to that on the non-injured side and given a score of 0 (no movement) to 3 (strong normal movement). To examine reinnervation of the whisker pad, at

day 28 rats had fluorogold pads inserted into their control and experimental whisker pad for retrograde labelling and then were sacrificed at day 30.

Functional improvement was observed in PBS (Fig. 14A- blue line) and Poly I:C (Fig. 14A- pink line)-injected rats but neither reached full recovery. Poly I:C-treated rats showed greater recovery than PBS–treated rats at days 9,11, 14, 23, 26 and 28 (all $p<0.05$ in an unpaired samples T-test).

Finally, to evaluate target reinnervation fluorogold labelled facial motor neurons were quantified, the percentage fluorogold positive neurons (experimental/control) in the Poly I:C (53%±7%) injected rats were somewhat different from PBS (46%±1%), but this was not statistically significant ($p>0.05$ in an unpaired samples T-test).

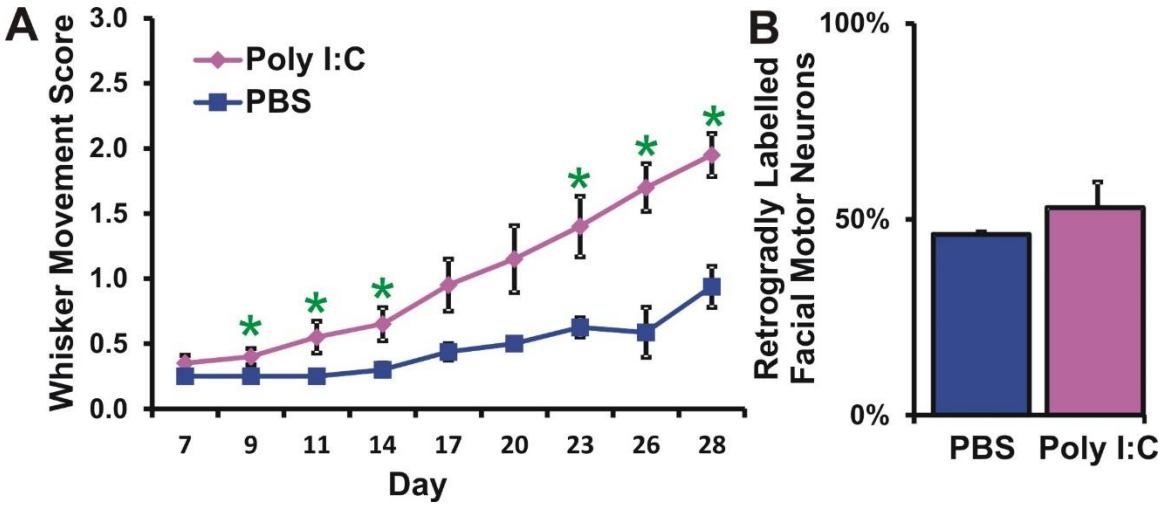

Figure 14: Poly I:C injection to rat hindbrain led to increased functional recovery after facial nerve axotomy. **A:** Histogram shows the whisker movement assessment score (0-3) at days 7 to 28 following facial nerve axotomy combined with and Poly I:C (pink line) or PBS (blue line) injections. The improvement in functional recovery in Poly I:C-injected compared to PBS-injected animals was statistically significant at days 9, 11, 14, 23, 26 and 28. (*) $p<0.05$ in an unpaired student T-test. **B:** Histogram represent the mean number of axons in the injured facial motor nucleus as a percentage of the number of neurons at the uninjured facial nucleus of rats injected with PBS (pink bar) or Poly I:C (blue bars), which underwent facial nerve axotomy

Discussion

The level of perineuronal inflammation around axotomised neurons has been correlated with their ability to regenerate axons (Leon et al., 2000; Lu and Richardson, 1991; Shokouhi et al., 2010). In this study Poly I:C, a synthetic double stranded RNA, was used to enhance inflammation around regeneration-

incompetent corticospinal neurons and regeneration-competent facial motor neurons and the effects on the neuronal response to axonal injury were assessed. In the motor cortex, Poly I:C at 1mg/ml was established as the preferred dose, as it was associated with widespread microgliosis and astrogliosis, but produced little tissue loss. Temporal analysis of Poly I:C revealed a peak in cortical microglial and astrocyte activation, and the recruitment of T-cells at day 3. Inflammation in the motor cortex was apparent without corticospinal neuron cell loss.

In the rat corticospinal tract and facial nerve injury models Poly I:C mediated a protective and a pro-regenerative effect, respectively. Following delivery of Poly I:C into the motor cortex and a concomitant C4 dorsal corticospinal tract injury, rats demonstrated an overall greater number of CST axons in the cervical spinal cord, with little evidence of axonal retraction from the injury site. In rats with facial nerve axotomy, Poly I:C injections adjacent to the facial nucleus enhanced the regenerative response by accelerating functional recovery, but we did not demonstrate an increased number of neurons retrogradely labelled from the whisker pad in Poly I:C-injected rats.

Poly I:C-mediated activation of microglia and astrocytes in the motor cortex

Poly I:C has been shown to mimic the effects of systemic viral infection (Cunningham et al., 2007). In the CNS, Poly I:C can be recognised by microglia, astrocytes and even neurons, through cell surface or endosomal TLR3 (Bsibsi et al., 2002; Bsibsi et al., 2003; Cameron et al., 2007; Jack et al., 2005) and cytoplasmic recognition has been postulated to also involve RIG (Peltier et al., 2010) and MDA-5 (Yoneyama and Fujita, 2010) receptors in neurons and astrocytes, respectively. In vitro and in vivo studies have shown that Poly I:C exposure results in a signalling cascade that leads to the expression of cytokines, chemokines, and oxidative species which are associated with neurodegenerative effects (Cameron et al., 2007; Deleidi et al., 2010; Patro et al., 2010).

We have evaluated the effect of increasing doses (0.1, 1 or 5.6 mg/ml) of Poly I:C on cortical microglia and astrocytes. In line with previous in vivo studies, we have shown that Poly I:C exposure is associated with a dose-dependent increase in numbers of reactive microglia and microglia taking on a phagocytic phenotype

by the retraction of their processes. Patro et al.(2010) found that infusion of a low dose (0.01 mg/ml) of Poly I:C into the lateral ventricle of rats provoked some microgliosis in periventricular areas. In addition, Deleidi et al. (2010) injected larger doses (2.5-10mg/ml) of Poly I:C into the substantia nigra, and found a dose-dependent effect on microglia. Furthermore widespread neurotoxicity was seen when Poly I:C was injected at the highest dose of 10mg/ml (Deleidi et al., 2010). This is compatible with our results, in which 5.6mg/ml Poly I:C produced necrotic areas around the injection site. In addition to the microglial response, increased GFAP expression in astrocytes was found in the Poly I:C-injected motor cortex. This effect was also reported by Town et al., (2006), where an increase in GFAP expression in the mouse cerebral cortex was found after intracerebroventricular Poly I:C (50ug/ml) injections.

At day 3 in our study Poly I:C appeared to have a strong effect on microglia and only a mild one on astrocytes, which is contrary to the results reported by Town et al. (2006), which showed a greater density of GFAP-positive astrocytes than CD11b-positive microglia at 24 and 48 hours post intracerebroventricular injections. This discrepancy might be attributable to the use of different species (rat vs mouse) and the time-point at which the brains were examined. (Town et al., 2006) also used a different marker to detect microglia. The current experiment used IBA1 to identify microglia. IBA1 is a marker that can be used to identify microglia at all activation states (Ito et al., 1998) but is highly upregulated in the reactive and phagocytic states. CD11b, the α-m integrin receptor used to detect microglia by Town et al., (2006), is very weakly expressed in the resting state and difficult to detect in well-fixed sections, but is strongly upregulated by reactive and phagocytic microglia (Kloss et al., 1999). If we had used the more capricious OX-42 antibody to detect CD11b in our rats, it would have provided a better comparison for the results in Town et al., (2006). However, the level of TLR3 expressed in microglia in vitro (Olson and Miller, 2004) is around six times more than that in astrocytes (Carpentier et al., 2005) suggesting that microglia are better candidates to respond rapidly to Poly I:C than astrocytes.

The results from the time course experiments demonstrated that cortical microglial and astrocyte activation peaked at day 3 and gradually declined over

time, as could be seen at day 7 and 14. However, unlike the effects on astrocytes, the effects of Poly I:C on cortical microglia were still present at day 14. This pattern is somewhere in between that seen following intraventricular infusion (Patro et al., 2010), where the peak was reached at day 7 and effects were gone by day 14, and the effect of nigrostriatal injection that peaked at day 12 and were still present a month later (Deleidi et al., 2010). This pattern might be explained by the differences in delivery method and site of injection, as well as by the doses used in the different studies. The dose used in the present study was 3 times higher than that used by Patro et al., (2010) and around 6 times lower than Deleidi et al., (2010).

Compared to other agents Poly I:C appears to be a potent inflammatory substance with relatively lower cytotoxic effects. Other substances have been used in the past to promote perineuronal inflammation. (Hossain-Ibrahim et al., 2006), used topical application of LPS to the adult motor cortex in rats and found weaker, less widespread and less prolonged inflammation than what we can see with Poly I:C, disappearing 7 days following application. However, others have reported that the effects of Poly I:C may be more transient than those of LPS. (Patro et al., 2013) reported that intraperitoneal injections of Poly I:C had acute effects whilst those of LPS were chronic.

Poly I:C is a strong inflammatory substance and can causes necrosis at the highest dose; however, when Zymosan was applied to the motor cortex, it caused high levels of necrosis (Hossain-Ibrahim et al., 2006). Therefore, Poly I:C can be considered a more potent and safer candidate to promote perineuronal inflammation than LPS or Zymosan.

T-cell recruitment to the Poly I:C injection site

Peripheral immune cell infiltration to the CNS is critical for defence against infection and for repair after injury (Hauwel et al., 2005). Three days post Poly I:C (1mg/ml) injection we found a surge of T-cells infiltrating the injection site from the periphery. Leukocyte recruitment involves the adherence of leukocytes to vascular endothelial cells in a 4 step process: 1) the lymphocyte makes transient contact with the vascular endothelium, allowing the cell to roll along the endothelial cell surface and sample the environment for chemokines. 2) T-cells

are activated by chemokines. 3) T-cell activation leads to the increased expression of integrins, such as VCAM and ICAM1, which then mediate firm arrest of the lymphocyte to the vessel wall. 4) Following T-cell adherence to the vascular wall, T-cells migrate across the BBB through the endothelial tight junctions (Engelhardt, 2006).

In vitro studies have shown that upon Poly I:C exposure, microglia and astrocytes are able to produce cytokines IL-6 and TNF-α, which are associated with the increase in intercellular adhesion molecules (ICAMs) (Furie and Randolph, 1995; Wahl et al., 1996), which may help T-cells traversing the walls of blood vessels to enter the injection site. In vivo, a peripheral challenge with intraperitoneal Poly I:C in mice evokes a global upregulation of a range of chemokines, including CXL1 and 2 and CCL2 and 4. The CXC family of chemokines (IL-8/CXCL8, CXCL1,2,3,10, MIP-2) attract neutrophils and CC chemokines (MCP-1, MIP1α, MIP1β, RANTES), summon monocytes, lymphocytes, eosinophils and basophils (Bajetto et al., 2001; Bell et al., 1996; Hausmann et al., 1998). In vitro data shows that neonatal and adult microglia produce chemokines MIP1β and RANTES (Pattison et al., 2013; Pratt et al., 2013), and astrocytes IL-8 and IP-10 (CXCL-10) (Park et al., 2006) upon challenge with Poly I:C, which may be involved in the T-cell migration seen in this study. In addition to the indirect effects, Poly I:C can act on the T-cell TLR3 receptor and lead to their activation (Funderburg et al., 2008). Poly I:C promotes the production of MIP-1, GMCSF and IL-10 and TGF-β by bovine T-cells (McGill et al., 2013).

Poly I:C and corticospinal neuron death

Intracerebroventricular (Melton et al., 2003) and systemic (Field et al., 2010) administration of Poly I:C is associated with neuronal cell death in various regions of the brain. To evaluate the level of toxicity we injected rats with Poly I:C at 1mg/ml and retrogradely labelled their corticospinal neurons with fluorogold. We found that Poly I:C-treated rats showed microglial activation in the motor cortex but had similar numbers of fluorogold-positive corticospinal neurons as controls.

In these retrograde labelling studies the axons of corticospinal neurons were injured, which might have promoted axotomy-induced cell death. Reports in rats (Barron et al., 1988; Kneubuhl and Steward, 2008; McBride et al., 1989; McBride

et al., 1991), hamsters (Barron et al., 1988; Merline and Kalil, 1990; Ramirez and Kalil, 1985), and primates (Wannier et al., 2005) show no corticospinal cell death following corticospinal tact injury in the spinal cord. Nonetheless, Hains et al., (2003) observed substantial apoptotic cell death of corticospinal neurons 7 days after injury to the thoracic spinal cord. Field et al., (2010) reported that systemic challenge with Poly I:C in mice with a model of Alzheimer's disease, amplified CNS inflammation and exacerbated neuronal cell death in the hippocampus and thalamus. The rats in the present study survived 7 days like those reported in (Hains et al., 2003). However, there was no exaggerated neuronal cell death following Poly I:C injection compared to control rats.

The effect of Poly I:C on regeneration of the PNS and CNS

Facial nerve axotomy: regenerative effects of Poly I:C

In the present study, injection of Poly I:C into the brainstem close to the facial motor nucleus of rats accelerated functional recovery following facial nerve axotomy. Poly I:C may encourage fast regeneration by enhancing inflammation around the neuronal cell bodies. PBS-treated rats did not show complete functional recovery following facial nerve axotomy. Heaton et al., (2008) determined functional recovery of whisker movements in Wistar rats with facial nerve transection by measuring the amplitude and speed of movement occurring both spontaneously, as well as following a stimulus (puff of air). At six weeks, the measurement for whisker movement of injured rats was 80% lower than that achieved by sham injured or intact rats. In the present experiment, the whisker movements on the injured side was 70% lower at four weeks post-injury compared to the non-injured side.

Although Poly I:C had a positive effect on functional recovery, it apparently had no effect on the number of axons that successfully reinnervate the whisker pad. The disparity between the functional and anatomical effects of Poly I:C, may be explained by the methodology used to identify a regenerating neurons. Fluorogold is a retrograde tracer that can label neurons whose axons have formed endplates on muscle fibres and those that have not (Richmond et al., 1994). Fluorogold labelling cannot resolve small differences in the speed of regeneration of axons. In the present study, the fluorogold pad inserted in the

whisker pad would label both neurons that have rapidly regenerated their axons and formed endplates with the muscles of the whisker pad, and those that are more slowly regenerating their axons, have not formed endplates but are in close proximity to the whisker pad. Accordingly, it could be that Poly I:C-injected animals have regenerated their axons and formed functional endplates with the muscle fibres faster than the PBS-injected rats. A better method to evaluate the effect of Poly I:C on the speed of regeneration, would involve examining longitudinal sections of facial nerves taken 4 days after axotomy, stained for the neuropeptides galanin or calcitonin gene-related peptide (CGRP) that accumulate in the growth cones (Makwana and Raivich, 2005). Subsequently, the speed of axonal regeneration can be determined by measuring the distance travelled by fastest (most distal) growth cone from the crush side.

Alternatively, Poly I:C may have an effect on axonal branching and muscle reinnervation. The facial motor nucleus contains 5 subnuclei; lateral, dorsal, intermediate, medial and ventromedial (Kempf and Schwab, 2013; Martin and Lodge, 1977; Papez, 1927; Semba and Egger, 1986). The dorsal, lateral and intermediate subnuclei contain neurons that extend their axons into the zygomatic, buccal and mandibular branches of the facial nerve that control movements of the eyelid, whisker and lip movements. Streppel et al., (2002), used triple retrograde labelling to estimate the degree of collateral branching of axons. They injected retrograde tracers Dil (red) Fluorogold (yellow) and Fast Blue (blue) into the zygomatic, buccal and mandibular branches in intact rats, or rats with facial nerve axotomy and ligation. In intact rats the motor neurons that extend their axons through these branches were not double or triple labelled, suggesting that intact neurons send only one unbranched axon to the different branches. However, following injury there is around 53% of double or triple labelled neurons, suggesting that there is collateral branching following injury. Collateral branching has been associated with polyinnervation of neuromuscular junctions and the poor functional recovery observed in the rat following peripheral nerve injury (Al-Majed et al., 2000a; Zhang et al., 2013).The method described by Streppel et al., (2002), could be used to shed light on weather Poly I:C can exacerbate or prevent axonal branching following axonal transection.

Finally, Poly I:C could have an effect on the number of axons forming connections with the muscle fibre. Grosheva et al., (2008) estimated the degree of reinnervation of the levator labii superioris muscle, which is the main muscle that controls whisker movement in the rat. They counted the number of axons and endplates in confocal images of longitudinal muscle sections staining for bungarotoxin to visualise motor endplates and neuronal class III β-tubulin to visualise intramuscular axons. The same technique could be used to evaluate the number of axons innervating endplates following Poly I:C injection into the hindbrain of rats with an ipsilateral facial nerve axotomy.

Corticospinal tract injury: protective effects of Poly I:C

The corticospinal tract relays instructions for voluntary movements. Following injury the corticospinal tract cannot regenerate. To determine whether Poly I:C-mediated perineuronal inflammation enhances axonal regeneration following a dorsal corticospinal tract injury, a mixture of BDA and Poly I:C was injected into the motor cortex in adult rats and a contralateral corticospinal tract injury was carried out. There were more anterogradely labelled axon in the spinal cord than in the pyramids in both Poly I:C-injected and PBS-injected animals. This suggests that the corticospinal axons in the pyramids had branched or sprouted in the spinal cord. There was a higher axonal density in the spinal cord, rostral to the injury site, in the Poly I:C-treated group compared to PBS controls. This effect was not explained by differences in the efficacy of anterograde labelling between groups, as the number of axons at the level of the pyramids was the same for both. Thus it appears that Poly I:C might either protect axons from dying back after spinal cord injury or promote axonal sprouting.

Completely severed axons in the spinal cord undergo retrograde degeneration (dieback) (RamonyCajal, 1928). The distance the corticospinal axons retract has been reported to increase with time, from approximately 1.4 mm at 1 week and 4.1 mm at 16 weeks post injury (Seif et al., 2007). Our results somewhat reflect this since at 2 weeks post injury the greatest numbers of corticospinal axons were found about 2mm from the lesion site.

Axonal retraction can also be evaluated by counting the number of axonal retraction bulbs present at varying levels from the injury site. (RamonyCajal,

1928) reported that areas of axonal swelling may be sites of axonal retraction. The ends of severed spinal axons develop into spherical swellings known as terminal bulbs, which are clearly seen within 1 day after injury and persist many months (Fishman and Kelly, 1984a; Pallini et al., 1988; Pasquale-Styles et al., 2003). Terminal bulbs contain dense accumulations of axoplasmic organelles and are surrounded by a fluid filled microcyst, were BDA can be stored. These spherical swellings are consistently retracted away from the original site of injury after significant time intervals post injury (Borgens et al., 1986; Fishman, 1987; Hill et al., 2001; Houle and Jin, 2001; Kalil and Schneider, 1975; Pallini et al., 1988; Pasquale-Styles et al., 2003). We found that there was no significant difference in the numbers of axonal bulbs in Poly I:C-injected rats and PBS-injected controls.

As well as axonal degeneration, a weak regenerative response is provoked in corticospinal axons following injury without any intervention, in the form of axonal sprouting (Li and Raisman, 1995). In the current experiment, rostral to the injury site there was a greater number of axons in the Poly I:C-injected than PBS-injected rats, which may be explained by a greater presence of axonal sprouts in the Poly I:C-injected rats. However, the current study did not directly address this point due to the methodology employed in axonal counting. To evaluate axonal sprouts images can be taken at the level of the lesion, 1mm rostral to lesion and 4mm rostral to the lesion, for each consecutive sections. A virtual transverse plane perpendicular to the CST can then be created for each image and the number of CST branches and sprouts intersecting this virtual plane can be counted (Schnell and Schwab, 1993).

It is important to note that Poly I:C has been shown to inhibit neurite growth in vitro (Cameron et al., 2007; Leinster et al., 2013) by acting on TLR-3 receptors at the growth cone (Cameron et al., 2007). In the present study, the corticospinal axons did not regenerate past the lesion even in PBS-treated animals, so it would have been difficult to measure any inhibitory effects on regeneration.

Conclusion

In this chapter we have demonstrated that injection of Poly I:C to the rat motor cortex produces inflammation and glial activation that is dose dependent, and

which can be seen up to 14 days following administration. Poly I:C was also found to increase the expression of regeneration related transcription factors in nuclei that appear to belong to glial cells. In addition to its inflammatory effects, injections of Poly I:C into the motor cortex are associated with an axon-protective effect after spinal cord injury. Furthermore, injection of Poly I:C near the axotomised facial nucleus enhanced functional recovery after facial nerve injury.

CHAPTER FOUR

Characterising the effects of prolonged perineuronal inflammation using GM-CSF lentivirus in the rat CNS

Introduction

Achieving long-distance axonal growth that results in functional recovery after central axonal injury remains one of the biggest practical challenges in experimental biology. The failure of the CNS to regenerate their axons may be at least in part due to CNS neurons mounting a weak, transient or incomplete molecular response to axonal injury. This muted response to injury has been shown to be associated with low or absent perineuronal inflammation (Shokouhi et al., 2010) probably wrong reference. Previous studies aiming to enhance axonal regeneration through perineuronal inflammation had a number of limitations that may have restricted the extent of axonal regrowth, such as the agents used may have not been potent enough inflammogens and their effects may have been too transient (Hossain-Ibrahim et al., 2006; Yin et al., 2000).

An alternative inflammatory agent that could be suitable to promote perineuronal regeneration is the cytokine Granulocyte Macrophage-Colony Stimulating Factor (GM-CSF). GM-CSF is a potent microglial mitogen (Kloss et al., 1997) which also enhances microglial production of the pro-inflammatory cytokines IL1β and TNFα, (Kloss et al., 1997). GM-CSF promotes phagocytosis and functional antigen presentation by cultured brain-derived macrophages (Giulian and Ingeman, 1988) as well as microglia in vivo (McQualter et al., 2001; Mirski et al., 2003; Ponomarev et al., 2007). In addition to its intrinsic immunological actions, recombinant GM-CSF peptide delivered by intraperitoneal injection has been shown to be neuroprotective and to promote functional recovery following spinal cord injury (Bouhy et al., 2006; Ha et al., 2005; Huang et al., 2009).

To evaluate the effects of long-term inflammation around neuronal perikarya, a non-integrating lentiviral vector expressing GM-CSF was developed for this study. The ability of lentiviruses to transduce non-dividing cells, their ease of production and the option to change their cell tropism by pseudotyping make

them useful gene delivery vectors. However, recent in vivo and clinical trial data has highlighted the potential risk of insertion mutagenesis following integration of the viral DNA into sensitive areas of the host genome (Hacein-Bey-Abina et al., 2003). The concern surrounding insertional mutagenesis has naturally led to interest in using non-integrating lentiviruses, by introducing class 1 mutations into the integrase gene. The result is a failure of vector DNA to integrate so that it exists episomally in a functional double-stranded circular form produced by host nuclear enzymes.

The following chapter is divided into three parts: Part 1: shows the successful in vitro expression of lentiviral genes, GM-CSF and enhanced green fluorescent protein (eGFP). Part 2: evaluates in vivo the time-dependent effects of high doses of GM-CSF non-integrating lentiviruses on the CNS and blood. Part 3: demonstrates in vivo the dose necessary to produces optimal microglia activation and little cell death in the motor cortex.

Results

To determine the effect of prolonged inflammation in the rodent CNS, two viruses were created: the experimental encoding for GM-CSF and eGFP (GM-CSF-virus) and the control that only encodes for eGFP (eGFP). Figure 1 shows the two lentiviral plasmids. The eGFP-virus plasmid used was previously described by Yanez-Muñoz et al. (2006); here the spleen focus-forming virus (SFFV) promoter drives eGFP expression (Fig. 1A). The GM-CSF plasmid, was created by cloning the GM-CSF gene and the xIRES genes between the SFFV and eGFP genes (see Methods). Therefore the expression of GM-CSF is driven by SFFV promoter and the expression of eGFP is controlled by xiap derived Internal Ribosome Entry Site (xIRES) (Fig. 1B).

To produce the non-integrating lentivirus particles, the lentiviral plasmids (eGFP-virus or GM-CSF-virus), the non-integrating virus packaging plasmid and the vesicular stomatitis virus (VSVG) envelope plasmid were used to transduced HEK293T cells, which are required for viral assembly (see Methods). Previous research has demonstrated that pseudotyping the lentiviral particle with VSVG is associated with efficient gene delivery to neurons (Rahim et al., 2009).

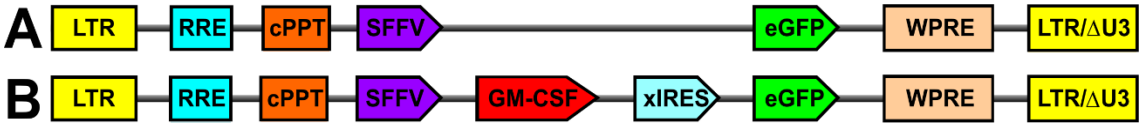

Figure 1: Schematic representation of the lentiviral plasmid constructs used in the study. A) The eGFP lentiviral plasmid (eGFP-virus). In this study this plasmid was used as a control to the current GM-CSF virus. B) The GM-CSF lentiviral plasmid, carrying the GM-CSF gene, xIRES, and eGFP. SFFV directs the expression of GM-CSF and xIRES permits bicistronic expression of eGFP (GM-CSF/eGFP).

Part 1: In vitro studies

GM-CSF-virus produces expression of eGFP protein in vitro

The first step of the project was to evaluate whether the GM-CSF-virus can cause the production of eGFP. The expression of eGFP permits the identification of virally transduced cells. The eGFP-virus has consistently been shown to strongly produce expression of eGFP protein in vitro and in vivo (Rahim et al., 2009; Yanez-Munoz et al., 2006). To examine whether GM-CSF virus can produce eGFP in vitro, six different volumes of GM-CSF-virus or eGFP-virus virus were added to HEK293T cells: 0µl, 0.032µl, 0.016µl, 0.08µl, 0.4µl and 2µl. The following day the percentage of eGFP-positive cells was measured as well as the median fluorescence intensity (MFI), using flow cytometry.

Delivering increasing volumes of eGFP-virus (Fig. 2-green) or GM-CSF-virus (Fig. 2-red) to HEK293T cells increased the percentage of transfected cells and the intensity of eGFP fluorescence. In comparison to eGFP-virus, GM-CSF-virus displayed a lower level of eGFP fluorescence intensity between 2% and 75% of HEK293T cell transfection.

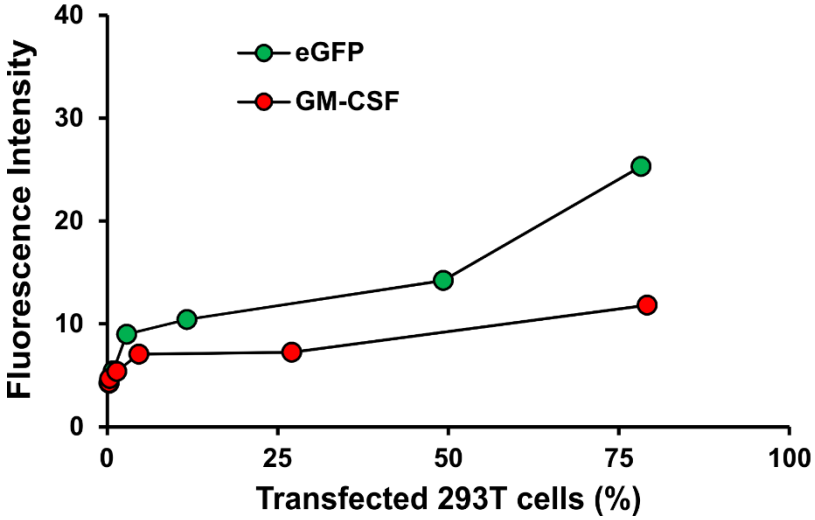

Figure 2: Comparative eGFP expression efficiency of eGFP and GM-CSF viruses in HEK293T cells. Five volumes of eGFP (green) or GM-CSF (red) virus was added to HEK293T cells: 0µl, 0.032µl, 0.016µl, 0.08µl, 0.4µl and 2µl. Using flow cytometry the median fluorescent intensity for each vector (Y axis) was measured along with the percentage of infected cells (X axis). The MFI of cells transduced by GM-CSF virus is lower than the MFI of cells transduced by the eGFP-virus, between 2% and 75% of transfection.

A viral vector producing GM-CSF enhances microglial proliferation in-vitro

To test viral vector-mediated production of GM-CSF in vitro; supernatant from eGFP-virus or GM-CSF-virus infected HEK 293T cells was applied onto BV2 microglial cells. As a positive control BV2 cells were separately treated with murine GM-CSF recombinant protein. The next day BV2 cells were incubated with 3(4,5-dimethythiazol-2-yl)-25-diphenyltetrazolium bromide (MTT) to assess cell number and viability, MTT is an insoluble tetrazolic salt that is hydrolysed by mitochondrial dehydrogenases to produce an insoluble formazan that has a purple colour (van Meerloo et al., 2011). The activity of this enzymes can reflect the number of viable cells present. Therefore, if the number of viable cells increases this would increase the purple colouring. Here, the amount of formazan formation by the viable cells was quantified by measuring the level of light absorbance.

As shown in figure 3, the MTT colometric assay demonstrated no effect of eGFP-condition medium on BV2 cell proliferation, as the amount of light absorbance remained constant (Fig. 3-green bars). In contrast, conditioned medium from HEK293T cells transduced with GM-CSF-virus elicited a 1.5-fold increase in light absorbance, with half-maximal effect at 1:1000 dilution, which is equivalent to a

viral titre of 100 (TU/ml) (Fig. 3-red bars). Addition of recombinant GM-CSF peptide to otherwise untreated BV2 cells, showed a 2.2-fold increase and a half-maximal effect at 1ng/ml in comparison the control (Fig. 3-blue bars).

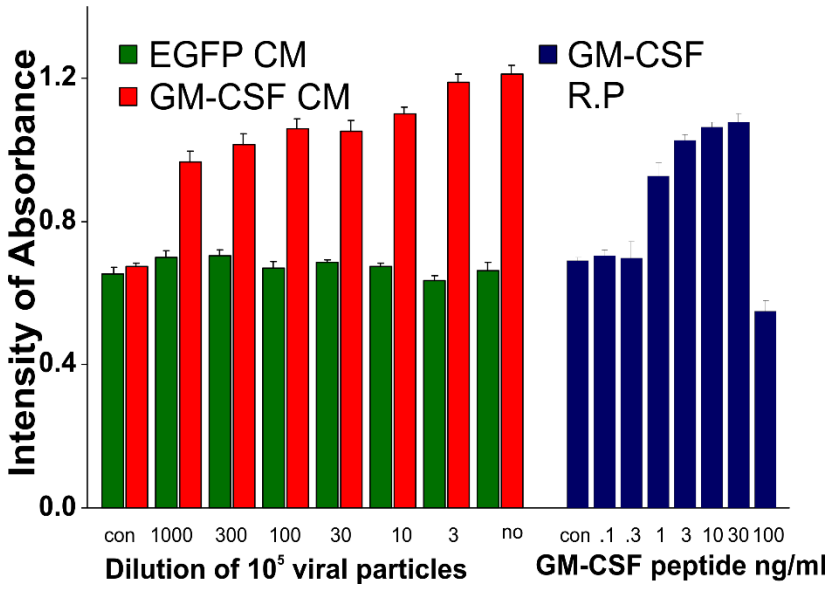

Figure 3: Viral vector-mediated production of GM-CSF causes microglial cell proliferation in vitro. Histogram showing the intensity of light absorbance by BV2 cells following treatment with conditioned medium (CM) from HEK293T cells treated with increasing concentrations of EGFP (green bars) or GM-CSF (red bars) viral vectors. Blue bars represent the effect of increasing GM-CSF concentrations. GM-CSF condition medium was a more effective mitogen that 30ng/ml GM-CSF. Bars and error bars represent the mean and standard error of the mean (SEM), respectively.

Part 2: Time course in vivo

Delivery of GM-CSF-virus to the motor cortex of Sprague Dawley rats increases microglial numbers

Following confirmation that the GM-CSF-virus works in vitro, the next step was to analyse whether the virus would work in vivo. To determine the effect of prolonged expression of GM-CSF, rat motor cortex was injected with eGFP-virus (10^8 TU/ml) or a mixture of GM-CSF-virus (10^7 TU/ml) and eGFP-virus (10^8 TU/ml) (GM-CSF/eGFP-virus). Rats were allowed to survive for 3 (eGFP n=1 & GM-CSF/eGFP n=4), 7 (n=2 & n=4), 14 (n=2 & n=4) or 28 (n=2 & n=4) days after viral delivery.

At day three there was little evidence of eGFP-positive cells in the motor cortices of animals injected with eGFP-virus or GM-CSF/eGFP-virus. However, at days 7 (Fig. 4C), 14 (Fig. 4E) and 28 (Fig. 4G), motor cortices injected with eGFP-virus (Fig. 4-right column) showed numerous eGFP-positive neurons up to 200µm away from the needle track, and normal consistency of injected tissue, In contrast, rats injected with GM-CSF/EGFP-virus (Fig 4-left column), revealed a high number of eGFP-positive glial-like cells at day 7 (Fig. 4D). However, at days 14 (Fig. 4F) and 28 (Fig. 4H) there was only a moderate number of eGFP-positive cells and evidence of fluid filled spaces at the site of the needle track.

To quantify the level of viral transduction, eGFP-positive cells were counted in layers II to V along the needle track using a 40x objective lens (Fig. 5A). After eGFP-virus injection (Fig 5. A-green bars) there was a strong increase in the number of eGFP-positive cells per field as time increased. However, this increase was more moderate after intracranial delivery of GM-CSF/eGFP-viral mixture (Fig 5. A-red bars). At each time point, the number of transduced cells present per field was considerably less after GM-CSF/eGFP-viral mixture injection to the motor cortex than after an eGFP-virus injection. However, this difference did not reach statistical significance ($p>0.05$; unpaired student's T-test).

Since GM-CSF is a microglial mitogen, the numbers of IBA1-positive microglia were counted in sections through the injection sites. At three days after delivery of eGFP-virus to the motor cortex (Fig.4A), IBA1-positive microglia demonstrated a rounded morphology typical of phagocytic microglia. At 7 (Fig. 4B), 14 (Fig. 4C) and 28 days (Fig. 4D) microglia surrounding the numerous green-fluorescent cells had a ramified (resting) morphology. However, at day 3 the GM-CSF/eGFP-injected cortex (Fig. 4E) showed IBA1-positive microglia that had short process that is associated with a state of activation. By day 7 (Fig. 4F), the density of activated microglia surrounding eGFP-positive cells increased. At 14 (Fig. 4G) and 28 (Fig.4H) days post injection of GM-CSF/eGFP virus, most local IBA1-positive microglia/macrophages showed rounded phagocytic morphology, with many densely packed clusters around the injection site. A large number of microglial clusters were seen at the boundaries of the of fluid filled spaces and

tissue, but many spread as far as the white matter of the internal capsule and corpus callosum, approximately 100µm away from the eGFP-positive cells.

IBA1-positive microglia were counted Using a 40x objective lens in four fields along the needle track of eGFP (Fig. 5B-green bars) and GM-CSF/eGFP-injection sites (Fig. 5B-red bars). Initially, the total numbers of microglial cells at the resting, reactive and phagocytic activation states were quantified. Following eGFP-virus injection, at day 3 there were 101 microglia per field. However, this increase was transient and gradually disappeared at later time points: the eGFP-virus injection was associated with 91±4 microglia per field at day 7, 58±18 microglia per field at day 14, and 20±15 microglia per field at day 28. In contrast, following injection of GM-CSF/eGFP-viral mixture, there were 102±15 microglia per field at day 3, 151±15 microglia per field at day 7, 155±29 microglia per filed at day 14 and 158±15 microglia per field at day 28. The GM-CSF/eGFP viral mixture produced a significantly higher number of IBA1-positive microglial cells per field than eGFP-virus at all time-points apart from day 3 ($p<0.05$; unpaired student's T-test).

To assess the effect of GM-CSF on microglial morphology, the numbers of IBA1-positive cells that had a round or amoeboid shape (phagocytic microglia) were quantified along the injection site. At day 3 the eGFP-virus treated (Fig. 5C-green bars) and eGFP/GM-CSF-treated animals (Fig. 5C-red bars), both showed phagocytic cells at the injection site. These phagocytes disappeared at later time points in the cortices injected with eGFP-virus, but increased in number following the GM-CSF/eGFP virus injection. Cortices injected with GM-CSF/eGFP virus had 111±21 phagocytic microglia per field at day 14 and 113±24 microglia per field at day 28, which was significantly higher than the 23±1 phagocytic microglia per field found at 14 days and 4±4 microglia per field counted at 28 days post eGFP-virus injection ($p<0.05$ unpaired student's t-test).

Since microglial phagocytes tend to form clusters – defined as 3 or more tightly aggregating phagocytes - cluster formation was also examined. Although, there was a trend for more clusters per field to be present in GM-CSF/eGFP- injected rats (Fig. 5D-red bars) than in those injected with eGFP (Fig. 5D-green bars) at days 14 and 28, this did not reach statistical significance ($p>0.05$; unpaired student's t-test).

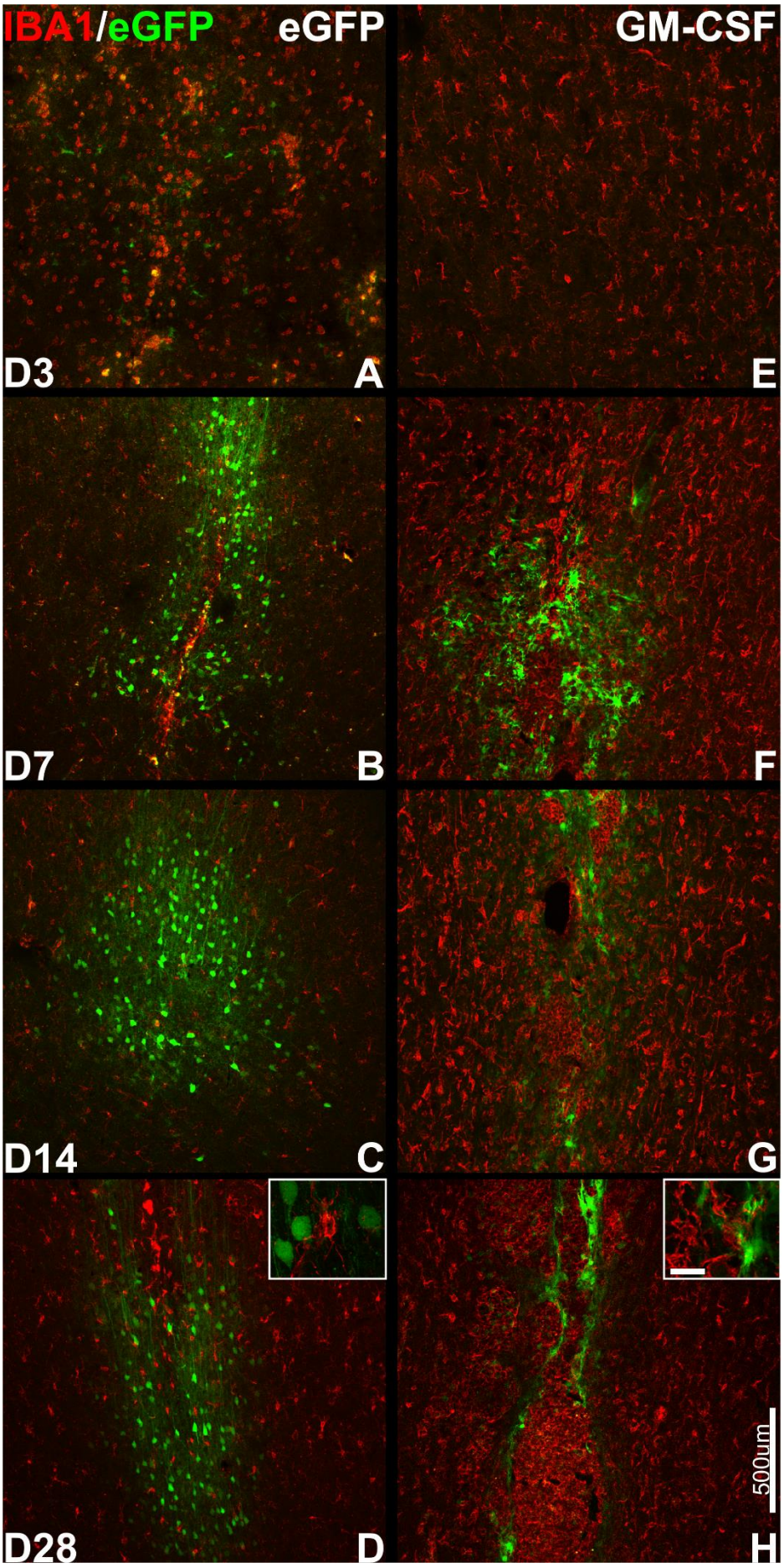
IBA1/eGFP
eGFP
GM-CSF
D3
A
E
D7
B
F
D14
C
G
D28
D
H
500um

Figure 4: Long-term expression of GM-CSF-virus increases microglial activation in the motor cortex. Coronal brain sections of motor cortex stained for IBA1 (in red), and also showing eGFP-positive cells (in green), at 3 (A&E), 7 (B&F), 14 (C&G) or 28 days (D&E) following eGFP-virus or GM-CSF/eGFP-virus injections. From day 7 to 28, GM-CSF virus increased the number of microglia (F-H), but the control virus produced no increment (B-D). The number of eGFP-positive cells decreased in cottices injected with GM-CSF virus (F-H), but increased in those injected with the control virus (B-D). High magnification inserts, show that rounded microglia can be seen surrounding the green cells only at day 28 following GM-CSF virus treatment. Scale Bar: 50um

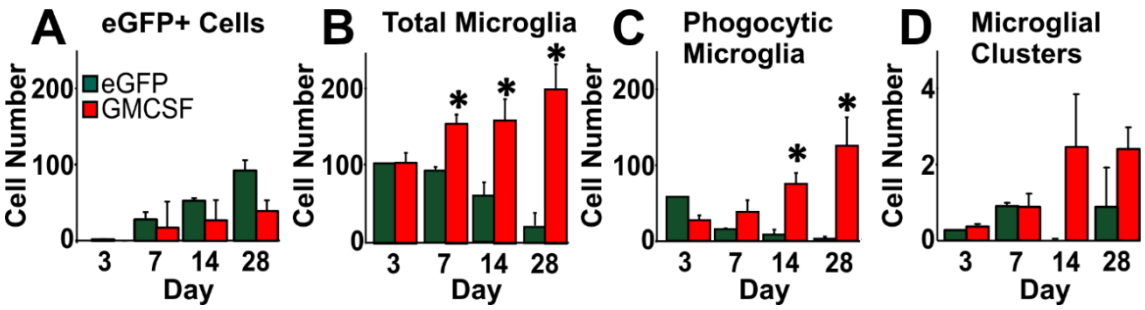

Figure 5: Quantitation of microglial and eGFP-positive cell numbers following eGFP- or GM-CSF/eGFP- virus injections to the motor cortex. **A-D**: Histograms representing the number of eGFP-positive (+) cells per field (A), total microglia per field (B), phagocytic microglia per field (C) or microglial clusters per field (D), 3, 7, 14, or 28 days post eGFP-virus (green bars) or GM-CSF/eGFP-virus (red bars) injection to the motor cortex. (*) $p<0.05$; unpaired student's t-test. Bars and error bars represent the mean and standard error of the mean (SEM).

GM-CSF-mediated microglial activation is associated with a reduction in the numbers of corticospinal neurons

To examine the potentially toxic effects that GM-CSF-mediated inflammation may have on corticospinal neurons, a rat was injected with eGFP-virus (10^8 TU/ml) to the left motor cortex and GM-CSF/eGFP-virus (10^7 & 10^8 TU/ml) to the right motor cortex. Corticospinal neurons were retrogradely labelled with fluorogold from the fourth cervical segment of the spinal cord. Coronal brain sections containing fluorogold-labelled corticospinal neurons (Fig. 6A & B-gold) were fluorescently stained for IBA1 to visualise microglia (Fig. 6 A & B-red).

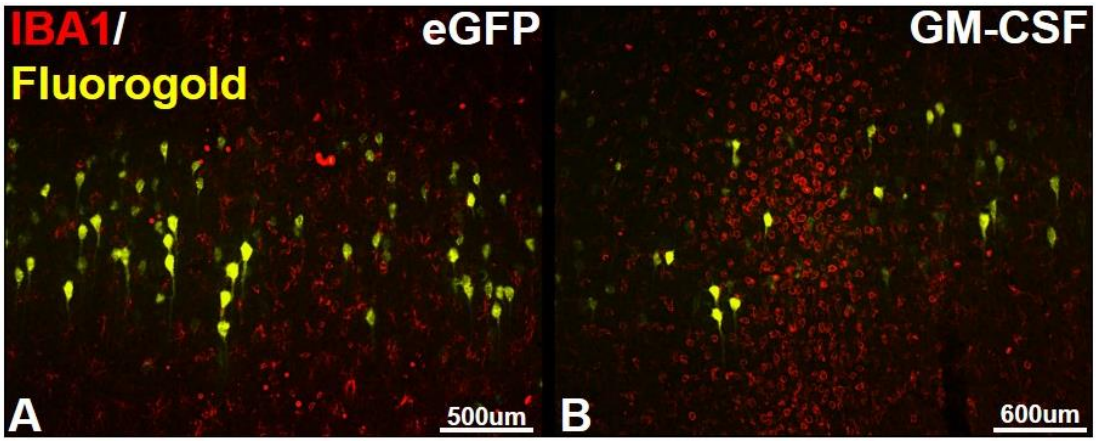

Figure 6: GM-CSF viral expression is associated with corticospinal neuron cell death. **A-B:** Coronal sections of IBA1-stained (in red) motor cortex with fluorogold-positive (in gold) neurons through the injection sites of eGFP (A) or GM-CSF/eGFP (B) viruses. The GM-CSF/eGFP injected cortex has greater numbers of phagocytic microglia but fewer fluorogold-positive neurons.

Fourteen days following eGFP-virus delivery (Fig. 6A), there were numerous fluorogold-labelled neurons present in layer V of the motor cortex. The IBA1-positive microglia surrounding these fluorogold-positive neurons had a ramified morphology typical of the resting state (Fig. 6A-red). However, the GM-CSF/eGFP-injected cortex had fewer fluorogold-positive corticospinal neurons than the eGFP-virus injected cortex (Fig. 6) but had a higher density of IBA1-positive phagocytic microglia surrounding the fluorogold-labelled neurons (Fig. 6B-red). This shows that the delivery of GM-CSF viral vector at this titre to the motor cortex was toxic to corticospinal neurons, either by direct effects on neurons or via the induction of phagocytic microglia.

Prolonged exposure to GM-CSF virus increases astrocyte density

As well as having effects on microglia (Lee et al., 1994), GM-CSF has been shown to stimulate the proliferation of astrocytes in primary cultures derived from simian brains (Guillemin et al., 1996). To characterise the effects of GM-CSF on astrocytes, coronal sections of cortex injected with GM-CSF/eGFP or eGFP viruses were examined at 3 (eGFP-virus group n=1 & GM-CSF/eGFP group n=4), 7 (n=2 & n=4), 14 (n=2 & n=4), and 28 (n=2 & n=4) days post injection.

Three days following eGFP (Fig. 7A-green) or GM-CSF/eGFP (Fig. 7B-green) injections there was no evidence of eGFP positive cells. However, the expression of GFAP was higher in the motor cortex of GM-CSF/eGFP-injected rats (Fig. 7B-

red) than in the motor cortex injected with eGFP (Fig. 7A-red). Longer exposure to eGFP-virus (Fig. 7C-green) produced an increase in the number of eGFP-positive cells that had a neuronal shape. In comparison, the GM-CSF/eGFP-injected cortex (Fig. 7D-green) had a lower number of eGFP-positive cells and they resembled glia rather than neurons. eGFP-injected cortex had few GFAP-positive astrocytes and these cells had thin processes (Fig. 7C-red & insert). In contrast, the GM-CSF/eGFP virus injection (Fig. 7D-red) produced a greater density of astrocytes and they demonstrated a hypertrophic appearance with thick GFAP-positive processes (Fig. 7D-red insert). In addition, there were clear astrocytic scars surrounding areas of tissue damage in the GM-CSF/eGFP injected cortex.

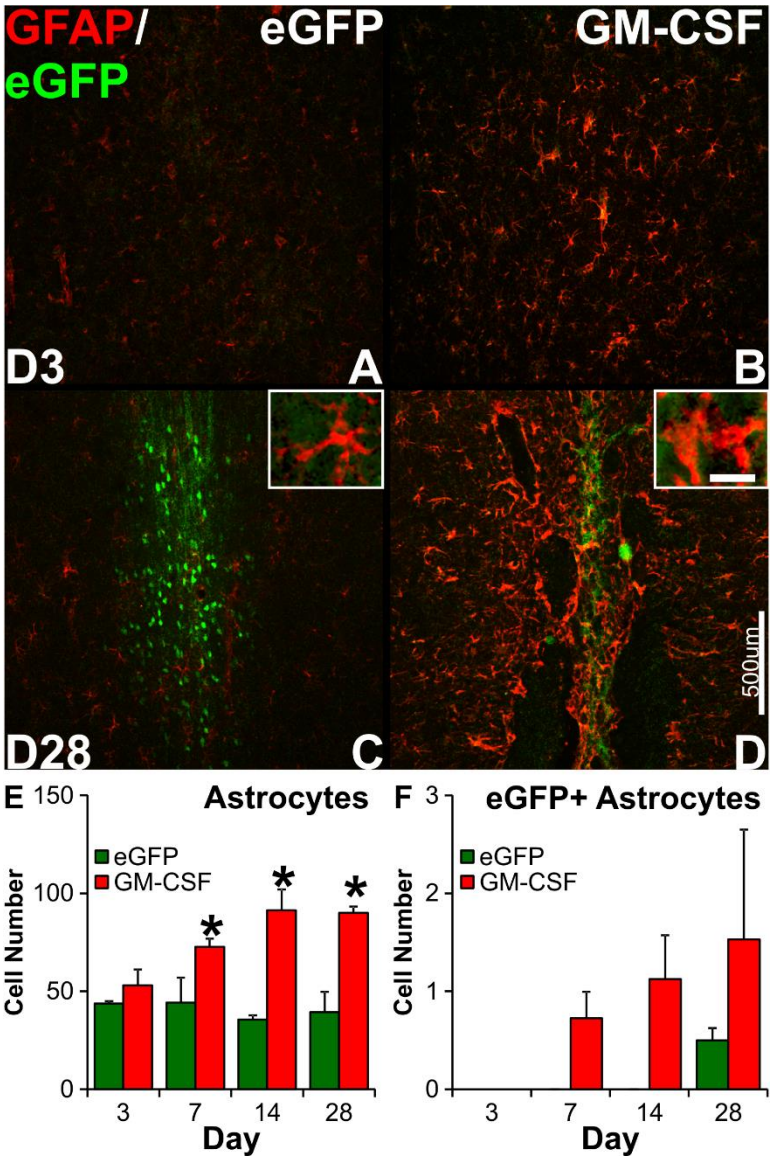

Figure 7: The effect of long-term expression of GM-CSF on astrocyte activation. **A-D:** Coronal brain sections of motor cortex, showing eGFP-positive cells (in green) and GFAP-positive (red) astrocytes, at 3 (A&B) or 28 days (C&D) following injections of eGFP-virus or GM-CSF/eGFP-virus into the motor cortex. **E-F:** Histograms representing the number of GFAP-positive astrocytes per field (E) or eGFP-positive (+) astrocytes per field (F), 3, 7, 14, or 28 days after injection of eGFP-virus (green bars) or GM-CSF/eGFP-virus (red bars) into the motor cortex. (*) $p<0.05$; unpaired student's t-test. Bars and error bars represent the mean and standard error of the mean (SEM).

Using a 40x objective, the number of GFAP-positive astrocytes were counted along the eGFP (Fig. 7D-green bars) or GM-CSF/eGFP injection sites (Fig. 7D-red bars). The number of GFAP-positive astrocytes per field remained constant after longer exposure to the eGFP viruses. However, the GM-CSF/eGFP-injected motor cortex showed a gradual increase in the number of GFAP-positive astrocytes per field. There was a significantly greater number of GFAP-positive

astrocytes per field following GM-CSF/eGFP-injections at day 7, 14 and 28 in comparison to eGFP-injected brains. The GM-CSF/eGFP-injected cortex showed 73±4 GFAP-positive astrocytes per field at day 7, 91±10 at day 14 and 90±3 at day 28. In contrast there were 44±13 GFAP+ astrocytes per field at day 7, 36±2 at day 14 and 39±10 at day 28 ($p<0.05$; unpaired student's t-test) in eGFP-injected brains.

In addition, to find out if astrocytes were being transduced by the viral vectors, the number of cells that were both GFAP- and eGFP-positive were counted along the eGFP (Fig. 7E-green bars) or GM-CSF/eGFP (Fig. 7E-red bars) injection sites. The presence of eGFP-positive astrocytes was evident at 7, 14 and 28 days following GM-CSF/eGFP injection to the motor cortex. However, eGFP-positive astrocytes were found only at 28 days after eGFP-virus injection. At all time-points except day 3, the GM-CSF/eGFP-injected motor cortex appeared to have more eGFP-positive astrocytes per field than those injected with eGFP. However this difference was not significant ($p>0.05$; unpaired student's t-test).

The effect of cortical injection of GM-CSF viral vectors on leukocytes.

To further evaluate the inflammatory response to GM-CSF granulocytes, T-cells and monocytes where counted along the injection sites in brains injected with eGFP-virus (10^8 TU/ml) or GM-CSF/eGFP viral mixture (10^7 & 10^8 TU/ml). The animals were killed at 3 (eGFP-virus group n=1 & GM-CSF/eGFP group n=4), 7 (n=2 & n=4), 14 (n=2 & n=4), or 28 (n=2 & n=4) days post injection.

Granulocyte recruitment

To identify granulocytes, sections demonstrating eGFP-positive cells (Fig. 8-green) along the needle tack were fluorescently stained for endogenous peroxidase (Fig. 8-red). Three days after injection of eGFP-virus there was a strong recruitment of endogenous peroxidase-positive cells to the site of injection (Fig. 8A). However, by day 28 post injection the numbers of presumptive granulocytes had declined (Fig. 8B). There was also an extensive granulocyte influx at 3 days after injection of GM-CSF/eGFP viral mixture (Fig. 8C) but these numbers remained high even at day 28 post injection (Fig. 8D). Unlike microglial activation, GM-CSF-mediated granulocyte recruitment did not extend far beyond the injection sites.

These observations were quantified. eGFP-virus injection produced 124 granulocytes per field at day 3 (Fig. 9A-green bars) but less than one granulocyte per field by day 7. At day 14 and 28 there were 2±1 and 4±2, granulocytes per field respectively. Like eGFP-virus, GM-CSF/eGFP-virus injection was associated with an initial increase and subsequent decrease in granulocyte numbers (Fig. 9A-red bars). At day 3 there were 91±7 granulocytes present, this number decreased to 12±6 at day 7 and to 5±2 at day 14. At the day 28 time point there was a second peak; there were 50±11 granulocytes per field in the GM-CSF/eGFP-injected motor cortex. In comparison to eGFP-virus, GM-CSF/eGFP-delivery resulted in a greater granulocyte influx at day 28 ($p<0.05$; unpaired student's t-test). All other comparisons were not significant.

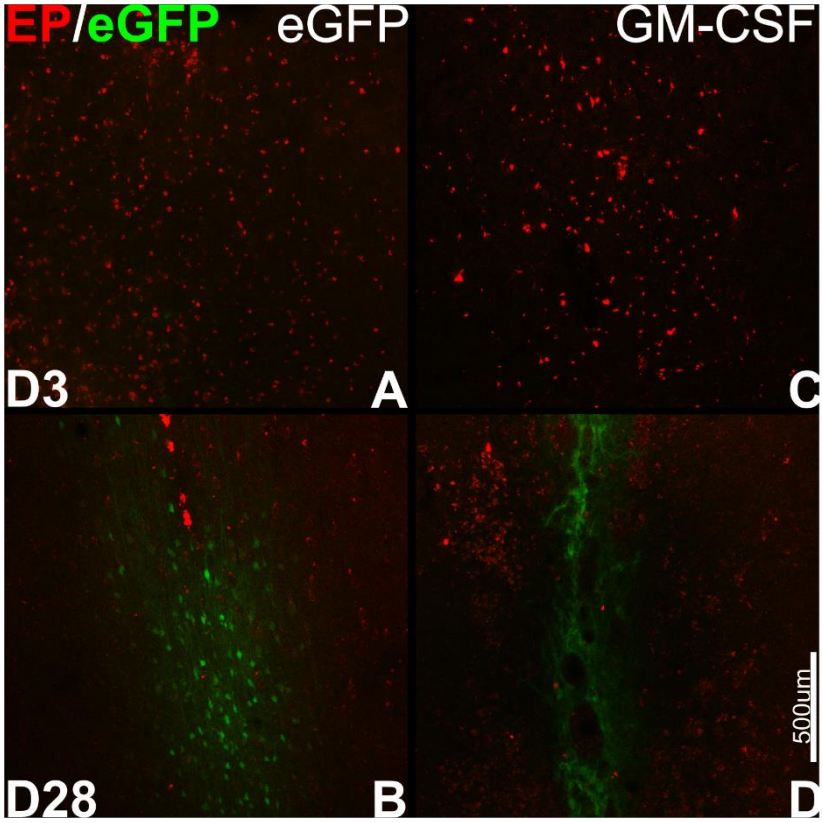

Figure 8: GM-CSF increases granulocyte recruitment to the motor cortex. **A-D:** Coronal brain sections of motor cortex stained for endogenous peroxidase (EP) to identify granulocytes (in red), and showing eGFP-positive cells (in green), at 3 (A&C) or 28 days (B&D) following eGFP-virus or GM-CSF/eGFP-virus injections to the motor cortex. At 28 days there is greater granulocyte recruitment to the motor cortex following injection of GM-CSF/eGFP-virus rather than eGFP-virus.

T-cells recruitment

To examine the effect of GM-CSF/eGFP-virus on T-cell recruitment, sections through the eGFP-virus (Fig. 9B-green bars) and GM-CSF/eGFP-virus (Fig. 9B-red bars) injection sites were stained for T-Cell Receptor (TCR). As time increased, the number of T-cells per field being recruited to the site of eGFP-virus injection increased: three days following eGFP-virus injection to the motor cortex there were 2±2 T-cells per field and by day 28 there were 22±73 T-cells per field. In contrast T-cell recruitment following GMSF/eGFP injection remained constant: There were 18±3 T-cells per field at day 3 and 18±6 T-cells per field at day 28. In comparison to eGFP control, GM-CSF/eGFP viral mixture delivery to the motor cortex showed significantly higher recruitment of T-cells per field at day 3, suggesting that there is an earlier T-cell recruitment following GM-CSF/eGFP-virus injection than eGFP-virus injection.

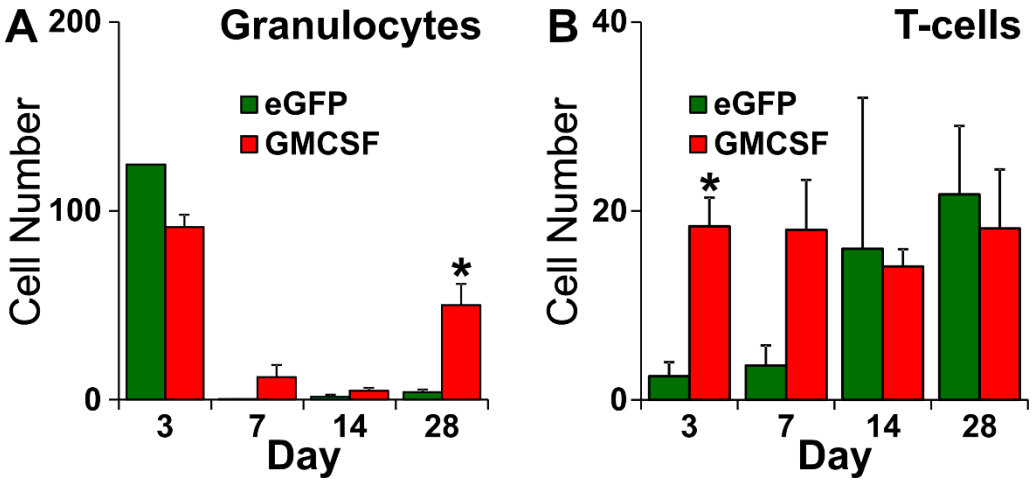

Figure 9: Quantitation of granulocytes and T-cell number following eGFP- or GM-CSF/eGFP-injections to the motor cortex. **A-D**: Histograms representing the number of granulocytes per field (A), or TCR-positive T-cells (B), at 3, 7, 14, or 28 days after injection of eGFP-virus (green bars) or GM-CSF/eGFP-virus (red bars) into the motor cortex. (*) $p<0.05$; unpaired student's t-test. Bars and error bars represent the mean and standard error of the mean (SEM).

Monocyte recruitment

Following GM-CSF/eGFP treatment to the motor cortex there was an abundant presence of IBA1-positive cells that had a rounded shape typical of a phagocytic microglia or a peripheral macrophage. To evaluate whether macrophages are being derived from the periphery, the effect of GM-CSF/eGFP on blood-derived monocytes recruitment to the motor cortex was assessed. Twenty-four hours

prior to perfusion, rats injected with eGFP-virus or GM-CSF/eGFP-virus received an intravenous injection of fluorospheres (10ul/g), which are red fluorescent spheres that can be phagocytosed by circulating monocytes. To distinguish between failed (Fig. 10 A) and successful (Fig. 10 B) intravenous injections, transverse sections through the spleen were taken and examined for fluorosphere presence. Only rats with successful fluorosphere delivery were examined at 3 (eGFP-virus n=0 & GM-CSF/eGFP-virus n= 3), 7 (n=1 & n= 2), 14 (n=2 & n=2), or 28 (n=2 & n=3) days post eGFP-virus or GM-CSF/eGFP intracranial injections.

First, the total number of leukocytes in the blood was measured by counting DAPI-positive nuclei using a 40x objective lens along the midline of blood smears of eGFP-virus or GM-CSF/eGFP-virus injected rats. Leukocytes were divided into two groups according to the shape of the nucleus: multilobulated nuclei corresponded to granulocytes (Fig. 10C-blue) and rounded nuclei belonged to monocytes/lymphocytes (Fig. 10D-blue). Following eGFP-virus (Fig. 10E-blue line) or GM-CSF/eGFP-virus (Fig. 10E-pink line) cortical injections, there were more monocytes/lymphocytes per field in the blood than granulocytes at all time-points. In addition, the percentage of monocytes/lymphocytes and granulocytes in the blood remained essentially unchanged across all time points post eGFP-virus or GM-CSF/eGFP-virus injections.

Next, the number of fluorospheres that were in close proximity to the nuclei of granulocytes or monocytes/lymphocytes (i.e. incorporated by the corresponding cell) were counted. It was observed that in both the eGFP and GM-CSF/eGFP groups, monocytes/lymphocytes (Fig. 10D-red) rather than granulocytes (Fig. 10C-red) avidly phagocytosed fluorospheres.

Fewer fluorospheres were incorporated by monocytes/lymphocytes as time passed in eGFP-virus injected rats. There were 20%±20% of monocyte/lymphocytes with an incorporated fluorosphere per field at day 14 but by day 28 there was no evidence of fluorosphere incorporation (Fig. 10G-blue line). In contrast, GM-CSF/eGFP-virus injection showed an initial decrease in the percentage of monocytes/lymphocytes that had incorporated fluorospheres from day 3 to 7 (Fig. 10G-pink line), then at day 14 and 28 there was an increase in

the percentage of monocyte/lymphocytes showing fluorosphere incorporation. Fluorospheres had been incorporated into 44%±12% of monocytes/lymphocytes per field at day 14 and 32%±32% at day 28. Nonetheless, there was no significant difference at day 14 and 28 ($p>0.05$; unpaired student's t-test) between the percentage of monocyte/lymphocytes that had incorporated fluorospheres between the eGFP and GMCSF/eGFP groups.

With regard to the non-incorporated fluorospheres, eGFP-virus injection was associated with an increasing percentage of free-floating fluorospheres per field as time increased (Fig. 10F-blue line). In contrast, across all time points the percentage of non-incorporated fluorospheres in the blood remained essentially unchanged in rats injected with GM-CSF/eGFP-virus at the motor cortex (Fig. 10F-pink line). Although, in the eGFP group there was a greater percentage of free floating fluorospheres at day14 and 28 than in the GM-CSF/eGFP group, this difference was not significant ($p>0.05$; unpaired student's t-test).

Finally, monocyte recruitment to the injection site in the motor cortex of rats injected with eGFP-virus (Fig. 10H-blue line) or GM-CSF/eGFP-virus (Fig. 10H-pink line) was determined by counting the number of fluorospheres co-localising with amoeboid-shaped IBA1-positive cells. The delivery of GM-CSF/eGFP-virus to the motor cortex failed to provoke the recruitment of IBA1-positive/fluorosphere-positive monocyte to the injection site. Following GM-CSF/eGFP injection there was around 1 IBA1-positive cell containing a fluorosphere per field at 14 and 28 days post virus delivery to the motor cortex, which was similar to that observed when eGFP-virus was injected.

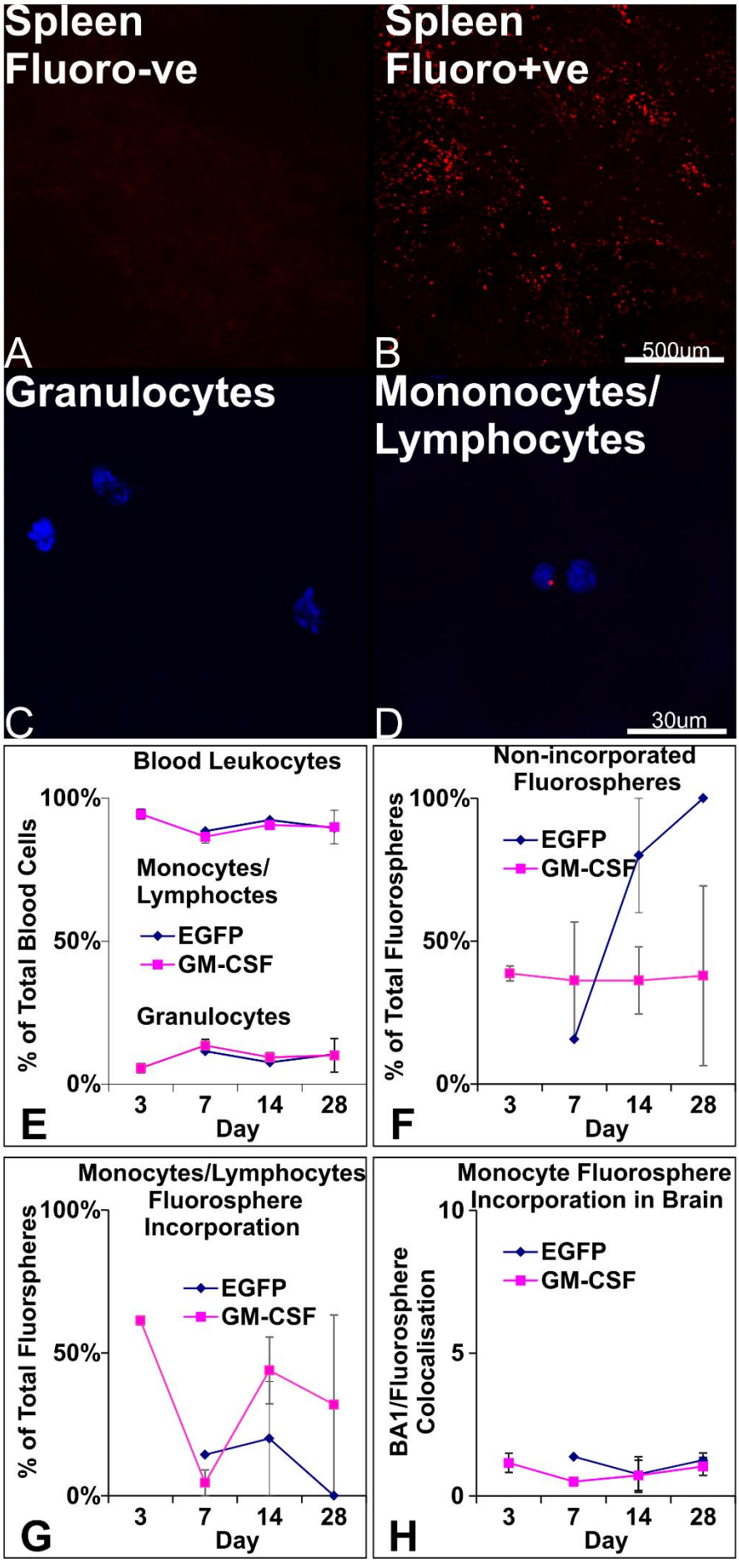
Spleen
Fluoro-ve
A
Spleen
Fluoro+ve
B
500um
Granulocytes
C
Mononocytes/
Lymphocytes
D
30um
Blood Leukocytes
% of Total Blood Cells
100%
50%
0%
Monocytes/
Lymphoctes
EGFP
GM-CSF
Granulocytes
3
7
14
28
Day
E
Non-incorporated
Fluorospheres
% of Total Fluorospheres
100%
50%
0%
EGFP
GM-CSF
3
7
14
28
Day
F
Monocytes/Lymphocytes
Fluorosphere
Incorporation
% of Total Fluorspheres
100%
50%
0%
EGFP
GM-CSF
3
7
14
28
Day
G
Monocyte Fluorosphere
Incorporation in Brain
BA1/Fluorosphere
Colocalisation
10
5
0
EGFP
GM-CSF
3
7
14
28
Day
H

Figure 10: The effect of GM-CSF on blood leukocytes and the recruitment of monocytes to the brain. **A-H:** Rats injected with eGFP-virus or GM-CSF/eGFP-virus into the motor cortex were injected i.v. with fluorospheres 24hrs before sacrifice. **A-B:** Sections through the spleen showing the absence (A) or presence (B) of fluorospheres (red) in the spleen, corresponding to a failed or a successful fluorosphere injection, respectively. **C-D:** Cells in the blood smear. Cells were identified by the shape of the DAPI-positive nucleus. Lobed nuclei allowed granulocytes(C) to be identified and rounded nuclei allowed monocytes/lymphocytes (D to be identified. **(E)** Line graphs representing the percentage of nucleated blood cells per field. **(F)** The percentage of non-incorporated fluorospheres in the blood. **(G)** The percentage of fluorospheres incorporated by monocyte/lymphocytes in the blood. **(H)** The percentage fluorospheres incorporated by IBA1-positive monocyte in the brain, at 3, 7, 14 or 28 days after injections of eGFP-virus (blue line) or GM-CSF/eGFP-virus into the motor cortex (pink line). Data points and error bars represent the mean percentage and standard error of the mean (SEM).

The inflammatory effect of GM-CSF-virus, injected into the motor cortex, at the level of the hindbrain and spinal cord

As intracortical injections of GM-CSF/eGFP-viral mixture have been found to promote microglia activation around corticospinal neurons, the next step was to evaluate whether GM-CSF/eGFP-virus can stimulate an inflammatory response in the CST, at the level of the pyramids and in the cervical spinal cord.

Rats injected with eGFP-virus (10^8 TU/ml) or GM-CSF/eGFP (10^7 & 10^8 TU/ml) to the motor cortex were allowed to survive for 3 days (eGFP-virus & GM-CSF/eGFP-virus: n=1 & n=4), 7 days (n=2 & n=4), 14 days (n=2 & n=2) and 28 days (n=2 & n=4). Coronal sections through the pyramids and longitudinal horizontal sections through the spinal cord, where stained for IBA1 to visualise microglia or GFAP to visualise astrocytes.

Microglia

In the pyramids, corticospinal axons are ipsilateral to their cells of origin. Transverse sections through the hindbrain at day 28 showed that eGFP-virus-injected rats (Fig. 11A) had fewer IBA1-positive microglia and weaker IBA1 immunoreactivity in both the ipsilateral (EXP) and contralateral (CON) pyramids than did GM-CSF/eGFP-virus- injected rats Fig. 11B).

The number of IBA1-positive microglia were counted in the control and experimental pyramids using a 40x objective lens. Prolonged exposure of eGFP-virus to the forebrain failed to show an increase in the number of IBA1–positive

microglia per field in the control (Fig. 11C-green patterned bars) and experimental pyramids as time passed (Fig. 11C-green bars). In contrast, GM-CSF/eGFP-injection was associated with a gradual increase in the number of IBA1-positve microglia per field in both the control (Fig. 11C-red patterned bars) and experimental pyramids (Fig. 11C- red bars).

Across all the time points studied, the GM-CSF/eGFP-group showed a greater number of microglia per field in both pyramids than the eGFP-group, but a significant difference was only observed at day 14 and 28. In the control pyramids, the GM-CSF/eGFP- group had 48±6 (eGFP: 29±4) microglia per field at day 14 and 57±10 (eGFP: 27±8) at day 28 whereas in the experiment pyramid, there were 61±18 (eGFP: 27±4) microglia per field at day 14 and 71±5 (eGFP: 29±3) at day 28 ($p<0.05$; unpaired student's t-test).

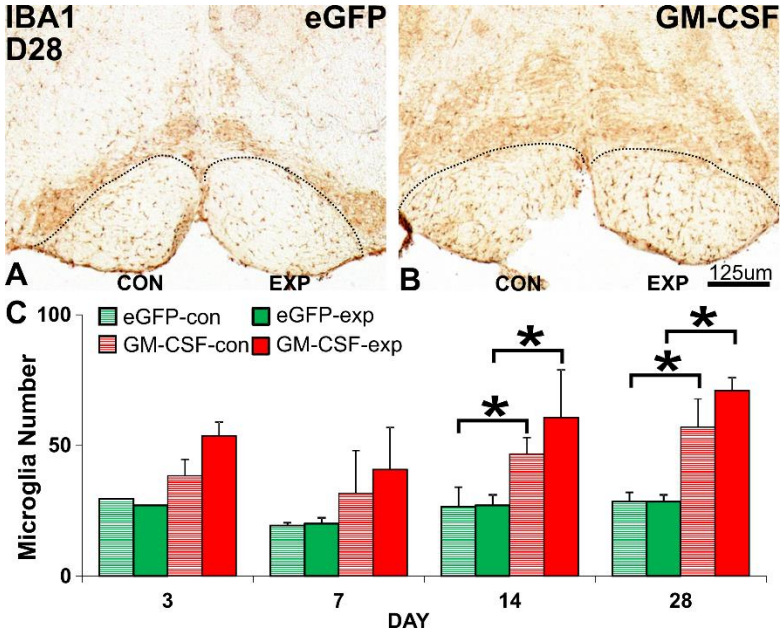

Figure 11: GM-CSF/eGFP virus increases microglia activation in the control and experimental pyramids. **A-B:** Coronal brain sections of hindbrain stained for IBA1 showing control pyramid (CON) and experimental pyramid (EXP), at 28 days after injection of eGFP-virus (A) or GM-CSF/eGFP-virus into the motor cortex (B). **C:** Histogram representing the number of IBA1-positive microglia per field in the control (patterned bars) or experimental pyramids (plain bars), at 3, 7, 14, or 28 days after injection of eGFP-virus (green bars) or GM-CSF/eGFP-virus (red bars) into the motor cortex. (*) $p<0.05$; unpaired student's t-test. Bars and error bars represent the mean and standard error of the mean (SEM).

In the spinal cord, the dorsal corticospinal tracts are contralateral to their cells of origin. Longitudinal horizontal sections through the cervical spinal cords showed the corticospinal tract that is ipsilateral (CON: control) and contralateral (EXP: experimental) to the eGFP-virus (Fig. 12A) or GM-CSF/eGFP-virus (Fig. 12B) injection site. At 28 days after injection of eGFP-virus, rats had few IBA1-positive microglia in the control and experimental corticospinal tracts and there was little difference between the two tracts. In contrast, after GM-CSF/eGFP-virus injection to the motor cortex, there was higher microglial density in the experimental corticospinal tract than in the control corticospinal tract. In comparison to the eGFP-virus group, the GM-CSF/eGFP injected rats had more IBA1-positive microglia in the control and experimental corticospinal tracts and they were more strongly immunoreactive.

The number of IBA1-positive microglia was counted along the corticospinal tract using four fields of a 40x objective lens. As with the pyramids, eGFP-virus at the motor cortex had little effect on IBA1-positive microglia in the control (Fig. 10C-green patterned bars) and experimental corticospinal tracts (Fig. 10C-green bars). However, from 3 to 28 days following GM-CSF/eGFP-injection, there was a steady increase in the number of IBA1–positive microglia in both the control and experimental corticospinal tracts. In comparison to the eGFP-group, the GM-CSF/eGFP-injected groups had greater microglial density in both corticospinal tracts at all time-points and a significant difference was evident at day 14 and 28. The experimental corticospinal tracts of the GM-CSF/eGFP treated animals had 10±0 microglia per field at day 14 and 15±1 at day 28; this was significantly higher than the 8±1 microglia per field found at day 14 and 8±0 at day 28 in those injected with eGFP-virus to the motor cortex ($p<0.05$; unpaired student’s t-test).

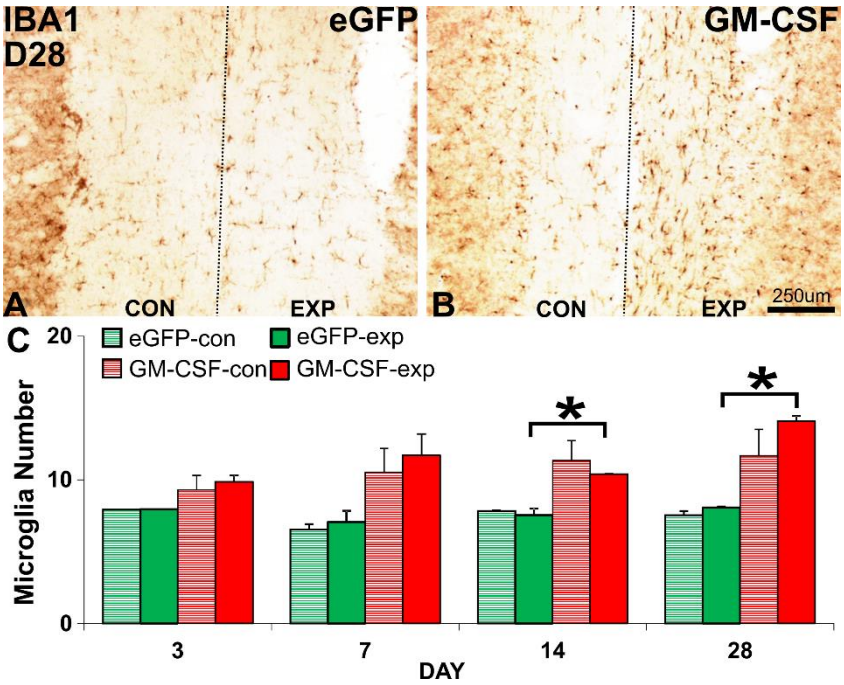

Figure 12: GM-CSF/eGFP-virus increases microglial activation in the control and experimental corticospinal tracts. **A-B:** Longitudinal horizontal sections of spinal cords stained for IBA1 showing control corticospinal tract (CON) and experimental corticospinal tract (EXP), 28 days after injection of eGFP-virus (A) or GM-CSF/eGFP-virus (B) into the motor cortex. **C:** Histogram showing the number of IBA1-positive microglia per field in the control corticospinal tract (patterned bars) or experimental corticospinal tract (plane bars), 3, 7, 14, or 28 days after injection of eGFP-virus (green bars) or GM-CSF/eGFP-virus (red bars) into the motor cortex. (*) $p<0.05$; unpaired student's t-test. Bars and error bars represent the mean and standard error of the mean (SEM).

Astrocytes

Astrogliosis was also evident in the pyramids of animals injected with GM-CSF/eGFP-virus at the motor cortex, although it was not as pronounced as microgliosis. At day 28, rats injected with GM-CSF/eGFP-virus (Fig. 13A) had stronger immunoreactivity for GFAP in the control and experimental pyramids than did rats injected with eGFP-virus (Fig. 13B). To quantify this effect, GFAP-positive astrocytes in the control and experimental pyramids were counted using a 40x objective lens. The effect of eGFP-virus on the number of GFAP-positive astrocytes per field in the control (Fig. 13C-green patterned bars) and experimental pyramids was minimal (Fig. 13C-green bars), as there was no change in astrocyte density between 3 to 28 days post injection. Rats exposed to GM-CSF/eGFP-virus also showed little change with time in the number of GFAP-

positive astrocytes per field in the control (Fig. 13C-red patterned bars) and experimental pyramids (Fig. 13C-red bars). Nonetheless, GM-CSF/eGFP-injected rats had a greater number of GFAP-positive astrocytes from day 3 to day 28 in the control and experimental pyramids. At 28 days post GM-CSF/eGFP injections to the motor cortex, the experimental pyramid had 32±3 astrocytes per field, which was significantly higher than the 21±2 astrocytes per field present in the eGFP-virus injected rats ($p<0.05$; unpaired student's t-test). All other comparisons were not significant.

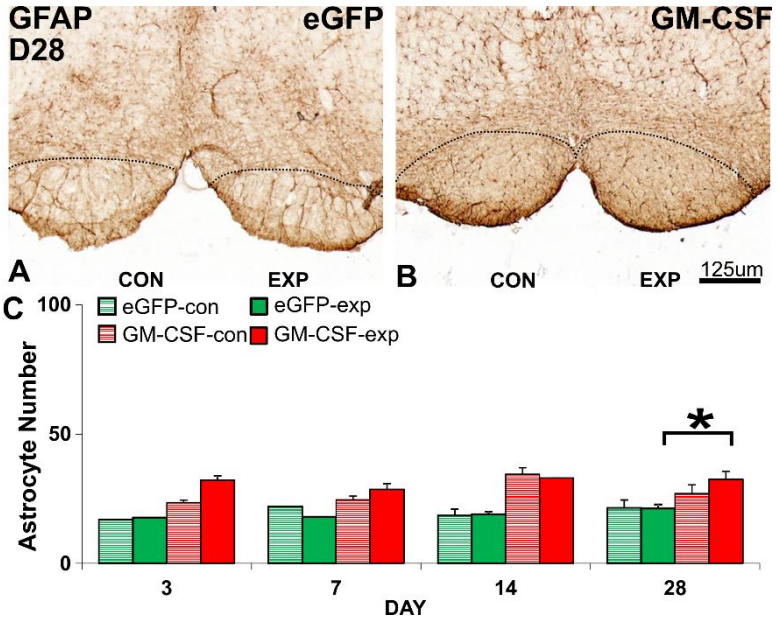

Figure 13: GM-CSF/eGFP virus increases astrocyte activation in the experimental pyramid at day 28. **A-B:** Coronal brain sections of hindbrains stained for GFAP showing the control pyramid (CON) and experimental pyramid (EXP), 28 days after injection eGFP-virus (A) or GM-CSF/eGFP-virus into the motor cortex (B). **C:** Histogram representing the number of GFAP-positive astrocytes per field in the control (patterned bars) or experimental pyramids (plane bars), 3, 7, 14, or 28 days after injection of eGFP-virus (green bars) or GM-CSF/eGFP-virus (red bars) into the motor cortex. (*) $p<0.05$; unpaired student's t-test. Bars and error bars represent the mean and standard error of the mean (SEM).

Astrocyte activation was also evident at the corticospinal tract in the cervical spinal cord. At 28 days post GM-CSF/eGFP-injection (Fig. 14B) to the motor cortex there was higher astrocyte density and GFAP immunoreactivity in the control and experimental corticospinal tracts than eGFP-injected rats (Fig. 14A). Quantification of GFAP-positive astrocytes, revealed that EGFP-virus injection failed to have an effect on astrocyte activation in the control (Fig. 14C- green patterned bars) and experimental corticospinal tracts as time increased (Fig. 14C-

green bars). In comparison, from day 3 to day 28, GM-CSF/eGFP-injected rats had an increasing number of GFAP-positive astrocytes per field in the control (Fig. 14C- red patterned bars) and experimental corticospinal tracts (Fig. 14C- red bars). Although there were greater numbers of astrocytes per field in the control corticospinal tract of the GM-CSF/eGFP injected rats than eGFP-injected rats at all of the time points, it was only at day 7 that there was a significant effect. However, the experimental corticospinal tract showed significantly higher numbers of GFAP-positive astrocytes in GM-CSF/eGFP injected rats than it did in eGFP-injected rats, at day 7 (GM-CSF= 11±2 vs eGFP= 7±0), 14 (11±1 vs 8±0) and 28 (12±2 vs 8±0) ($p<0.05$; unpaired student's t-test).

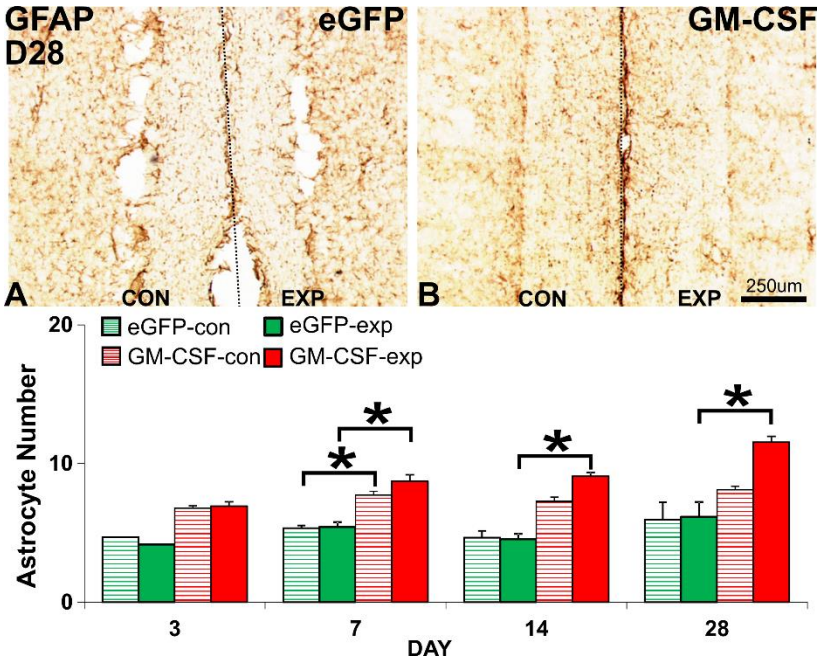

Figure 14: GM-CSF/eGFP virus increases astrocyte activation in the control and experimental corticospinal tracts. **A-B:** Horizontal sections of spinal cords stained for GFAP showing the control corticospinal tract (CON) and experimental corticospinal tract (EXP), 28 days after injections of eGFP-virus (A) or GM-CSF/eGFP-virus into the motor cortex (B). **C:** Histogram showing the number of GFAP-positive astrocytes per field in the control corticospinal tract (patterned bars) or experimental corticospinal tract (plain bars), 3, 7, 14, or 28 days after injections of eGFP-virus (green bars) or GM-CSF/eGFP-virus (red bars) into the motor cortex. (*) $p<0.05$; unpaired student's t-test. Bars and error bars represent the mean and standard error of the mean (SEM).

Part 3: Dose response

Increasing dose of GM-CSF virus increases cell death and microglial proliferation, and decreases the number of surviving transduced cells

The time course experiments have demonstrated that injecting GM-CSF virus at 10^7 TU/ml successfully increases perineuronal inflammation. However this effect is associated with substantial tissue damage and corticospinal neuron loss. Therefore, the next step was to find a concentration that causes moderate microglia activation and little tissue damage.

Rats received intracranial injections of eGFP-virus at 10^8 TU/ml (n=2) or GM-CSF/eGFP virus mixture at the following dilutions: 10^3 (GM3: n=2), 10^4 (GM4: n=2), 10^5 (GM5: n=2), 10^6 (GM6: n=2), or 10^7 (n=2) TU/ml. Animals were allowed to survive 14 days after injection. Coronal sections through the injection site containing eGFP-positive cells were fluorescently stained for IBA1 to visualise microglia and for TUNEL, to identify cell death associated with DNA damage.

Fourteen days following eGFP-virus injection to the motor cortex (Fig. 15A) there were very few or no TUNEL positive cells (Fig. 15A- in red), a large number of eGFP-positive neurons (Fig. 15A-in green) and no surrounding phagocytic microglia (Fig. 15A-in blue). However, delivery of GM-CSF/eGFP at a concentration of 10^7 (TU/ml) to the motor cortex (Fig. 15B) produced fluid-filled spaces, a high number of TUNEL-positive cells (Fig. 15B-in red), few eGFP-positive cells (Fig. 15B- in green) and a high density of phagocytic microglia.

Using a 40x objective lens, the number of resting, reactive and phagocytic IBA1-positive microglia (Fig. 15C-all MG) were counted along the injection site. Injecting higher doses of GM-CSF/eGFP-virus into the motor cortex, increased the number of IBA1-positive microglia per field. Concentrations GM4 (Fig. 15C-yellow bar), GM5 (Fig. 15C-blue bar) and GM6 (Fig. 15C-purple bar) showed a trend towards producing more IBA1 positive microglia than did eGFP-virus (Fig. 15C-green bar). However, GM7-injected cortices (Fig. 15C-red bar) had a significantly higher number of IBA1-positive microglia per field than those injected with eGFP, GM3, GM4 and GM5 ($p<0.05$; Tukey post hoc test to a univariate ANOVA).

From all the microglia analysed at the injection site, the subpopulation of microglia with a rounded morphology, typical of the phagocytic state, were counted separately (Fig. 15C-Phagocytic). The number of phagocytic microglia per field increased with higher doses of GM-CSF/eGFP-virus. In comparison to eGFP (0±0), there was a trend towards more phagocytic microglia per field in the motor cortex of rats injected with GM4 (16±6). Concentrations GM5 (27±6) and GM6 (50±1) produced a greater phagocytic microglia density than did the eGFP and GM3 (1±0) groups. Finally, the GM7-injected motor cortex had more phagocytic microglia per field (83±112) than did eGFP, GM3, GM4 and GM5 ($p<0.05$; Tukey post hoc test to a univariate ANOVA).

As well as increasing the number of phagocytic microglia, the presence of higher doses of GM-CSF/eGFP-virus also increased the number of TUNEL-positive cells (Fig. 15C-TUNEL). Injecting control virus or lower doses of GM-CSF/eGFP virus (GM3 to GM5) resulted in a few cells being TUNEL-positive. However, a sharp increase in the number of TUNEL-positive cells per field was evident at concentrations GM6 (65±26) and GM7 (101±9). Injecting GM6 to the motor cortex was associated with a trend towards higher numbers of TUNEL-positive cells per field than eGFP (7±2) and GM3 (6±2). A significantly higher number of tunnel-positive cells per field was found in the cortex of rats injected with GM-CSF/eGFP-virus at GM7 than in the cortex of eGFP, GM3, GM4 (13±3) and GM5 (15±1)-injected animals ($p<0.05$; Tukey post hoc test to a univariate ANOVA).

The increase in the number of TUNEL-positive cells coincided with a reduction in the number of eGFP-positive cells following GM-CSF/eGFP-injections. Increasing the concentration of GM-CSF/eGFP virus produced a decrease in the number of eGFP-positive cells per field (Fig. 15C-eGFP). There were significantly fewer eGFP-positive cells per field in the motor cortex of rats injected with GM4 (40±7), GM5 (22±6), GM6 (19±4) or GM7 (13±3), when compared to cortex injected with eGFP-virus (85±4) (Fig. 13: C-green bar) ($p<0.05$; Tukey post hoc test to a univariate ANOVA).

Despite moderate microglial activation, there was little cell death and a low number of phagocytic microglia at the GM-CSF 10^4-10^5 TU/ml doses; this makes them good candidates to investigate effects of inflammation without toxicity.

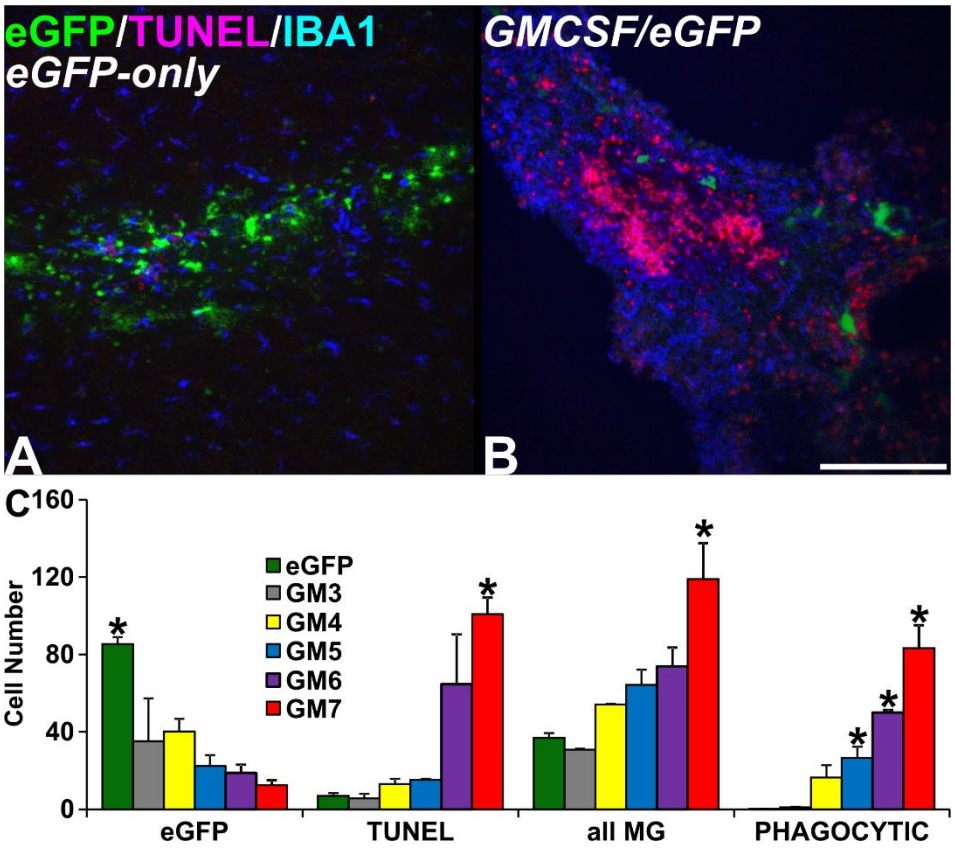

Figure 15: Dose dependent effects of GM-CSF/eGFP virus in the motor cortex of rats. A-B: Coronal brain sections of motor cortex stained for IBA1 (in blue) and TUNEL (in red) and showing eGFP-positive cells (in green), 14 days after injection of eGFP-virus (A) or GM7-virus (B) into the motor cortex. Bar Scale: 250 C: Histogram representing the number of eGFP-positive cells per field, TUNEL-positive nuclei per field, IBA1-positive microglia per field, or IBA1-positive phagocytic microglia per field, following cortical injections of eGFP-virus (green bar), or GM-CSF/eGFP-virus at 10^3 TU/ml (GM3:grey bar), 10^4 TU/ml (GM4: yellow bar), 10^5 TU/ml (GM5: blue bar), 10^6 TU/ml (GM6: purple bar), or 10^7 TU/ml (GM7: red bar). (*) $p<0.05$ Tukey post hoc test to univariate ANOVA. Bars and error bars represent the mean and standard error of the mean (SEM).

GM-CSF-induced inflammation is evident in the corticospinal tracts

It has been shown above that 14 days after cortical injections of GM-CSF/eGFP there is a dose-dependent increase in cell death and phagocytic microglia in the motor cortex. The inflammatory effects of GM-CSF expression in the corticospinal tracts in the pyramids and the cervical spinal cord were also studied. Fourteen days after intracortical injections of eGFP-virus (10^8 TU/ml: n=2) or different

doses of GM-CSF/eGFP (10^3 to 10^7 TU/ml: n=2 per dose), transverse sections through the hindbrain and longitudinal horizontal sections through the cervical spinal cord were collected. Sections were immunostained for IBA1 to visualise microglia.

Delivery of moderate to high doses of GM-CSF/eGFP virus to the motor cortex increased the level of IBA1 immunoreactivity in the control (Fig. 16-CON) and experimental (Fig. 16-EXP) pyramids in rats injected with GM5 (Fig. 16B) or GM7 (Fig. 16C) than those injected with eGFP (Fig. 16A).

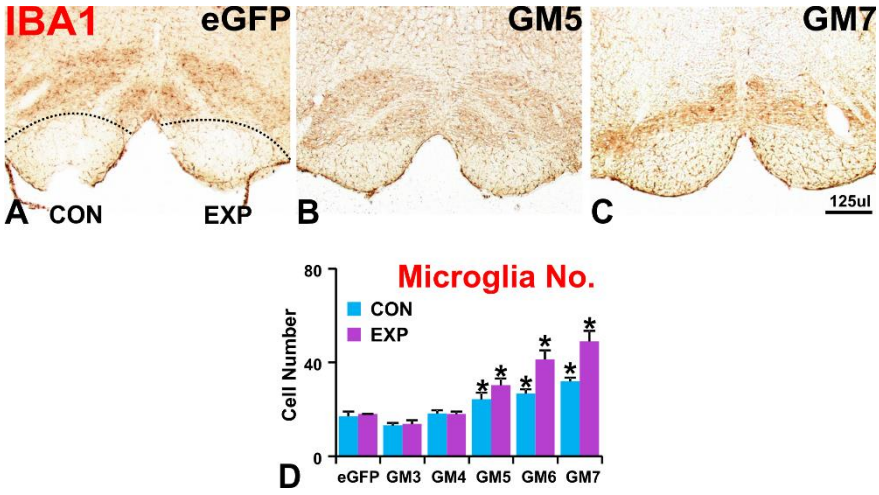

Figure 16: GM-CSF/eGFP-virus increases microglial activation in the control and experimental pyramids. **A-C:** Coronal brain sections of hindbrains stained for IBA1 showing control pyramid (CON) and experimental pyramid (EXP), 14 days after injection of eGFP (A), GM5 (B) or GM7 (C) into the motor cortex (B). **D:** Histogram representing the number of IBA1-postive microglia per field (D) in the control pyramid (blue bars) and experimental pyramids (purple bars), following cortical injections of eGFP-virus, or GM-CSF/eGFP virus at 10^3 TU/ml (GM3), 10^4 TU/ml (GM4), 10^5 TU/ml (GM5), 10^6 TU/ml (GM6), or 10^7 TU/ml (GM7). (*) $p<0.05$ Tukey post hoc test to univariate ANOVA. Bars and error bars represent the mean and standard error of the mean (SEM).

To quantify this effect, the number of IBA1-positive microglia were counted in the control (Fig. 16D-blue bar) and experimental pyramids (Fig. 16D-pink bar) using a 40x objective lens. The experimental pyramid of the rats injected with GM-CSF/eGFP at doses GM5 (30±3), GM6 (41±4) and GM7 (49±5) had more IBA1-positive microglia than those injected with eGFP (18±0), GM3 (14±1), GM4 (18±1) and GM5 (30±3) ($p<0.05$; Tukey post hoc test to a univariate ANOVA).

It was noted that there was also an increased microglial density in the control pyramid in rats injected with GM-CSF/eGFP-virus at GM6 (27±2) and GM7 (32±2)

compared to those injected with eGFP-virus (17±3) or GM3 (13±1). ($p<0.05$; Tukey post hoc test to a univariate ANOVA).

A heightened microglial response was also seen in the corticospinal tract at the level of the cervical spinal cord. Horizontal sections through the cervical spinal cord of rats injected with GM7-virus into the motor cortex (Fig. 17B) showed stronger immunoreactivity for IBA1 in the control and experimental corticospinal tracts than those injected with eGFP-virus (Fig. 17A).

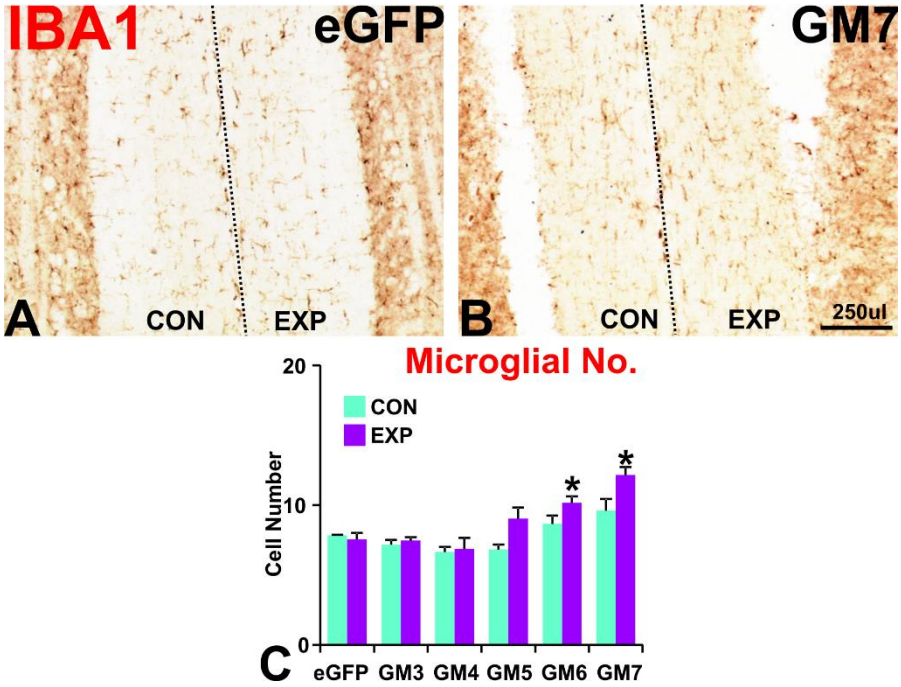

Figure 17: GM-CSF/eGFP virus increases microglial in the corticospinal tracts. A-B: Horizontal sections of spinal cords stained for IBA1 showing the control pyramid (CON) and the experimental corticospinal tracts (EXP), 14 days after injection of eGFP (A), or GM7 (B) into the motor cortex. C: Histogram representing the number of IBA1-postive microglia per field in the control corticospinal tract (blue bars) and experimental corticospinal tract (purple bars), following cortical injections of eGFP-virus, or GM-CSF/eGFP virus at 10^3 TU/ml (GM3), 10^4 (GM4), 10^5 TU/ml (GM5), 10^6 TU/ml (GM6), or 10^7 TU/ml (GM7). (*) $p<0.05$ Tukey post hoc test to univariate ANOVA. Bars and error bars represent the mean and standard error of the mean (SEM).

To confirm this observation, the number of IBA1-positive microglia were counted along the control and experimental corticospinal tracts using a 40x objective lens. The control side corticospinal tract in the eGFP group, concentrations GM3 to GM7 failed to show any significant difference in the number of IBA1-postive microglia compared with eGFP-injected animals (Fig. 17C-blue bars) ($p>0.05$; univariate ANOVA). With regard to the experimental corticospinal tract (Fig. 17C-purple bars), only rats injected with the GM7 (12±1) dose showed a greater IBA1-

positive microglia per field than eGFP–injected animals (8±1) ($p<0.05$; Tukey post hoc test to a univariate ANOVA).

Discussion

GM-CSF is a 14.5-35 kDa glycoprotein that exerts its effects on a large variety of cells by binding to GM-CSF receptor, which is made of an α-subunit and a β-subunit (Chiba et al., 1990). GM-CSF induces granulocyte and macrophage maturation from myeloid progenitor cells (Francisco-Cruz et al., 2014). It can promote the expression of pro-inflammatory cytokines and cytotoxic molecules during inflammation (Hamilton, 1993; Hamilton, 2002), but it has also been associated with pro-regenerative effects in spinal cord injury models (Bouhy et al., 2006; Ha et al., 2005; Huang et al., 2009).The GM-CSF-virus created in this study was efficient at expressing GM-CSF and eGFP protein in vitro. In vivo, prolonged exposure of rat motor cortex to GM-CSF/eGFP virus at high concentration (10^7TU/ml) was found to produce areas of tissue damage, a reduction in the number of eGFP-positive cells, extensive microglial/macrophage and astrocyte activation, recruitment of peripheral granulocytes and T-cells to the injection site. This was associated with reduced numbers of corticospinal neurons. In addition, activation of microglia and astrocytes was seen along the corticospinal tracts of rats injected with high doses of GM-CSF in the motor cortex. A dose-response experiment was therefore performed to determine a viral concentration that resulted in moderate microglial activation with little CNS damage. From 10^3 to 10^7 TU/ml there was a dose-dependent increase in overall microglia density and in the number phagocytic microglia/macrophages, correlated with an increase in TUNEL labelling and a decrease in eGFP-positive cells. Motor cortex injections with 10^4-10^5 TU/ml of GM-CSF virus produced moderate microglia activation but little or no cell death and little phagocytosis. Therefore, this range of doses makes them good candidates to investigate the possible pro-regenerative effects GM-CSF-mediated perineuronal inflammation may have in models of spinal cord injury (Nimmervoll et al., 2013; Taylor et al., 2005).

Efficient lentiviral-mediated expression of GM-CSF in vitro

The GM-CSF-virus in this study was shown to be effective in producing the expression of GM-CSF protein in vitro. Application of supernatant from GM-CSF-virus transfected HEK 293T cells provoked the proliferation of mouse microglia-derived BV2 cells in a titre-dependent manner. GM-CSF-condition medium was a more effective mitogen than 30ng/ml GM-CSF recombinant protein. The proliferative effect caused by GM-CSF on BV2-cells, is line with previous studies using primary microglial cultures (Giulian and Ingeman, 1988; Kloss et al., 1997). Giulian and Ingeman (1988), demostrated that increasing concentrations of mouse GM-CSF recombinant protein augmented the number of rat ameboid microglia per field. It was also shown that GMCSF was a more potent microglial mitogen than M-CSF, G-CSF, IL-1, , IL-2, IL-3, IFN-ɣ and TNF-α. In addtion, Kloss et al., (1997), showed that ramified mouse microglia grown on a rat astrocyte monolayer proliferated in the presence of mouse GM-CSF in a dose-dependent manner.

In the current study the effect of GM-CSF on microglial morphology and function in vitro was not specifically analysed. However, other studies have suggest that GM-CSF promotes microglial ramification in vitro (Fujita et al., 1996), phagocytosis (Giulian and Ingeman, 1988) and antigen presentation (Fischer et al., 1993). Fujita et al. (1996), showed that GMCSF facilitated the ramification of rat microglia in a mixed brain cell culture. In addition, Giulian and Ingeman (1988) showed that cultured rat microglia treated with GM-CSF showed greater incorporation of fluorescently labelled microspheres than M-CSF, G-CSF, IL-1, IL-2, and FGF. Fischer et al., (1993) showed that microglial cultures of new born rats exposed to GM-CSF acquired characteristics of macrophages, such as the expression of complement receptor macrophage-1 (MAC-1) and F4/80, which is a transmembrane protein found in macrophages. In addition, GM-CSF rather than M-CSF was able to efficiently induce antigen-directed proliferation of helper T cells in culture.

Work on BV-2 cells has found that the effect of GM-CSF on microglial proliferation is mediated by the JAK/STAT and MAK pathways. Following exposure to GM-

CSF, BV-2 microglial cells expressed components of the JAK/STAT pathway, such as JAK2, STAT5A and STAT5B. In addition, GM-CSF exposure mediated the phosphorylation of MAP kinases, ERK1 and ERK2 in BV-2 cells (Liva et al., 1999). The expression of JAK2, STAT5A, STAT5B and ERKs are known to be important in controlling cellular proliferation (Francisco-Cruz et al., 2014)

Inflammation and astrogliosis in the motor cortex following GM-CSF delivery using a lentiviral vector

Microglia activation

The current study shows that the prolonged exposure of GM-CSF-virus in the rat motor cortex at a high titre increases the number of IBA1-positive microglia, induces a phagocytic phenotype in microglial, and promotes phagocytic microglial cluster formation at the injection site and at the borders of fluid filled areas. There is limited research specifically evaluating the effect of GM-CSF in the cortex of rats. However, support for the finding that GM-CSF produces microglial proliferation and activation in vivo comes from Giulian et al. (1988). Forty-eight hours following injection of recombinant GM-CSF into the cortex of rats, a large number of mononuclear phagocytes were present at the injection site. In addition, co-injecting GM-CSF with polystyrene microspheres showed an accelerated clearance of polystyrene microspheres from the brain compared to rats injected with PBS and polystyrene microspheres. A similar effect was also seen following the intracerebral delivery of IL-3 and a less intense effect when M-CSF or G-CSF was injected. Another study looking at the effect of GM-CSF in the cortex of organotypic slice cultures showed that GM-CSF stimulated proliferation and migration of small round microglia from a rat cortex slice. These cells were positive for CD11b (Ox42), isolectin B4-lectin-binding, the monocyte marker ED1 and partially expressed major histocompatibility complex (MHC) II (Schermer and Humpel, 2002).

The present study has shown that high concentrations of GM-CSF may be having a toxic effect. In addition to the presence of phagocytic microglia, there is apparent tissue damage characterised by the appearance of fluid-filled areas, and a reduction in the number of eGFP-positive cells and corticospinal neurons present in the motor cortex. Activated microglia are known to contribute to secondary damage by releasing cytotoxic molecules. Intracerebroventricular

injections of recombinant mouse GM-CSF protein in C57/BL6 mice increased the production of pro-inflammatory cytokines TNF-α, IL1-β and IL-6 in the cerebral cortex (Reddy et al., 2009). These cytokines have been associated with neuronal damage in the CNS.

Astrocyte activation

Astrocytes play an important role in the regulation of immune-mediated processes in the central nervous system. They are able to proliferate, to form the glial scar in astrogliosis, to perform phagocytosis, to express MHC class I and II (Aloisi et al., 1992a; Frei et al., 1994; Sawada et al., 1989; Vidovic et al., 1990) and to secrete cytokines involved in the inflammatory process (Aloisi et al., 1992b; Malipiero et al., 1990; Rubio and Sierra, 1993; Sawada et al., 1989).

The expression of GM-CSF in the rat motor cortex increased astrocyte activation, characterised by a change in morphology, GFAP fluorescence intensity and astrocyte density. Reddy et al. (2009) showed that following intracerebroventricular injections of GM-CSF there was increased expression of GFAP mRNA in the brain C57/BL6 mice as well as GFAP immunoreactivity by astrocytes in the hippocampus and midbrain. However, it may be that astrocyte activation may be mediated by the secretion of inflammatory cytokines by microglia rather than GM-CSF directly affecting astrocytes. Microglia secrete TNF-α in response to LPS exposure, when murine astrocytes were grown in the presence of TNF-α it induced astrocyte activation and the secretion of GM-CSF (Malipiero et al., 1990). However, evidence of GM-CSF having a direct effect on astrocytes comes from work on simian astrocyte cultures by Guillemin et al., (1996). They found that the α-subunit of the GM-CSF receptor is expressed in the membrane of cultured simian astrocytes. Furthermore, they demostrated that similar to TNF-α and IL-6, GM-CSF stimulated in vitro the proliferation of simian astrocytes in primary cultures; this was further confirmed by using an antibody against GM-CSF to block proliferation. Nonetheless, little is known about the effect of GM-CSF in astrocytes of rats. An in vitro study of rat astrocyte cultures would confirm whether GM-CSF expressed by the virus can directly stimulating astrocyte proliferation.

Leukocyte recruitment

GRANULOCYTES

The current experiment shows that the GM-CSF attracts large numbers of granulocytes to the injection site, which coincides with tissue damage. GM-CSF supports the proliferation and survival of granulocytic precursors in the bone marrow. GM-CSF potentiates the release of oxygen and nitrogen radical ions, and phagocytosis by neutrophils (Bourgoin et al., 1992; Corey and Rosoff, 1989; Kumaratilake et al., 1996) and inhibits their apoptosis (Bourgoin et al., 1992; Corey and Rosoff, 1989; Kumaratilake et al., 1996). In addition, GM-CSF has been found to have a potent effect in inducing the expression on neutrophils of receptors for CC chemokines (Cheng et al., 2001). These are cytokines that have chemoattractant properties whose main documented role is leukocyte recruitment to inflammatory sites.

The recruitment of granulocytes may be due to the direct or indirect effects of GM-CSF. GM-CSF-mediated chemotaxis has been demonstrated using transwell plates, here human granulocytes have been shown to choose to migrate to a chamber containing GM-CSF buffer rather than PBS buffer (Gomez-Cambronero et al., 2003). In an in vivo mouse model of intestinal inflammation GM-CSF neutralisation using antibodies reduced infiltration of neutrophils into the intestine (Khajah et al., 2011). However, leucocyte influx into the central nervous system is frequently a feature of severe brain pathology. The amount and number of different cell types being recruited is dependent on the severity of brain pathology. In contrast to slight or indirect injury, direct brain injury, infection and autoimmune disease results in granulocyte influx into the brain parenchyma (Holmin et al., 1998; Popovich et al., 1997). In the current experiment the influx of granulocytes to the injected motor cortex might be due to the direct chemotactic effects of GM-CSF or the secondary brain damage associated with GM-CSF mediated inflammation.

T-CELLS

There was faster T-cell recruitment to the motor cortex following injection of GM-CSF-virus than eGFP-virus. GM-CSF is known to be released by activated T-cells (Ponomarev et al., 2007) and the release of GM-CSF by autoreactive T-cells

is required for the onset of experimental autoimmune encephalomyelitis (Ponomarev et al., 2007). There is evidence that T-cells contain the GM-CSF receptor α-subunit in their cell membrane, but the direct effect of GM-CSF on T-cells remain elusive (Shi et al., 2006). As GM-CSF can stimulate the production of IL-6 and TNF-α by microglia (Reddy et al., 2009), evidence points to GM-CSF having an indirect effect on T-cell recruitment. IL-6 and TNF-α can increase ICAM expression (Furie and Randolph, 1995; Wahl et al., 1996), which may help T-cells to cross blood vessels and enter the injection site. GM-CSF has also been reported to induce in microglia the transcription of genes important for T-cell chemotaxis (MIP-1α), and antigen processing (MHC II proteins) (Re et al., 2002), which suggest that the T-cell recruitment may be mediated by microglia.

MONOCYTES/MACROPHAGES

The fluorosphere experiments showed that only a few monocytes/macrophages are recruited following GM-CSF injection. Monocytes are hematopoietic cells belonging to the myeloid lineage (van Furth et al., 1979). Monocytes originate from the bone marrow and seed into the tissue to become tissue specific macrophages (Varol et al., 2007). Differentiating between activated microglia and monocytes is difficult because microglia do not express unique surface markers. The similarity between monocytes and activated microglia has led to the idea that microglia are derived from the bone marrow to become brain macrophages (Ginhoux et al., 2010). In the adult brain there is recruitment of low numbers of haematogenous cells that become microglia in the brain. Using adult parabiotic mice, which are mice that have undergone conjoined surgery to share the same blood circulation, it was demonstrated that less than 5% of microglia were of donor origin at 1 and 12 months post-parabiosis (Ginhoux et al., 2010). However, 95% of microglia were of host origin and were derived from mesodermal cells during development (Alliot et al., 1999; Ginhoux et al., 2010). This may suggest that microglia are maintained independently of circulating monocytes throughout life. Following GM-CSF-injection to the motor cortex there were very few recruited monocytes in motor cortex, which may suggest that the abundant round IBA1-positive cells present in the motor cortex injected with GM-CSF may be microglia that have taken up a phagocytic phenotype. However, in models of intracerebral inflammation following experimental contusion injury, it was claimed that there

was monocyte/macrophage recruitment to the site of injury (Holmin et al., 1998). However, they identified the monocytes/macrophages by staining for ED1 antigen and ED1 is also a microglial marker (Graeber et al., 1988a). The presence of ED1-positivwe cells coincided with that of T-cells. The low number of monocytes/macrophages found in the GM-CSF injection site may be due to the technique used to visualise macrophages not being sensitive enough. The macrophages were recognised as round IBA1-positive cells containing fluorospheres. The success rate of injecting fluorospheres intravenously was around 70%, which considerably reduced the number of animals per group; this reduces the statistical power and could have masked any effects GM-CSF-virus may be having on macrophage recruitment.

The effect of GM-CSF on leukocytes circulating in the blood

GM-CSF can cross the blood brain barrier. Schaebitz et al. (2008) showed that rats injected i.v with iodinated GM-CSF had more radioactivity in the brain than those injected with iodinated bovine serum albumin, which suggests that GM-CSF can cross the intact blood brain barrier. This result was in concordance with a previous report that showed the transport of GM-CSF across the blood brain barrier (McLay et al, 1997). For this reason it was hypothesised that GM-CSF expressed in the motor cortex following injection of the viral vector could have an effect on monocytes, lymphocytes or granulocytes circulating in the blood. When mouse GM-CSF protein was injected in mice i.v., there was a trend towards more monocytes/lymphocytes and neutrophils being present in the blood compared to controls (Verdrengh and Tarkowski, 1998). However, rats injected with GM-CSF-virus into the motor cortex showed no increase in the number of monocytes/lymphocytes or granulocytes in the blood when compared to those injected with eGFP-virus. In addition, GM-CSF can have an effect on the phagocytic activity of monocytes. When monocytes isolated from human peripheral blood were grown in serum containing GM-CSF, they increased in size and granularity, had increased phagocytic activity, and expressed various adhesion molecules, CD14 and major histocompatibility complex (MHC) class II. In our study, monocytes/lymphocytes of GM-CSF-injected rats did not show an effect on phagocytosis, as the level of fluorosphere incorporation by monocytes/lymphocytes in rats injected with GM-CF-virus into the motor cortex

was similar to those injected with eGFP-virus. This may be explained by presumably low concentrations of GM-CSF protein entering the blood from the brain, concentrations which fail to produce a significant increase in the number of leukocytes or the phagocytic activity of monocytes/lymphocytes circulating in the blood.

Cell-death is associated with the production of GM-CSF

Cell death can be characterised by morphological changes in cells, such as DNA damage fragmentation (Stoica and Faden, 2010). TUNEL detects DNA fragmentation by labelling the terminal end of nucleic acids (Gavrieli et al., 1992). Cortical delivery of GM-CSF-virus at high concentrations produced TUNEL-positive cell death. This is in line with research by Holmin and Mathiesen (2000), who evaluated the effect of proinflammatory cytokines IL-1 and TNF-α in the rat cerebral cortex. Twenty-four hours after rats received an intracerebral injection of IL-1, rather than TNF-α, there was a significantly higher number of TUNEL-positive cells at the injection site compared to those injected with PBS. In addition, when rats were injected with IL-1 rather than PBS, a large number of macrophages/phagocytic microglia and T-cells were evident at the injection site. The effects of injecting IL-1 into the cerebral cortex returned to baseline at 72 hours post injection. Holmin and Mathiesen (2000), found that 40% of the TUNEL-positive cells were neurons, 20% were mononuclear phagocytes was also detected, and 5% oligodendrocytes. However, there were no GFAP-positive astrocytes that were also TUNEL-positive (Holmin and Mathiesen, 2000). In the current study the identity of the dying cells remains to be characterised. It would appear that GM-CSF-virus injection to the motor cortex is killing neurons, as a reduction in corticospinal neuron number was observed in the GM-CSF-virus injection site compared to the eGFP-virus injection site, but whether they were dying by apoptosis is unknown. Finally, Holmin and Mathiesen (2000) found that the activation of caspase pathway may be promoting TUNNEL-positive cell death. Cells that were TUNEL-positive were in the majority also Bax-positive. Bax is a molecule of the Bcl-2 family that can directly permeabilise mitochondria, which then release cytochrome c from the mitochondrial intermembrane space to the intracellular fluid, which in turn can activate caspases leading to the fragmentation of DNA resulting in cell death (Oltvai et al., 1993).

Microgliosis and astrogliosis along the corticospinal tracts

Corticospinal neurons have long-range axonal projections to the spinal cord so viral transduction of their cell bodies could lead to actions at distant sites along the corticospinal tract (Wong et al., 2006). In fact, mice injected with eGFP-virus to the motor cortex showed eGFP-protein in corticospinal axons within the spinal cord (Rahim et al., 2009). In both the control and experimental pyramidal tracts of the hindbrain there was an increase in the number of microglia and astrocytes following injections into the motor cortex of GM-CSF-virus rather than eGFP-virus. The increased microgliosis and astrogliosis in the control pyramid may be the product of GM-CSF protein diffusing through the corticospinal fluid from the motor cortex to the control corticospinal tract in the pyramid. If this was the case then there would be increased inflammation throughout the CNS rather than specifically in the corticospinal tracts. To examine this it would be necessary to evaluate whether other areas within the control forebrain, hindbrain and spinal cord are also show enhanced inflammation. Alternatively, GM-CSF diffusion may occur at the level of the hindbrain and spinal cord. The corticospinal tracts from the right and left motor cortices remain predominantly segregated before and after the pyramidal decussation. Thus the increased inflammation seen within the control tract may be explained by GM-CSF travelling along the experimental corticospinal axons, being released by those axons and then diffusing from the experimental to control pyramid.

The present study has provided evidence that at high concentrations GM-CSF virus cause corticospinal neuron cell death so inflammation in the experimental pyramid and spinal cord could have been produced by Wallerian degeneration. We found an approximately 50% increase in number of microglia in the control pyramid after 10^7 TU/ml GM-CSF-virus treatment. Microglial activation in the experimental corticospinal tract could be causing by-stander activation of microglia in the control corticospinal tract through the diffusion of microglial-derived factors. However, Jacobowitz and colleagues (2012) reported the presence of increased microglial reactivity around degenerating axons along the length of the experimental corticospinal tract following traumatic brain injury in rats. Activated microglia were, however, not observed on the control side. It is

thus likely that the microgliosis observed in the control corticospinal tract in our study could be due to the GM-CSF diffusion from the experimental to control CST.

Conclusion

A non-integrating lentiviral vector that encodes for both GM-CSF and eGFP was created. In vitro, the virus led the production of eGFP and bioactive GM-CSF. In vivo, injections of high titre GM-CSF virus causes chronic inflammation and astrocyte activation in the rat motor cortex which is associated with neurotoxic effects. Microglia and astrocyte activation was also observed along the corticospinal tract following cortical injections of the virus. Action of GM-CSF in the brain and spinal cord appears to be mediated locally without any systemic effect on peripheral leucocytes.

CHAPTER FIVE

Mouse strain-dependent neuroinflammatory response to lentiviral delivery of GM-CSF: Modelling toxic effects of microglia activation

Introduction

In peripheral tissues, macrophages can be classified in two main groups: classically activated macrophages that express pro-inflammatory cytokines (TNF-α, IL1-β, IL-12 and IL-6), chemokines (CXCL1, CCL5) and NO (Chhor et al., 2013; Colton, 2009; Ransohoff and Perry, 2009). In contrast, alternatively activated macrophages are characterized by the release of anti-inflammatory cytokines IL-10 and IL-1RA (IL-1 receptor antagonist) (Rutschman et al., 2001). Microglia can also acquire diverse activation states or phenotypes known as classical activation or alternative activation (Colton, 2009; Schwartz et al., 2006; Thored et al., 2009). Classical activation can cause bystander damage in the CNS by the production of pro-inflammatory cytokines, while alternative activation may be supportive to the CNS by the expression of anti-inflammatory or neurotrophic factors (Giunti et al., 2014).

The role of GM-CSF in the CNS is dual, as it can be proinflammatory and protective. GMCSF induces the secretion by microglia of proinflammatory cytokines, such as IL1-β and TNF-α (Kloss et al., 1997; Malipiero et al., 1990) and promotes phagocytosis and functional antigen presentation in cultured brain-derived macrophages (Giulian and Ingeman, 1988) as well as microglia in vivo (McQualter et al., 2001; Mirski et al., 2003; Ponomarev et al., 2007). In addition, GM-CSF can enhance regeneration and functional recovery in models of spinal cord injury (Bouhy et al., 2006; Ha et al., 2005; Huang et al., 2009).

White matter damage in both term and preterm infants is strongly associated with motor disabilities in adulthood such as cerebral palsy (Devries et al., 1993). The factors that have been identified to cause white matter damage in the immature brain include hypoxia, ischemia, infection and/or inflammation (Bell and Hallenbeck, 2002; Dammann and Leviton, 1997; Pleasure et al., 2006; Volpe,

2009). Inflammation may cause injury to the cerebral white matter via microglial activation. Activated microglia can cause white matter injury by the production of neurotoxins, nitric oxide and proinflammatory cytokines. During development, amoeboid microglia can be found in clusters in the supraventricular corpus callosum and are known as fountains of microglia (Del Rio-Hortega, 1932). They can be found in the 2nd gestational trimester in humans (Monier et al., 2006; Rezaie and Male, 1999), and in mice and rats from a week before to 10 days after birth (Brockhaus et al., 1996; Hirasawa et al., 2005; Hurley et al., 1999; Leong and Ling, 1992) It has been found that an increase in microglial cell density in the cerebral white matter of the human foetus coincides with the peak window of vulnerability for periventricular leukomalacia (Billiards et al., 2006; Monier et al., 2006). Activated phagocytes in the vicinity of vulnerable white matter could play an important role in the axonal damage in the foetus and premature neonate (Lechpammer et al., 2008; Rezaie and Dean, 2002; Tahraoui et al., 2001; Yoon et al., 1997b).

The use of transgenic mice allows the analysis of mechanisms through which GM-CSF may be having its proinflammatory or protective effects in the CNS. This chapter evaluates the inflammatory effect of lentiviral-mediated expression of GM-CSF in adult mice of one outbred and six inbred strains. In addition, since undue perinatal activation of periventricular phagocytes has been suggested to result in white matter damage (Wang et al., 2009), the lentiviral delivery of GM-CSF in the FVB/N mouse strain was chosen to model potential neurotoxic effects of inflammatory processes in the immature brain.

Results

CD1 mouse-strain shows variable responses to GM-CSF-virus

Since there is a wide choice of transgenic mutant mice that could help us to study the molecular mechanisms of GM-CSF action on the CNS, we wanted to investigate the effect of GM-CSF-virus in the mice. This study used two non-integrating lentiviruses: one that contains GM-CSF and eGFP genes (GM-CSF-virus), and one with only eGFP (eGFP-virus) (Fig.1A&B). As a starting point, it was decided to investigate the effects of eGFP-virus and GM-CSF-virus on the comparatively widely-used outbred CD1 mouse strain. CD1 mice were injected

with eGFP-virus (10^7 TU/ml) or GM-CSF-virus (10^7 TU/ml) into the motor cortex and were allowed to survive for 3 days, 7 days, 14 days or 28 days following cortical injections. Coronal sections through the motor cortex were immunoreacted for IBA1. As seen in figure 1, at 14 days following virus injection there was some microglial activation in response to eGFP-virus (Fig. 1C). This was not evident in saline-injected controls (not shown). The results were variable in mice injected with GM-CSF-virus. A minority (~ ¼) showed small fluid-filled areas, clusters of activated microglia and a small number of eGFP positive cells (Fig. 1D). In contrast, the majority of mice had no tissue damage, a large number of eGFP positive cells and little sign of microglial activation (Fig. 2E). Similar, predominantly low level of microglia activation was also observed at other time points following GM-CSF-virus injections into the motor cortex (day 3-7 and day 28) (not shown).

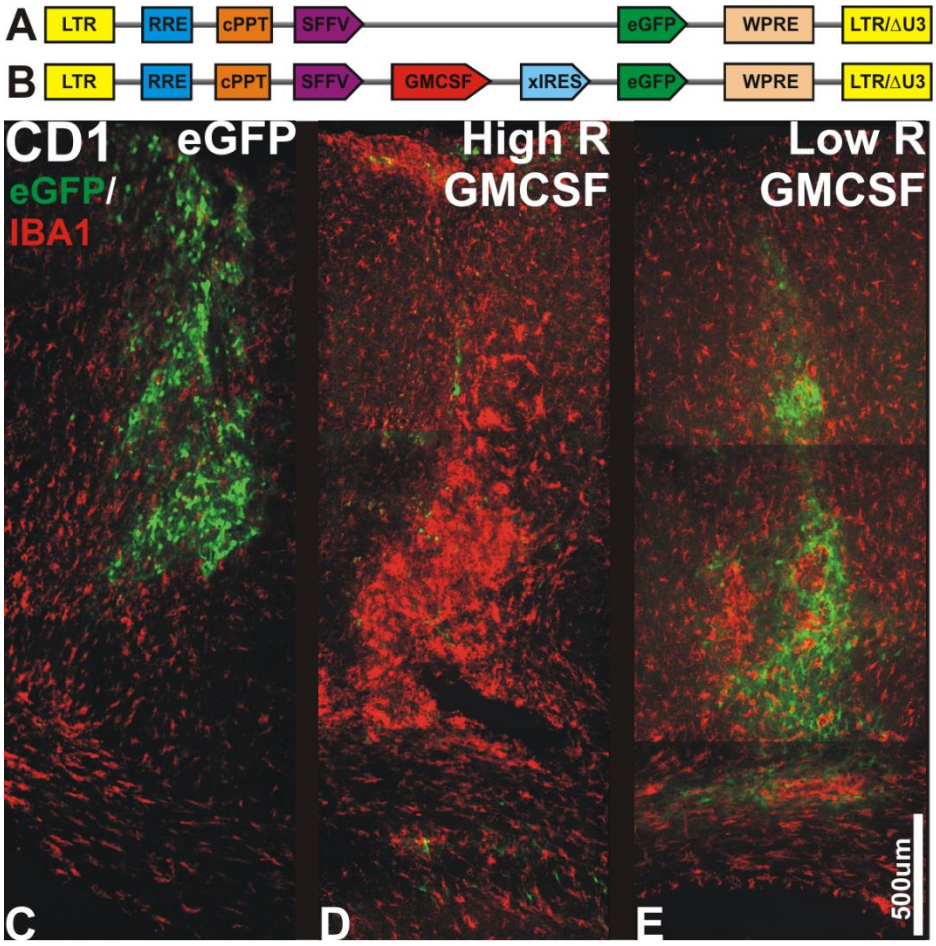

Figure 1: The outbred CD1 mice demonstrate a variable microglial response to GMCSF virus, and also respond to eGFP-virus. **A-B:** Schematic representation of the eGFP-lentiviral (eGFP-virus) (A) and the GM-CSF-lentiviral plasmid constructs used in the study. **C-E:** Coronal brain sections of motor cortex of CD1-mice stained for IBA1 (red) and also showing eGFP-positive cells (green) following eGFP-virus (C) or GM-CSF-virus injection (D-E). The left, middle and right pictures correspond to eGFP-virus controls, high-responders (High R), and low-responders (Low R) to GM-CSF-virus, respectively.

Inbred and outbred mice show a strain-dependent response to GM-CSF-virus

To investigated whether the response in this outbred mouse strain was representative of all mice. CD1 and six inbred strains: 129S2/Sv, FVB/N, SJL, Balb/C, C3H/N, C57/BL6 received striatal injections of GM-CSF-virus at 10^7 TU/ml.

Firstly, it was necessary to establish whether the effect of GM-CSF in mouse CNS was reproducible. The 7 strains were injected two months apart in two batches of 3 animals per strain (42 animals in total). Mice were sacrificed 14 days following striatal injections. Coronal sections through the injection site in the striatum were stained for microglial IBA1, and granulocyte endogenous peroxidase. Using a 40x objective lens, sections through the injection site in the striatum were given a score from 0-3 for granulocyte density (Fig. 2A), local reactive microglial density (Fig. 2B), spread of reactive microglia (Fig. 2C), phagocytic microglial density (Fig. 2D), amount of necrosis (Fig. 2E), and astrocyte activation (Fig. 2F) (0 being the lowest score and 3 being the highest). Scores obtained for each strain in batch 1 and batch 2 were correlated and the R-squared correlation coefficient was taken as a representative for the strength of correlation.

A high variability and therefore a low correlation was observed between average scores obtained for each strain in batch 1 and batch 2 for granulocyte density (R^2=0.01) and reactive microglia density (R^2=0.001) at the GM-CSF-virus injection site. However, the inter-batch scores showed a moderate positive correlation for necrosis at (R^2= 0.33), a strong positive correlation for phagocytic microglia (R^2= 0.58) and astrocyte density (R^2=0.41) at the injection site, and for reactive microglia 2mm away from the injection site (R^2= 0.51).

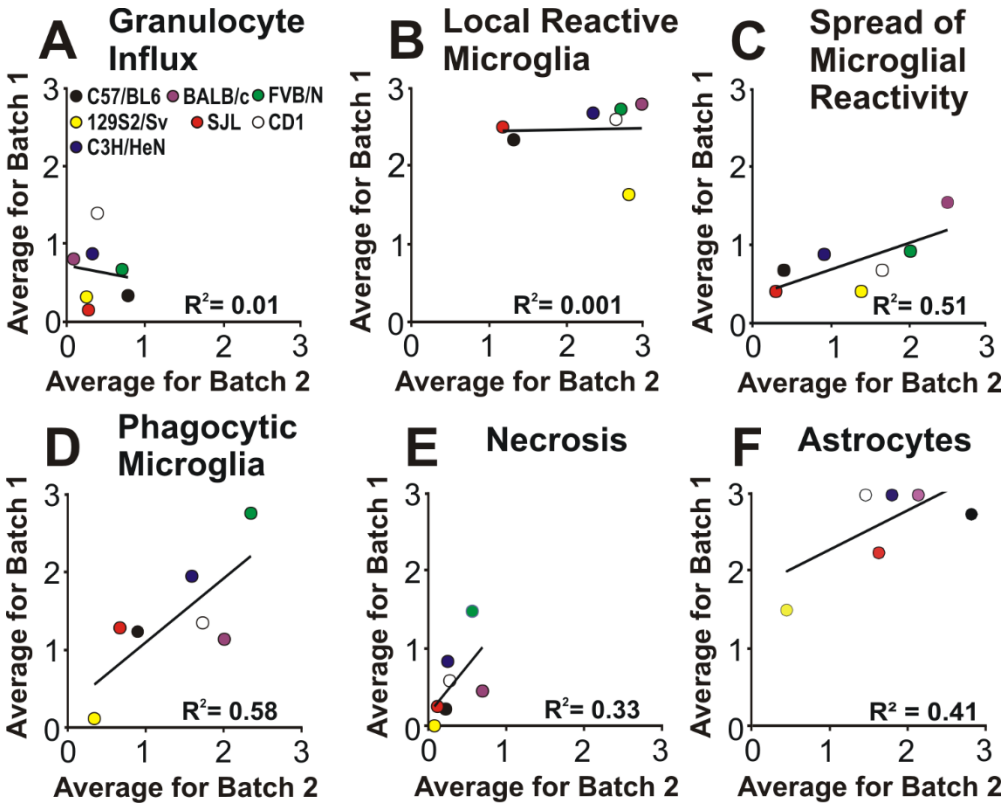

Figure 2: Correlating the effects of GM-CSF-virus injection into the striatum of inbred and outbred mice from two separate batches. Scatter plots representing the average score from 0 to 3 given for C57/BL6 (black dot), BALB/c (purple dot), FVB/N (green dot), 129S2/Sv (yellow dot), SJL (red dot) or CD1 (white dot) mice injected with GM-CSF/eGFP-virus in two separate batches; Batch 1 and Batch 2. The R^2 correlation coefficient shows no correlation for the average scores of granulocyte influx (A) and local reactive microglia (B). A good correlation was found for microglia spread (C), phagocytic microglia (D), necrosis (E) and astrocytes (F).

Secondly, inter-strain differences were analysed for the parameters that showed good correlation namely; spread of reactive microglia, phagocytic microglia, necrosis, and astrocytes activation. This was achieved by averaging the scores obtained per parameter for each strain in batch 1 and 2.

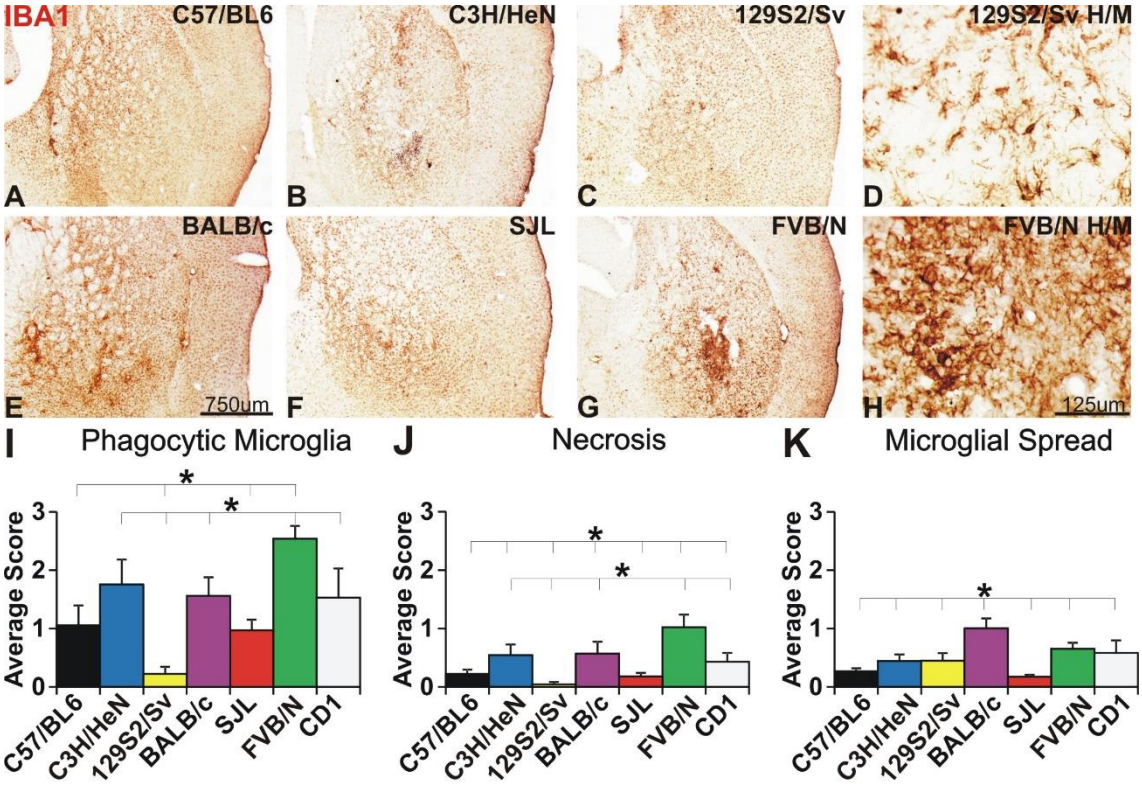

Figure 3: Inbred and outbred mice show a strain dependent inflammatory response to GM-CSF. **A-H:** Coronal brain sections of the striatum of six different inbred mouse strains (A-C & E-G) immunostained for microglial IBA1 at 14 days following injections of GM-CSF-virus. Mouse strains showed weak (C), medium (A, B & F), widespread (E), and strong local responses (G). High magnification micrographs (H/M) showed that in the high (H) responder strain the microglia were of a rounded morphology and more densely packed than in the low responder (D). **I-K:** Histograms representing the average scores given for phagocytic microglia, necrosis or microglial spread in the striatum of the outbred and six different inbred strains that received striatal injections of GM-CSF-virus. (*) $p<0.05$ Tukey post hoc test to univariate ANOVA. Bars and error bars represent the mean and standard error of the mean (SEM).

Fourteen days following injection of GM-CSF-virus into the striatum, there was low IBA1-immunoreactivity in the 129S2/Sv strain (Fig. 3C), moderate in C57/BL6 (Fig. 3A), C3H/N (Fig. 3B) and SJL (Fig. 3F), widespread though moderate in BALB/c (Fig. 3E), and high immunoreactivity in the FVB/N strain (Fig. 3G). It was observed that the high responder FVB/N-strain (Fig. 3H) had more amoeboid-shaped IBA1-positive monocytes/macrophages at the GM-CSF-virus injection site than the 129S2/Sv-mice, which showed predominantly ramified IBA1-positive microglia (Fig. 3D).

This observation was reflected in the statistical analysis. The FVB/N mouse (Mean=3± SEM=0.3) showed more phagocytic microglia per field following injection into the striatum of GM-CSF-virus (Fig. 3I-green bar), than the 129S2/Sv (0.2±0.1) (Fig. 3I-yellow bar) C57/BL6 (1±0.3) (Fig. 3I-black bar), and SJL mouse

strains (1±0.2) (Fig. 3I-red bar) ($p<0.05$; Tukey post hoc test to a univariate ANOVA). The enhanced microglial response to GM-CSF-virus in the striatum of FVB/N mice was also accompanied with high levels of necrosis. FVB/N (1±0.2) had more necrotic areas in the GM-CSF-virus injection site than any other mouse strain ($p<0.05$; Tukey post hoc test to a univariate ANOVA). When the level of microglial activation 2mm away from the GM-CSF-virus injection site was studied, there was more widespread microglial activation in the BALB/c (1±0.2) strain than C57/BL6 (0.3±0.1), 129S2/Sv (0.4±0.1), SJL (0.2±0), C3H/N (0.4±0.1) and CD1 (0.6±0.2) ($p<0.05$; Tukey post hoc test to a univariate ANOVA). The 129S2/Sv mouse strain (0.2±0.1) had significantly fewer phagocytic microglia than FVB/N (3±0.3), BALB/c (2±0.3), C3H/N (2±0.4) and CD1 (2± 0.5) and negligible necrotic damage ($p<0.05$; Tukey post hoc test to a univariate ANOVA). In addition, 129S2/Sv mice (1.2±0.4) had less astrocyte activation than BALB-c (2±0.2) or C57/BL6 mice (3±0.2) (Fig. 3) ($p<0.05$; Tukey post hoc test to a univariate ANOVA). In summary, this study revealed that the inflammatory response to the expression of GM-CSF was strain-dependent; low in the 129S2/Sv strain, widespread though moderate in BALB/c, and high in the FVB/N strain.

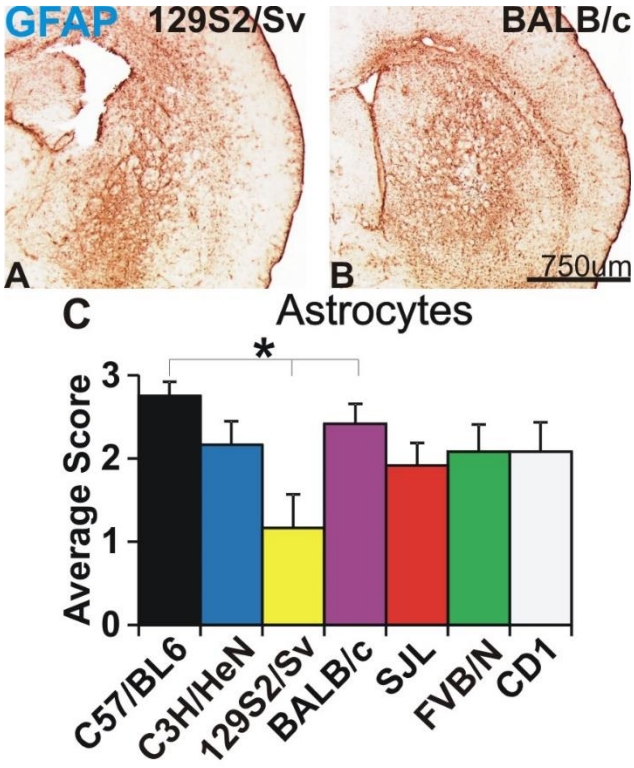

Figure 4: Astrocyte activation following GM-CSF delivery is mouse strain dependent. The 129S2/Sv mice (A), showed a lower astrocytic response to GM-CSF expression in the striatum compared to BALB/c mice (B). The 129S2/Sv mouse strain showed more GFAP-immunoreactivity than BALB/c 14 days after injection of the vector. **C:** Histogram representing the average scores given for astrocyte density in the striatum of the outbred and six different inbred strains that received striatal injections of GM-CSF-virus. (*) $p<0.05$ Tukey post hoc test to univariate ANOVA. Bars and error bars represent the mean and standard error of the mean (SEM).

Exploring the effects of different doses of viral GM-CSF in the 129S2/Sv, BALB/c and FVB/N mouse strains

Building on the work on mouse strain specific responses to GM-CSF, the inflammatory effects of increasing GM-CSF doses in the three most interesting strains namely, 129S2/Sv, BALB/c and FVB/N, were examined. Mice received striatal injections of a mixture of GM-CSF/eGFP-virus from 10^3 to 10^7 (TU/mL) (n=3-4 per concentration per strain) or eGFP-virus (10^8 TU/mL) (n=2-3 per concentration per strain). Animals survived for 14 days. Coronal sections were immunoreacted for eGFP+ cells, microglia (IBA1), astrocytes (GFAP) and T cells (CD4).

eGFP-positive cells

There was a trend for the number of eGFP-positive cells to decrease in the striatum of FVB/N mice when exposed to high concentrations of GM-CSF/eGFP-virus. Following eGFP-virus injection to the striatum (CON) of 129S2/Sv (Fig. 5A), BALB/c (Fig. 5B) or FVB/N (Fig. 5C) mice, the eGFP-positive cells had a neuronal morphology. However, when GM-CSF/eGFP-virus at 10^7 TU/mL (GM7) was injected to the striatum of 129S2/Sv (Fig. 5D), BALB/c (Fig. 5E) or FVB/N (Fig. 5F) the eGFP-positive cells were glial-shaped. When the number of eGFP-positive cells were counted along the eGFP-injection site in the striatum there were 28±9 eGFP-positive cells per field in 129S2/Sv mice, 14±6 in BALB/c, and 27±1 in FVB/N (Fig. 5G-eGFP+ cells). In contrast, following injection of GM-CSF/eGFP 10^7 TU/mL into the striatum the number of eGFP-positive cells per field was similar in BALB/c mice (19±3) and 129S2/Sv mice (19±2), while there was a strong decrease in FVB/N mice (4±3). Nonetheless, comparisons did not reach statistical significance ($p>0.05$; univariate ANOVA).

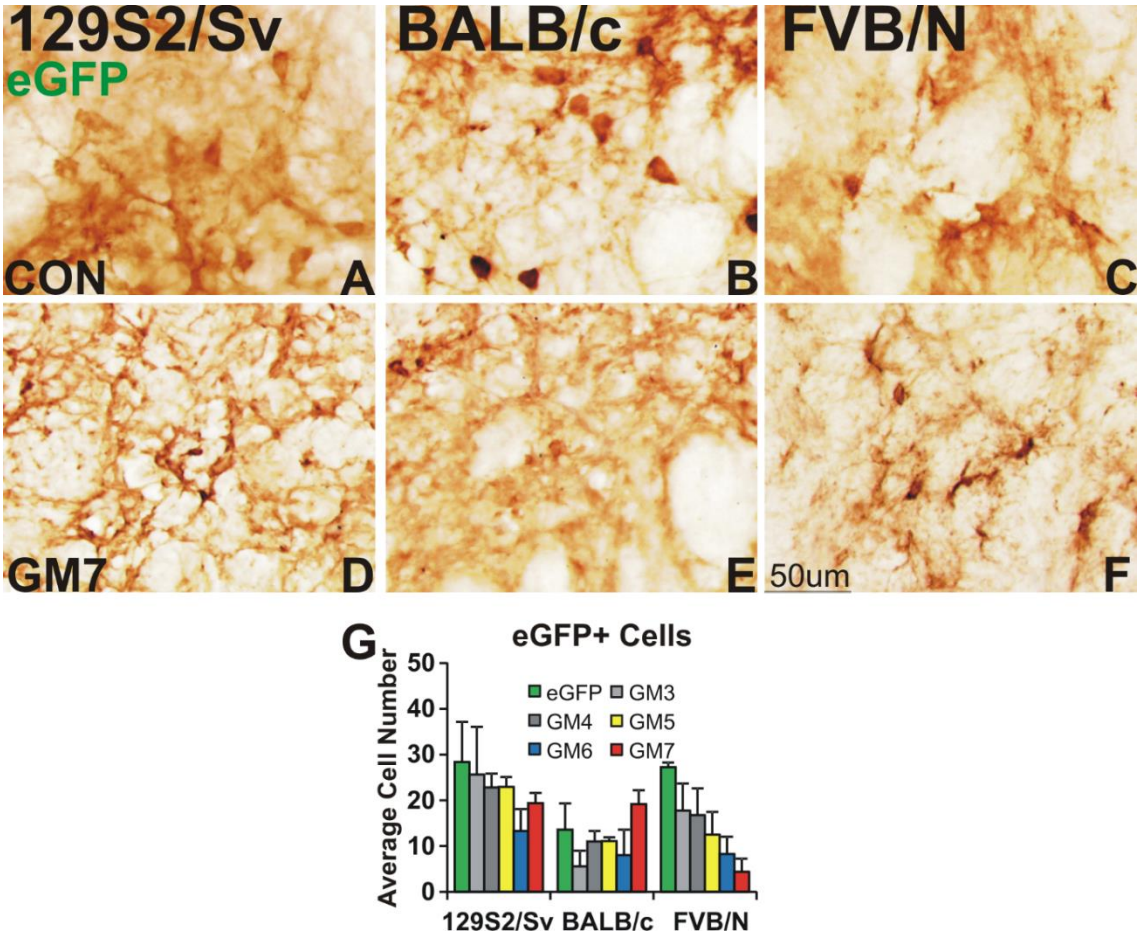

Figure 5: The FVB/N strain injected with high concentrations of GM-CSF/eGFP-virus shows a trend for fewer eGFP-positive cells. **A-F:** Coronal brain sections of the striatum 14 days after injection of eGFP-virus (A-C) or GM7-virus (D-F) immunoreacted for eGFP (visualized with DAB). **C:** Histogram representing the average number of eGFP-positive cell per field following injection of eGFP-virus (green bar) or GM-CSF/eGFP-virus a t10^3 TU/ml (GM3: light grey bar), 10^4 TU/ml (GM4: dark grey bar), 10^5 TU/ml (GM5: yellow bar), 10^6 TU/ml (GM6: blue bar), or 10^7 TU/ml (GM7: red bar). Bars and error bars represent the mean and standard error of the mean (SEM).

Microglia

Microglia change morphology in the striatum of 129S2/Sv BALB/c and FVB/N mice following GM-CSF/eGFP-virus treatment. Microglia had a reactive morphology in the striatum of 129S2/Sv (Fig. 6D) and BALB/c (Fig. 6E) mice, and a phagocytic morphology in FVB/N mice (Fig. 6F) following an striatal injection of GM-CSF/eGFP-virus at 10^7 TU/mL (GM7). In contrast, injecting eGFP-virus (control) into the striatum of 129S2/Sv (Fig. 6A), BALB/c (Fig. 6B) or FVB/N (Fig. 6C) mouse-strains resulted in in no microglial activation- the cells maintained a resting morphology.

Using a 40x objective, the numbers of IBA1-positive microglial cells with a resting, reactive and phagocytic morphology were counted along the injection sites of eGFP-virus or GM-CSF/eGFP-virus (Fig. 6G-Total Microglia). 129S2/Sv, BALB-c or FVB/N mice injected with GM-CSF/eGFP-virus showed a dose-dependent increase in the number of IBA1-positive microglia in the striatum (Fig. 6G-Total Microglia).

When phagocytic microglia were specifically counted, there was an increase in the number of phagocytic microglia with GM-CSF exposure. The striatum of 129S2/Sv mice or BALB/c mice injected with GM-CSF/eGFP-virus at 10^7 TU/ml had more phagocytic microglia at the injection site than those injected with eGFP ($p<0.05$; Tukey post hoc test to a univariate ANOVA). The FVB/N strain had more phagocytic microglia in the striatum following GM-CSF/eGFP-virus at 10^5 TU/mL (GM5) (7±0), 10^6 TU/mL (GM6) (9±0), or 10^7 TU/mL (GM7) (21±8) than in eGFP-injected mice ($p<0.05$; Tukey post hoc test to a univariate ANOVA), showing that microglia in the FVB/N strain change morphology in response to lower viral titres.

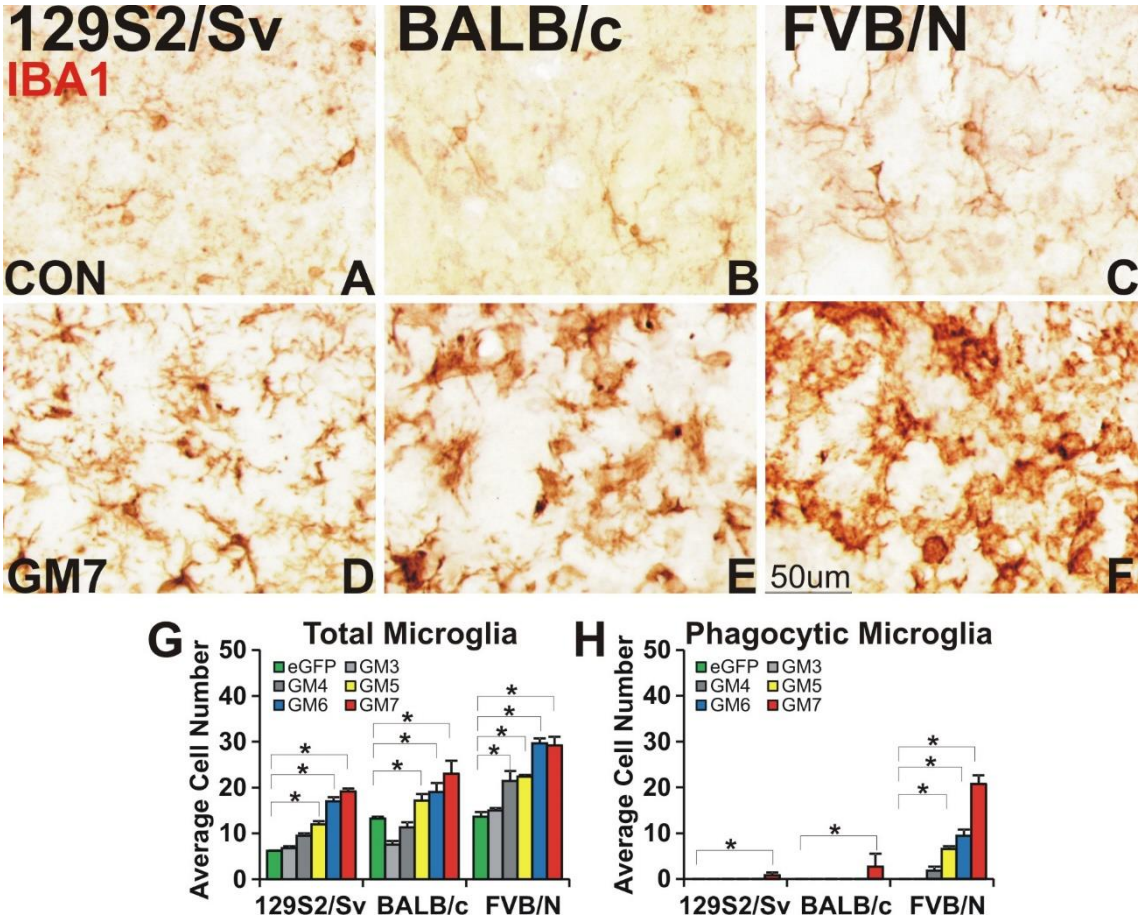

Figure 6: Microglial activation is dose-dependent and strain dependent. **A-F**: Coronal sections of the striatum stained for IBA1 14 days after injection of eGFP-virus (A-C) or GM7-virus (D-F) into the striatum. **C:** Histogram representing the average number of IBA1-positive microglia per field following injection of eGFP-virus (green bar) or GM-CSF/eGFP-virus at 10^3 TU/ml (GM3: light grey bar), 10^4 TU/ml (GM4: dark grey bar), 10^5 TU/ml (GM5: yellow bar), 10^6 TU/ml (GM6: blue bar), or 10^7 TU/ml (GM7: red bar). (*) $p<0.05$ Tukey post hoc test to univariate ANOVA. Bars and error bars represent the mean and standard error of the mean (SEM).

Astrocytes

The number of GFAP-positive astrocytes in the striatum of 129S2/Sv, BALB/c and FVB/N mice increased in animals injected with GM-CSF/eGFP-virus. There was more GFAP immunoreactivity in 129S2/Sv (Fig. 7D), BALB/c (Fig. 7E) and FVB/N (Fig. 7F) mice were injected with GM-CSF/eGFP-virus at 10^7 TU/mL (GM7) than those injected with the eGFP-virus (Fig. 7A-C). The number of GFAP-positive astrocytes increased in a dose dependent manner in 129S2/Sv, BALB/c and FVB/N mice following the injection of GM-CSF/eGFP-virus at 10^4-10^7 TU/ml ($p<0.05$; Tukey post hoc test to a univariate ANOVA).

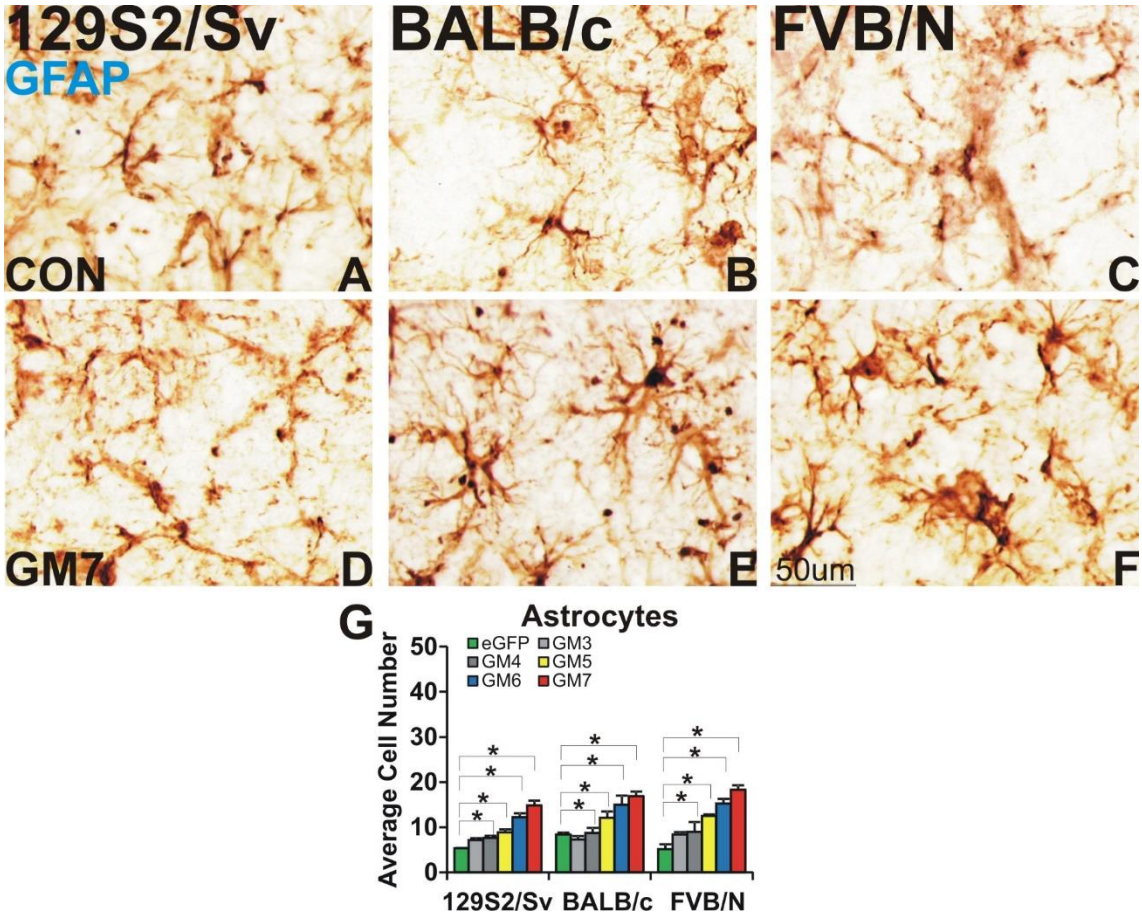

Figure 7: There is more astrocyte activation at higher doses of GM-CSF/eGFP-virus. **A-F**: Coronal brain sections of the striatum stained for GFAP 14 days after injection of eGFP-virus (A-C) or GM7-virus (D-F) into the striatum. **C:** Histogram representing the average number of GFAP-positive astrocytes per field following injection of eGFP-virus (green bar) or GM-CSF/eGFP-virus at 10^3 TU/ml (GM3: light grey bar), 10^4 TU/ml (GM4: dark grey bar), 10^5 TU/ml (GM5: yellow bar), 10^6 TU/ml (GM6: blue bar), or 10^7 TU/ml (GM7: red bar). (*) $p<0.05$ Tukey post hoc test to univariate ANOVA. Bars and error bars represent the mean and standard error of the mean (SEM).

T-cells

There was no CD3-positive T-cells influx into the striatum of 129S2/Sv, BALB-c or FVB/N mice injected with eGFP virus. In contrast, GM-CSF/eGFP-virus injection into the striatum of FVB/N mice was associated with the presence in the striatum of large numbers of CD3-positive T-cells. The effects of the GM-CSF/eGFP-virus were less in other strains of mice: there were a few CD3-postive T-cells in 129S2/Sv mice (Fig. 8A), moderate numbers in BALB/c mice (Fig. 8B), and abundant in FVB/N mice (Fig. 8C).

Taken together this data is in line with our previous observations where a high inflammatory response was found in the FVB/N mouse strain, moderate in BALB/c and low in 129S2/Sv.

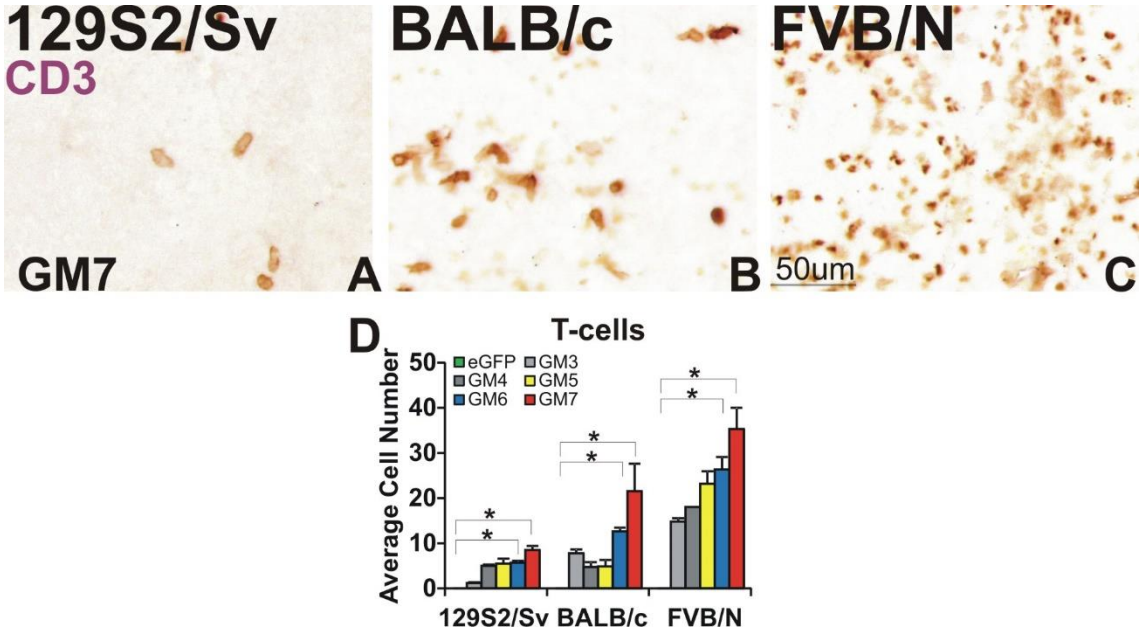

Figure 8: FVB/N mice are avid T-cell recruiters on exposure to GM-CSF/eGFP-virus. **A-F**: Coronal brain sections of the striatum stained for CD3 14 days after injection of eGFP-virus (A-C) or GM7-virus (D-F) into the striatum. **C:** Histogram representing the average number of CD3-positive T-cells per field following injection of eGFP-virus (green bar) or GM-CSF/eGFP-virus at 10^3 TU/ml (GM3: light grey bar), 10^4 TU/ml (GM4: dark grey bar), 10^5 TU/ml (GM5: yellow bar), 10^6 TU/ml (GM6: blue bar), or 10^7 TU/ml (GM7: red bar). (*) $p<0.05$ Tukey post hoc test to univariate ANOVA. Bars and error bars represent the mean and standard error of the mean (SEM).

The effect of injecting GM-CSF-virus into the foetal mouse brain

Perinatal infants that are exposed to inflammation may be at risk of white matter injury that can cause motor disabilities such as cerebral palsy in adulthood (Wang et al., 2009). A preliminary study was carried out to investigate whether expression of GM-CSF in the immature mouse brain will lead to microglial activation in the white matter. The 129S2/SV strain was chosen for its low response to GM/CSF virus and the FVB/N strain was used for its neurotoxic response. In collaboration with Dr Simon Waddington (UCL), pregnant 129S2/SV (n=2) or FVB/N (n=2) mice (Fig. 9A) at embryonic day 14 had full-depth midline laparotomy to expose the uterus (Fig. 9B). Foetuses received intrauterine

injections of GMCSF/eGFP-viral mixture or eGFP-virus into the lateral ventricle of brain (Fig. 9C). In contrast to pregnant FVB/N mice, the two pregnant 129S2/SV failed to handle the procedure, as one cannibalised her stillborn neonates and the other miscarried.

FVB/N pups were taken at P0, P3 and P7. Coronal brain sections were collected and stained for eGFP and microglial IBA1. Injections resulted in the presence of eGFP-positive cells in the cerebral cortex, ventricular epithelium, choroid plexus and meninges. As we aimed for GM-CSF production to be in the vicinity of the white matter, animals were determined to have had successful injections if transduced cells were found in all of the above regions except the meninges. There were no successful injections of GMCSF/eGFP at P0 or and P7, but there was 1 out of 2 (1/2) pups at P3 that had choroid plexus transduction. With eGFP-only delivery, 2/3 neonates had successful injections at P0, 2/2 at P3, and 2/2 at P7. When IBA1 stained sections of P3 GMCSF/eGFP group (Fig. 9E) were compared with those of the eGFP-only group (Fig. 9D), it was evident that the GMCSF/eGFP-injected mouse had lower eGFP-expression in the left and right choroid plexus in the lateral ventricles, but had higher IBA1-positive microglial density at the subcortical and periventricular white matter than the control.

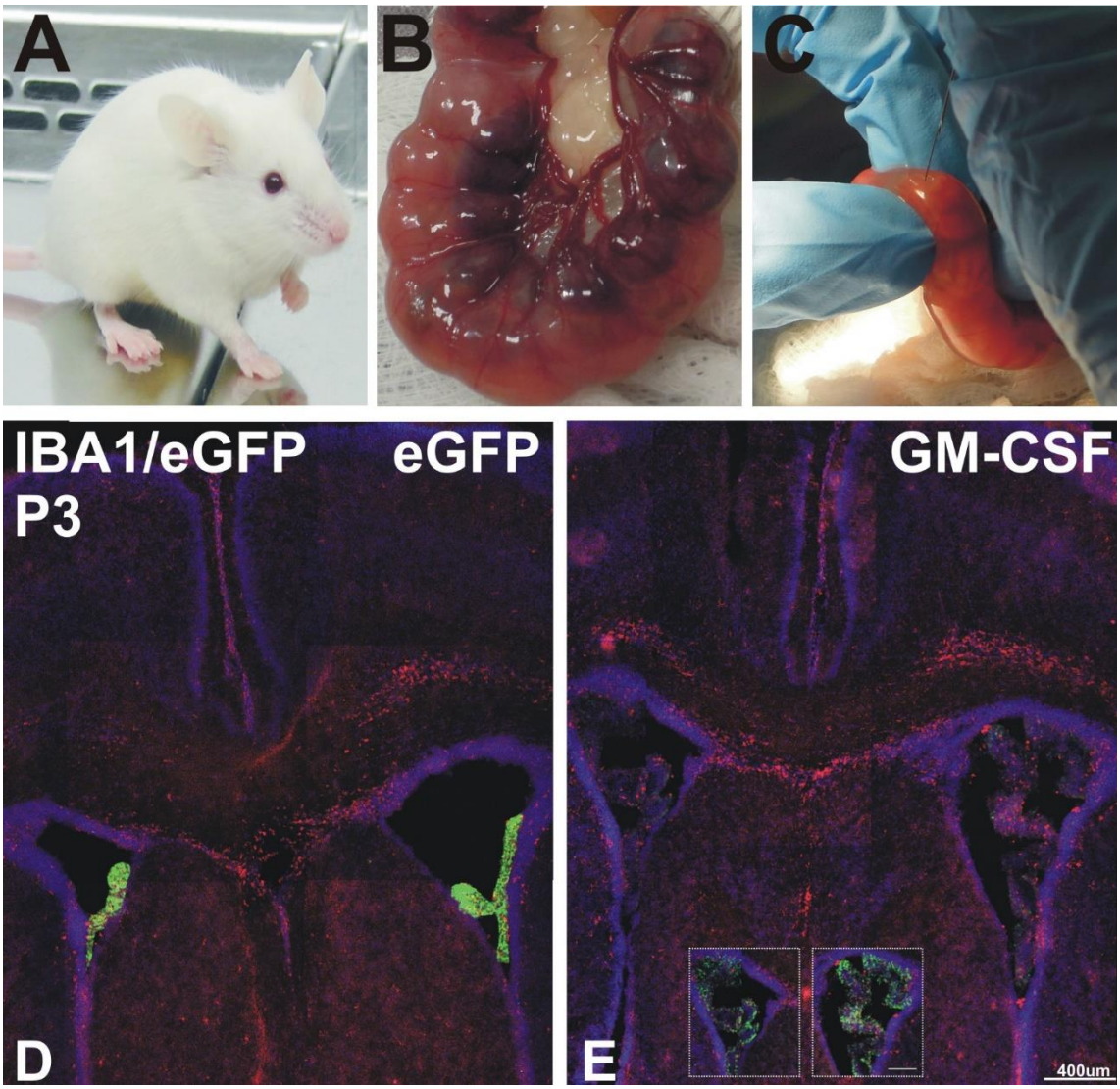

Figure 9: Delivery of GM-CSF-virus in foetal FVB/N mice causes a heightened inflammatory response in the subcortical and periventricular white matter. **A-E**: Pregnant FVB/N mice (A) had a midline laparotomy, the uterus was exposed (B) and foetal mice at embryonic day 14 were injected with GM-CSF-virus or eGFP-virus control (C). At P3, injection of eGFP-virus (E) or GM-CSF-virus (F) resulted in eGFP-positive (green) choroid plexus in the left and right lateral ventricle, which was associated with IBA1-positive (red) phagocytic microglia at the subcortical and periventricular white matter in the GM-CSF injected mouse compared to the eGFP treated mice. Insert: Enhanced eGFP-positive cells of the choroid plexus of the animal injected with GM-CSF-virus. **Bar Scale**: 200um.

eGFP positive cells are present in foetal FVB/N mice injected with GM-CSF/eGFP-virus

To confirm whether the above result was reproducible and if the difference between the effects of GM-CSF/eGFP-virus and eGFP-virus are consistent at other post-natal time points, FVB/N foetuses at embryonic day 14 received eGFP-virus or GM-CSF/eGFP-viral mixture injection to the lateral ventricles. The eGFP-

virus or GM-CSF/eGFP-virus injected pups were taken at postnatal day 0 (GM-CSF/eGFP-virus vs eGFP-virus: n=11 vs n=3), day 3 (n= 11 vs n=2), and day 7 (n=19 vs n=2). Coronal sections through the lateral ventricles and hippocampus were immunostained for IBA1 or eGFP. Eight brain areas were analysed: cortex, white matter, septum, striatum, hippocampus, ventricular epithelium, choroid plexus and meninges.

eGFP-positive cells were widespread. Animals injected with eGFP or GMCSF/eGFP, had eGFP-positive cells in the choroid plexus/ventricular epithelium (Fig. 10A-F), meninges, cortex (Fig. 11A-F), septum, striatum and hippocampus (Fig. 12A-F).

To quantify the level of viral transduction the eight brain areas were given a score of 0-3 for eGFP (0 being none, 1 low, 2 medium and 3 high stain intensity). Across all areas studied there was no significant difference in eGFP immunoreactivity between the control eGFP-virus (Fig. 13A-G-blue bars) and the mixture of GMCSF/eGFP-virus at any postnatal time point (Fig. 13 A-G -purple bars), demonstrating that there may be no difference in the levels of virus transduction or subsequent gene expression between the two lentiviral vectors ($p > 0.05$; Students t-test). This therefore suggests that the presence of GM-CSF did not affect the ability of eGFP-virus, in the experimental viral mixture, to transduce cells. It also suggests that the expression of GM-CSF may fail to kill cells that were transduced by the virus.

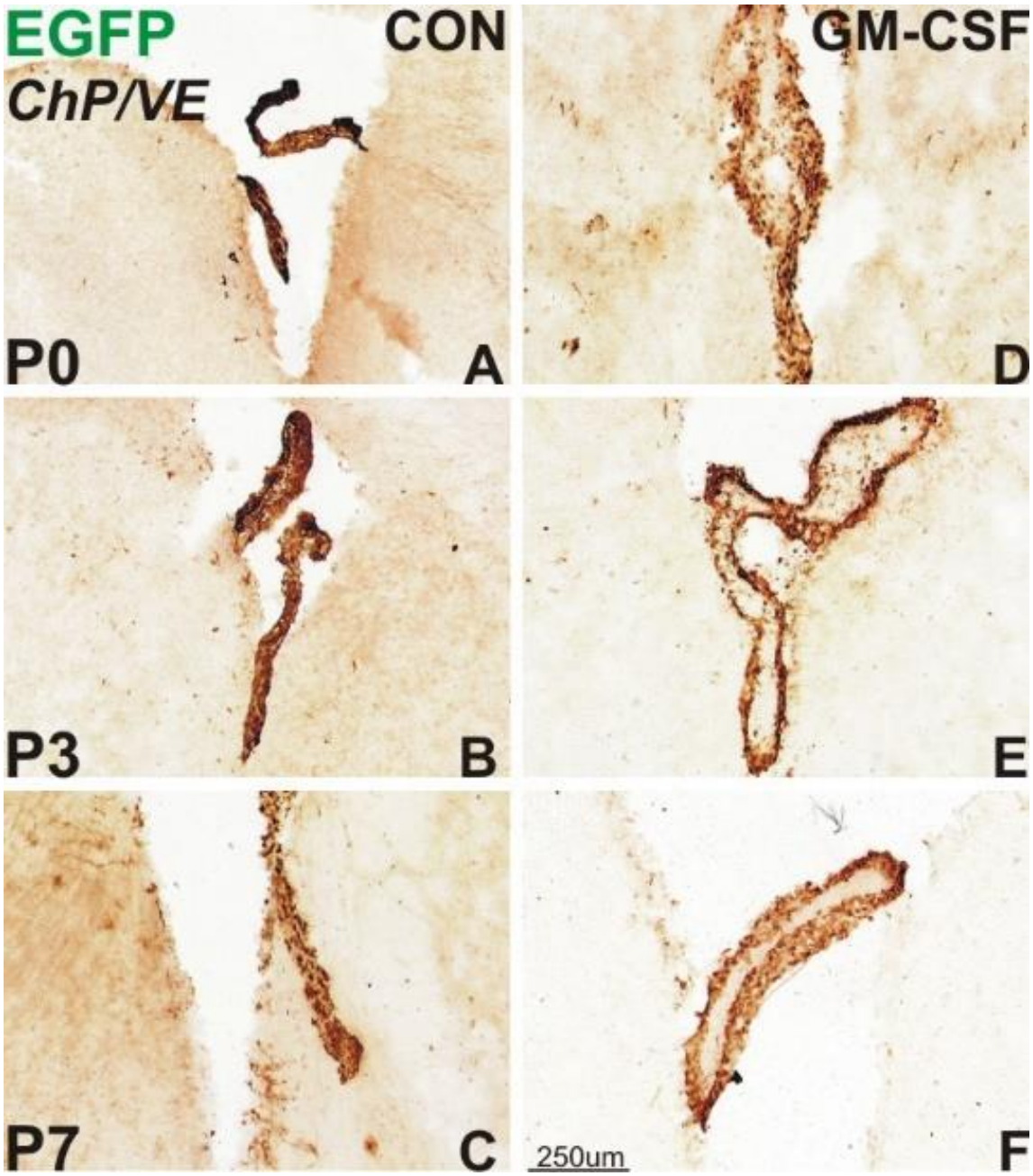

Figure 10: FVB/N foetal mice intraventricular injections of GM-CSF/eGFP-virus or eGFP-virus results in the expression of eGFP in the choroid plexus and ventricular epithelium. Coronal brain sections through the lateral ventricles, immunostained for eGFP, of FVB/N mice injected in utero at gestational day 14 with control **(A-C)** or GM-CSF/eGFP virus mixture **(D-F)**. Mice were killed at postnatal day 0 (P0-top row), 3 (P3-middle row) and 7 (P7- bottom row). Similar eGFP expression can be seen in the choroid plexus (ChP) and ventricular epithelium (VE) at all time-points in the eGFP-injected and GM-CSF/eGFP-injected groups.

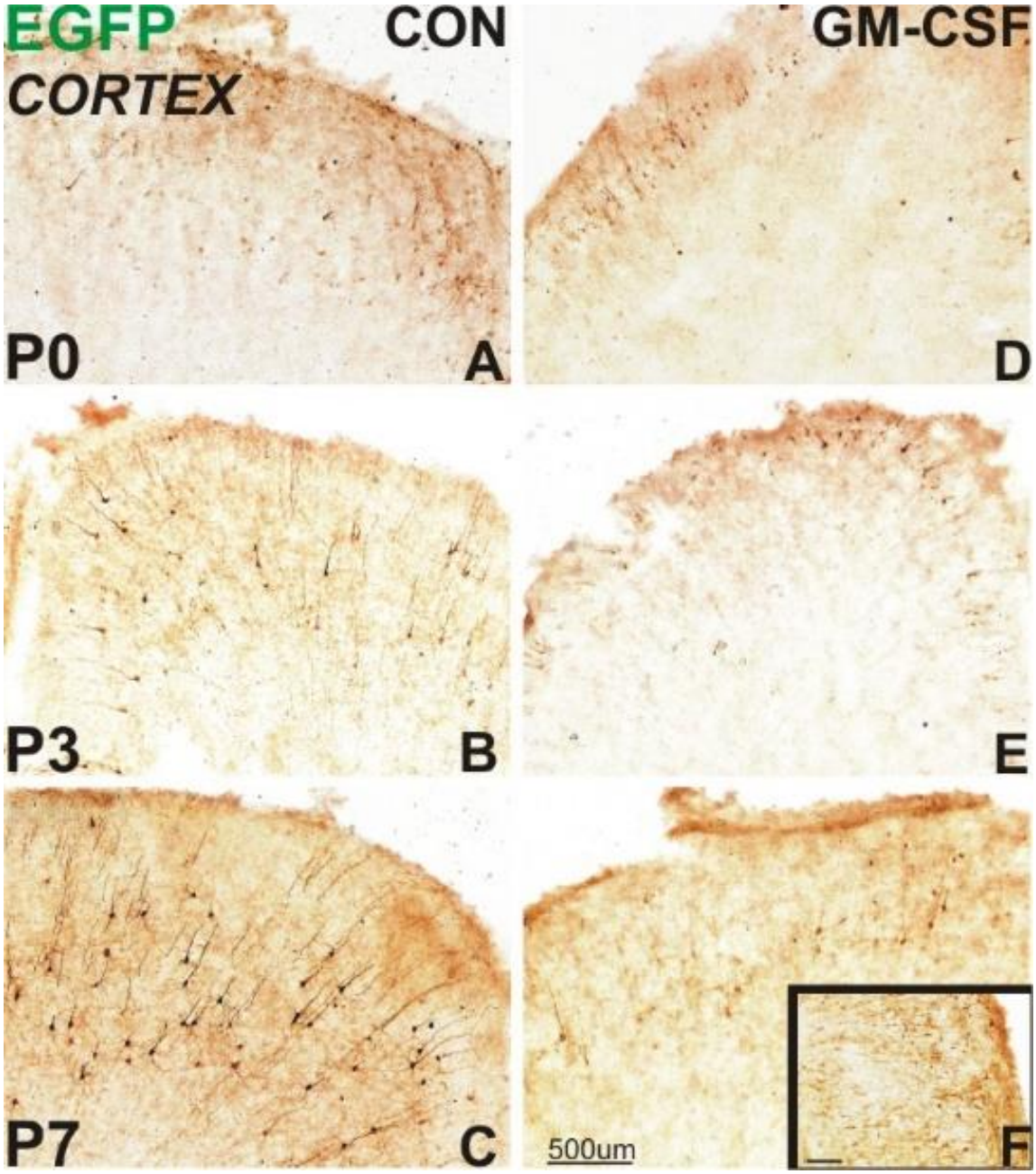

Figure 11: There is widespread eGFP-expression in the cortex of FVB/N mice that received intraventricular injections of GM-CSF/eGFP-virus or control-virus. Coronal brain sections through the cortex, immunostained for eGFP, of FVB/N mice that were injected in utero at gestational day 14 with control **(A-C)** or GM-CSF/eGFP virus mixture **(D-F).** Mice were killed at postnatal day 0 (P0-top row), 3 (P3-middle row) and 7 (P7- bottom row). Neuronal expression of eGFP can be seen in the motor and somatosensory cortex of mice injected with the control-virus (A-C) or GM-CSF/eGFP-virus (D-F). Insert shows further expression in the granular insular area at P7 in the GM-CSF/eGFP-virus injected mouse. Bar scale: 200um

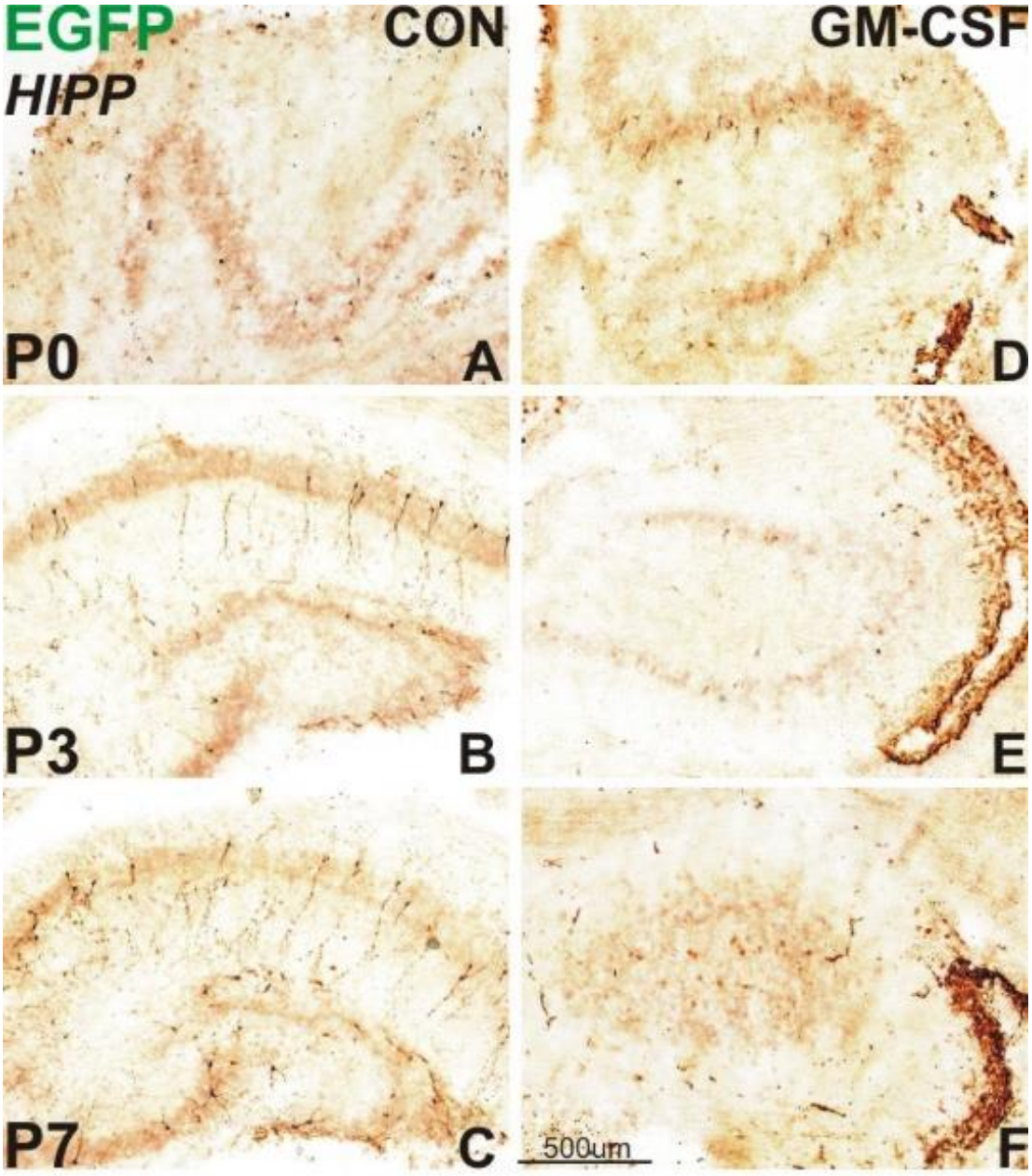

Figure 12: eGFP-expression is also evident in the hippocampus of FVB/N mice that received intraventricular injections of GM-CSF/eGFP-virus or control-virus. Coronal brain sections through hippocampus immunostained for eGFP of FVB/N mice that were injected in utero at gestational day 14 with control **(A-C)** or GM-CSF/eGFP virus mixture **(D-F)**. Mice were killed at postnatal day 0 (P0-top row), 3 (P3-middle row) and 7 (P7- bottom row). Hippocampal neurons can be seen expressing eGFP in mice injected with control-virus or GM-CSF/eGFP-virus.

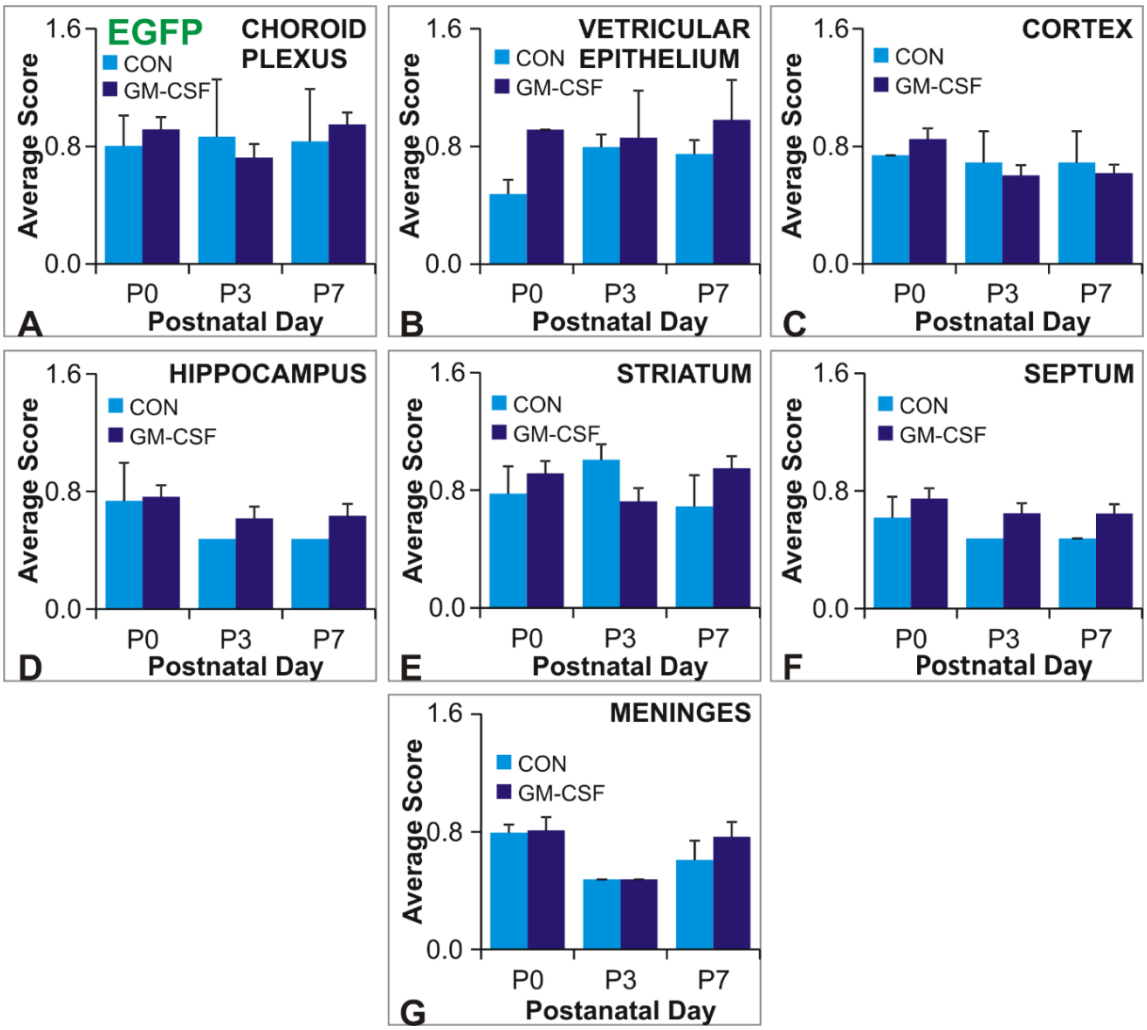

Figure 13: The level of eGFP expression is similar between control-virus and GM-CSF-virus injected FVB/N mice. Histograms show average eGFP intensity scores, normalised using the log (x+0.01) algorithm, of mouse brains injected with control (blue bars) or GFMCSF/eGFP virus (purple bars) at gestational day 14 that survive up to postnatal day 0 (P0), 3 (P3) or 7 (P7). Intensity was specifically evaluated in the choroid plexus, ventricular epithelium, cortex (top row), hippocampus, striatum, septum (middle row), and meninges (bottom row). Note no significant difference between mice injected with control or GMCSF virus, and that the expression of eGFP does not increase with time. Bars and error bars represent the mean and standard error of the mean (SEM).

There are activated and phagocytic microglia in various areas in the brain following foetal GM-CSF-virus injection

In comparison to eGFP-virus treated pups (Fig.14-19A, B, C), those injected with the GM-CSF/eGFP-viral mixture had more IBA1 immunoreactivity and reactive and/or phagocytic microglia in the ventricular white matter (Fig.14D, E, F) and in areas where eGFP immunoreactivity was present, such as choroid plexus and ventricular epithelium (Fig. 15 D, E, F), septum (Fig. 16D, E, F), striatum (Fig. 17, E, F), and hippocampus (Fig. 18D, E, F).

Using a 40x objective, these areas were given a score from 0-3 for IBA1-microglial activation (0 resting-activated, 1-reactive-phagocyic and 2-completely phagocytic 3-tissue necrosis). Pups injected with GM-CSF/eGFP-virus (Fig. 19-purple bars) had more reactive and phagocytic microglia in the ventricular epithelium at postnatal day 0 and 3 (P0 & P3) (Fig. 19B) than those injected with eGFP-virus (Fig. 19- blue bars). In the white matter (Fig. 19A), cerebral cortex (Fig. 19C), septum (Fig 19D) and striatum (Fig. 19E) more reactive and phagocytic microglia were seen only at P0. Overall, this GM-CSF-mediated microglial activation in the brain of perinatal FVB/N mice was transient. It peaked at day 0 and decreased by day 7 (Fig. 19-purple bars). Injection of EGFP-only vector showed that injection per se was not a source of significant microglial activation (Fig. 19-blue bars).

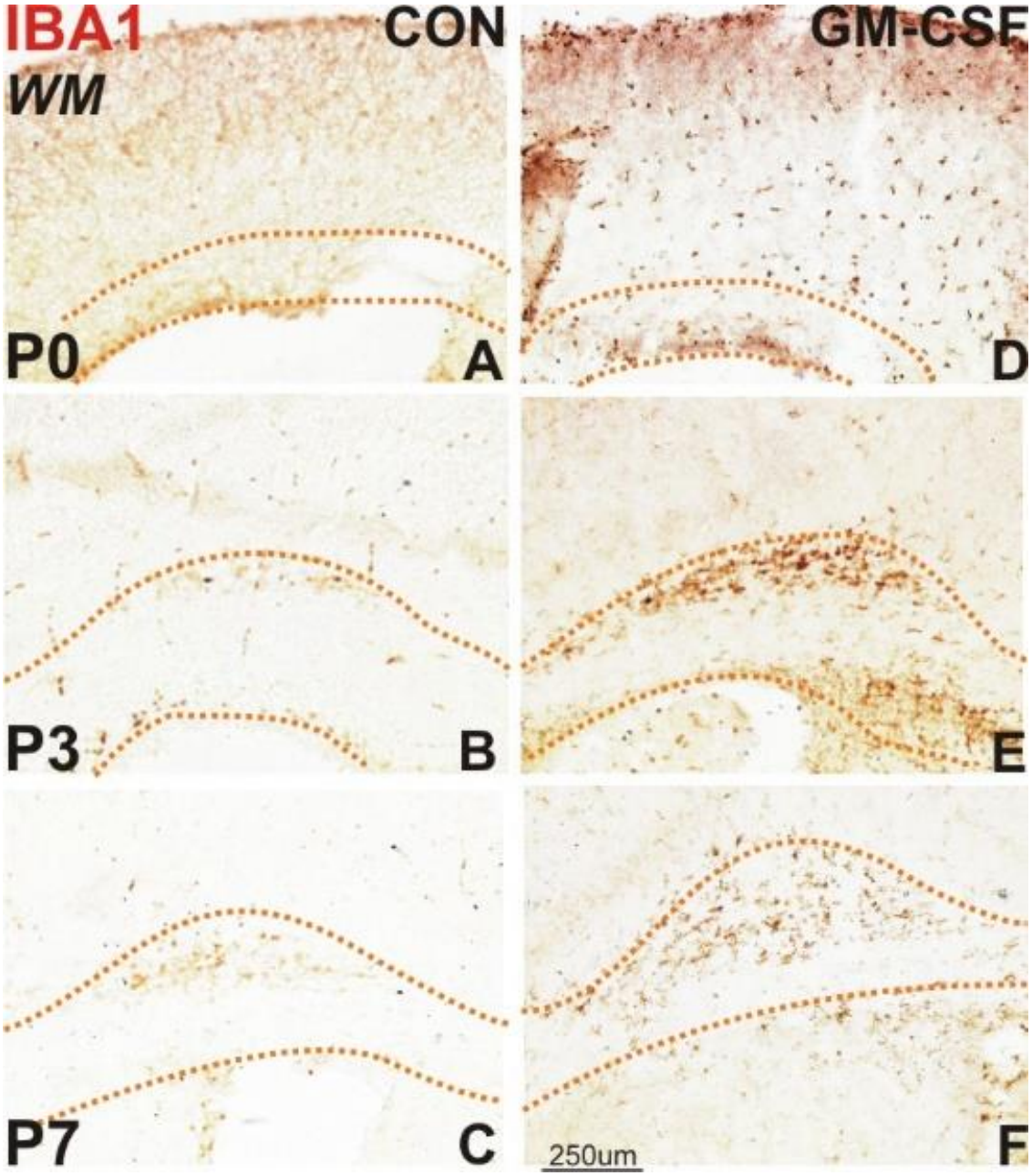

Figure 14: Microglial activation is evident in the white matter of FVB/N mice that received intraventricular GM-CSF/eGFP-virus injection. Coronal brain sections, immunostained for IBA1, of FVB/N mice that were injected in utero at gestational day 14 with control **(A-C)** or GM-CSF/eGFP virus mixture **(D-F)** and were collected at postnatal day 0 (P0-top row), 3 (P3-middle row) and 7 (P7- bottom row). Dashed lines in orange highlight the boundaries of the white matter. There are more phagocytic microglia at P0 (D), phagocytic and reactive microglia at P3 (E) and reactive microglia at P7 (F) in comparison to controls (A-C).

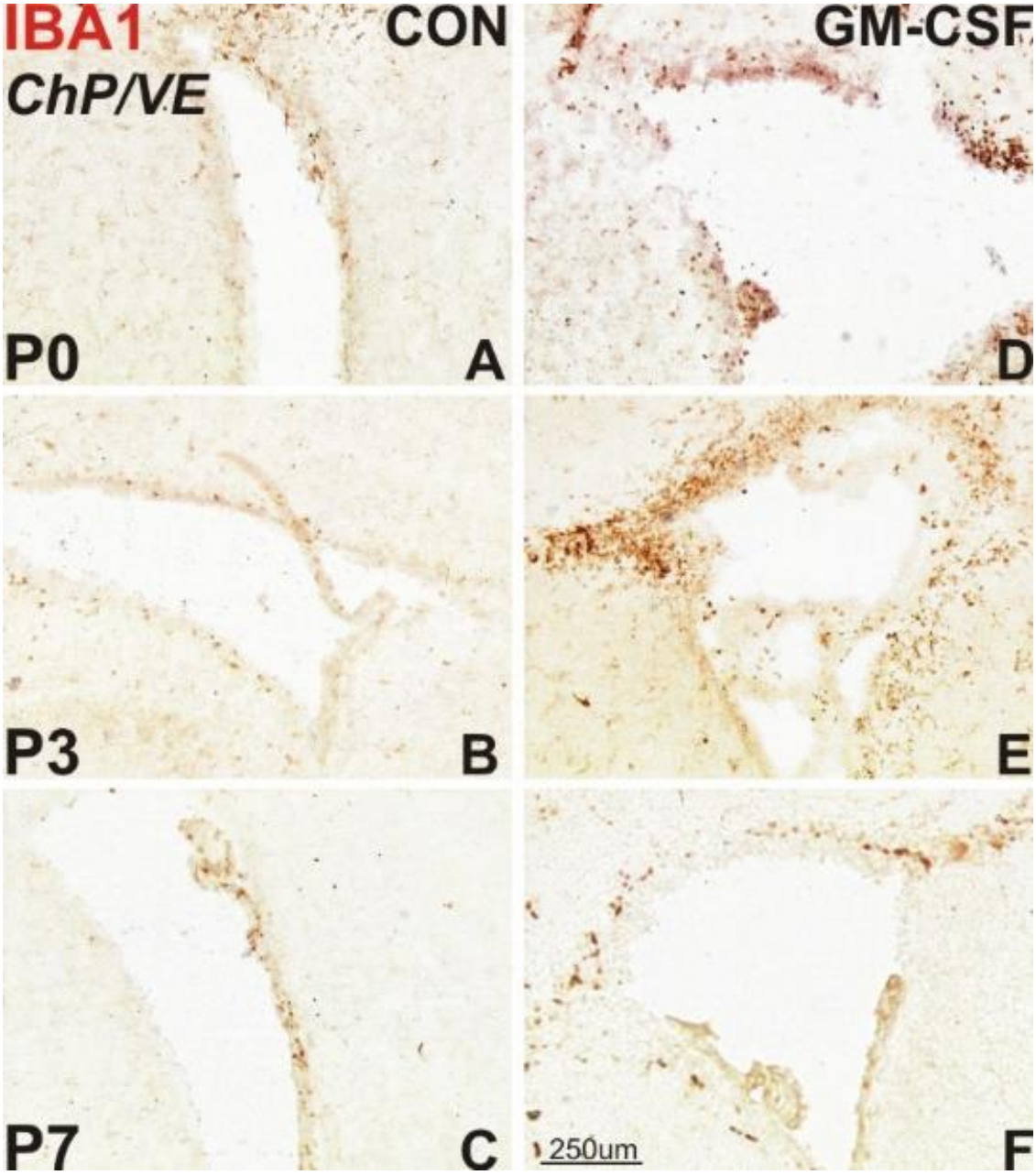

Figurer 15 Higher levels of microglial activation are present in the ventricular epithelium in GM-CSF/eGFP-injected mice than those injected with control virus. Coronal brain sections through the lateral ventricle, immunostained for IBA1, of FVB/N mice that were injected in utero at gestational day 14 with control **(A-C)** or GM-CSF/eGFP virus mixture **(D-F).** Animals were killed at postnatal day 0 (P0-top row), 3 (P3-middle row) and 7 (P7- bottom row). There is more microglial activation in the ventricular epithelium of GM-CSF/eGFP-injected mice than those injected with control particularly at P0 and P3.

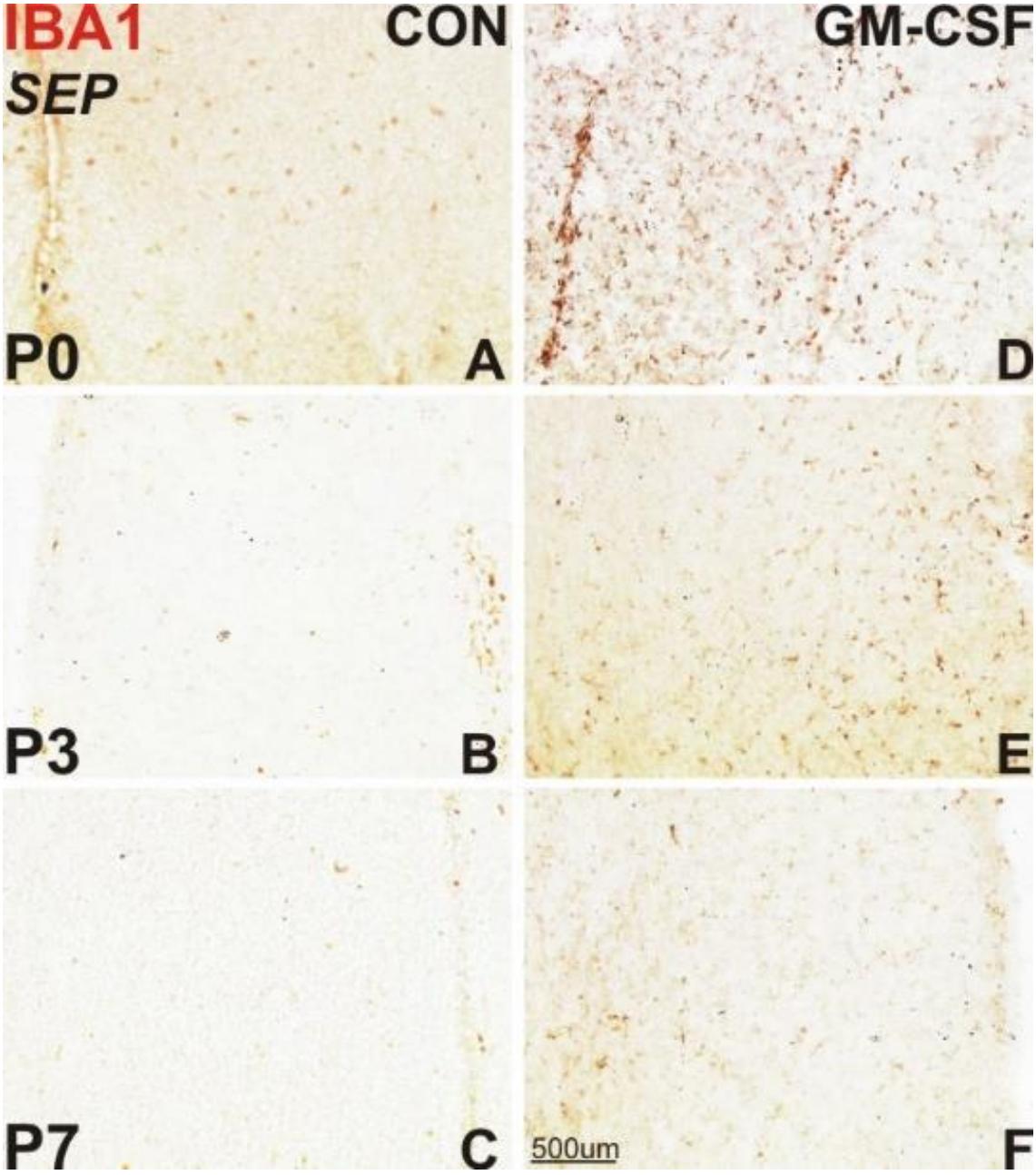

Figure 16: The septum of GM-CSF/eGFP-injected mice shows more IBA1 immunoreactivity than that of mice injected with control virus. Coronal brain sections through the septum (SEP), immunostained for IBA1, of FVB/N mice that were injected in utero at gestational day 14 with control **(A-C)** or GM-CSF/eGFP virus mixture **(D-F).** Mice were killed at postnatal day 0 (P0-top row), 3 (P3-middle row) and 7 (P7- bottom row). Microglial activation appears to be particularly high at P0 mice injected with GM-CSF/eGFP-virus rather than eGFP-virus

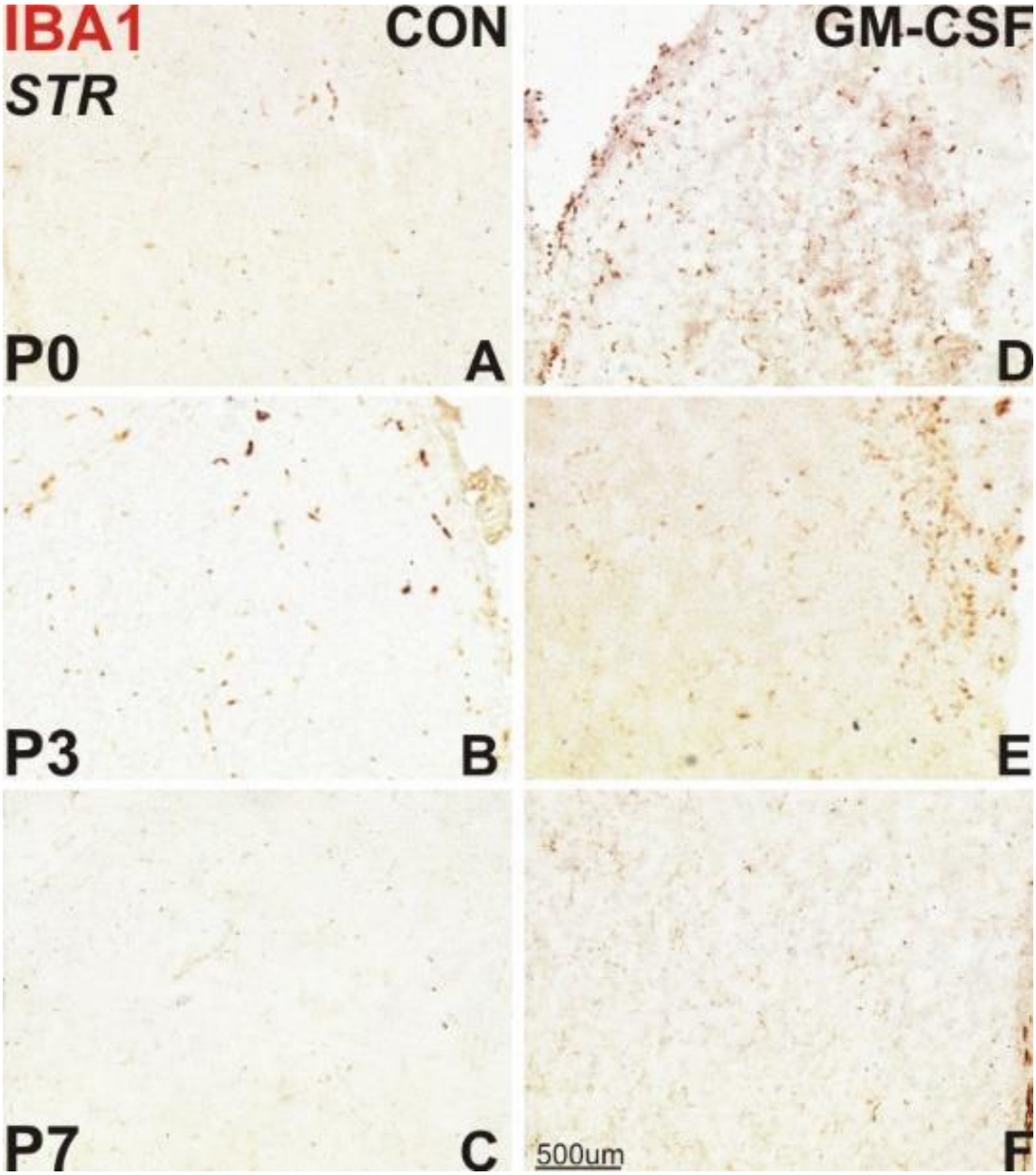

Figure 17: The striatum of GM-CSF/eGFP-injected mice shows more IBA1 immunoreactivity than that of mice injected with control virus. Coronal brain sections through the striatum (STR), immunostained for IBA1, of FVB/N mice that were injected in utero at gestational day 14 with control **(A-C)** or GM-CSF/eGFP virus mixture **(D-F).** Mice were killed at postnatal day 0 (P0-top row), 3 (P3-middle row) and 7 (P7- bottom row).

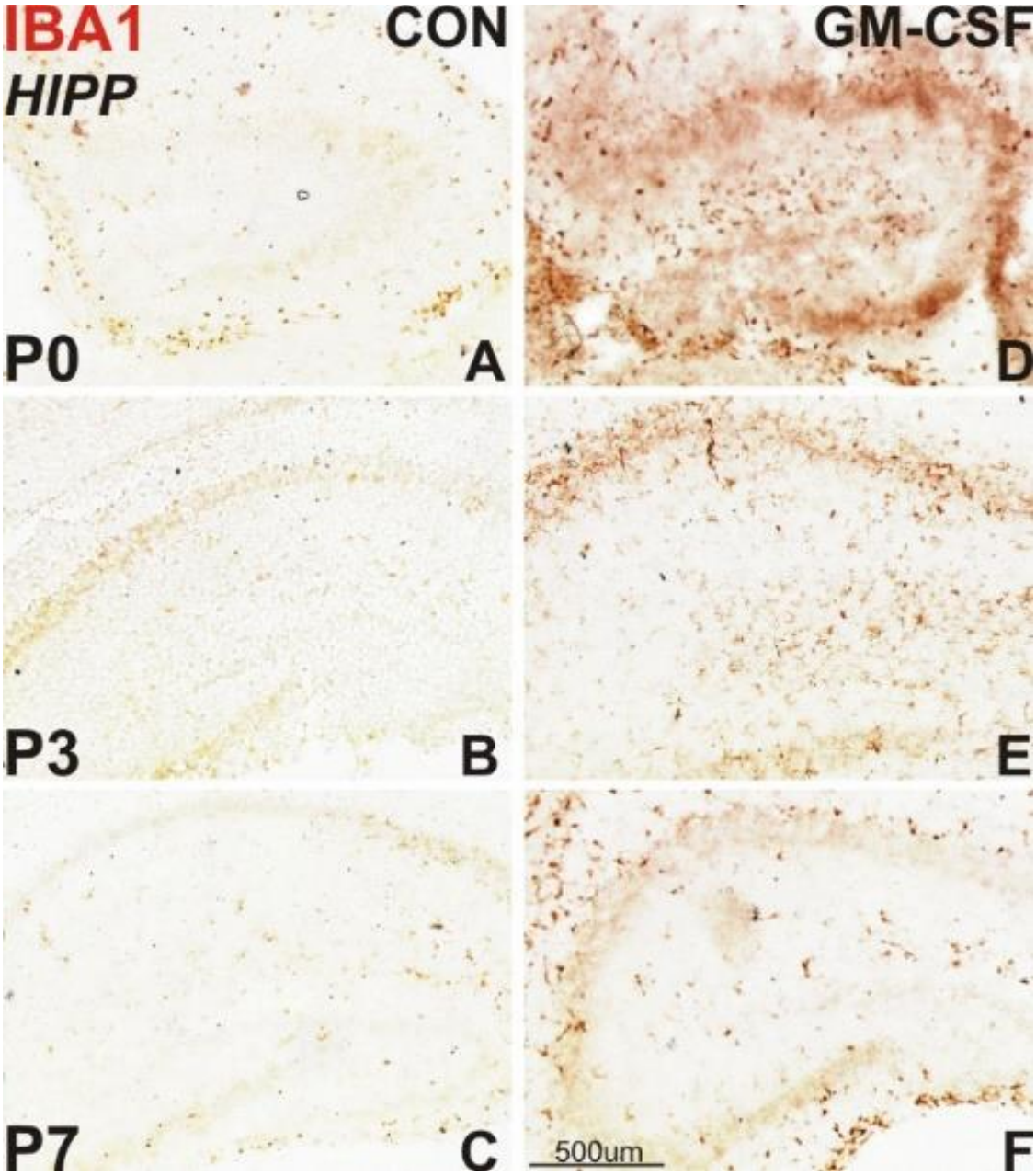

Figure 18: The hippocampus of GM-CSF/eGFP-injected mice shows more IBA1 immunoreactivity than that of mice injected with control virus. Coronal brain sections through the hippocampus (HIPP), immunostained for IBA1, of FVB/N mice that were injected in utero at gestational day 14 with control **(A-C)** or GM-CSF/eGFP virus mixture **(D-F)**. Mice were killed at postnatal day 0 (P0-top row), 3 (P3-middle row) and 7 (P7- bottom row).

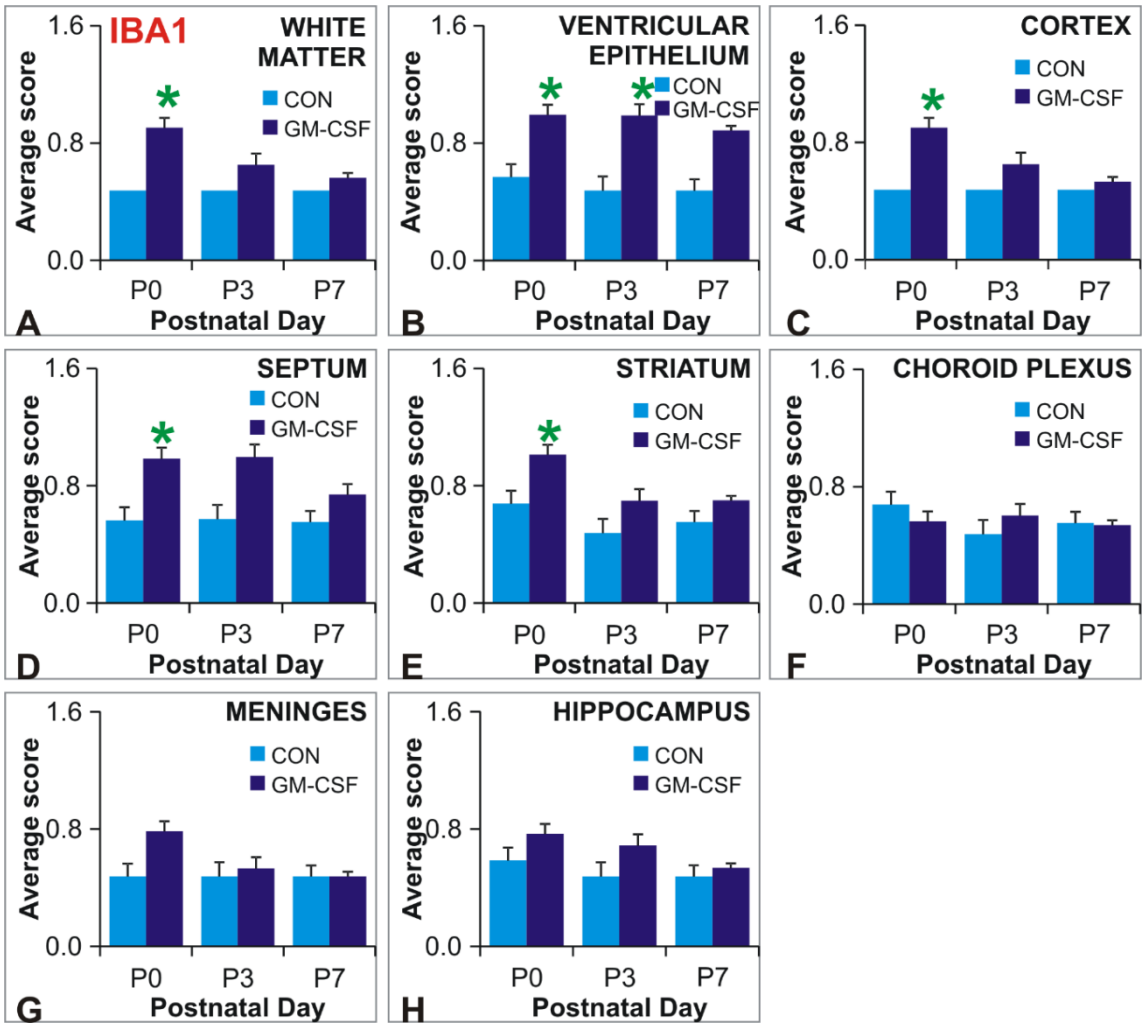

Figure 19: FVB/N mice injected with GM-CSF/eGFP-virus showed widespread activation of IBA1-positive microglia that decreases with increasing time to control levels. Histograms show average IBA1 microglia morphology scores, normalised using the log (x+0.01) algorithm, of mouse brains injected with control (CON-blue bars) or GFMCSF/eGFP virus (purple bars) in utero. The mice were killed at postnatal day 0 (P0), 3 (P3) or 7 (P7). Resting, reactive and phagocytic microglia were evaluated in the following areas: white matter (WM), ventricular epithelium (PVE) and cortex (top row), septum, striatum, choroid plexus (ChPx) (middle row), meninges and hippocampus (bottom row). In the white matter, ventricular epithelium, cortex, septum and striatum there were significantly higher levels of IBA1-positive microglia in GMCSF-virus-injected mice than eGFP-virus-injected mice at day 0, as indicated by the green asterisks. Note that in all brain areas the level of microglial activation is dampened with increasing time. (*) $p<0.05$; Students t-test. Bars and error bars represent the mean and standard error of the mean (SEM).

Discussion

The wide choice of transgenic mutant mice available could help to identify the molecular mechanisms through which GM-CSF effects CNS regeneration or degeneration. As a starting point, the widely-used outbred CD1 mouse strain was evaluated. The majority of the tested CD1 mice demonstrated little microglial activation, and only a minority showed a prominent microglial response following

GM-CSF/eGFP injection. To evaluate whether the genetic background influenced the effects of GM-CSF, GM-CSF/eGFP-virus was injected into six different inbred strains of mice. In each of these strains the effect of GM-CSF on the level of phagocytic microglia, necrosis, the spread of reactive microglia and astrocyte activation was reproducible. The mouse strains 129S2/Sv, BALB/c and FVB/N showed a low, medium and high inflammatory response to GMCSF/eGFP-virus, respectively. Subsequently, the FVB/N mouse strain was used to evaluate potential neurotoxic effects of GM-CSF in the immature mouse CNS. Transuterine injections of control or GMCSF/eGFP virus targeting the lateral ventricles of mice at embryonic day 14, resulted in virally transduced cells being widespread in the cerebral cortex, hippocampus, striatum, septum, meninges, ventricular epithelium, and choroid plexus. More reactive and phagocytic microglia were present in the areas of viral transduction. Of particular interest, there was a successful increase in inflammation at the subcortical and periventricular white matter. Although, the level of transduction remained relatively constant with increasing time, inflammation decreased, suggesting that sensitivity to GM-CSF is highest before or around birth.

The effect of GM-CSF on microglial activation is reproducible in the striatum of adult mice

Injecting GM-CSF into the CNS of one outbred strain and six inbred strains in two separate batches that were two months apart, showed that the effects of GM-CSF were reproducible for the spread of microglia activation from the injection site, and for phagocytic microglia, necrosis and activated astrocytes at the injection site. In previous studies there is consistent evidence for microglial and astrocyte activation following GM-CSF treatment into the mouse CNS. Infusing GM-CSF into the substantia nigra of C57/BL6 mice stimulated microglial and astrocyte activation as identified by the expression of alpha-M integrin and GFAP, respectively (Mangano et al., 2011). In addition, delivering GM-CSF into the lateral ventricle of BALB/c mice produced high levels of phagocytic microglia (Mausberg et al., 2009). Furthermore, C57/BL6 mice had more GFAP immunoreactivity in the hippocampus and midbrain following intracerebroventricular injections of GM-CSF compared to PBS (Reddy et al., 2009)

GM-CSF failed to produce a consistent effect on granulocyte recruitment into the injected striatum. The delivery of mouse GM-CSF protein intravenously has been associated with the recruitment of neutrophils into inflamed areas such as the joints in arthritic mouse models (Bischof et al., 2000), the intestine in a mouse model of intestinal inflammation (Khajah et al., 2011), and the cortex of rats injected with GM-CSF/eGFP-virus (Chapter 4).This might suggest that lentiviral GM-CSF in the mouse striatum does not have significant systemic effects that lead to a consistent granulocyte recruitment to the striatum. As direct injury to the brain has been associated with granulocyte influx into the brain parenchyma (Holmin et al., 1998), the varying levels of granulocytes in the injected striatum may be explained by the extent of mechanical injury caused by the injections of the virus. In fact, the level of granulocyte recruitment correlated well with the level of reactive microglia found directly at the injection site (another parameter that was not reproducible); the more reactive microglia present at the injection site resulted in more granulocyte influx to the injection site (data not shown).

The degree of microglial activation in the adult mouse striatum is strain specific

The phenotype that microglia acquire depends on the stimuli acting on different microglial receptors. The classical activation phenotype of microglia can be induced by LPS or amyloid-β. Stimulated microglia release great amounts of TNF-α and NO (Butovsky et al., 2005; Schwartz et al., 2006) which are associated with neuronal death (de Bock et al., 1998; Long-Smith et al., 2010; Ono et al., 2010). Similarly, GM-CSF can promote the production of pro-inflammatory cytokines by microglia. Intracerebroventricular injection of GM-CSF in C57/BL6 mice leads to the expression of IL-1β, IL-6 and TNF-α by microglia (Reddy et al., 2009), which are cytokines that can promote neuronal death (de Bock et al., 1998; Long-Smith et al., 2010; Ono et al., 2010). In the current experiments, FVB/N mice injected into the striatum with GM-CSF/eGFP-virus at high concentrations showed fluid-filled areas in the brain parenchyma that were surrounded by abundant phagocytic microglia. The expression of GM-CSF in the striatum of FVB/N mice may be stimulating microglia to differentiate into the classically activated subtype that promotes the production of pro-inflammatory factors that can cause tissue damage.

In contrast, the alternative activation state of microglia can be induced by low doses of interferon gamma or the anti-inflammatory cytokine IL-4, leading to the release of growth factors including BDNF and IGF-1 (Butovsky et al., 2005; Schwartz et al., 2006). Although, GM-CSF is a pro-inflammatory cytokine that can cause tissue damage, it has also been associated with promoting the production of BDNF by microglia (Bouhy et al., 2006; Ha et al., 2005; Huang et al., 2009), and treatment with GM-CSF can be protective in stroke models (Kong et al., 2009; Schaebitz et al., 2008), and pro-regenerative in spinal cord injury models (Bouhy et al., 2006; Ha et al., 2005; Huang et al., 2009). In the current experiment, GM-CSF expression in the striatum of the 129S2/Sv and BALB/c strains failed to promote tissue damage but resulted in a mild and moderate microglial activation, respectively. As the microglial response to GM-CSF in the 129S2/Sv and BALB/c strains is lower in comparison to the FVB/N strain, whereas the outbred CD-1 strain showed a variable response, it suggests that the effects of GM-CSF are dependent not only on the type of stimulus but also on the genetic background of the mice. Furthermore, a disparity in the toxic effects of LPS-activated microglia from different mouse strains has also been reported. When neurons from rats were grown with LPS-activated microglia from the C57/BL6 or SWR/J mouse strains, there were fewer surviving neurons in the cultures containing microglia derived from C57/BL6 mice than in those containing microglia derived from SWR/J mice. Microglia from C57/BL6 mice produced higher levels of prostaglandin-E2 a major inflammatory mediator and inducible nitric oxide synthase, an enzyme that catalyses the production of nitric oxide (McLaughlin et al., 2006).

There are at least two reasons why some mouse strains should show less inflammation following injection of GM-CSF virus: less GM-CSF may be produced in some strains or the microglia and astrocytes may be less sensitive to the GM-CSF that is produced. In the three mouse strains there is no significant difference between the number of eGFP-positive cells in the GM-CSF-virus injected and eGFP-injected mice. This suggests that the mice allow similar expression of transgenes, therefore the difference in inflammatory responses in these strains may be presumably down to the sensitivity to GM-CSF. Nonetheless, to further investigate the differences between high and low responders to GM-CSF-virus, it

will be important to carry out in situ hybridisation and ELISA experiments to establish the levels of bioactive GM-CSF protein produced in the low-responding mouse strains. The responses of different strains to injection of recombinant GM-CSF could be compared. In addition, the striatal tissue treated with GM-CSF/eGFP-virus or control-virus should be extracted for gene expression profiling using DNA microarray technology. The results may identify candidate genes whose expression may mediate the toxic effects of GM-CSF.

Finally, the mouse strains where GM-CSF expression results in moderate microglia activation may be used to evaluate the possible pro-regenerative effects of that cytokine.

Why was the mouse striatal response to GM-CSF different between gross analysis and cell counting?

To study whether the glial and inflammatory responses to a striatal injection of GM-CSF virus was different between mouse strains, a semi-quantitative and a quantitative analysis was carried out. To measure the glial and inflammatory response in six mouse strains a semi-quantitative scoring system that took into account cellular morphology and antibody reactivity was used, while to further analyse the differences between three strains the numbers of cells were counted. When the results of the semi-quantitative and quantitative studies were compared, it was found that the difference in astrocyte activation between mouse strains was inconsistent. In the semi-quantitative study astrocyte activation in the striatum of 129S2/SV mice was significantly lower than that in FVB/N mice. In contrast, the quantitative study failed to reveal any difference between these strains in terms of astrocyte activation. In addition, the semi-quantitative study apparently shows an obvious difference between strains in the amount of microglial activation and phagocytic microglial density, while in the quantitative study the differences between strains were dampened. This discrepancy may be due to the inherent differences between a semi-quantitative and quantitative analysis. In the semi-quantitative analysis an ordinal scale was used, where the differences between adjacent scale values do not necessarily represent equal intervals. Therefore it is difficult to compare the results of the two experiments. In addition, in the semi-quantitative study glial activation was characterised by a gross analysis of cell density as well as the level of antibody immunoreactivity.

However, in the quantitative analysis only the number of cells were considered. It would be interesting to carry out immunoreactivity measures to find out if the difference between strains is still exists.

Mechanisms of GM-CSF- mediated inflammation

When microglia become activated by GM-CSF they can produce pro-inflammatory cytokines, such as IL-6 and TNF-α (Reddy et al., 2009), which are known to activate astrocytes (Malipiero et al., 1990) and can cause cell death (de Bock et al., 1998; Long-Smith et al., 2010; Ono et al., 2010). GM-CSF also increases ICAM expression (Furie and Randolph, 1995; Wahl et al., 1996), which may help T-cells to be recruited to the injection site. These mechanisms are discussed in greater detail in chapter four.

Foetal FVB/N mice injected with GM-CSF/eGFP-virus into the lateral ventricles had virally- transduced cells present in several brain areas

As FVB/N mice are high responders to GM-CSF, it was next investigated whether GM-CSF/eGFP-virus could be used to cause inflammation in cerebral white matter of the immature brain. Injury to the white matter is a common cause of cerebral brain injury leading to cerebral palsy. The causes of perinatal cerebral white matter injury are multifactorial: hypoxia, ischemia, infection and inflammation are thought to be involved (Volpe, 2009). A widely used model of infection and inflammation is the systemic or uteroplacental administration of LPS in pregnant female rodents (Hagberg et al., 2002; Silbereis et al., 2010). However, the effects of LPS are only transient and multiple injections are often required (Duncan et al., 2002). To model the effect of chronic inflammation in the immature brain, GM-CSF/eGFP-virus was injected into the lateral ventricles of foetal FVB/N mice.

In the current study it was found that the lentiviral vector can be successfully delivered to the foetal brain and that there is long-term expression of the transgene. Foetal mice injected with eGFP-virus or GM-CSF/eGFP-virus had widespread eGFP-positive cells in the brain at postnatal day 0, 3 and 7. These results are in agreement with Rahim et al. (2009), who showed that mice which received an intraventricular injection of eGFP-lentiviral vector at embryonic day

14 had eGFP-positive neurons in the cingulate cortex, sensory motor cortex and hippocampus at day 21.

The widespread expression of eGFP in the brain following viral vector injection may be due to cell migration. Tabata and Nakajima (2001) found that foetal mice injected with a DNA plasmid encoding for eGFP into the lateral ventricles at embryonic day 14 had eGFP-expressing cells in the ventricular zone at embryonic day 15. The ventricular zone is a pseudostratified epithelium containing multipotent neural stem cells located next to the ventricle walls. At embryonic day 16 neuroblasts had entered the intermediate zone, which recedes between the marginal zone and the pia mater in the developing cortex. At postnatal day 3 the eGFP-positive cells were observed beneath the marginal zone, were migration terminates and neuroblasts differentiate into mature neurons. By day 21 neurons were present in the layer II, III and IV of the cerebral cortex (Tabata and Nakajima, 2001). As there was eGFP-positivity in the choroid plexus and ventricular epithelium migration of virally-transduce neuroblasts from the ventricular zone to other cortical layers may be possible. However, it is also likely that the eGFP-virus and GM-CSF/eGFP virus diffused trough the brain transducing local cells.

Microglial activation is transient in the immature CNS of FVB/N mice

Mice injected with GM-CSF/eGFP-virus at embryonic day 14 had more phagocytic microglia in the white matter, cerebral cortex, septum, striatum and ventricular epithelium, at postnatal day 0 than those injected with eGFP-virus. The GM-CSF/eGFP-mediated increase in microglial activation decreased by day 7. The transient increase in microglial activation may be reflecting the process of microglial maturation during development. In the foetal and neonatal brain microglia have a rounded amoeboid morphology that changes to a ramified one as the brain matures (Alliot et al., 1999; Ginhoux et al., 2010; Hristova et al., 2010; Prinz and Mildner, 2011). In mice phagocytic microglia in the white matter and cortex are present at postnatal day 0, processes protrude from the microglial cell body at day 7, and at day 14 microglia are fully ramified, having an almost adult phenotype (Hristova et al., 2010). Phagocytic microglia in the new-born mice may be more sensitive to GM-CSF than ramified microglia. Indirect evidence for this

comes from adult rats. In the facial motor nucleus of rats that have undergone facial nerve axotomy there is an increase in the expression of the GM-CSF receptor, which coincides with microglial proliferation and the transformation of microglia from a ramified to an activated morphology (Raivich et al., 1991a). In new born mice there may be greater expression of GM-CSF receptors in microglia making them more susceptible to the effects of GM-CSF.

Alternatively, the transient effects of GM-CSF may be pertinent to the mouse brain being particularly vulnerable to damage during the embryonic and perinatal periods. In the developing cerebral white matter, premyelinating oligodendrocytes are more vulnerable to excitotoxic, oxidative and inflammatory forms of injury than mature oligodendrocytes (Volpe, 2009). In addition, subplate neurons have been shown to be vulnerable to excitotoxic cell death (Ghosh et al., 1990; Ghosh and Shatz, 1992) and hypoxic-ischemic injury (McQuillen et al., 2003). Subplate neurons are located beneath the immature cerebral cortex (Kostovic and Rakic, 1990; Luskin and Shatz, 1985). They are transient cells (Alghoul and Miller, 1989; Chun and Shatz, 1988; Price et al., 1997) that undergo programmed cell death in the first postnatal week in mice (McQuillen et al., 2002). They are required for the formation of mature thalamocortical connections and for the proper development of motor, visual and cognitive functions in rodents and humans (McQuillen and Ferriero, 2005). Subplate neurons are selectively destroyed when the glutamate agonist kainate is injected into the brain of embryonic and postnatal kittens (Ghosh et al., 1990; Ghosh and Shatz, 1992). In addition, in the neonatal rat model of hypoxia-ischemia, selective subplate neuronal death is seen. This is associated with deficits in motor function, as in babies with periventricular white matter damage (McQuillen et al., 2003). Microglia stimulated with GM-CSF have been shown to produce proinflammatory factors that can cause cell death (Reddy et al., 2009) and further increase the level of microglial activation.

In summary, the experiments have enabled the development of models of severe and moderate inflammation in the adult mouse brain and of inflammatory injury in the foetal mouse brain. The foetal mouse model offers a method of testing the effects of prolonged inflammation in the immature brain. Previous infectious/inflammatory models that have been developed, include intrauterine

administration of LPS, the direct delivery of LPS into the subcortical white matter, intravenous injection of LPS into the foetus, or intraperitoneal injection into the mothers or the pup (Wang et al., 2006). In these models the time points investigated are between 1 to 72 hours post injection as LPS-induced inflammation is transient. In contrast, using the current model the chronic effect of inflammation in the immature brain can be investigated. In addition, the delivery of GM-CSF into the ventricles of the foetal brain permits inflammation to be restricted to the CNS. In some other models inflammation this is both systemic and central (Wang et al., 2006). However, using the virally-delivered GM-CSF model the effects of local inflammation in the brain rather than that caused by circulating factors can be evaluated. The model could be used to test therapeutic strategies using pharmacological agents, e.g. hemichannel blockers (Takeuchi et al., 2006). In addition, brain injury is exacerbated in neonate mice injected with LPS when they undergo hypoxia-ischemia insult, which involves unilateral carotid ligation and exposure to 8% oxygen for 30 minute, (Kendall et al., 2011). Future experiments should investigate whether GM-CSF-virus has a similar preconditioning effect on cerebral hypoxia-ischemia.

Conclusion

In this chapter the viral delivery of GM-CSF to the brain of different mouse strains produces strain specific effects. The inflammatory and glial response was low in the 129S2/Sv strain, widespread though moderate in BALB/c, and high in the FVB/N strain. The FVB/N mouse strain was used to study the effect of GM-CS-virus mediated inflammation in the foetal brain with the aim of modelling perinatal white matter damage. Intraventricular delivery of GM-CSF-virus enhances microglial activation in the early post natal period in various areas brain, including the white matter.

CHAPTER SIX

Delivery of lentiviral GM-CSF to the motor cortex protects corticospinal axons and improves functional recovery in rats with corticospinal tract injury

Introduction

The neurons of the peripheral nervous system (PNS) have a well-documented ability to regenerate their axons following injury leading to successful functional recovery. This spontaneous recovery is associated with a cell body response that includes the upregulation of growth associated genes, adhesion molecules and structural proteins (Anderson and Lieberman, 1999; Becker, 2006), and pronounced activation and proliferation of microglia surrounding the neuronal perikarya (Kreutzberg, 1996; Liu et al., 1998). In contrast, neurons projecting within the central nervous system (CNS), such as corticospinal neurons, show no microglial activation and a weak or absent neuronal response to axonal damage, (Barron et al., 1990; Leong et al., 1995) and limited behavioural improvement (Whishaw et al., 1993).

Microglial activation can be induced by Granulocyte Macrophage Colony Stimulating Factor (GM-CSF), a potent microglial mitogen that has been shown to strongly enhance microglial synthesis of neurotrophins such as BDNF, increase expression of regeneration-related proteins such as GAP-43, promote neuronal survival, increasing neurite outgrowth in vivo and improving functional recovery after spinal cord injury (Bouhy et al., 2006; Ha et al., 2005; Huang et al., 2009). However, previous studies demonstrating pro-regenerative effects of GM-CSF concentrated on inflammatory changes at the site of spinal cord injury and focused only on short-term effects of GM-CSF.

The following chapter describes the effect of long-term GM-CSF/eGFP-virus mediated cortical inflammation on axonal regeneration and functional recovery. The chapter reports the histological assessments and behavioural tests carried out on rats with corticospinal tract injury injected into the motor cortex with GM-CSF/eGFP-virus.

Results

GM-CSF-virus has a protective effect on injured corticospinal axons

To examine the effect of GM-CSF on corticospinal tract regeneration, Sprague-Dawley rats had injections of eGFP control-virus (n=4) (Fig. 1A) or GM-CSF/eGFP-viral mixture at titres 10^4 (GM4: n=4), $10^{5.5}$ (GM5.5: n=4), 10^7 (GM7: n=4) /ml into the motor cortex (Fig.1B). The contralateral dorsal corticospinal tract was transected at the fourth cervical segment. Two weeks before sacrifice, BDA was injected into the motor cortex to label axons in the injured corticospinal tract. Rats were allowed to survive 42 days after initial surgery, and their BDA-positive axons were visualized using DAB enhanced with cobalt nickel.

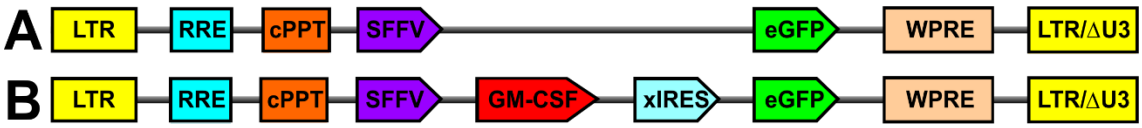

Figure 1: Schematic representation of the lentiviral plasmids used in this study. A: The enhanced Green Fluorescent Protein (eGFP) lentiviral plasmid (control-virus). B: The Granulocyte Macrophage Colony Stimulating Factor (GM-CSF) lentiviral plasmid. In these experiments the GM-CSF virus was diluted from 10^8 TU/ml to 10^7,$10^{5.5}$, and 10^4 TU/ml using control-virus at a 10^8 titre.

To examine whether the cortical injections of virus altered the numbers of labelled corticospinal axons in the brainstem, BDA-positive corticospinal axons were counted in transverse sections of the pyramidal decussation using two fields of a x40 objective. The GM4-virus group had 35±6 BDA-labelled axons per field (Fig. 2B & E-grey bar), those injected with GM5.5-virus had 39±7 (Fig. 2C & E-yellow bar), and GM7-virus injected rats had 45±10 (Fig. 2D & E-red bar). The GM-CSF-virus injected groups were not significantly different from the control-injected group that had 31±6 per field (Fig. 2A & E-green bar) ($p<0.05$; univariate ANOVA). This result shows that there was a similar success in the anterograde labelling of the corticospinal tract in GM-CSF/eGFP-virus injected and control-virus injected groups and that the proximal parts of corticospinal axons were not adversely affected by the viral injections.

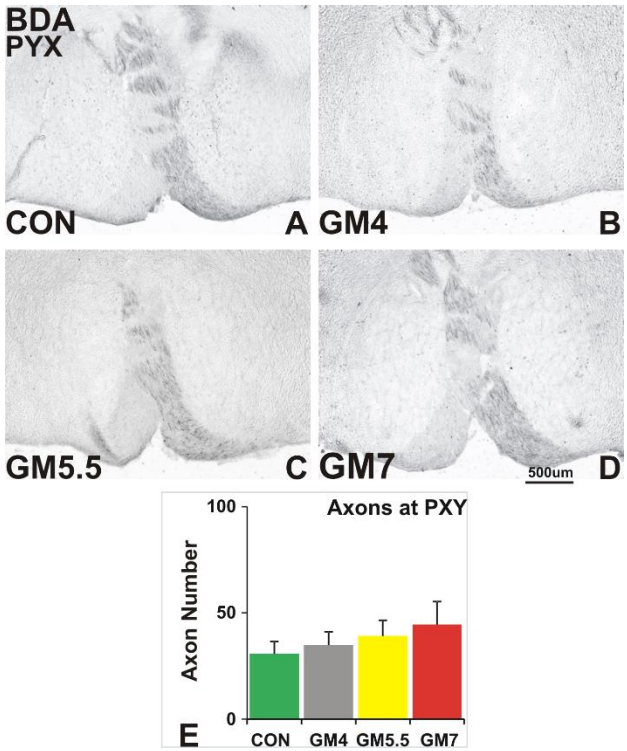

Figure 2: CST axonal density at the pyramidal decussation is the same following control-virus or GM-CSF/eGFP-virus injections into the motor cortex. Histogram representing the mean number of BDA positive axons per field in the pyramidal decussation (PXY) of rats injected with control-virus (green bars), GM4 (grey bars), GM5.5 (yellow bars) or GM7 (red bars). Cortical injections were contralateral to a C4 corticospinal tract injury. There was no difference between the groups: $p>0.05$ univariate ANOVA. Error bars show the standard error of the mean (SEM).

Longitudinal horizontal sections through the spinal cord demonstrated that after injecting control-virus into the motor cortex (Fig. 3A), there were a few axons and retraction bulbs in close proximity to the injury site. These increased in those animals injected with GM4 (Fig. 3B), were highest in those injected with GM5.5 (Fig. C), and decreased in rats injected with GM7 (Fig. 3D)

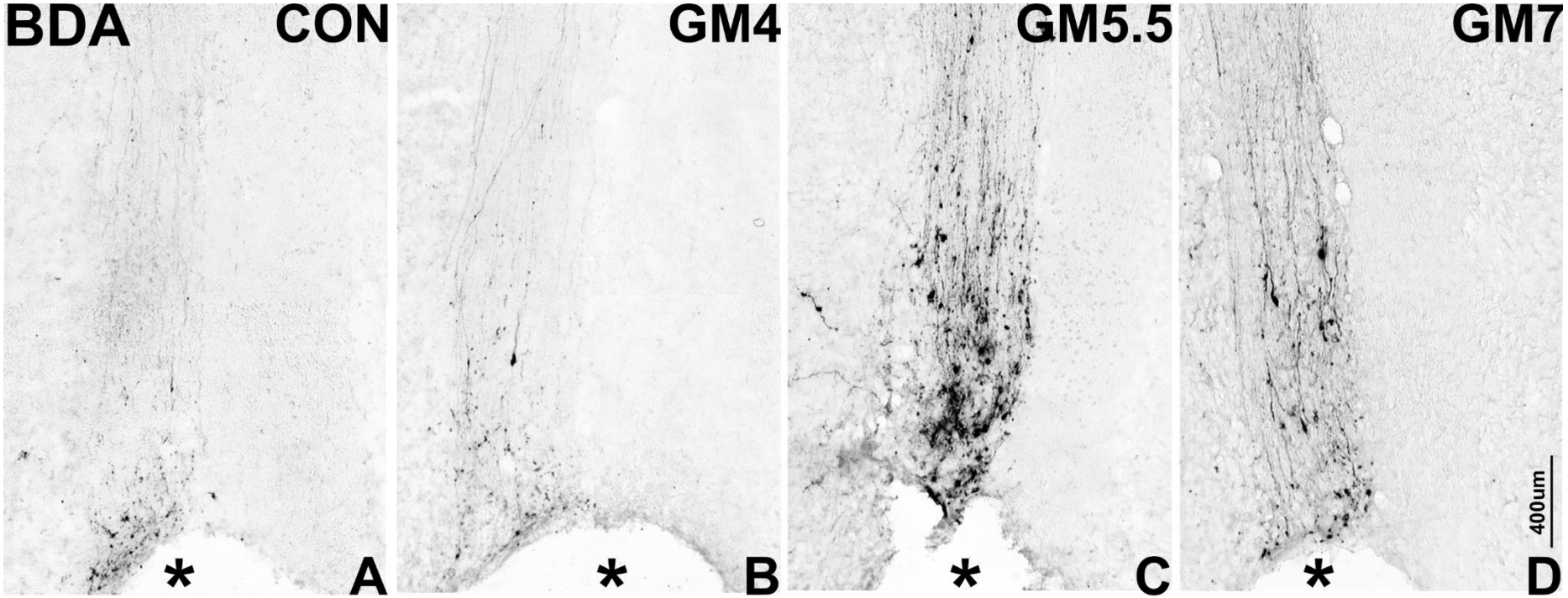

Figure 3: The effect of GM-CSF/eGFP virus on axon and retraction bulb density after injury. A-D: Micrographs showing horizontal longitudinal sections through the cervical corticospinal tract of rats with C4 corticospinal tract injury, which received control-virus (A), or GM-CSF/eGFP-virus (B-D) at 10^4 TU/ml (GM4), $10^{5.5}$ TU/ml (GM5.5) or 10^7 TU/ml (GM7) injected into the motor cortex. Cobalt Nickel -stained sections showing BDA-positive axons with the injury site (*) at the bottom of each image.

Using a 40x objective lens, the number of BDA-labelled axons in the corticospinal tracts and their retraction end bulbs were quantified rostral (-4.5mm to -0.5mm) and caudal (0.5mm to 4.5mm) to the injury site (0mm). Corticospinal tract axon counts were normalised for the success of anterograde labelling in each animal by comparison with the corresponding count of labelled axons in the pyramidal decussation. Rats treated with GM5.5-virus (Fig. 4-yellow bars) and GM7-virus (Fig. 4-red bars) titres had significantly more corticospinal axons close to the injury site (1mm rostral) than those treated with control-virus (Fig. 4-green bars) ($p<0.05$; Tukey post hoc test to a univariate ANOVA).

In addition, an overall effect of GM-CSF-virus treatment independent of distance from the injury site was also found. The average number of axons in the corticospinal tract within the spinal cord at all distances rostral to the injury site was over four times greater in the GM4 (Fig. 4- insert grey bar), GM5.5 (Fig. 4- insert yellow bar) and GM7-treated groups (Fig. 4- insert red bar) compared to control-virus treated group (Fig. 4- insert green bar) ($p<0.05$; Tukey post hoc test to a univariate ANOVA).

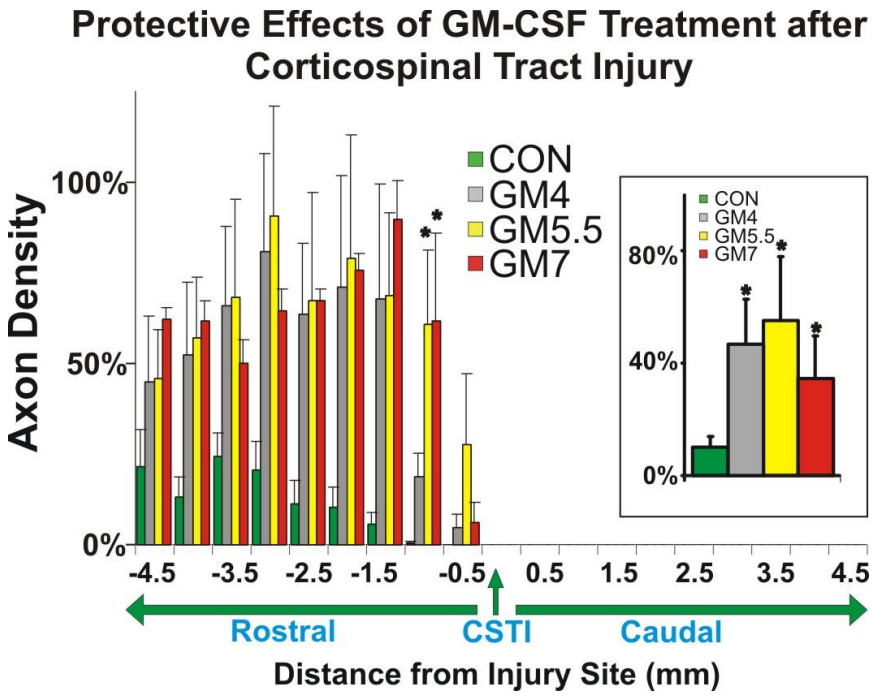

Figure 4: GM-CSF/eGFP-virus injection into the motor cortex has a protective effect on CST axons following injury. Histogram showing the axonal density rostral (-0.5 to -4.5 mm) and caudal (0.5 to 4.5 mm) to the corticospinal tract injury site (CSTI). Green bars represent animals injected with control virus, grey bars represent those injected with GM4-virus, yellow GM5.5-virus, red GM7-virus. Rats injected with GM5.5 and GM7 have significantly more axons 1mm rostral to the lesion site that those injected with control virus. Insert: Histogram showing the axonal density after averaging the counts for all distances rostral to the injury site. Animals injected with GM4, GM5.5 and GM7 have significantly more axons in the cervical corticospinal tracts than those injected with control virus. (*) $p<0.05$ Tukey post hoc test to a univariate ANOVA. Bars represent the ratio between the numbers of axons in the spinal cord to those in the pyramidal decussation. Error bars show the standard error of the mean (SEM).

To further evaluate the axonal response, the number of BDA-filled axonal retraction bulbs were counted. Retraction bulb quantifications were normalised with spinal axon counts. Rats treated with GM5.5-virus (Fig. 5-yellow bars) or GM7-virus (Fig. 5-red bars) had more retraction bulbs at 1mm and 1.5mm rostral to the injury site, than those treated with control-virus virus (Fig. 5-green bars). Overall, independent of distance, all GMCSF/eGFP-virus treated animals had greater numbers retraction bulbs at spinal cord than the eGFP virus (Fig. 5-insert) ($p<0.05$; Tukey post hoc test to a univariate ANOVA).

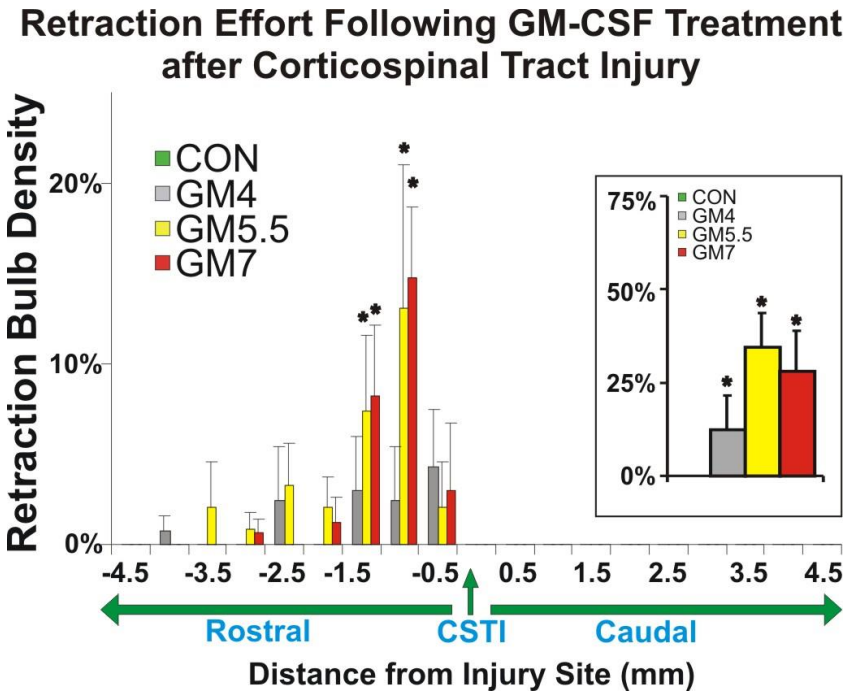

F**igure *5***: Quantification of axonal retraction following GM-CSF/eGFP-virus treatment. Histogram showing the retraction bulb density rostral (-0.5 to -4.5 mm) and caudal (0.5 to 4.5 mm) to the corticospinal tract injury site (CSTI). Green bars represent animals injected with control virus, grey bars represent those injected with GM4-virus, yellow GM5.5-virus, red GM7-virus. Rats injected with GM5.5 and GM7 have significantly more retraction bulbs 1mm and 1.5mm rostral to the lesion site that those injected with control virus. Insert: Histogram showing the retraction bulb density after averaging the counts for all distances rostral to the injury site. Animals injected with GM4, GM5.5 and GM7 have significantly more retraction bulbs in the cervical corticospinal tracts than those injected with control virus. (*) $p<0.05$ Tukey post hoc test to a univariate ANOVA. Bars represent the ratio between the numbers of retraction bulbs in the spinal cord to the number of axons in the corticospinal tract in the spinal cord. Error bars show the standard error of the mean (SEM).

Inflammation, gliosis and expression of growth-related proteins in the motor cortex accompanied the GM-CSF-mediated axonal protection

Inflammation and astrogliosis

The next step was to analyse whether the axonal protection previously described could be correlated with the production of inflammation and astrogliosis in the motor cortex. Coronal sections through the motor cortex of rats with corticospinal tract injuries, injected with control-virus (n=4), GM4-virus (n=4), GM5.5-virus (n=4) or GM7-virus (n=4), were fluorescently stained to visualise microglia or astrocytes.

Microglial and astrocyte activation was dose-dependent. At six weeks after injection coronal brain sections through the injection site stained for IBA1, contained microglia with a ramified morphology in rats injected with the control-virus (Fig. 6A), an activated morphology in those injected with GM5.5-virus (Fig. 6B), and a phagocytic morphology in GM7-virus injected rats (Fig. 6C). The numbers of IBA1-positive microglia were counted along the injection site using a x40 objective lens. Rats injected with GM5.5-virus (Fig 6. D-yellow bar) or GM7-virus had more microglia at the injection site (Fig 6. D-red bar), than those injected with control-virus virus (Fig 6. D-green bar) ($p<0.05$; Tukey post hoc test to a univariate ANOVA).

Similarly, astrocytes in the motor cortex changed in morphology with GM-CSF treatment. Astrocytes had a hypertrophic appearance with thick GFAP-positive processes in rats injected with GM5.5-virus (Fig. 6F) or GM7-virus (Fig. 6G), compared to those injected with control-virus (Fig. 6E). In addition, there was clear glial scaring in GM7 injected rats, which was not evident in control-virus or

GM5.5-virus-injected rats. Finally, the number of astrocytes per field was greater in those injected with GM5.5-virus (Fig. 6H-yellow bar) or GM7-virus (Fig. 6H-red bar), than those injected with control-virus (Fig. 6H-green bar) ($p<0.05$; Tukey post hoc test to a univariate ANOVA).

Growth-associated proteins

Regeneration competent neurons increase expression of regeneration-associated genes such as *ATF3* and *c-Jun*. Increasing inflammation in the vicinity of the injured neuronal perikarya is associated with the cell body response. With this in mind, the expression of growth-associated factors in the inflamed motor cortex was next examined. Brain sections of rats injected with control-virus or GM4-virus, GM5.5-virus or GM7-virus were fluorescently stained for c-Jun or ATF3. Sections were also stained with DAPI to visualise nuclei. DAPI-positive nuclei that were c-Jun- or ATF3-positive were counted using a x40 objective lens at various levels along the injection site.

Coronal sections through the injection site showed that there was little expression of these transcription factors in the control-injected cortex, but there was more expression in and around the injection sites of GM5.5-virus and GM7-virus. However, the small size of c-Jun- (Fig.7-left column) and ATF3- (Fig. 7-right column) positive nuclei suggests that they belonged to glial cells rather than cortical neurons.

There were more c-Jun-positive nuclei per field in rats injected with GM5.5 (Fig.7D-yellow bar) and GM7 (Fig.7D-red bar) than in those injected with control-virus (Fig.7D-green bar). Similarly, in comparison to control-virus injected rats (Fig.7H-green bar), GM7-virus injected rats had significantly more ATF3-positive nuclei (Fig.7D-red bar) ($p<0.05$; Tukey post hoc test to a univariate ANOVA).

Figure 6: Long-term expression of GM-CSF-virus increases microglial and astrocyte activation in the motor cortex of rats with C4 corticospinal tract injuries. A-C&E-G: Coronal brain sections through motor cortex stained for IBA1 or GFAP (in red), and also showing eGFP-positive cells (in green), six weeks following injections of control-virus, GM4, GM5.5 or GM7-virus. Bar Scale: 20um. The number of microglia (A-C) and astrocytes (E-G) increase with increasing GM-CSF/eGFP-virus concentration. The number of eGFP-positive cells decreased in cortices injected with GM-CSF virus (A-C&E-H). D&H: Histograms representing the number of IBA1-positive (+) microglia per field (D) and GFAP-positive astrocytes per field (H), 6 weeks after injection into the motor cortex of control virus (green bars), GM4-virus (grey bars), GM5.5-virus (yellow bars) or GM7-virus (red bars). (*) $p<0.05$ following an univariate ANOVA statistical analysis. Bars and error bars represent the mean and standard error of the mean (SEM), respectively.

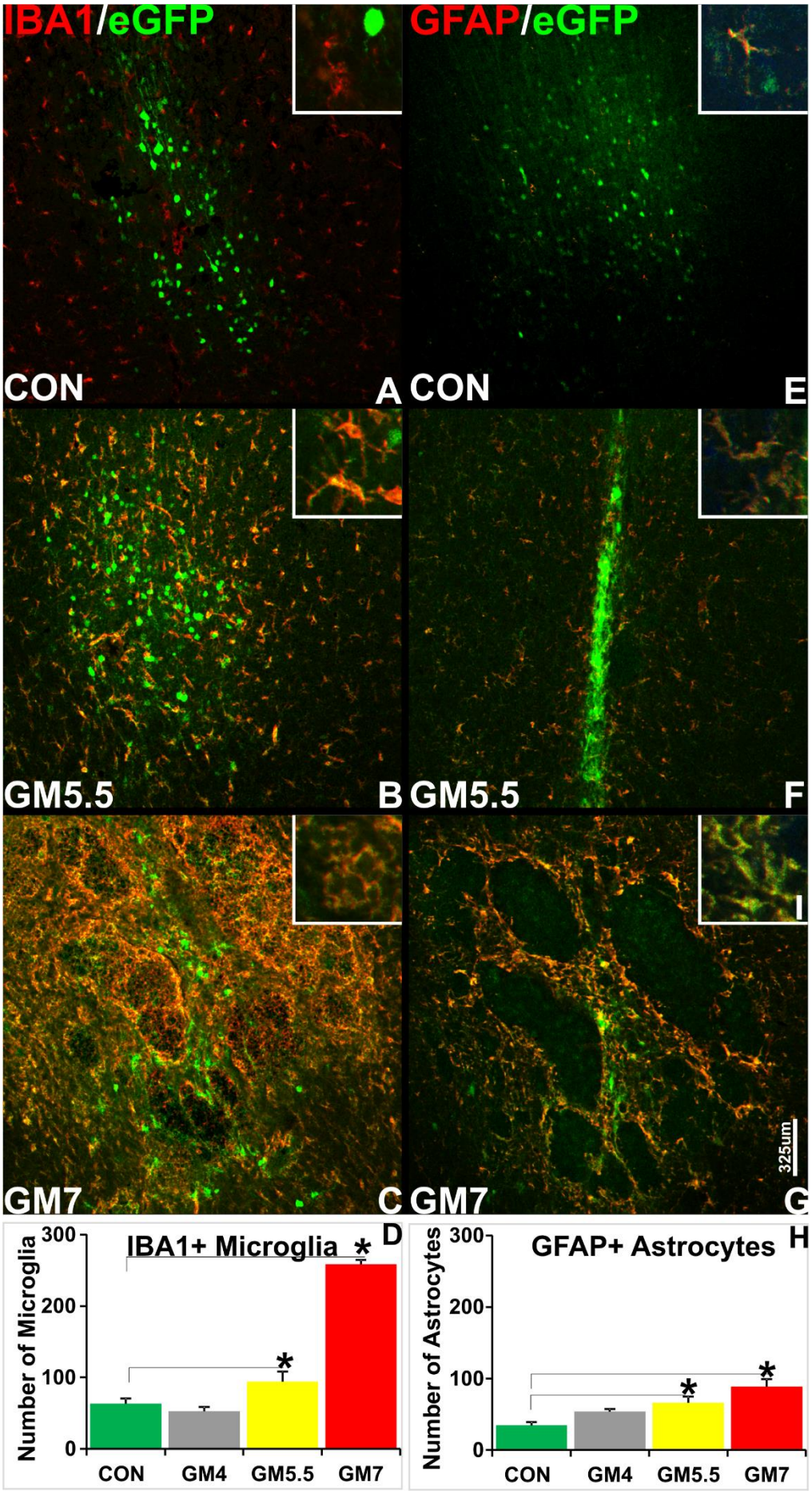
IBA1/eGFP
GFAP/eGFP
CON
A
CON
E
GM5.5
B
GM5.5
F
GM7
C
GM7
G
I
325um
IBA1+ Microglia
D
Number of Microglia
300
200
100
0
CON
GM4
GM5.5
GM7
GFAP+ Astrocytes
H
Number of Astrocytes
300
200
100
0
CON
GM4
GM5.5
GM7

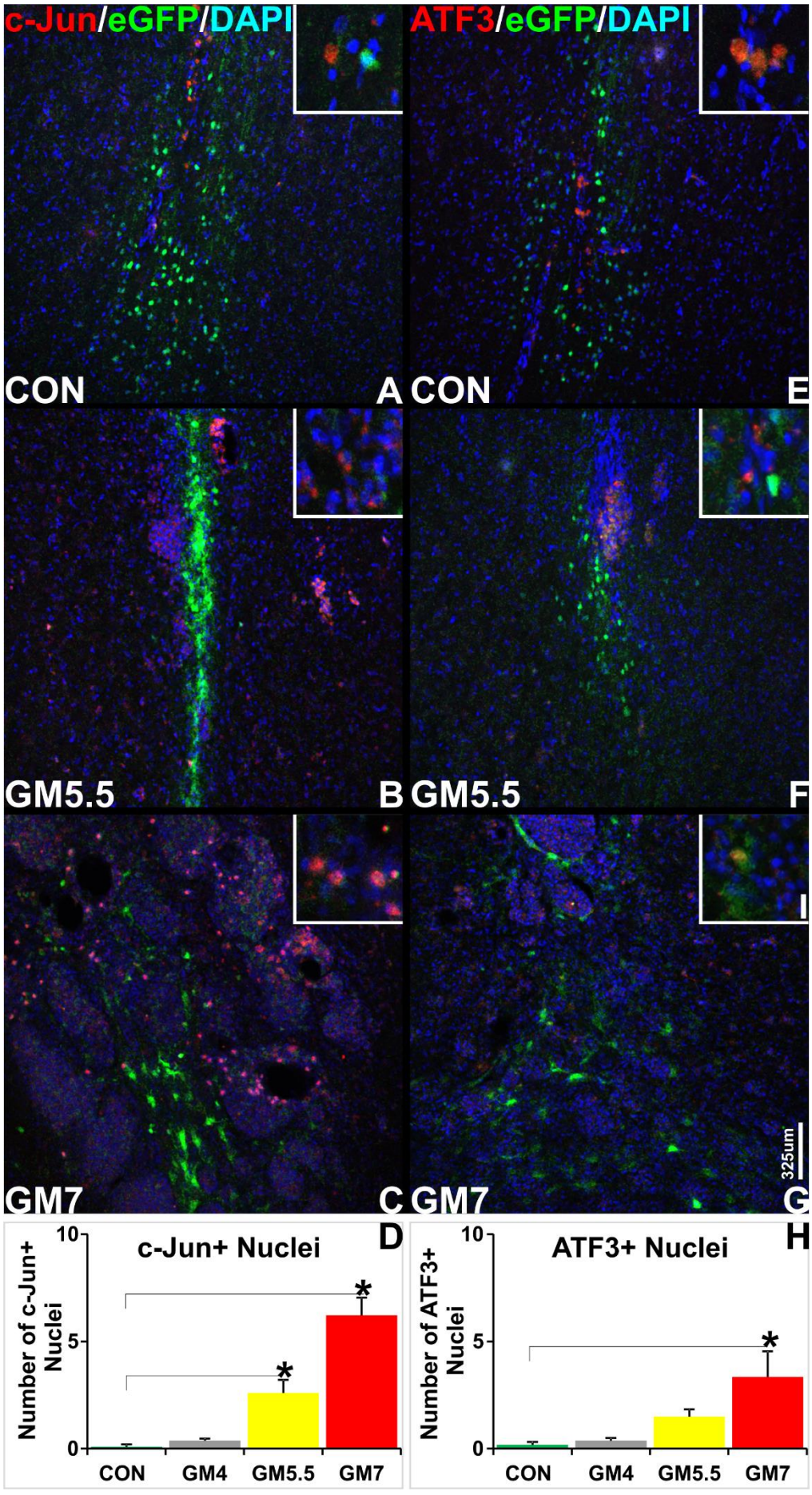
c-Jun/eGFP/DAPI
ATF3/eGFP/DAPI
CON
A
CON
E
GM5.5
B
GM5.5
F
GM7
C
GM7
G
325um
I
c-Jun+ Nuclei
D
Number of c-Jun+ Nuclei
10
5
0
CON
GM4
GM5.5
GM7
ATF3+ Nuclei
H
Number of ATF3+ Nuclei
10
5
0
CON
GM4
GM5.5
GM7

Figure 7: Long-term expression of GM-CSF-virus increases c-Jun and ATF3 expression in the motor cortex of rats with C4 corticospinal tract injuries. A-C&E-G: Coronal brain sections through motor cortex stained for c-Jun or ATF3 (in red), nuclei (in blue), and also showing eGFP-positive cells (in green), six weeks following injections of control-virus, GM4, GM5.5 or GM7-virus. Bar Scale: 20um. With increasing GM-CSF/eGFP-virus concentration, the number of c-Jun-positive nuclei (A-C) and ATF3-positive nuclei increased (E-G). D&H: Histograms representing the number of c-Jun-positive (+) nuclei per field (D) and ATF3-positive nuclei per field (H), 6 weeks after injection into the motor cortex of control-virus (green bars), GM4-virus (grey bars), GM5.5-virus (yellow bars) or GM7-virus (red bars). (*) $p<0.05$ following an univariate ANOVA statistical analysis. Bars and error bars represent the mean and standard error of the mean (SEM), respectively.

Increased microglial activation was also found along the corticospinal tract within the spinal cord

In Chapter Four it was found that intracortical injections of GM-CSF/eGFP-viral mixture into the motor cortex of intact rats promoted microglial activation in the corticospinal tract. The next step evaluated whether rats with corticospinal tract injuries that received intracortical injections of control-virus (n=4), GM4-virus (n=4), GM5.5-virus (n=4), or GM7-virus (n=4) showed signs of an inflammatory response in the corticospinal tract within the cervical spinal cord. Longitudinal horizontal sections through the spinal cord were stained for IBA1 to visualise microglia and BDA to visualise axons in the corticospinal tract.

The injured and intact corticospinal tracts were visualized in longitudinal horizontal sections through the cervical spinal cord. Six weeks after injection, the rats injected with GM5.5-virus had more microglia with a phagocytic morphology surrounding the BDA positive axons in the injured and intact corticospinal tracts than those injected with control-virus. Microglial activation in the corticospinal tract was highest in the injured corticospinal tract and less in the intact corticospinal tract. This effect was not present in the rats injected with control virus (Fig. 8).

The number of IBA1-positive microglia was counted along the corticospinal tract, rostral to the injury site, using four fields of a 40x objective lens. In comparison to the control-group, the GM5.5-virus injected rats had significantly more microglia in the experimental corticospinal tract rostral to the injury site ($p<0.05$; Tukey post hoc test to a univariate ANOVA). However, GM-CSF-virus had no effect on the number of microglia in the intact corticospinal tract.

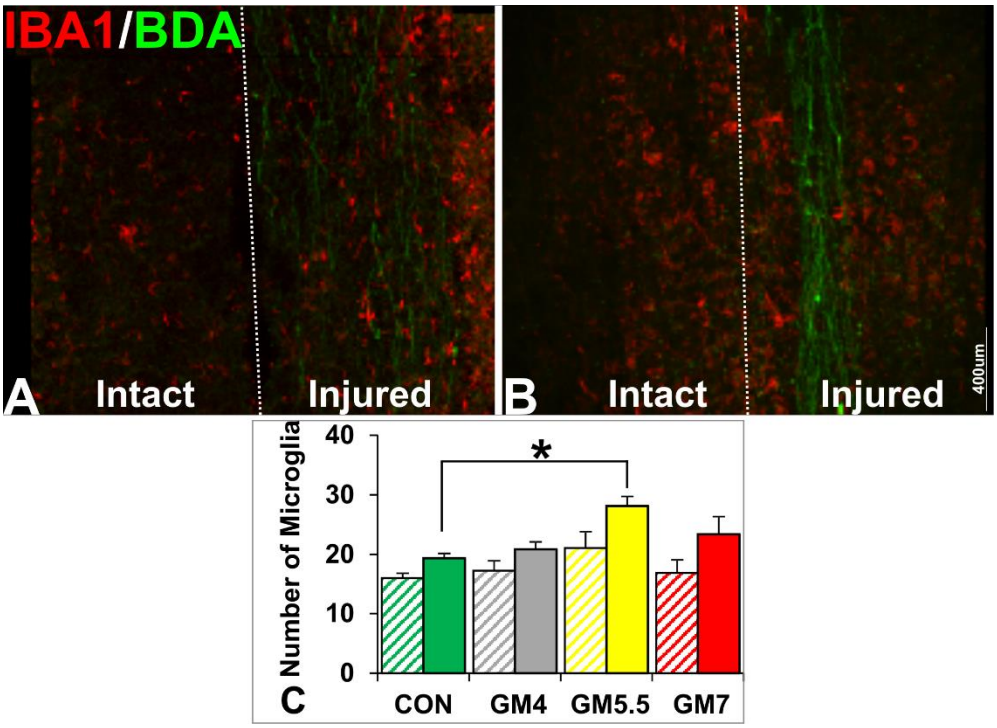

Figure 8: GM-CSF/eGFP virus increased the number of microglia in the corticospinal tract within the spinal cord. A-B: Horizontal sections of spinal cords stained for IBA1 showing the intact and the injured corticospinal tracts, 6 weeks after injection of control-virus (A), or GM5.5-virus (B) into the motor cortex. C: Histogram showing the number of IBA1-postive microglia per field in the intact corticospinal tract (patterned bars) and injured corticospinal tract (plain bars), following cortical injections of control-virus, GM3-virus, GM5.5-virus, or GM7-virus. There were significantly more microglia in the injured corticospinal tract of GM5.5 animals compared to animals injected with control virus. (*) $p<0.05$ Tukey post hoc test to univariate ANOVA. Bars and error bars represent the mean and standard error of the mean (SEM).

Preliminary assessment of functional recovery of rats with corticospinal tract injury

The anatomical analysis has shown that rats that received cortical injections of moderate and high doses of GM-CSF lentivirus have more axons in the injured corticospinal tract than those that received the control-virus. To determine if this effect produces functional improvement, a rearing test and the directed forepaw reaching test were used to evaluate asymmetrical use of forelimb for weight bearing or forepaw reaching and food grasping, respectively.

Preliminary experiments were carried out using four rats. With the direction of Dr Li Ying and Prof Raisman (UCL), the apparatus for the directed forepaw reaching test was produced by adapting a rat cage so as to have a vertical slit (8 cm x 1.5 cm) in the middle of cage with a rectangular platform (3 cm x 4 cm) protruding at the bottom of the slit (Fig. 9A). For the rearing test, we used a transparent vertical

Plexyglas cylinder (30 cm height and 20 cm diameter) (Gharbawie, Wishaw & Wishaw, 2003) with two mirrors (30 cm x 30 cm) placed at 90^{o} behind the cylinder, so that a 360^{o} view of the rat was available (Fig. 9B).

Preliminary behavioural studies allowed us to optimise environmental factors, such as levels of light and sound, necessary to have efficient and effective data collection. In addition, for the food reaching task a battery of food samples were tested including noodles, raisins, marshmallows, Cheerios, etc. Sprague Dawley rats had a preference for Cheerios. To ease the rats' manipulation of food each Cheerios were fragmented into thirds. Furthermore, for the rearing test, it was found that sticking four cotton buds covered in honey at different heights inside the cylinder promoted rearing.

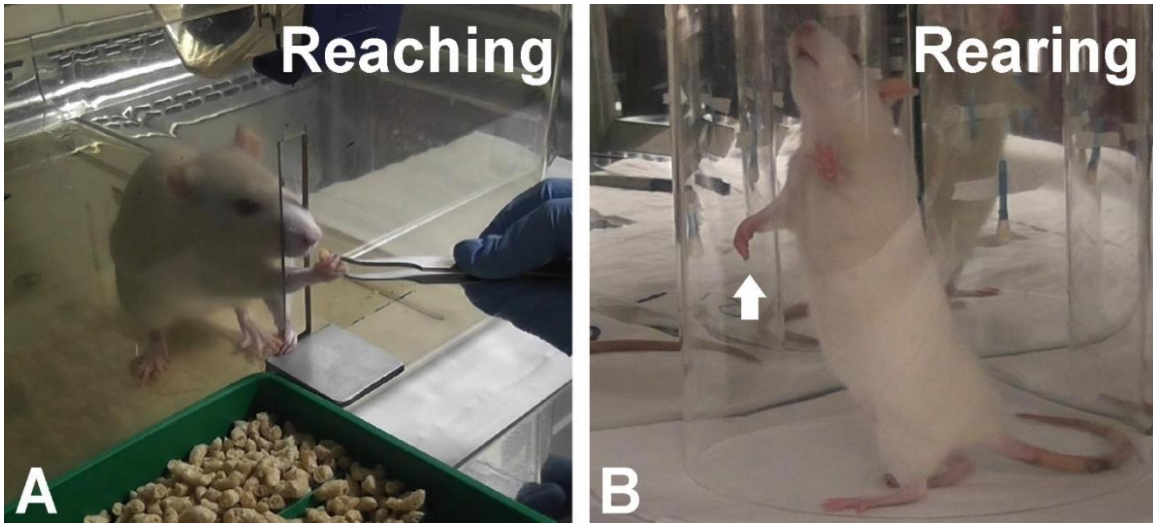

Figure 9: Measuring functional recovery of rats with spinal cord injury using the directed forepaw reaching test and rearing test. **A:** Shows a rat grasping a Cheerio fragment; this action is obliterated in rats with corticospinal tract hemisection. **B:** A rat with right C4 corticospinal tract injury in the standing position using only the left forepaw to balance. Notice the inability to use the injured right forepaw for weight bearing. The arrows points at the paw on the side of the corticospinal tract injury.

Rearing movements spontaneously improve following corticospinal tract injury

Rats with right dorsal corticospinal tract injury at cervical segment 4 were injected into the left motor cortex with control-virus (CON: n=8) or a GM-CSF/eGFP-viral mixture at 10^{4} (GM4: n=9), $10^{5.5}$ (GM5.5: n=7) or 10^{7} (GM7: n=8) (TU/ml). In addition, rats were injected with the anterograde tracer BDA at the motor cortex

3 weeks before sacrifice. To evaluate functional recovery of the right (injured side) paw the rearing assessment was used. The rearing action was broken down into three movements- push off (Fig.10A), rearing (Fig. 10C) and landing (Fig. 10E). The use of left (uninjured) paw, the right paw or both paws for weight bearing were quantified. Two baselines were taken prior to injury and data at 12 post-injury time points, from day 3 to 42, were collected. The involvement of the injured right forepaw in the push off, rearing and landing movements was calculated using the index (2 x RP + BP)/(LP + RP +BP)/2, where RP, LP and BP are the number of times the right paw, left paw and both paws were used, respectively. Behavioural assessment was carried out blind by an examiner using video recordings.

In all the different conditions, the right paw in the push off (Fig 10B), rearing (10D) and landing functions was used around 50% of the time in the pre-surgery time points. At day three in all the tested groups, the push off and rearing movements were more affected by the right corticospinal axotomy than the landing movement. The push off and rearing movements decreased to 2% and 9%, respectively, while the landing movements only decreased to 20%. All rats in each of the groups showed spontaneous recovery of the push off, rearing and landing functions, from day 7 to day 42 following corticospinal tract injury. When the GM-CSF/eGFP groups (GM4, GM5.5 and GM7) were averaged together and compared to the control, there was no significant difference ($p>0.05$; unpaired student t-test).

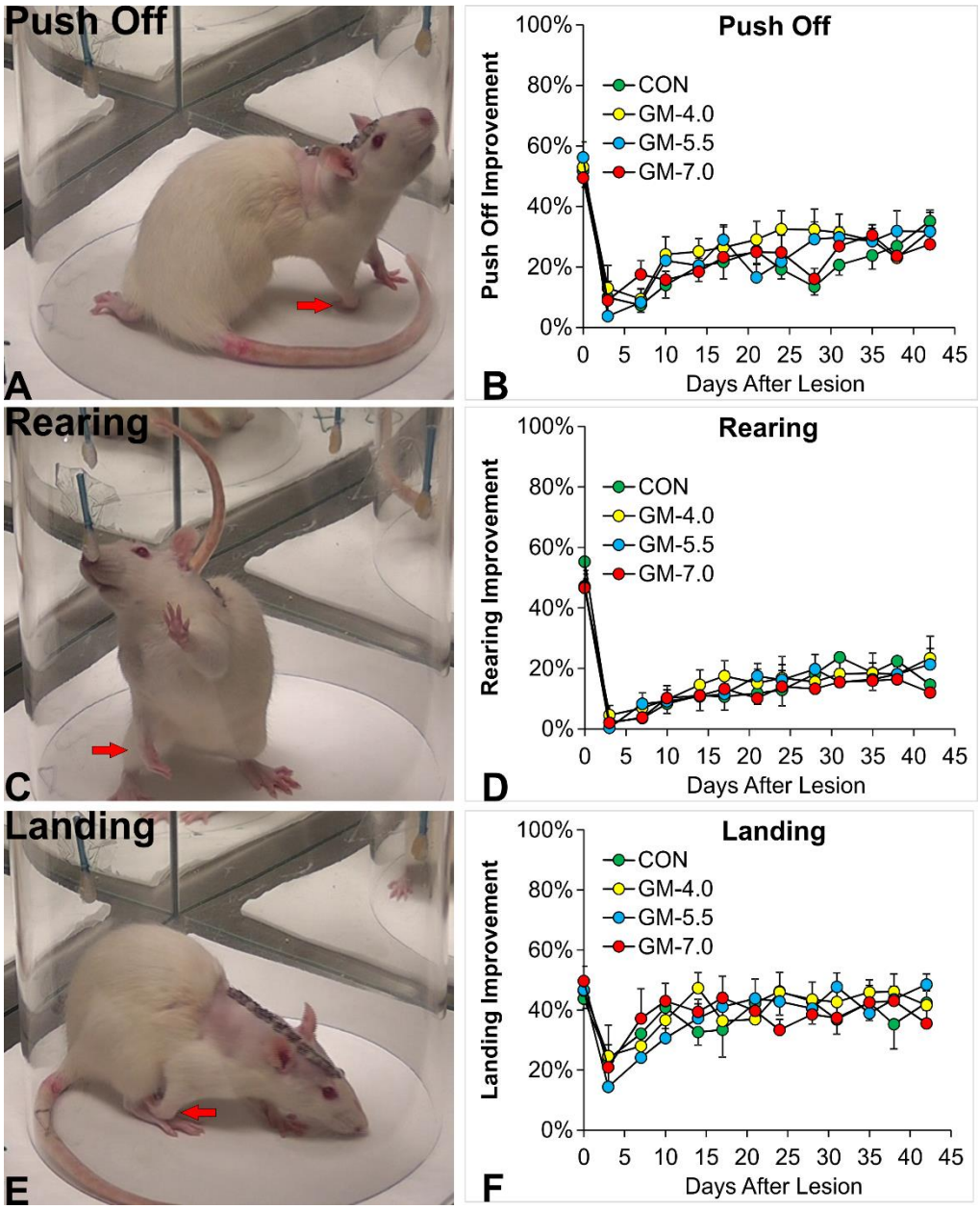

Figure 10: Rats with corticospinal tract injury show spontaneous recovery of rearing movements independent of treatment. A, C & E: Photographs show the movements which were quantified in the rearing assessment. A rat with right C4 corticospinal tract injury uses only the left (uninjured) paw to balance when pushing off the floor (A), rearing (B) and landing (C). Red arrow points to the right (injured side) paw. B,D &F: Line graphs represent the percentage improvement of the right paw of C4 corticospinal tract injured rats injected with control-virus (CON-green) or increasing concentrations of GM-CSF/eGFP-virus at 104 (GM-4.0: yellow), 105.5 (GM-5.5: blue) or 107 (GM-7: red) at 0-42 days post lesion.

GM-CSF/eGFP-virus cortical injection improves behavioural recovery in the directed forepaw reaching test

To further investigate the effect of GM-CSF on functional recovery, rats were evaluated on the directed forepaw reaching test. This task measures fine and voluntary movement, which are controlled by the corticospinal tract (Whishaw et

al., 1992; Whishaw et al., 1998). The reaching movement was separated into three categories, including eating success, distal muscle and proximal muscle movements.

A successful eating movement consisted of the following sequence: lifting paw from floor (Fig. 11A), exiting the slit (Fig. 11B), grasping the Cheerio fragment (Fig. 11C), withdrawing the Cheerio fragment and transporting it to mouth to eat (Fig. 11C). The number of successful eating movement by the right (injured side) paw was calculated as a percentage of the total number of successful eating movement by the injured and intact paws.

Distal muscle function was evaluated by assessing the movements of the lower forelimb and paw: wrist flexion and extension (Fig. 11G-H), and paw opening and closure (Fig. 11E-F). Proximal muscle function was assessed by the shoulder movements, which included abduction (Fig. 11I-J), adduction (Fig. 11K-L) and flexion (Fig. 11M-N), and biceps flexion (Fig. 11O-P). Ability to perform these movements was scored on a scale of 1-3 (1-attempted but ineffective, 2-partial use, or 3-complete use). To measure functional improving, for each movement a percentage score was calculated using the following index: (1 x ineffective + 2 x partial + 3 x complete)/ (ineffective + partial + complete)/3.

Corticospinal tract injury produces loss of distal limb function

During pre-surgery baseline testing, rats randomly assigned to the four experimental groups showed complete movements with the left and right forelimbs. Following a right C4 corticospinal tract injury a clear reduction in all movements was found in the right but not the left forelimb at the first postoperative date (Day 3). These effects were observed in rats injected into the left motor cortex with control-virus (n=8) as well as with GM4 (n=7), GM5.5 (n=6) or GM7 (n=9) (TU/mL) (Fig. 12).

Movements of injured side showed a graded response, with distal muscles being more affected than proximal. A strong effect, with a drop in function to just grade 1 (i.e. attempted movement but of no use, =33%) was found for paw opening and closure (Fig. 12B-C). A more moderate decrease, between grade 1 and 2 (2 is equivalent to partial use, =67%) was observed for wrist extension and flexion (Fig.

12D-E), biceps flexion (Fig. 12F), and shoulder abduction (Fig.12G). Only very mild functional loss (between grade 2 and 3-complete use, =100%) was noted for shoulder adduction and flexion (Fig. 12H-I).

Eating success (Fig. 12A) was especially heavily affected, dropping to 0% immediately after injury. Thus, in line with past research, current results demonstrate that injury to the corticospinal tract is primarily associated with deficits in the movement of distal limb, particularly the precision of reaching and grasping (Whishaw et al., 1993).

Functional recovery

As shown in Figure 12, GM-CSF improved eating success. Averaging across GM-CSF/eGFP groups and comparing against eGFP controls, the rats showed a significant improvement in their ability to complete the eating task (Fig. 12A) at 14, 17, 21, 31, 35 and 38 days post-surgery. There was no apparent dose-dependence in the experimental groups that received the GMCSF vector at GM4, GM5.5 or GM7 ($p<0.05$; unpaired student t-test).

Sub-movements controlled by distal muscles also showed a trend towards better recovery in rats treated with GM-CSF/eGFP-virus, again with no clear difference between different dosages. Thus, paw opening and closing functions showed a trend for improvement (Fig. 12B-C) at day 14 (p= 6%) and 17 (p= 6%; unpaired student t-test) following GM-CSF/eGFP-virus cortical injections rather than control-virus injection. In addition, there was a trend for GM-CSF/eGFP-virus to accelerate recovery of wrist flexion and extension (Fig. 12D-E), biceps flexion (Fig. 12F) and shoulder abduction (Fig. 12G) (p =6-9%; unpaired student t-tests). Spontaneous recovery of proximal movements, such shoulder adduction (Fig. 12H) or flexion (Fig. 12I), were generally independent of treatment ($p>0.05$; unpaired student t-test).

As with eating success, all recoveries seemed to plateau and show little improvement beyond approximately three weeks after corticospinal tract lesion. This suggests that the first 3 weeks is a sensitive phase for treatment with GM-CSF/eGFP-virus.

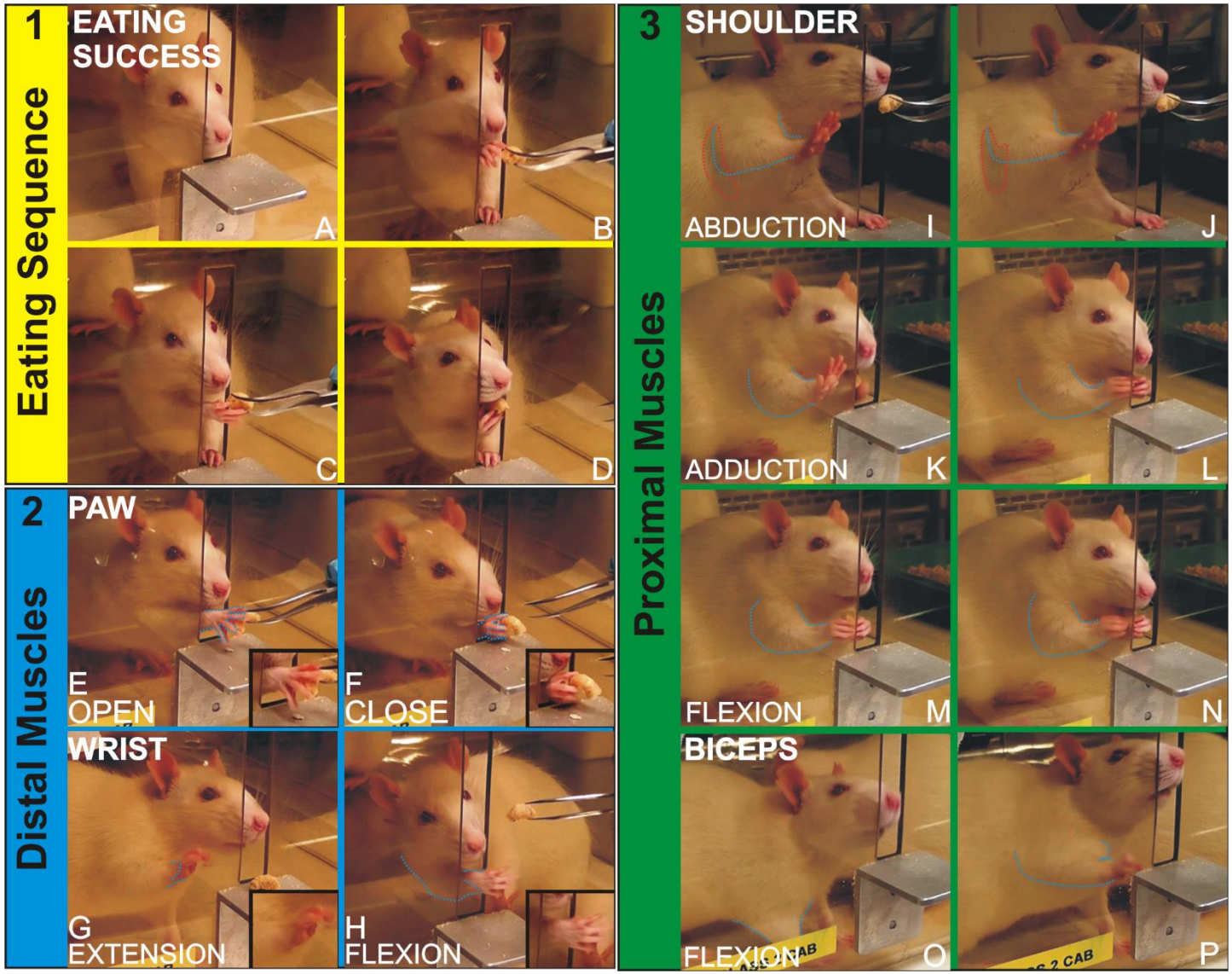
1
Eating Sequence
EATING SUCCESS
A
B
C
D
2
Distal Muscles
PAW
E
OPEN
F
CLOSE
WRIST
G
EXTENSION
H
FLEXION
3
Proximal Muscles
SHOULDER
ABDUCTION
I
J
ADDUCTION
K
L
FLEXION
M
N
BICEPS
FLEXION
O
P

Figure 11: Movements used to determine functional recovery in rats with C4 corticospinal tract injury injected with control-virus or increasing GMCSF/eGFP-virus concentrations. 1-3: Accurate/complete right arm movements of intact rats involved in the eating sequence (1-yellow outline), the proximal (2- blue outline) and distal muscles (3-green outline) used during reaching. Contours of forelimb and forepaw are highlighted with blue dotted lines and shadows in red (I&J). 1A-D: An eating success (yellow outline) was quantified only when rats completed the following sequence of movements: A-B: lifting the forepaw from the floor, exiting the slit, covering the food, opening paw, B: closing paw and withdrawing food, and D: transporting it to mouth to eat the pellet. 2E-H: Movements of proximal muscles namely of the wrist and paw involved during the food reaching and grasping motions. Wrist extension (E) was determined by the arm being parallel to the floor and digits point upwards. Wrist flexion (F) was evident when the joint was bent resulting with the palm of the paw moving toward the forearm. Digits moving laterally away from the axial line showed a paw opening motion (G), and paw closing (H) was found when digits flexed around the food fragment. Inserts show close up of the wrists and paw movements. 3 I-P: Show proximal muscle movements in the shoulder (I-N) and biceps (O-P). Shoulder abduction (I-J) involved the lateral movement of the elbow away from the midline of the body; notice the shadow (red contour) of the arm expanding when the arm moves literally. Adduction (K-L) was noticed when elbow and paw toward the midline of the body in a horizontal plane. Flexion (M-L) was determined by the movement of the upper arm upward to the front. Biceps flexion (O-P) was determined by the rat lifting the forepaw from the floor.

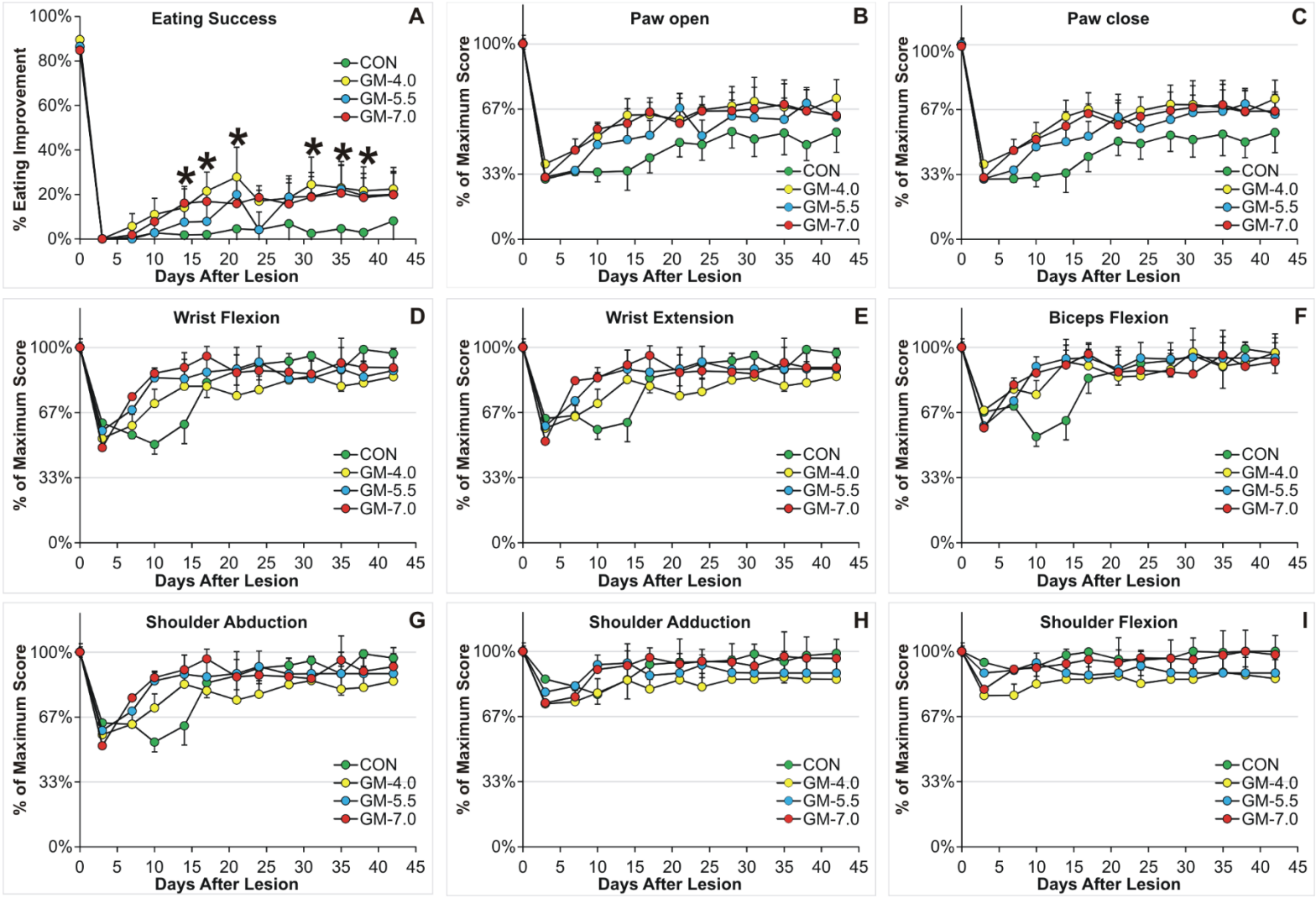
Eating Success
A
% Eating Improvement
100%
80%
60%
40%
20%
0%
CON
GM-4.0
GM-5.5
GM-7.0
0 5 10 15 20 25 30 35 40 45
Days After Lesion
Paw open
B
% of Maximum Score
100%
67%
33%
0%
Paw close
C
Wrist Flexion
D
Wrist Extension
E
Biceps Flexion
F
Shoulder Abduction
G
Shoulder Adduction
H
Shoulder Flexion
I

Figure 12: Eating success was most affected following right spinal cord injury and showed significant improvement following GM-CSF treatment. A-I: Line graphs represent the percentage (%) improvement of the right arm and paw of C4 corticospinal tract injured rats injected with control-virus (CON-green) or increasing concentrations of GM-CSF/eGFP-virus at 10^4 (GM-4.0: yellow), $10^{5.5}$ (GM-5.5: blue) or 10^7 (GM-7: red) at 0-42 days post lesion. Eating success movements (A) were quantified, and the precision of the following sub-movements were scored: paw opening (B) and closing (C), wrist flexion (D), wrist extension (E) bicep flexion (F), shoulder abduction (G), adduction (H) and flexion (I). At post-operative day 3, a graded response to injury emerged with proximal to distal muscles showing little to high functional deterioration, respectively. Similarly, shoulder adduction (H) and flexion (I) movements showed spontaneous recovery; shoulder abduction, bicep flexion, wrist flexion and extension revealed acceleration towards recovery, and paw opening and closing showed a strong tend towards improvement. The average grades 1, 2 and 3 are represented on the graphs by the first, second and third intermediate grid lines. Eating success was most affected by injury and GM-CSF treatment was associated with significant recovery. (*) $p<0.05$ significance following unpaired student t-test.

Discussion

The current study demonstrates for the first time that injections of GM-CSF/eGFP-virus into the motor cortex of rats with corticospinal tract injuries can have a protective effect on injured corticospinal axons and promote functional recovery. It was also shown that cortical injections of GM-CSF/eGFP-virus results in prolonged microglial and astrocyte activation in the motor cortex and microglial activation in the corticospinal tract in the cervical spinal cord. The positive action of GM-CSF/eGFP-virus observed in C4 corticospinal tract injured rats may be at least partially mediated by enhancing the inflammatory response around the cell body and axons of injured corticospinal neurons.

GM-CSF/eGFP-virus mediates the preservation of corticospinal tract axons

Rats with C4 corticospinal tract injuries that received injections of GM-CSF/eGFP-virus into the motor cortex, had more axons in the dorsal corticospinal tract of the spinal cord and these extended closer to the site of injury than those in animals injected with control-virus. The differences in the efficacy of anterograde labelling between groups could not explain this effect, as the number of axons at the level of the pyramids was similar for all the groups. GM-CSF may be mediating this effect by: a) activating a regenerative response in the injured neurons, b) suppressing the activation of an intrinsic neuronal program that leads to neurodegeneration, c) or by local effects on axonal viability (Luo and O'Leary, 2005). Although the current study did not specifically examine these factors, other studies suggest that GM-CSF may play a role in all three processes.

GM-CSF/eGFP-injections into the motor cortex may promote axonal regeneration following injury. In the present study there was a pronounced increase in microglial activation in the motor cortex of GM-CSF/eGFP-injected rats with corticospinal tract injury. Following corticospinal tract injury there is no microglial activation around the cell bodies of corticospinal neurons (Leong et al., 1995). Stimulating microglial activation around the cell bodies of neurons that project their axons into the central nervous system is associated with enhanced axonal regeneration. Lu and Richardson, (1991) found that injection of Corynebacterium to the DRG activates macrophages and was associated with axonal regeneration following dorsal rhizotomy (central axotomy). Similarly, Leon et al., (2000) showed that macrophage activation following the intraocular injection of zymosan or injury to lens is associated with RGC survival and vigorous axonal regeneration following optic nerve crush.

Peripheral nerve graft experiments have also demonstrated that the extent of perineuronal microglial activation correlates well with axonal regeneration. Shokouhi et al. (2010) demonstrated that axonal growth into peripheral nerve implants provokes a substantial increase in perineuronal neuroinflammation, which is most obvious around the highly regenerative thalamic reticular neurons. Increased microglial activity is also found around rubrospinal neurons which regenerate into peripheral nerve grafts in the spinal cord (Harvey et al., 2005; Richardson et al., 1980). Interestingly, neurons that regenerate their axons into peripheral nerve grafts show a transient upregulation of regeneration associated molecules (GAP-43, CAP-23, SCG-10) following injury, which is prolonged in response to the implantation of the graft. However, neurons which do not regenerate into peripheral nerve grafts, such as corticospinal neurons, do not mount such a response (Campbell et al., 1991; Chaisuksunt et al., 2000; Mason et al., 2002; Vaudano et al., 1995; Zhang et al., 1995). The current study evaluated the expression of c-Jun or ATF3 transcription factors, which are key players in the neuronal response to injury by participating in the transcriptional regulation of growth-associated genes. It was found that c-Jun or ATF3 may be expressed by glial cells rather than corticospinal neurons of GM-CSF/eGFP-

injected rats. Nonetheless, more detailed analysis must be carried out to confirm this rather than just relying on the nuclear morphology. Coronal brain sections should be double-stained for neuronal marker (e.g. NeuN) and c-Jun or ATF3. In addition, other factors involved in the growth and guidance of regenerating neurons, such as GAP-43, CAP-23, SCG10, L1 and CHL1 (Mason et al., 2003), must be evaluated.

In addition, GM-CSF has been found to promote axonal regeneration following injury by the enhancing expression of neurotrophic factors. Bouhy et al. (2006), investigated the effect of injecting GM-CSF intraperitoneally into rats four weeks after a closed spinal cord compression injury at the T8-T9 level. At 8 and 24 weeks post injury they detected more regenerating fibres of the corticospinal tract entering the lesion site in GM-CSF treated rats than those injected with the vehicle. This was mediated by a transient increase in the number of macrophages at the injury site. These macrophages were expressing BDNF. Bouhy et al. (2006), concentrated on the changes in the spinal cord. However, when rats with a dorsal corticospinal injury to the thoracic spinal cord received BDNF near the cell bodies of the injured neurons, there was a significant increase in collateral sprouting by corticospinal fbres within the spinal cord (Vavrek et al., 2006). It remains to be investigated whether neurotrophic factors are produced in the vicinity of the cell bodies of corticospinal neurons in our experiments.

Microglia can produce proinflammatory cytokines that can cause astrocyte activation and cell death. The current study found that high levels of microglial and astrocyte activation in the motor cortex following the injection of high concentrations of GM-CSF/eGFP was associated with a decrease in the number of virally-transduced (eGFP+) cells. Accordingly, the number of BDA-positive corticospinal axons appeared to decreased in rats injected with high concentration of GM-CSF/eGFP-virus compared to those injected with a medium concentration. Nonetheless, rats injected with medium and high concentrations had more axons closer to the injury site than those injected with eGFP-virus. GM-CSF has been associated with increasing survival of neurons. Rats that underwent focal cerebral ischemia following unilateral occlusion of the middle

cerebral artery and were administered GM-CSF for five consecutive days had a decreased cerebral infarction volume. This was associated with the decreased expression of apoptosis-related genes, including *Bcl-2, Bax, caspase 3, and p53*. In vitro, experimenters found that GM-CSF increased the viability of a neuroblastoma cell line subject to glutamate-induced excitotoxicity, by reducing *Bax* gene expression and increasing *Bcl-2* gene (anti-apoptotic) expression (Kong et al., 2009). Similarly, Schaebitz et al., (2008), reported that exposure of vulnerable neurons to GM-CSF was protective. GM-CSF induced anti-apoptotic *BCL-2* and *BCL-Xl* gene expression in mouse and rat primary cortical neurons treated with nitric oxide. GM-CSF was also found to highly activate the PI3K/Akt pathway. When PI3K/Akt neuronal signalling was inhibited it strongly decreased the anti-apoptotic activity of GM-CSF, suggesting that the PI3K/Akt pathway is important in protection of primary cortical neurons. It remains to be investigated if GM-CSF/eGFP-virus enhances the survival of corticospinal neurons and whether this plays a role in axonal protection.

Finally, GM-CSF has been found to preserve axonal integrity. Rats with a T9/10 spinal cord injury induced using a vascular clip had GM-CSF administrated via intraperitoneal injection or administration on the dural surface using Gelfoam at the time of SCI. GM-CSF was shown to preserve the corticospinal axonal morphology and myelin structure after spinal cord injury. Longitudinal horizontal sections were immunostained for neurofilament and Luxol fast blue, to detect axon fibres and myelin/myelinated axons, respectively. Axons were relatively well arranged and the myelin sheath was preserved relatively intact in the GM-CSF groups (Huang et al., 2009). The effect of GM-CSF/eGFP injection into the motor cortex of rats with corticospinal tract injury on axonal morphology needs to be evaluated in more detail.

Distal movements are more affected by a corticospinal tract injury

In the rat, axons of corticospinal neurons travel down to all levels of the spinal cord in the dorsal, ventral and lateral corticospinal tracts (Weidner et al., 2001). At different spinal cord segments, corticospinal axons can form synapses directly with motor neurons or, more frequently, indirectly through interneurons in the grey

matter of the spinal cord. These motor neurons innervate muscles involved in fine, voluntary and skilled movement (Arslan, 2001). In the current study, the directed forepaw reaching task was used to evaluate fine and voluntary movement (Whishaw et al., 1992; Whishaw et al., 1993). It was found that movements, such as those of the wrist and paw produced by distal muscles were more affected by a dorsal corticospinal tract injury at the fourth cervical segment than movements produced by proximal muscles, such as those of the shoulder and biceps. Findings from anatomical studies suggest that the level of the spinal cord at which the injury was carried out may produce the difference between proximal and distal muscles. Tosolini and Morris (2012) used fluorogold to identify the motor pools of 11 muscles in the forelimbs of Long-Evans rats. Motor neuron columns innervating the shoulder muscles span across cervical spinal cord segments 2–6 (C2-C6). Those innervating the upper forelimb muscles span across C3–C8, whereas the majority of the motor neurons innervating the lower forelimb muscles span across C5–C8 (Tosolini and Morris, 2012). In the current study rats had a dorsal corticospinal tract injury at spinal cord level C4 so more motor neurons for proximal limb muscles would have retained their corticospinal control.

In agreement with Tosolini and Morris (2012) results, Whishaw et al. (1993) found that rats with a unilateral corticospinal tract lesion in the medullary pyramids had significant deficits in the function of both proximal and distal forelimb muscles. Using a reaching test, similar to the one used in the current study, Whishaw et al. (1993) found that advancing the forepaw to the pellet (proximal muscles), grasping the pellet (distal muscles), then retracting the limb into the testing box (proximal muscles) while the paw maintains a grip on the pellet (distal muscles), were significantly impaired following lesions of the pyramids. However, it was interesting to note that injured rats retained the ability to open their paw digits but had impaired their grasping ability. Other studies have reported that lesions of the pyramids show deficits in the ability to open their paw digits (Castro, 1972a; Kalil and Schneider, 1975). In the present study, the opening and closing of paw digits were both highly impaired, which is compatible to the studies of Castro, (1972) and Kalil and Schneider (1975), which have shown the importance of the corticospinal tract in the use of forepaw digits in rodents.

Spontaneous functional recovery following corticospinal tract injury

It has been reported that rats with unilateral lesions of the corticospinal tract, at the level of the spinal cord or medullary pyramid, may retain or resume forelimb function without intervention (McKenna and Whishaw, 1999; Metz and Whishaw, 2002; Weidner et al., 2001; Whishaw et al., 1993; Whishaw et al., 1998). In the current study, rats showed spontaneous recovery in the rearing test and in some movements of the directed forepaw reaching test four weeks after a dorsal corticospinal tract injury. The extent of spontaneous functional recovery has been associated to sprouting. Weidner et al. (2001) investigated the effect of different forms of corticospinal tract lesions on behavioural recovery. Rats received a unilateral dorsal-only, ventral-only or dorsal and ventral corticospinal tract transection. Using a reaching test to assess behaviour, they quantified the number of successful pellet retrievals. They also evaluated specific movement of forelimb use, including failed advances (proximal muscle function); missed aims (proximal muscle function); digit spread (distal muscle function); and food pellet drops, (either proximal or distal muscle function). Movements of the forelimb which required the use of both proximal and distal muscles, were transiently impaired in rats with a dorsal- or ventral- corticospinal tract transection. Rats with both dorsal and ventral corticospinal tract injury showed a permanent deficit in movements. Experimenters found that the rats with a dorsal corticospinal tract injury only had more corticospinal tract axon terminals on motor neurons in the medial motor columns in lamina IX of spinal grey matter, than rats that where intact. The greater number of motor neuron synapses were explained to originate from the uninjured ventral corticospinal tract. Correlational analysis suggested that rats with more corticospinal tract sprouts to the spinal grey matter showed greater functional recovery (Weidner et al., 2001).

In the current study the eating success function did not show spontaneous recovery, as at 6 weeks, this function remained severely impaired in control-virus injected rats with a dorsal corticospinal tract injury. Weidner et al., (2001) evaluated successful pellet retrievals and found that after four weeks, rats with a dorsal corticospinal tract lesion recovered function similar to that of non-injured rats. At least two reasons may explain the difference between the current result

and those of Weidner et al. Firstly, the criteria used to measure function are slightly different. In the present study an eating success was counted if the rat lifted the paw from floor, the paw exited the slit, and the Cheerio fragment was grasped, withdrawn and transported to the mouth to eat. However, Weidner et al., (2001) did not include the transportation of the food to the mouth. Secondly, it may be that the injury in the rats of the present study was more extensive. Due to the nature of the dorsal corticospinal tract transection, rats may have had other areas of the spinal cord injured, such as the grey matter of the spinal cord or the lateral dorsal corticospinal tract. The extent of loss of directed forelimb reaching is indeed affected by the extent grey matter injury (Yamamoto et al., 2009). Yamamoto and colleagues found that rats that showed no return of function had extensive destruction through the medio-lateral extent of the grey matter, in addition to the dorsal corticospinal tract injury. However, further work analysing the extent of grey matter injury remains to be carried out to clarify this point.

GM-CSF/eGFP-virus improves functional recovery

Rats injected with GM-CSF-virus showed significantly more functional improvement in eating success, a trend towards more improvement in the paw opening and closing movements and a trend towards faster recovery of movements that required wrist flexion and extension, biceps flexion and shoulder abduction. Intact spinal interneurons that bypass the spinal lesion are capable of receiving new inputs from cut axons (Bareyre et al., 2004; Vavrek et al., 2006). Axons of the corticospinal tract (ventral CTS projections when dorsal CTS is damaged but ventral fibres are preserved) have been reported to sprout into spinal grey matter following spinal cord injury (Weidner et al., 2001). It could be that GM-CSF/eGFP-virus may be intensifying this sprouting effect, leading to the formation of new synapses, which in turn results in improved functional recovery. The current study found that rats injected with GM-CSF/eGFP-virus had more axons closer to the injury site than those injected with control virus. However, it failed to characterise the level of axonal sprouting into the grey matter of the spinal cord. Thus future studies need to analyse the extent of axonal sprouting to see if it could play a role in functional improvement.

Nonetheless, axonal sprouting may be mediated by GM-CSF-stimulated production of neurotrophic molecules. Researchers have shown improvement of function in spinal cord injured rodents injected with GM-CSF-protein (Bouhy et al., 2006; Ha et al., 2005; Hayashi et al., 2009). Bouhy et al., (2006) used open field Basso, Beattie, and Bresnahan (BBB) scores to record the extent of functional recovery of rats with a spinal cord injury at T8-T9 level, treated with intraperitoneal injections of GM-CSF. Rats treated with GM-CSF had more corticospinal axons regenerating past the injury site than those injected with PBS. In addition, more BDNF was expressed by microglia in the spinal cord of GM-CSF injected rats than the rats injected with PBS control. It would be interesting to measure the levels of BDNF and other neurotrophins in the spinal cord and motor cortex of rats injected with the GM-CSF virus.

Limitation

In the current study, a histological assessment and behavioural assays were used to evaluate whether producing inflammation around injured corticospinal neurons enhances axonal regeneration and functional recovery. This revealed that cortical injections of medium and high concentrations of GM-CSF-virus were efficient at both promoting inflammation in the motor cortex and functional recovery. However, cortical injections of a lower concentration of GM-CSF-virus, namely GM4, resulted in better functional recovery, but failed to produce noticeable inflammation in the motor cortex. However, at least two factors can explain the lack of inflammation in GM4-injected rats: 1) the experimental set up and 2) the sensitivity/accuracy in measuring inflammation. In terms of the experimental set up, the histological assessments of the effects that GM4 on inflammation were carried out at different times after injection. In Chapter 4 a heightened inflammatory response to GM4-virus was found in the motor cortex of intact rats14 days after cortical injections. In the current chapter histological assessment of inflammation was carried out at 42 days after injection. This suggest that GM4 can produce inflammation at relatively early time-points, but this may have declined by 42 days after injection. It would be interesting to find out at which day inflammation peaks; the time points evaluated should be between 14 and 42 days after injecting GM4-virus into the motor cortex of rats with CST injury. Regarding the sensitivity/accuracy in measuring inflammation,

the histological assay presented in this chapter characterised inflammation by the increased density of microglial cells, irrespective of the activation states. A failure in evaluating the different activation states of microglia may mask the effect GM4 has on inflammation. Microglial activation should be evaluated by also quantifying the number of activated microglia and phagocytic microglia, separately. It is possible that GM4-virus is promoting cortical inflammation by causing morphological changes in microglia.

Conclusion

In this study we have demonstrated that at high concentrations GM-CSF virus increases inflammation and astrogliosis in the motor cortex of rat, and produces axon protective effects following corticospinal tract injury. The cortical delivery of GM-CSF was associated with an improvement in reaching function. The anatomical and molecular mechanisms mediating functional improvement require further investigation.

CHAPTER SEVEN

General Discussion

This thesis has investigated the dual effects of inflammation on the central nervous system. Like peripheral macrophages, activated microglial cells – their CNS counterparts - express a number of potentially cytotoxic molecules which could impair neuronal survival (Raivich et al., 1999). However, there is accumulating evidence suggesting that microglia also produce signals which change neuronal gene expression to promote regeneration (Bouhy et al., 2006; Lalancette-Hebert et al., 2007; Makwana et al., 2007; Schroeter et al., 2006; Yin et al., 2006).

The aim of the current project was to use perineuronal microglia as a tool to enhance corticospinal tract and facial nerve regeneration after axotomy. In addition, we explored the neurotoxic effect of microglial activation in the adult and neonate rodent brain. To provoke inflammation Poly I:C and viral GM-CSF were used.

Perineuronal inflammation can be protective and enhance regeneration following central and peripheral axonal injury

The difference in regenerative capacity between the central (CNS) and peripheral nervous system (PNS) has been primarily attributed to the non-supportive environment the injured CNS presents to regenerating axons, compared to the more permissive environment of the injured PNS (Filbin, 2003). However, the ability of neuronal cell bodies to mount an appropriate response to injury could also be a significant factor to create differences in PNS and CNS (Anderson et al., 1998; Raivich et al., 2004; Raivich and Makwana, 2007). The neuronal cell body response to axonal injury is accompanied by perineuronal inflammation around the cell body of the axotomised neurons. Interestingly, while axonal injury causes inflammation around PNS projecting neurons, axonal injury to CNS neurons does not cause perikaryal inflammation (Anderson et al., 1998).

When inflammation is induced around the axotomised centrally projecting neurons by stimulating surrounding macrophages, neurons are able to extend their axons into the CNS (Lu and Richardson, 1991; Leon et al., 2000). The

improved axonal regeneration mediated by increased perineuronal inflammation is associated with increased upregulation of regeneration-related proteins (Leon et al., 2000; Lu and Richardson, 1991).

This thesis demonstrates the effect of acute and chronic inflammation around the cell bodies of injures neurons on axonal regeneration and functional recovery. The inflammation produced by Poly I:C in the CNS appears to be short lived, peaking at day 3 after injection and decreasing thereafter. Injections of Poly I:C to the motor cortex are associated with a greater number of axons in the corticospinal tract after spinal cord injury. In addition, functional recovery following facial nerve transection is also improved by Poly I:C injections to the brainstem near the facial motor nucleus. Similarly, viral delivery of GM-CSF to the motor cortex promotes chronic inflammation which can be seen up to 42 days. Viral GM-CSF mediated inflammation in the motor cortex was associate with a greater number of corticospinal axons closer to the injury site after spinal cord injury, as well as functional recovery in reaching tasks.

These results support previous evidence that perineuronal inflammation promotes axonal regeneration. Improvement in central axonal regeneration by mediating perineuronal inflammation has previously been demonstrated on central rhizotomy and optic nerve injury models. Like Hossain-Ibrahim et al. (2006), this thesis extends the application of this approach to spinal cord injury. In contrast to Hossain-Ibrahim and colleagues, who applied lipopolysaccharide (LPS) to the rat motor cortex and found no effect in the spinal cord, in this thesis a protective effects on injured axons and increased functional recovery were demonstrated.

In addition, that Poly I:C has been shown to enhance functional recovery following facial nerve transection in rats. Previous studies using a number of different approaches have failed to demonstrate such robust functional recovery in the rat after peripheral nerve transection (Al-Majed et al., 2000b; Brushart et al., 2002; Hadlock et al., 2010; McQuarrie et al., 1977; Zhang et al., 2013). Peripheral nerve regeneration in the rat is robust with almost complete target reinnervation achieved within 8 weeks (Al-Majed et al., 2000b; Sinis et al., 2009). However, functional recovery is absent even up to 15 weeks following injury (Hadlock et al.,

2010; Knox et al., 2013). The lack of functional recovery has been explained by polyinnervated non-functioning neuromuscular junctions (Zhang et al., 2013). The enhancement of functional recovery mediated by Poly I:C in this thesis appear to be independent of target reinnervation. Future work should concentrate on determining the effect perineuronal Poly I:C may have on neuromuscular junction reinnervation patterns and function.

The effects observed on axonal regeneration in the spinal cord following perineuronal inflammation with Poly I:C and viral GMC-SF appear to be very mild. Despite their axon protective effects following spinal cord injury we failed to observe axonal regeneration into the injury site. Other experimental therapeutic approaches, which have mainly concentrated on the injury site, have shown avid growth into the glial scar and robust sprouting (Bradbury et al., 2002; Carter et al., 2008; Fabes et al., 2007; Goldshmit et al., 2011; Yick et al., 2003; Yick et al., 2004). Targeting the inhibitory injury site which lacks neurotrophic support in combination with enhancing the neuronal cell body response may work in synergy to cause pronounced beneficial effects on axonal regeneration and recovery following spinal cord injury.

How can inflammation promote axonal regeneration?

The current study used GM-CSF and Poly I:C to produce inflammation around the soma of axotomised neurons, with the aim of producing or enhancing axonal regeneration. Inflammation may be affecting axonal regeneration by promoting mammalian target of rapamycin (mTOR)-mediated protein synthesis in the axon. mTOR is an atypical serine/threonine kinase, whose upstream regulators are PI3K and Akt, and PTEN (phosphatase and tensin homolog) and TCS 1/2 (tuberous sclerosis), which act as inhibitors of PI3K and AKT, respectively (Hay and Sonenberg, 2004). There is indirect and direct evidence to show that mTOR is involved in axonal protein synthesis. Injured adult peripheral axons contain mTOR and its downstream targets, such as P-S6K, PS6, P-4E-BP1, ribosomal-P0 and phospho-eIF-4E, which are components of the translational machinery responsible for ribosome-recruitment to mRNA (Jimenez-Diaz et al., 2008; Verma et al., 2005). Additionally, mTOR controls the axonal translation of the regeneration-associated protein GAP-43 (Abe et al., 2010) and the membrane

protein syntaxin-13 (Cho et al., 2014), which is involved in endosomal recycling of plasma membrane proteins (Prekeris et al., 1998). Functionally, the activation of mTOR results in robust axonal regeneration, after axonal injury of CNS neurons (Hu et al., 2010; Liu et al., 2010; Park et al., 2008).

Proinflammatory cytokines can activate mTOR. The cytokine IL-6 has been shown to activate mTOR in the soma of spinal neurons of rats with CST injury and enhance spinal cord regeneration (Yang et al., 2012). Since both GM-CSF and Poly I:C can cause the production of IL-6 by microglia, it could be suggested that mTOR activation in neurons may be at least caused by IL-6 production. Currently, only GM-CSF has been shown to directly activate the upstream constituents of the mTOR pathway; in cultured rat primary neurons challenged by NO the activation of this pathway was associated with increased neuronal survival (Schaebitz et al., 2008). Additionally, GM-CSF promotes neurite growth from postnatal RGCs mediated by mTOR (Legacy et al., 2013). It remains to be evaluated whether Poly I:C can also modulate the mTOR pathway. Nonetheless, it is possible that the regenerative effects associated with treating rats with GM-CSF or Poly I:C may be mediated at least in part by the mTOR pathway.

Enhanced axonal protein synthesis mediated by mTOR may lead to better axonal regeneration. Following injury, axonal processes of regeneration-competent neurons synthesize proteins from pre-existing mRNA (Merianda et al., 2009; Willis et al., 2005; Zheng et al., 2001). Locally synthesised proteins include endoplasmic reticulum chaperone proteins (Willis et al., 2005), the transcription factor STAT3 (Ben-Yaakov et al., 2012), and proteins important for retrograde signalling such as importin-β1 (Hanz et al., 2003) and vimentin (Perlson et al., 2005). The ability of an injured axon to continue synthesising protein is correlated with its ability to regenerate (Verma et al., 2005). In addition, when protein synthesis is blocked in injured axons, a retraction of growth cones is evident (Zheng et al., 2001). Therefore, synthesis of proteins in the axons promotes axonal regeneration and the initiation of retrograde transport of injury signals.

More protein production in the axons may lead to a stronger retrograde transport to the cell body, thereby increasing the cell body response and subsequently causing axonal regeneration. Retrograde transport of injury signals is important

for triggering a cell body response following injury. Signalling molecules (p38, JNKs, MAPKs, ERKs) can be transported from the axons to the neuronal cell body via macromolecular signalling complexes trafficked by dynein motors (Rishal and Fainzilber, 2010). Among the components of these macromolecular signalling complex is importin, which is a scaffolding protein that links the signalling molecules to the dynein motors. Importin has two isoforms, importin-α and importin-β. In adult sensory axons, importin-α is constitutively expressed in normal conditions and its expression remains the same after injury, while the expression of importin-β increases after injury, due to the local translation of mRNA (Hanz et al., 2003). The role of importin on axonal regeneration has been demonstrated in vitro and in vivo. In vitro, selective depletion of importin-β1 from axons attenuated the cell body response to injury in sensory neurons, with a reduction of over 60% of genes that are activated in the cell body after injury (Perry et al., 2012). In addition, lack of axonal importin-β1 delayed functional recovery from sciatic nerve injury (Perry et al., 2012). Additionally, importin on the dynein motors can also bind to vimentin, which itself can bind to phosphorylated ERK (Perlson et al., 2005) and to locally translated STAT3 (Ben-Yaakov et al., 2012). These proteins are known to have an effect on gene regulation after axonal injury and are known to promote regeneration (Patodia and Raivich, 2012a). Interestingly, intravitreal injection of GM-CSF upregulates STAT3 protein in the retina of rats with retinal degenerative disease; this was associated with increased photoreceptor survival (Schallenberg et al., 2012). In this thesis, the protective or regenerative effects of GM-CSF treatment in rats with spinal cord injury could be in part mediated by increased retrograde trafficking of STAT3, synthesised in injured axons. Future work should evaluate whether perineuronal inflammation produced by GM-CSF and Poly I:C increases regeneration of injured neurons by promoting a cell body response, which is mediated by the mTOR pathway, axonal protein production and retrograde signalling to the cell body.

Inflammation is toxic in the CNS

Injections of Poly I:C at high concentration and GM-CSF virus at high titres were associated with necrosis and cell death in the motor cortex. Inflammation mediated neural injury can be part of neurological disease processes (Raivich et

al., 1999). In this way, the toxic effects produced by Poly I:C and viral GM:CSF might help model inflammatory CNS disease.

In this thesis has studied the inflammatory response to injections of GM-CSF-virus into the striatum of different mouse strains. It was found that the inflammatory and glial response was low in the 129S2/Sv strain, widespread though moderate in BALB/c, and high in the FVB/N strain. Expanding the analysis of viral GM-CSF mediated inflammation to mice, opens an avenue of research using transgenics. This might permit the analysis of the molecular mechanisms through which GM-CSF may promote neuroprotective or neurotoxic effects.

Work on producing a mouse model of inflammatory perinatal brain injury using the FVB/N strain has been presented in this thesis. Unlike, other models of inflammatory perinatal brain injury which rely on transient systemic effects (Bell and Hallenbeck, 2002), transuterine injections of GM-CSF-virus targeting the ventricles of the developing mouse brain, provides a prolonged inflammatory stimulus. Here it was shown that intraventricular viral GM-CSF causes microglia activation in various brain areas including the white matter. This response was transient disappearing as the mouse brain matures postnatally. Future work should concentrate in determining whether GM-CSF induced microglia activation causes white matter damage and behavioural deficits in adulthood, as observed in Cerebral Palsy.

In the adult 129SV2 and BALB/c mice injected with GM-CSF virus into the striatum demonstrated mild to moderate responses. Microglia activation can result in two diverse phenotypes known as classical activation or alternative activation (Colton, 2009; Schwartz et al., 2006; Thored et al., 2009). Classical activation is associated with damage in the CNS and the production of pro-inflammatory cytokines, while alternative activation may be supportive to the CNS by the expression of anti-inflammatory or neurotrophic factors (Giunti et al., 2014). The absence of injury in the 129SV2 and BALB/c in the presence of microglia activation makes these strains suitable for the study of the effects of non-toxic inflammation on regeneration.

Limitations

Chapter 3

The conclusions that can be derived from the experiments on the effect of motor cortex injections of Poly I:C on corticospinal tract regeneration are limited. This is because of the absence of information on a number of parameters that have not yet been studied.

First, no description of the effects of Poly I:C in the motor cortex of rats with spinal cord injury has been performed. Similarly no formal analysis has been carried out of the possible effects cortical Poly I:C might have on inflammation and regenerative gene expression at the level of the CST. Second, the description of Poly I:C effects on the neuronal response to injury was limited to the expression of two transcription factors. There is a large number of other regeneration associated genes and proteins that should also be studied to determine whether Poly I:C has an effect by promoting regeneration associated gene expression. Third, analysis was limited to the count of BDA labelled axons and retraction bulbs at the level of the spinal cord after injury. Data must be obtained on axonal sprouting from the CST, first to explain the observed increase in axonal number at the spinal cord and second to determine if there are any further effects that may represent an enhance regenerative effort. Finally, behavioural analysis could be carried out to determine whether the axon protective effect of Poly I:C promote recovery of motor function.

There are also limitations on the study of perineuronal Poly I:C on facial nerve regeneration. The robust enhancement of functional recovery described in this thesis lacks neuroanatomical correlates. First, analysis of the effects of Poly I:C on inflammation and neuronal response at the level of the facial nucleus must be carried out. Second, the rate of axonal elongation at the level of the facial nerve must be determined. Third, effects of Poly I:C on collateral branching and neuromuscular innervation must be ascertained. These parameters would provide a possible mechanism by which increased functional recovery was achieved from perineuronal Poly I:C delivery.

Chapter 4

A thorough description of the in vivo effects of viral GM-CSF injections to the motor cortex was carried out in this thesis. However, a number of questions remain to be answered. First, the cellular identity of cells transfected by the virus is unclear as morphology of eGFP positive cells in the GM-CSF/eGFP injected cortices is atypical of neurons. Double labelling with specific cellular markers for glia and neurons may be used to answer this question. Second, although microglia activation was demonstrated in a dose dependent manner with GM-CSF virus in vivo, there is no direct evidence that GM-CSF protein or RNA was present following injections of the virus. This question can be addressed with the use of western blotting, ELISA, In-Situ Hybridization or RT-PCR for the virus encoded murine GM-CSF. Third, it is unclear whether the inflammatory effects of GM-CSF seen distally, in the pyramids and spinal cord, are due to global CNS inflammation or a diffusion effect of GM-CSF protein travelling down the CST from transfected corticospinal neurons. This can be assessed by determining levels of inflammation in areas not in close proximity to the CST or motor cortex and by determining whether there is murine GM-CSF protein or RNA at the pyramids and spinal cord.

Chapter 5

The study on the inflammatory effects of viral GM-CSF on different mouse strains is limited by a lack of information on gene expression on each of the strains. There is no direct evidence to demonstrate that the difference in response to viral GM-CSF injection between strains is not due to differences in GM-CSF expression. In addition, the strain dependent responses have not been characterised at the molecular levels. The importance of both of these factors may be effectively determined using comparative gene expression arrays to profile each strain response to viral GM-CSF injections.

The work on the effects of intrauterine delivery of GM-CSF virus on the perinatal brain is limited by the use of scoring instead of formal quantification. In addition, no direct measurements of neuronal or axonal injury have been performed. These along with behavioural assessment of adult mice that have received GM-CSF in utero would help determine the value of this strategy as a model of cerebral palsy.

Chapter 6

This thesis has demonstrated that viral delivery of GM-CSF to the rat motor cortex is associated with proregenerative effects following corticospinal tract injury. However, there remains a number of parameters that should be analysed to draw reliable conclusions from the presented data. First, no neuroanatomical evidence has yet been obtained from the animals from which the functionally recovery data was obtained. Second, no formal assessment of axonal sprouting and inflammation has been carried out at the level of the spinal cord. Third, the analysis of proregenerative gene expression was limited to immunofluorescence for c-Jun and ATF3 transcription factors in the motor cortex. Further work on these two areas would help elucidate the mechanism through which cortical delivery of viral GM-CSF is beneficial for functional recovery following spinal cord injury.

General conclusion

This thesis describes Poly I:C and lentiviral GM-CSF mediated inflammation in central nervous system. Inflammatory responses produced by these substances have been shown to be both protective and toxic. It has been demonstrated that perineuronal Poly I:C promotes axon protection following spinal cord injury and enhances functional recovery after facial nerve axotomy. Inflammatory response to lentiviral GM-CSF was found to be strain dependent in mice; being low in the 129S2/Sv, widespread though moderate in BALB/c, and high in the FVB/N strain. Intrauterine injection of viral GM-CSF to the perinatal FVB/N mouse brain is associated with gliosis in periventricular brain areas. In the rat, GM-CSF induced perineuronal inflammation is associated with axon protective effects and improved functional recovery following spinal cord injury. The work presented here contributes to the understanding of the role of inflammation in neurodegeneration and axonal regeneration. It also promotes a new mouse model for perinatal white matter damage and a novel experimental therapeutic strategy for spinal cord injury.

References

Abe, N., Borson, S.H., Gambello, M.J., Wang, F., Cavalli, V., 2010. Mammalian Target of Rapamycin (mTOR) Activation Increases Axonal Growth Capacity of Injured Peripheral Nerves. Journal of Biological Chemistry. 285**,** 28034-28043.

Akiyama, H., McGeer, P.L., 1990. Brain microglia constitutively express Beta-2 integrins. Journal of Neuroimmunology. 30**,** 81-93.

Al-Majed, A.A., Brushart, T.M., Gordon, T., 2000a. Electrical stimulation accelerates and increases expression of BDNF and trkB rnRNA in regenerating rat femoral motoneurons. European Journal of Neuroscience. 12**,** 4381-4390.

Al-Majed, A.A., Neumann, C.M., Brushart, T.M., Gordon, T., 2000b. Brief electrical stimulation promotes the speed and accuracy of motor axonal regeneration. Journal of Neuroscience. 20**,** 2602-2608.

Alexopoulou, L., Holt, A.C., Medzhitov, R., Flavell, R.A., 2001. Recognition of double-stranded RNA and activation of NF-kappa B by Toll-like receptor 3. Nature. 413**,** 732-738.

Alghoul, W.M., Miller, M.W., 1989. Transient expression of ALZ-50 immunoreactivity in developing rat neocortex - a marker for naturally-occurring neuronal death. Brain Research. 481**,** 361-367.

Alheim, K., Bartfai, T., 1998. The interleukin-1 system: Receptors, ligands, and ICE in the brain and their involvement in the fever response. In Neuroimmunomodulation: Molecular Aspects, Integrative Systems, and Clinical Advances. Annals of the New York Academy of Sciences, Vol. 840, S.M. McCann, J.M. Lipton, E.M. Sternberg, G.P. Chrousos, P.W. Gold, C.C. Smith, pp. 51-58.

Alliot, F., Godin, I., Pessac, B., 1999. Microglia derive from progenitors, originating from the yolk sac, and which proliferate in the brain. Brain research. Developmental brain research. 117**,** 145-52.

Aloisi, F., Borsellino, G., Samoggia, P., Testa, U., Chelucci, C., Russo, G., Peschle, C., Levi, G., 1992a. Astrocyte cultures from human embryonic brain - characterization and modulation of surface molecules by inflammatory cytokines. Journal of Neuroscience Research. 32**,** 494-506.

Aloisi, F., Care, A., Borsellino, G., Gallo, P., Rosa, S., Bassani, A., Cabibbo, A., Testa, U., Levi, G., Peschle, C., 1992b. Production of hemolymphopoietic cytokines (IL-6, IL-8, Colony-Stimulating Factors) by normal human

astrocytes in response to IL-1-beta and Tumor-Necrosis-Factor-Alpha. Journal of Immunology. 149**,** 2358-2366.

Amador, M.J., Guest, J.D., 2005. An appraisal of ongoing experimental procedures in human spinal cord injury. Journal of neurologic physical therapy : JNPT. 29**,** 70-86.

Amr, S.M., Gouda, A., Koptan, W.T., Galal, A.A., Abdel-Fattah, D.S., Rashed, L.A., Atta, H.M., Abdel-Aziz, M.T., 2014. Bridging defects in chronic spinal cord injury using peripheral nerve grafts combined with a chitosan- laminin scaffold and enhancing regeneration through them by co-transplantation with bone-marrow-derived mesenchymal stem cells: Case series of 14 patients. Journal of Spinal Cord Medicine. 37**,** 54-71.

Anderson, D.K., Means, E.D., Waters, T.R., Green, E.S., 1982. Micro-vascular perfusion and metabolism in injured spinal-cord after Methylprednisolone treatment. Journal of Neurosurgery. 56**,** 106-113.

Anderson, P., Zhang, J., Ahmed, B., et al., 2006. Deletion of CAP-23 in adult mouse motor neurons delays axonal regeneration following facial nerve transection. Vol. 522. Soc Neurosci Abstr, pp. C46.

Anderson, P.N., Campbell, G., Zhang, Y., Lieberman, A.R., 1998. Cellular and molecular correlates of the regeneration of adult mammalian CNS axons into peripheral nerve grafts. Neuronal Degeneration and Regeneration: from Basic Mechanisms to Prospects for Therapy. 117**,** 211-232.

Anderson, P.N., Lieberman, A.R., 1999. Intrinsic determinants of differential axonal regeneration by adult mammalian CNS neurons. In Degeneration and Regeneration in the Nervous System. N.R. Saunders, Dziegielewska,K.M. Harwood Academic Press, pp. 53-75.

Anderson, P.N., Lieberman, A.R., 2000. Intrinsic determinants of differential axonal regeneration by adult mammalian central nervous system neurons. In *Degeneration and Regeneration in the Nervous System*, N.R. Saunders, K.M. Dziegielewska. Overseas Publisher Association, Singapore, pp. 93-120.

Andersson, P.B., Perry, V.H., Gordon, S., 1991. The kinetics and morphological-characteristics of the macrophage microglial response to Kainic Acid-induced neuronal degeneration. Neuroscience. 42**,** 201-214.

Arakawa, H., 2005. P53, apoptosis and axon-guidance molecules. Cell Death and Differentiation. 12**,** 1057-1065.

Armand, J., 1982. The origin, course and terminations of corticospinal fibers in various mammals. Progress in Brain Research. 57**,** 329-360.

Arslan, O., 2001. Neuroanatomical Basis of Clinical Neurology, CRC Press.

Arteaga, M.F., Gutierrez, R., Avila, J., Mobasheri, A., Diaz-Flores, L., Martin-Vasallo, P., 2004. Regeneration influences expression of the Na+,K+-ATPase subunit isoforms in the rat peripheral nervous system. Neuroscience. 129**,** 691-702.

Baas, P.W., Ahmad, F.J., 2001. Force generation by cytoskeletal motor proteins as a regulator of axonal elongation and retraction. Trends in Cell Biology. 11**,** 244-249.

Bajetto, A., Bonavia, R., Barbero, S., Florio, T., Schettini, G., 2001. Chemokines and their receptors in the central nervous system. Frontiers in Neuroendocrinology. 22**,** 147-184.

Bamber, N.I., Li, H.Y., Lu, X.B., Oudega, M., Aebischer, P., Xu, X.M., 2001. Neurotrophins BDNF and NT-3 promote axonal re-entry into the distal host spinal cord through Schwann cell-seeded mini-channels. European Journal of Neuroscience. 13**,** 257-268.

Baptiste, D.C., Fehlings, M.G., 2006. Pharmacological approaches to repair the injured spinal cord. Journal of Neurotrauma. 23**,** 318-334.

Barde, Y.A., Edgar, D., Thoenen, H., 1982. Purification of a new neurotrophic factor from mammalian brain. Embo Journal. 1**,** 549-553.

Bareyre, F.M., Kerschensteiner, M., Raineteau, O., Mettenleiter, T.C., Weinmann, O., Schwab, M.E., 2004. The injured spinal cord spontaneously forms a new intraspinal circuit in adult rats. Nature Neuroscience. 7**,** 269-277.

Barron, K.D., Dentinger, M.P., Popp, A.J., Mankes, R., 1988. Neurons of layer vb of rat sensorimotor cortex atrophy but do not die after thoracic cord transection. Journal of Neuropathology and Experimental Neurology. 47**,** 62-74.

Barron, K.D., Marciano, F.F., Amundson, R., Mankes, R., 1990. Perineuronal glial responses after axotomy of central and peripheral axons - a comparison. Brain Research. 523**,** 219-229.

Bartsch, U., Bandtlow, C.E., Schnell, L., Bartsch, S., Spillmann, A.A., Rubin, B.P., Hillenbrand, R., Montag, D., Schwab, M.E., Schachner, M., 1995. Lack of evidence that myelin-associated glycoprotein is a major inhibitor of axonal regeneration in the CNS. Neuron. 15**,** 1375-1381.

Bauer, J., Huitinga, I., Zhao, W.G., Lassmann, H., Hickey, W.F., Dijkstra, C.D., 1995. The role of macrophages, perivascular cells, and microglial cells in the pathogenesis of experimental autoimmune encephalomyelitis. Glia. 15**,** 437-446.

Becher, J.C., Bell, J.E., Keeling, J.W., McIntosh, N., Wyatt, B., 2004. The Scottish perinatal neuropatholo study: clinicopathological correlation in early neonatal deaths. Archives of Disease in Childhood. 89**,** F399-F407.

Becker, K., 2006. Innate and adaptive immune responses in CNS disease. Clinical Neuroscience Research. 6**,** 227-236.

Bell, M.D., Lopezgonzalez, R., Lawson, L., Hughes, D., Fraser, I., Gordon, S., Perry, V.H., 1994. Up-regulation of the macrophage scavenger receptor in response to different forms of injury in the CNS. Journal of Neurocytology. 23**,** 605-613.

Bell, M.D., Taub, D.D., Perry, V.H., 1996. Overriding the brain's intrinsic resistance to leukocyte recruitment with intraparenchymal injections of recombinant chemokines. Neuroscience. 74**,** 283-292.

Bell, M.J., Hallenbeck, J.M., 2002. Effects of intrauterine inflammation on developing rat brain. Journal of Neuroscience Research. 70**,** 570-579.

Bell, M.J., Hallenbeck, J.M., Gallo, V., 2004. Determining the fetal inflammatory response in an experimental model of intrauterine inflammation in rats. Pediatric Research. 56**,** 541-546.

Ben-Yaakov, K., Dagan, S.Y., Segal-Ruder, Y., Shalem, O., Vuppalanchi, D., Willis, D.E., Yudin, D., Rishal, I., Rother, F., Bader, M., Blesch, A., Pilpel, Y., Twiss, J.L., Fainzilber, M., 2012. Axonal transcription factors signal retrogradely in lesioned peripheral nerve. Embo Journal. 31**,** 1350-1363.

Bendella, H., Pavlov, S.P., Grosheva, M., Irintchev, A., Angelova, S.K., Merkel, D., Sinis, N., Kaidoglou, K., Skouras, E., Dunlop, S.A., Angelov, D.N., 2011. Non-invasive stimulation of the vibrissal pad improves recovery of whisking function after simultaneous lesion of the facial and infraorbital nerves in rats. Experimental Brain Research. 212**,** 65-79.

Benfey, M., Aguayo, A.J., 1982. Extensive elongation of axons from rat-brain into peripheral-nerve grafts. Nature. 296**,** 150-152.

Berezovskaya, O., Maysinger, D., Fedoroff, S., 1995. The hematopoietic cytokine, Colony-Stimulating Factor-1, is also a growth-factor in the CNS - congenital absence of CSF-1 in mice results in abnormal microglial response and increased neuron vulnerability to injury. International Journal of Developmental Neuroscience. 13**,** 285-299.

Bergsland, M., Werme, M., Malewicz, M., Perlmann, T., Muhr, J., 2006. The establishment of neuronal properties is controlled by Sox4 and Sox11. Genes & Development. 20**,** 3475-3486.

Berkemeier, L.R., Winslow, J.W., Kaplan, D.R., Nikolics, K., Goeddel, D.V., Rosenthal, A., 1991. Neurotrophin-5 - a novel neurotrophic factor that activates trk and TRKB. Neuron. 7**,** 857-866.

Bignami, A., Ralston, H.J., 1969. Cellular reaction to wallerian degeneration in central nervous system of cat. Brain Research. 13**,** 444.

Bignami, A., Eng, L.F., Dahl, D., Uyeda, C.T., 1972. Localization of Glial Fibrillary Acidic protein in astrocytes by immunofluorescence. Brain Research. 43**,** 429.

Billiards, S.S., Haynes, R.L., Folkerth, R.D., Trachtenberg, F.L., Liu, L.G., Volpe, J.J., Kinney, H.C., 2006. Development of microglia in the cerebral white matter of the human fetus and infant. Journal of Comparative Neurology. 497**,** 199-208.

Bisby, M.A., Keen, P., 1985. The effect of a conditioning lesion on the regeneration rate of peripheral-nerve axons containing Substance-P. Brain Research. 336**,** 201-206.

Bischof, R.J., Zafiropoulos, D., Hamilton, J.A., Campbell, I.K., 2000. Exacerbation of acute inflammatory arthritis by the colony-stimulating factors CSF-1 and granulocyte macrophage (GM)-CSF: evidence of macrophage infiltration and local proliferation. Clinical and Experimental Immunology. 119**,** 361-367.

Blakemore, W.F., 1975. Remyelination by schwann-cells of axons demyelinated by intraspinal injection of 6-Aminonicotinamide in rat. Journal of Neurocytology. 4**,** 745-757.

Blesch, A., Tuszynski, M.H., 2003. Cellular GDNF delivery promotes growth of motor and dorsal column sensory axons after partial and complete spinal cord transections and induces remyelination. Journal of Comparative Neurology. 467**,** 403-417.

Blesch, A., Tuszynski, M.H., 2007. Transient growth factor delivery sustains regenerated axons after spinal cord injury. Journal of Neuroscience. 27**,** 10535-10545.

Blight, A.R., 1985. Delayed demyelination and macrophage invasion: a candidate for secondary cell damage in spinal cord injury. Central nervous system trauma : journal of the American Paralysis Association. 2**,** 299-315.

Blight, A.R., Young, W., 1989. Central axons in injured cat spinal-cord recover electrophysiological function following remyelination by Schwann-cells. Journal of the Neurological Sciences. 91**,** 15-34.

Blitts, B., Oudega, M., Boer, G.J., Bunge, M.B., Verhaagen, J., 2003. Adeno-associated viral vector-mediated neurotrophin gene transfer in the injured

adult rat spinal cord improves hind-limb function. Neuroscience. 118**,** 271-281.

Boche, D., Perry, V.H., Nicoll, J.A.R., 2013. Review: Activation patterns of microglia and their identification in the human brain. Neuropathology and Applied Neurobiology. 39**,** 3-18.

Boeshore, K.L., Schreiber, R.C., Vaccariello, S.A., Sachs, H.H., Salazar, R., Lee, J., Ratan, R.R., Leahy, P., Zigmond, R.E., 2004. Novel changes in gene expression following axotomy of a sympathetic ganglion: A microarray analysis. Journal of Neurobiology. 59**,** 216-235.

Bogdan, C., Vodovotz, Y., Nathan, C., 1991. Macrophage deactivation by Interleukin-10. Journal of Experimental Medicine. 174**,** 1549-1555.

Bohatschek, M., Jones, L.L., Kreutzberg, G.W., Raivich, G., 1998. Expression of immunoregulatory molecules MHC1, MHC2 and B7-2 in the axotomized mouse facial motor nucleus. Clinical Neuropathology, pp. 286.

Bohatschek, M., Gschwendtner, A., von Maltzan, X., Kloss, C.U.A., Pfeffer, K., Labow, M., Bluthmann, H., Kreutzberg, G.W., Raivich, G., 1999. Cytokine-mediated regulation of MHC1, MHC2 and B7-2, in the axotomized mouse facial motor nucleus. Society for Neuroscience Abstracts. 25**,** 1535.

Bomstein, Y., Marder, J.B., Vitner, K., Smirnov, I., Lisaey, G., Butovsky, O., Fulga, V., Yoles, E., 2003. Features of skin-coincubated macrophages that promote recovery from spinal cord injury. Journal of Neuroimmunology. 142**,** 10-16.

Bomze, H.M., Bulsara, K.R., Iskandar, B.J., Caroni, P., Skene, J.H.P., 2001. Spinal axon regeneration evoked by replacing two growth cone proteins in adult neurons. Nature Neuroscience. 4**,** 38-43.

Bontioti, E., Dahlin, L.B., Kataoka, K., Kanje, M., 2006. End-to-side nerve repair induces nuclear translocation of activating transcription factor 3. Scandinavian Journal of Plastic and Reconstructive Surgery and Hand Surgery. 40**,** 321-328.

Borgens, R.B., Blight, A.R., Murphy, D.J., 1986. Axonal regeneration in spinal-cord injury - a perspective and new technique. Journal of Comparative Neurology. 250**,** 157-167.

Bouhy, D., Malgrange, B., Multon, S., Poirrier, A.-L., Scholtes, F., Schoenen, J., Franzen, R., 2006. Delayed GM-CSF treatment stimulates axonal regeneration and functional recovery in paraplegic rats via an increased BDNF expression by endogenous macrophages. Faseb Journal. 20**,** 1239.

Bourgoin, S., Poubelle, P.E., Liao, N.W., Umezawa, K., Borgeat, P., Naccache, P.H., 1992. Granulocyte-Macrophage Colony-Stimulating Factor primes

Phospholipase-D activity in human neutrophils invitro - role of Calcium, G-proteins and Tyrosine Kinases. Cellular Signalling. 4**,** 487-500.

Boyd, J.G., Gordon, T., 2001. The neurotrophin receptors, trkB and p75, differentially regulate motor axonal regeneration. Journal of Neurobiology. 49**,** 314-325.

Bradbury, E.J., Moon, L.D.F., Popat, R.J., King, V.R., Bennett, G.S., Patel, P.N., Fawcett, J.W., McMahon, S.B., 2002. Chondroitinase ABC promotes functional recovery after spinal cord injury. Nature. 416**,** 636-640.

Brahmachari, S., Fung, Y.K., Pahan, K., 2006. Induction of glial fibrillary acidic protein expression in astrocytes by nitric oxide. Journal of Neuroscience. 26**,** 4930-4939.

Bregman, B.S., Kunkelbagden, E., Schnell, L., Dai, H.N., Gao, D., Schwab, M.E., 1995. Recovery from spinal-cord injury mediated by antibodies to neurite growth-inhibitors. Nature. 378**,** 498-501.

Bregman, B.S., McAtee, M., Dal, H.N., Kuhn, P.L., 1997. Neurotrophic factors increase axonal growth after spinal cord injury and transplantation in the adult rat. Experimental Neurology. 148**,** 475-494.

Bregman, B.S., Coumans, J.V., Dai, H.N., Kuhn, P.L., Lynskey, J., McAtee, M., Sandhu, F., 2002. Transplants and neurotrophic factors increase regeneration and recovery of function after spinal cord injury. In Spinal Cord Trauma: Regeneration, Neural Repair and Functional Recovery. Progress in Brain Research, Vol. 137, L. McKerracher, G. Doucet, S. Rossignol, pp. 257-273.

Bretsche, P., Cohn, M., 1970. A theory of self-nonself discrimination. Science. 169**,** 1042.

Brockhaus, J., Moller, T., Kettenmann, H., 1996. Phagocytozing ameboid microglial cells studied in a mouse corpus callosum slice preparation. Glia. 16**,** 81-90.

Brodkey, J.A., Laywell, E.D., Obrien, T.F., Faissner, A., Stefansson, K., Dorries, H.U., Schachner, M., Steindler, D.A., 1995. Focal brain injury and up-regulation of a developmentally-regulated extracellular-matrix protein. Journal of Neurosurgery. 82**,** 106-112.

Brown, M.C., Perry, V.H., Lunn, E.R., Gordon, S., Heumann, R., 1991. Macrophage dependence of peripheral sensory nerve regeneration - possible involvement of nerve growth-factor. Neuron. 6**,** 359-370.

Bruce, A.J., Boling, W., Kindy, M.S., Peschon, J., Kraemer, P.J., Carpenter, M.K., Holtsberg, F.W., Mattson, M.P., 1996. Altered neuronal and microglial

responses to excitotoxic and ischemic brain injury in mice lacking TNF receptors. Nature Medicine. 2**,** 788-794.

Brushart, T.M., Hoffman, P.N., Royall, R.M., Murinson, B.B., Witzel, C., Gordon, T., 2002. Electrical stimulation promotes motoneuron regeneration without increasing its speed or conditioning the neuron. Journal of Neuroscience. 22**,** 6631-6638.

Bsibsi, M., Ravid, R., Gveric, D., van Noort, J.M., 2002. Broad expression of Toll-like receptors in the human central nervous system. Journal of Neuropathology and Experimental Neurology. 61**,** 1013-1021.

Bsibsi, M., Persoon, C., van Noort, H., 2003. The expression of toll-like receptors in human adult astrocytes and microglia in response to different ligands. Glia. 39-40.

Bsibsi, M., Persoon-Deen, C., Verwer, R.W.H., Meeuwsen, S., Ravid, R., Van Noort, J.M., 2006. Toll-like receptor 3 on adult human astrocytes triggers production of neuroprotective mediators. Glia. 53**,** 688-695.

Bundesen, L.Q., Scheel, T.A., Bregman, B.S., Kromer, L.F., 2003. Ephrin-B2 and EphB2 regulation of astrocyte-meningeal fibroblast interactions in response to spinal cord lesions in adult rats. Journal of Neuroscience. 23**,** 7789-7800.

Bunge, M.B., Holets, V.R., Bates, M.L., Clarke, T.S., Watson, B.D., 1994. Characterization of photochemically induced spinal-cord injury in the rat by light and electron-microscopy. Experimental Neurology. 127**,** 76-93.

Bungner, O., 1891. Uber die Degenerations und Regenerations-vorgange am Nerven nach Verletzungen. Vol. 10. Pathol. Anat, pp. 321-387.

Butovsky, O., Talpalar, A.E., Ben-Yaakov, K., Schwartz, M., 2005. Activation of microglia by aggregated beta-amyloid or lipopolysaccharide impairs MHC-II expression and renders them cytotoxic whereas IFN-gamma and IL-4 render them protective. Molecular and Cellular Neuroscience. 29**,** 381-393.

Butter, C., Oneill, J.K., Baker, D., Gschmeissner, S.E., Turk, J.L., 1991. An immunoelectron microscopic study of the expression of class-ii major histocompatibility complex during chronic relapsing Experimental Allergic Encephalomyelitis in Biozzi ab/h mice. Journal of Neuroimmunology. 33**,** 37-42.

Cafferty, W.B.J., Strittmatter, S.M., 2006. The Nogo-Nogo receptor pathway limits a spectrum of adult CNS axonal growth. Journal of Neuroscience. 26**,** 12242-12250.

Cafferty, W.B.J., Duffy, P., Huebner, E., Strittmatter, S.M., 2010. MAG and OMgp Synergize with Nogo-A to Restrict Axonal Growth and Neurological Recovery after Spinal Cord Trauma. Journal of Neuroscience. 30**,** 6825-6837.

Cai, Z.W., Pan, Z.L., Pang, Y., Evans, O.B., Rhodes, P.G., 2000. Cytokine induction in fetal rat brains and brain injury in neonatal rats after maternal lipopolysaccharide administration. Pediatric Research. 47**,** 64-72.

Cai, Z.W., Pang, Y., Lin, S.Y., Rhodes, P.G., 2003. Differential roles of tumor necrosis factor-alpha and interleukin-1 beta in lipopolysaccharide-induced brain injury in the neonatal rat. Brain Research. 975**,** 37-47.

Cajal, R.y., 1928. Degeneration and Regeneration of the Nervous System. Hafner Publishing Co, New York.

Cameron, J.S., Alexopoulou, L., Sloane, J.A., DiBernardo, A.B., Ma, Y., Kosaras, B., Flavell, R., Strittmatter, S.M., Volpe, J., Sidman, R., Vartanian, T., 2007. Toll-like receptor 3 is a potent negative regulator of axonal growth in mammals. Journal of Neuroscience. 27**,** 13033-13041.

Cammer, W., Tansey, F.A., 1988. Carbonic-Anhydrase immunostaining in astrocytes in the rat cerebral-cortex. Journal of Neurochemistry. 50**,** 319-322.

Campagne, M.V., Thibodeaux, H., van Bruggen, N., Cairns, B., Lowe, D.G., 2000. Increased binding activity at an antioxidant-responsive element in the metallothionein-1 promoter and rapid induction of metallothionein-1 and-2 in response to cerebral ischemia and reperfusion. Journal of Neuroscience. 20**,** 5200-5207.

Campbell, G., Anderson, P.N., Turmaine, M., Lieberman, A.R., 1991. GAP-43 in the axons of mammalian cns neurons regenerating into peripheral-nerve grafts. Experimental Brain Research. 87**,** 67-74.

Campbell, G., Hutchins, K., Winterbottom, J., Grenningloh, G., Lieberman, A.R., Anderson, P.N., 2005. Upregulation of activating transcription factor 3 (ATF3) by intrinsic CNS neurons regenerating axons into peripheral nerve grafts. Experimental Neurology. 192**,** 340-347.

Cao, Q.L., Zhang, Y.P., Howard, R.M., Walters, W.M., Tsoulfas, P., Whittemore, S.R., 2001. Pluripotent stem cells engrafted into the normal or lesioned adult rat spinal cord are restricted to a glial lineage. Experimental Neurology. 167**,** 48-58.

Carbonell, A.L., Boya, J., 1988. Ultrastructural-study on meningeal regeneration and meningo glial relationships after cerebral stab wound in the adult-rat. Brain Research. 439**,** 337-344.

Carlson, S.L., Parrish, M.E., Springer, J.E., Doty, K., Dossett, L., 1998. Acute inflammatory response in spinal cord following impact injury. Experimental Neurology. 151**,** 77-88.

Carpentier, P.A., Begolka, W.S., Olson, J.K., Elhofy, A., Karpus, W.J., Miller, S.D., 2005. Differential activation of astrocytes by innate and adaptive immune stimuli. Glia. 49**,** 360-374.

Carter, L.M., Starkey, M.L., Akrimi, S.F., Davies, M., McMahon, S.B., Bradbury, E.J., 2008. The Yellow Fluorescent Protein (YFP-H) Mouse Reveals Neuroprotection as a Novel Mechanism Underlying Chondroitinase ABC-Mediated Repair after Spinal Cord Injury. Journal of Neuroscience. 28**,** 14107-14120.

Castro, A.J., 1972a. Motor performance in rats - effects of pyramidal tract section. Brain Research. 44**,** 313.

Castro, A.J., 1972b. Effects of cortical ablations on digital usage in rat. Brain Research. 37**,** 173.

Chaisuksunt, V., Zhang, Y., Anderson, P.N., Campbell, G., Vaudano, E., Schachner, M., Lieberman, A.R., 2000. Axonal regeneration from CNS neurons in the cerebellum and brainstem of adult rats: Correlation with the patterns of expression and distribution of messenger RNAs for L1, CHL1, c-jun and growth-associated protein-43. Neuroscience. 100**,** 87-108.

Chau, C.H., Shum, D.K.Y., Li, H., Pei, J., Lui, Y.Y., Wirthlin, L., Chan, Y.S., Xu, X.M., 2004. Chondroitinase ABC enhances axonal regrowth through Schwann cell-seeded guidance channels after spinal cord injury. FASEB Journal. 18**,** 194-196.

Chen, M.S., Huber, A.B., van der Haar, M.E., Frank, M., Schnell, L., Spillmann, A.A., Christ, F., Schwab, M.E., 2000. Nogo-A is a myelin-associated neurite outgrowth inhibitor and an antigen for monoclonal antibody IN-1. Nature. 403**,** 434-439.

Cheng, H., Cao, Y.H., Olson, L., 1996. Spinal cord repair in adult paraplegic rats: Partial restoration of hind limb function. Science. 273**,** 510-513.

Cheng, H., Liao, K.K., Liao, S.F., Chuang, T.Y., Shih, Y.H., 2004. Spinal cord repair with acidic fibroblast growth factor as a treatment for a patient with chronic paraplegia. Spine. 29**,** E284-E288.

Cheng, H.R., Almstrom, S., Gimenez-Llort, L., Chang, R., Ogren, S.O., Hoffer, B., Olson, L., 1997. Gait analysis of adult paraplegic rats after spinal cord repair. Experimental Neurology. 148**,** 544-557.

Cheng, S.S., Lai, J.J., Lukacs, N.W., Kunkel, S.L., 2001. Granulocyte-macrophage colony stimulating factor up-regulates CCR1 in human neutrophils. Journal of Immunology. 166**,** 1178-1184.

Chhor, V., Le Charpentier, T., Lebon, S., Ore, M.V., Celador, I.L., Josserand, J., Degos, V., Jacotot, E., Hagberg, H., Savman, K., Mallard, C., Gressens, P., Fleiss, B., 2013. Characterization of phenotype markers and neuronotoxic potential of polarised primary microglia in vitro. Brain Behavior and Immunity. 32**,** 70-85.

Chiba, S., Shibuya, K., Piao, Y.F., Tojo, A., Sasaki, N., Matsuki, S., Miyagawa, K., Miyazono, K., Takaku, F., 1990. IDENTIFICATION AND CELLULAR-DISTRIBUTION OF DISTINCT PROTEINS FORMING HUMAN GM-CSF RECEPTOR. Cell Regulation. 1**,** 327-335.

Cho, Y., Di Liberto, V., Carlin, D., Abe, N., Li, K.H., Burlingame, A.L., Guan, S., Michaelevski, I., Cavalli, V., 2014. Syntaxin13 Expression Is Regulated by Mammalian Target of Rapamycin (mTOR) in Injured Neurons to Promote Axon Regeneration. Journal of Biological Chemistry. 289**,** 15820-15832.

Chong, M.S., Reynolds, M.L., Irwin, N., Coggeshall, R.E., Emson, P.C., Benowitz, L.I., Woolf, C.J., 1994. GAP-43 expression in primary sensory neurons following central axotomy. Journal of Neuroscience. 14**,** 4375-4384.

Chong, M.S., Woolf, C.J., Turmaine, M., Emson, P.C., Anderson, P.N., 1996. Intrinsic versus extrinsic factors in determining the regeneration of the central processes of rat dorsal root ganglion neurons: The influence of a peripheral nerve graft. Journal of Comparative Neurology. 370**,** 97-104.

Chun, J.J.M., Shatz, C.J., 1988.A fibronectin-like molecule is present in the developing cat cerebral-cortex and is correlated with subplate neurons. Journal of Cell Biology. 106**,** 857-872.

Cohen, S., 1960. Purification of a nerve-growth promoting protein from the mouse salivary gland and its neuro-cytotoxic antiserum. Proceedings of the National Academy of Sciences of the United States of America. 46**,** 302-311.

Colton, C.A., Mott, R.T., Sharpe, H., Xu, Q., Van Nostrand, W.E., Vitek, M.P., 2006. Expression profiles for macrophage alternative activation genes in AD and in mouse models of AD. Journal of Neuroinflammation. 3.

Colton, C.A., 2009. Heterogeneity of Microglial Activation in the Innate Immune Response in the Brain. Journal of Neuroimmune Pharmacology. 4**,** 399-418.

Compston, A., Zajicek, J., Sussman, J., Webb, A., Hall, G., Muir, D., Shaw, C., Wood, A., Scolding, N., 1997. Glial lineages and myelination in the central nervous system. Journal of Anatomy. 190**,** 161-200.

Connolly, E.S., Winfree, C.J., Springer, T.A., Naka, Y., Liao, H., Yan, S.D., Stern, D.M., Solomon, R.A., GutierrezRamos, J.C., Pinsky, D.J., 1996. Cerebral protection in homozygous null ICAM-1 mice after middle cerebral artery occlusion - Role of neutrophil adhesion in the pathogenesis of stroke. Journal of Clinical Investigation. 97**,** 209-216.

Conti, L., Gessani, S., 2008. GM-CSF in the generation of dendritic cells from human blood monocyte precursors: Recent advances. Immunobiology. 213**,** 859-870.

Corey, S.J., Rosoff, P.M., 1989. Granulocyte-Macrophage Colony-Stimulating Factor primes neutrophils by activating a pertussis toxin-sensitive G-protein not associated with Phosphatidylinositol turnover. Journal of Biological Chemistry. 264**,** 14165-14171.

Costigan, M., Befort, K., Karchewski, L., Griffin, R.S., D'Urso, D., Allchorne, A., Sitarski, J., Mannion, J.W., Pratt, R.E., Woolf, C.J., 2002. Replicate high-density rat genome oligonucleotide microarrays reveal hundreds of regulated genes in the dorsal root ganglion after peripheral nerve injury. BMC Neuroscience. 3.

Coumans, A.B.C., Middelanis, J., Garnier, Y., Vaihinger, H.M., Leib, S.L., Von Duering, M.U., Hasaart, T.H.M., Jensen, A., Berger, R., 2003. Intracisternal application of endotoxin enhances the susceptibility to subsequent hypoxic-ischemic brain damage in neonatal rats. Pediatric Research. 53**,** 770-775.

Coumans, J.V., Lin, T.T.S., Dai, H.N., MacArthur, L., McAtee, M., Nash, C., Bregman, B.S., 2001. Axonal regeneration and functional recovery after complete spinal cord transection in rats by delayed treatment with transplants and neurotrophins. Journal of Neuroscience. 21**,** 9334-9344.

Cruz-Orengo, L., Figueroa, J.D., Velazquez, I., Torrado, A., Ortiz, C., Hernandez, C., Puig, A., Segarra, A.C., Whittemore, S.R., Miranda, J.D., 2006. Blocking EphA4 upregulation after spinal cord injury results in enhanced chronic pain. Experimental Neurology. 202**,** 421-433.

Cruz-Orengo, L., Figueroa, J.D., Torrado, A., Puig, A., Whittemore, S.R., Miranda, J.D., 2007. Reduction of EphA4 receptor expression after spinal cord injury does not induce axonal regeneration or return of tcMMEP response. Neuroscience Letters. 418**,** 49-54.

Cui, Q., 2006. Actions of neurotrophic factors and their signaling pathways in neuronal survival and axonal regeneration. Molecular Neurobiology. 33**,** 155-179.

Cummings, B.J., Uchida, N., Tamaki, S.J., Salazar, D.L., Hooshmand, M., Summers, R., Gage, F.H., Anderson, A.J., 2005. Human neural stem cells

differentiate and promote locomotor recovery in spinal cord-injured mice. Proceedings of the National Academy of Sciences of the United States of America. 102**,** 14069-14074.

Cunningham, C., Campion, S., Teeling, J., Felton, L., Perry, V.H., 2007. The sickness behaviour and CNS inflammatory mediator profile induced by systemic challenge of mice with synthetic double-stranded RNA (Poly I : C). Brain Behavior and Immunity. 21**,** 490-502.

Dammann, O., Leviton, A., 1997. Intrauterine infection, cytokines, and brain damage in the preterm newborn. Pediatric Research. 42**,** 1-8.

David, S., Aguayo, A.J., 1985. Axonal regeneration after crush injury of rat Central Nervous-System fibers innervating peripheral-nerve grafts. Journal of Neurocytology. 14**,** 1-12.

Davies, S.J.A., Goucher, D.R., Doller, C., Silver, J., 1999. Robust regeneration of adult sensory axons in degenerating white matter of the adult rat spinal cord. Journal of Neuroscience. 19**,** 5810-5822.

de Bock, F., Derijard, B., Dornand, J., Bockaert, J., Rondouin, G., 1998. The neuronal death induced by endotoxic shock but not that induced by excitatory amino acids requires TNF-alpha. European Journal of Neuroscience. 10**,** 3107-3114.

de Heredia, L.L., Magoulas, C., 2013. Lack of the transcription factor C/EBP delta impairs the intrinsic capacity of peripheral neurons for regeneration. Experimental Neurology. 239**,** 148-157.

De Winter, F., Oudega, M., Lankhorst, A.J., Hamers, F.P., Blits, B., Ruitenberg, M.J., Pasterkamp, R.J., Gispen, W.H., Verhaagen, J., 2002. Injury-induced class 3 semaphorin expression in the rat spinal cord. Experimental Neurology. 175**,** 61-75.

de Wit, J., Verhaagen, J., 2003. Role of semaphorins in the adult nervous system. Progress in Neurobiology. 71**,** 249-267.

Deckert-Schluter, M., Rang, A., Weiner, D., Huang, S., Wiestler, O.D., Hof, H., Schluter, D., 1996. Interferon-gamma receptor-deficiency renders mice highly susceptible to toxoplasmosis by decreased macrophage activation. Laboratory Investigation. 75**,** 827-841.

Del Rio-Hortega, P., 1932. Microglia. In *Cytology and Cellular Pathology of the Nervous System*. Vol. 2, W. Penfield. P. B. Hoeber. New York, NY, USA., pp. 481-534.

Deleidi, M., Hallett, P.J., Koprich, J.B., Chung, C.-Y., Isacson, O., 2010. The Toll-Like Receptor-3 Agonist Polyinosinic:Polycytidylic Acid Triggers

Nigrostriatal Dopaminergic Degeneration. Journal of Neuroscience. 30**,** 16091-16101.

Dergham, P., Ellezam, B., Essagian, C., Avedissian, H., Lubell, W.D., McKerracher, L., 2002. Rho signaling pathway targeted to promote spinal cord repair. Journal of Neuroscience. 22**,** 6570-6577.

Desimone, R., Giampaolo, A., Giometto, B., Gallo, P., Levi, G., Peschle, C., Aloisi, F., 1995. The Costimulatory Molecule B7 is expressed on human microglia in culture and in Multiple-Sclerosis acute lesions. Journal of Neuropathology and Experimental Neurology. 54**,** 175-187.

Devries, L.S., Eken, P., Groenendaal, F., Vanhaastert, I.C., Meiners, L.C., 1993. Correlation between the degree of periventricular leukomalacia diagnosed using cranial ultrasound and MRI later in infancy in children with cerebral-palsy. Neuropediatrics. 24**,** 263-268.

Di Giovanni, S., Knights, C.D., Rao, M., Yakovlev, A., Beers, J., Catania, J., Avantaggiati, M.L., Faden, A.I., 2006. The tumor suppressor protein p53 is required for neurite outgrowth and axon regeneration. Embo Journal. 25**,** 4084-4096.

Dickson, B.J., 2002. Molecular mechanisms of axon guidance. Science. 298**,** 1959-1964.

Didier, M., Harandi, M., Aguera, M., Bancel, B., Tardy, M., Fages, C., Calas, A., Stagaard, M., Mollgard, K., Belin, M.F., 1986. Differential immunocytochemical staining for Glial Fibrillary Acidic (GFA) protein, S-100 protein and Glutamine-Synthetase in the rat subcommissural organ, nonspecialized ventricular ependyma and adjacent neuropil. Cell and Tissue Research. 245**,** 343-351.

Dobkin, B., Apple, D., Barbeau, H., Basso, M., Behrman, A., Deforge, D., Ditunno, J., Dudley, G., Elashoff, R., Fugate, L., Harkema, S., Saulino, M., Scott, M., Grp, S., 2006. Weight-supported treadmill vs overground training for walking after acute incomplete SCI. Neurology. 66**,** 484-492.

Dohm, S., Streppel, M., Guntinas-Lichius, O., Pesheva, P., Probstmeier, R., Walther, M., Neiss, W.F., Stennert, E., Angelov, D.N., 2000. Local application of extracellular matrix proteins fails to reduce the number of axonal branches after varying reconstructive surgery on rat facial nerve. Restorative Neurology and Neuroscience. 16**,** 117-126.

Dolga, A.M., Granic, I., Blank, T., Knaus, H.-G., Spiess, J., Luiten, P.G.M., Eisel, U.L.M., Nijholt, I.M., 2008. TNF-alpha-mediates neuroprotection against glutamate-induced excitotoxicity via NF-kappa B-dependent up-regulation of K(Ca)2.2 channels. Journal of Neurochemistry. 107**,** 1158-1167.

Donnelly, E.M., Strappe, P.M., McGinley, L.M., Madigan, N.N., Geurts, E., Rooney, G.E., Windebank, A.J., Fraher, J., Dockery, P., O'Brien, T., McMahon, S.S., 2010. Lentiviral vector-mediated knockdown of the neuroglycan 2 proteoglycan or expression of neurotrophin-3 promotes neurite outgrowth in a cell culture model of the glial scar. Journal of Gene Medicine. 12**,** 863-872.

Donnelly, E.M., Madigan, N.N., Rooney, G.E., Knight, A., Chen, B., Ball, B., Kinnavane, L., Garcia, Y., Dockery, P., Fraher, J., Strappe, P.M., Windebank, A.J., O'Brien, T., McMahon, S.S., 2012. Lentiviral vector delivery of short hairpin RNA to NG2 and neurotrophin-3 promotes locomotor recovery in injured rat spinal cord. Cytotherapy. 14**,** 1235-1244.

Duncan, J.R., Cock, M.L., Scheerlinck, J.P.Y., Westcott, K.T., McLean, C., Harding, R., Rees, S.M., 2002. White matter injury after repeated endotoxin exposure in the preterm ovine fetus. Pediatric Research. 52**,** 941-949.

Dusart, I., Schwab, M.E., 1994. Secondary cell-death and the inflammatory reaction after dorsal hemisection of the rat spinal-cord. European Journal of Neuroscience. 6**,** 712-724.

Dziennis, S., Alkayed, N.J., 2008. Role of Signal Transducer and Activator of Transcription 3 in Neuronal Survival and Regeneration. Reviews in the Neurosciences. 19**,** 341-361.

Eddleston, M., Mucke, L., 1993. Molecular profile of reactive astrocytes - implications for their role in neurologic disease. Neuroscience. 54**,** 15-36.

Eickholt, B.J., Ahmed, A.I., Davies, M., Papakonstanti, E.A., Pearce, W., Starkey, M.L., Bilando, A., Need, A.C., Smith, A.J.H., Hall, S.M., Hamers, F.P., Giese, K.P., Bradbury, E.J., Vanhaesebroeck, B., 2007. Control of Axonal Growth and Regeneration of Sensory Neurons by the p110 delta PI 3-Kinase. Plos One. 2.

Eidelberg, E., Straehley, D., Erspamer, R., Watkins, C.J., 1977. Relationship between residual hindlimb-assisted locomotion and surviving axons after incomplete spinal-cord injuries. Experimental Neurology. 56**,** 312-322.

Elde, R., Cao, Y.H., Cintra, A., Brelje, T.C., Pelto-Huikko, M., Junttila, T., Fuxe, K., Pettersson, R.F., Hokfelt, T., 1991. Prominent expression of acidic fibroblast growth factor in motor and sensory neurons. Neuron. 7**,** 349-64.

Eng, L.F., Ghirnikar, R.S., Lee, Y.L., 2000. Glial fibrillary acidic protein: GFAP-thirty-one years (1969-2000). Neurochemical Research. 25**,** 1439-1451.

Engelhardt, B., Martin-Simonet, M.T.G., Rott, L.S., Butcher, E.C., Michie, S.A., 1998. Adhesion molecule phenotype of T lymphocytes in inflamed CNS. Journal of Neuroimmunology. 84**,** 92-104.

Engelhardt, B., 2006. Molecular mechanisms involved in T cell migration across the blood-brain barrier. Journal of Neural Transmission. 113**,** 477-485.

Engesser-Cesar, C., Anderson, A.J., Basso, D.M., Edgerton, V.R., Cotman, C.W., 2005. Voluntary wheel running improves recovery from a moderate spinal cord injury. Journal of Neurotrauma. 22**,** 157-171.

Eriksson, C., Winblad, B., Schultzberg, M., 1998. Kainic acid induced expression of interleukin-1 receptor antagonist mRNA in the rat brain. Molecular Brain Research. 58**,** 195-208.

Fabes, J., Anderson, P., Yanez-Munoz, R.J., Thrasher, A., Brennan, C., Bolsover, S., 2006. Accumulation of the inhibitory receptor EphA4 may prevent regeneration of corticospinal tract axons following lesion. European Journal of Neuroscience. 23**,** 1721-1730.

Fabes, J., Anderson, P., Brennan, C., Bolsover, S., 2007. Regeneration-enhancing effects of EphA4 blocking peptide following corticospinal tract injury in adult rat spinal cord. European Journal of Neuroscience. 26**,** 2496-2505.

Farina, C., Krumbholz, M., Giese, T., Hartmann, G., Aloisi, F., Meinl, E., 2005. Preferential expression and function of Toll-like receptor 3 in human astrocytes. Journal of Neuroimmunology. 159**,** 12-19.

Fawcett, J.W., Keynes, R.J., 1990. Peripheral-nerve regeneration. Annual Review of Neuroscience. 13**,** 43-60.

Fenrich, K.K., Skelton, N., MacDermid, V.E., Meehan, C.F., Armstrong, S., Neuber-Hess, M.S., Rose, P.K., 2007. Axonal regeneration and development of de novo axons from distal dendrites of adult feline commissural interneurons after a proximal axotomy. Journal of Comparative Neurology. 502**,** 1079-1097.

Fenzi, F., Benedetti, M.D., Moretto, G., Rizzuto, N., 2001. Glial cell and macrophage reactions in rat spinal ganglion after peripheral nerve lesions: An immunocytochemical and morphometric study. Archives Italiennes De Biologie. 139**,** 357-365.

Fidler, P.S., Schuette, K., Asher, R.A., Dobbertin, A., Thornton, S.R., Calle-Patino, Y., Muir, E., Levine, J.M., Geller, H.M., Rogers, J.H., Faissner, A., Fawcett, J.W., 1999. Comparing astrocytic cell lines that are inhibitory or permissive for axon growth: the major axon-inhibitory proteoglycan is NG2. Journal of Neuroscience. 19**,** 8778-8788.

Field, R., Campion, S., Warren, C., Murray, C., Cunningham, C., 2010. Systemic challenge with the TLR3 agonist poly I:C induces amplified IFN alpha/beta

and IL-1 beta responses in the diseased brain and exacerbates chronic neurodegeneration. Brain Behavior and Immunity. 24**,** 996-1007.

Fields, R.D., Ellisman, M.H., 1986. Axons regenerated through silicone tube splices .1. Conduction properties. Experimental Neurology. 92**,** 48-60.

Figueroa, J.D., Benton, R.L., Velazquez, I., Torrado, A.I., Ortiz, C.M., Hernandez, C.M., Diaz, J.J., Magnuson, D.S., Whittemore, S.R., Miranda, J.D., 2006. Inhibition of EphA7 up-regulation after spinal cord injury reduces apoptosis and promotes locomotor recovery. Journal of Neuroscience Research. 84**,** 1438-1451.

Filbin, M.T., 2003. Myelin-associated inhibitors of axonal regeneration in the adult mammalian CNS. Nature Reviews Neuroscience. 4**,** 703-713.

Fischer, H.G., Nitzgen, B., Germann, T., Degitz, K., Daubener, W., Hadding, U., 1993. Differentiation driven by Granulocyte-Macrophage Colony-Stimulating Factor endows microglia with interferon-gamma-independent antigen presentation function. Journal of Neuroimmunology. 42**,** 87-96.

Fishman, P.S., Kelly, J.P., 1984a. The fate of severed corticospinal axons. Neurology. 34**,** 1161-1167.

Fishman, P.S., Kelly, J.P., 1984b. Identified central axons differ in their response to spinal-cord transection. Brain Research. 305**,** 152-156.

Fishman, P.S., 1987. Retrograde changes in the corticospinal tract of posttraumatic paraplegics. Archives of Neurology. 44**,** 1082-1084.

Flaris, N.A., Densmore, T.L., Molleston, M.C., Hickey, W.F., 1993. Characterization of microglia and macrophages in the Central-Nervous-System of rats - definition of the differential expression of molecules using standard and novel monoclonal-antibodies in normal CNS and in 4 models of parenchymal reaction. Glia. 7**,** 34-40.

Fontaine, V., Mohand-Said, S., Hanoteau, N., Fuchs, L., Pfizenmaier, K., Eisel, U., 2002. Neurodegenerative and neuroprotective effects of tumor necrosis factor (TNF) in retinal ischemia: Opposite roles of TNF receptor 1 and TNF receptor 2. Journal of Neuroscience. 22.

Forman, D.S., Berenberg, R.A., 1978. Regeneration of motor axons in rat sciatic-nerve studied by labeling with axonally transported radioactive proteins. Brain Research. 156**,** 213-225.

Fouad, K., Klusman, I., Schwab, M.E., 2004. Regenerating corticospinal fibers in the Marmoset (Callitrix jacchus) after spinal cord lesion and treatment with the anti-Nogo-A antibody IN-1. European Journal of Neuroscience. 20**,** 2479-2482.

Fournier, A.E., Takizawa, B.T., Strittmatter, S.M., 2003. Rho kinase inhibition enhances axonal regeneration in the injured CNS. Journal of Neuroscience. 23**,** 1416-1423.

Francisco-Cruz, A., Aguilar-Santelises, M., Ramos-Espinosa, O., Mata-Espinosa, D., Marquina-Castillo, B., Barrios-Payan, J., Hernandez-Pando, R., 2014. Granulocyte-macrophage colony-stimulating factor: not just another haematopoietic growth factor. Medical Oncology. 31.

Frei, K., Leist, T.P., Meager, A., Gallo, P., Leppert, D., Zinkernagel, R.M., Fontana, A., 1988. Production of B-cell Stimulatory Factor-II and interferon-gamma in the central nervous-system during viral meningitis and encephalitis - evaluation in a murine model infection and in patients. Journal of Experimental Medicine. 168**,** 449-453.

Frei, K., Lins, H., Schwerdel, C., Fontana, A., 1994. Antigen presentation in the Central-Nervous-System - the inhibitory effect of IL-10 on mhc class-II expression and production of cytokines depends on the inducing signals and the type of cell analyzed. Journal of Immunology. 152**,** 2720-2728.

Freund, P., Wannier, T., Schmidlin, E., Bloch, J., Mir, A., Schwab, M.E., Rouiller, E.M., 2007. Anti-Nogo-A antibody treatment enhances sprouting of corticospinal axons rostral to a unilateral cervical spinal cord lesion in adult macaque monkey. Journal of Comparative Neurology. 502**,** 644-659.

Freund, P., Schmidlin, E., Wannier, T., Bloch, J., Mir, A., Schwab, M.E., Rouiller, E.M., 2009. Anti-Nogo-A antibody treatment promotes recovery of manual dexterity after unilateral cervical lesion in adult primates - re-examination and extension of behavioral data. European Journal of Neuroscience. 29**,** 983-996.

Frey, D., Laux, T., Xu, L., Schneider, C., Caroni, P., 2000. Shared and unique roles of CAP23 and GAP43 in actin regulation, neurite outgrowth, and anatomical plasticity. Journal of Cell Biology. 149**,** 1443-1453.

Fricker, M., Neher, J.J., Zhao, J.-W., Thery, C., Tolkovsky, A.M., Brown, G.C., 2012a. MFG-E8 Mediates Primary Phagocytosis of Viable Neurons during Neuroinflammation. Journal of Neuroscience. 32**,** 2657-2666.

Fricker, M., Oliva-Martin, M.J., Brown, G.C., 2012b. Primary phagocytosis of viable neurons by microglia activated with LPS or A beta is dependent on calreticulin/LRP phagocytic signalling. Journal of Neuroinflammation. 9.

Fu, R., Shen, Q., Xu, P., Luo, J.J., Tang, Y., 2014. Phagocytosis of Microglia in the Central Nervous System Diseases. Molecular Neurobiology. 49**,** 1422-1434.

Fuhrmann, M., Bittner, T., Jung, C.K.E., Burgold, S., Page, R.M., Mitteregger, G., Haass, C., LaFerla, F.M., Kretzschmar, H., Herms, J., 2010. Microglial

Cx3cr1 knockout prevents neuron loss in a mouse model of Alzheimer's disease. Nature Neuroscience. 13**,** 411-413.

Fujita, H., Tanaka, J., Toku, K., Tateishi, N., Suzuki, Y., Matsuda, S., Sakanaka, M., Maeda, N., 1996. Effects of GM-CSF and ordinary supplements on the ramification of microglia in culture: A morphometrical study. Glia. 18**,** 269-281.

Fujitani, M., Yamagishi, S., Che, Y.H., Hata, K., Kubo, T., Ino, H., Tohyama, M., Yamashita, T., 2004. P311 accelerates nerve regeneration of the axotomized facial nerve. Journal of Neurochemistry. 91**,** 737-744.

Fukuzawa, H., Sawada, M., Kayahara, T., Morita-Fujisawa, Y., Suzuki, K., Seno, H., Takaishi, S., Chiba, T., 2003. Identification of GM-CSF in Paneth cells using single-cell RT-PCR. Biochemical and Biophysical Research Communications. 312**,** 897-902.

Funakoshi, H., Frisen, J., Barbany, G., Timmusk, T., Zachrisson, O., Verge, V.M.K., Persson, H., 1993. Differential expression of messenger-rnas for neurotrophins and their receptors after axotomy of the sciatic-nerve. Journal of Cell Biology. 123**,** 455-465.

Funderburg, N., Luciano, A.A., Jiang, W., Rodriguez, B., Sieg, S.F., Lederman, M.M., 2008. Toll-Like Receptor Ligands Induce Human T Cell Activation and Death, a Model for HIV Pathogenesis. Plos One. 3.

Furie, M.B., Randolph, G.J., 1995. Chemokines and tissue-injury. American Journal of Pathology. 146**,** 1287-1301.

Gabbott, P.L.A., Bacon, S.J., 1996. Localisation of NADPH diaphorase activity and NOS immunoreactivity in astroglia in normal adult rat brain. Brain Research. 714**,** 135-144.

Gall, C., Rose, G., Lynch, G., 1979. Proliferative and migratory activity of glial cells in the partially deafferented hippocampus. Journal of Comparative Neurology. 183**,** 539-549.

Gallo, P., Frei, K., Rordorf, C., Lazdins, J., Tavolato, B., Fontana, A., 1989. Human Immunodeficiency Virus Type-1 (HIV-1) infection of the Central Nervous-System - an evaluation of cytokines in Cerebrospinal-Fluid. Journal of Neuroimmunology. 23**,** 109-116.

Garcia, J.H., Liu, K.F., Relton, J.K., 1995. Interleukin-1 receptor antagonist decreases the number of necrotic neurons in rats with middle cerebral-artery occlusion. American Journal of Pathology. 147**,** 1477-1486.

Gavrieli, Y., Sherman, Y., Bensasson, S.A., 1992. Identification of programmed cell-death insitu via specific labeling of Nuclear-DNA fragmentation. Journal of Cell Biology. 119**,** 493-501.

Geddes, J.W., Pettigrew, L.C., Holtz, M.L., Craddock, S.D., Maines, M.D., 1996. Permanent focal and transient global cerebral ischemia increase glial and neuronal expression of heme oxygenase-1, but not heme oxygenase-2, protein in rat brain. Neuroscience Letters. 210**,** 205-208.

Geiger, K.D., Nash, T.C., Sawyer, S., Krahl, T., Patstone, G., Reed, J.C., Krajewski, S., Dalton, D., Buchmeier, M.J., Sarvetnick, N., 1997. Interferon-gamma protects against herpes simplex virus type 1-mediated neuronal death. Virology. 238**,** 189-197.

Gharbawie, O.A., Whishaw, I.Q., 2003. Cholinergic and serotonergic neocortical projection lesions given singly or in combination cause only mild impairments on tests of skilled movement in rats: evaluation of a model of dementia. Brain Research. 970**,** 97-109.

Ghosh, A., Antonini, A., McConnell, S.K., Shatz, C.J., 1990. Requirement for subplate neurons in the formation of thalamocortical connections. Nature. 347**,** 179-181.

Ghosh, A., Shatz, C.J., 1992. Involvement of subplate neurons in the formation of ocular dominance columns. Science. 255**,** 1441-1443.

Gibson, R.M., Rothwell, N.J., Le Feuvre, R.A., 2004. CNS injury: the role of the cytokine IL-1. Veterinary Journal. 168**,** 230-237.

Giftochristos, N., David, S., 1988. Laminin and Heparan-Sulfate proteoglycan in the lesioned adult mammalian Central Nervous-System and their possible relationship to axonal sprouting. Journal of Neurocytology. 17**,** 385-397.

Ginhoux, F., Greter, M., Leboeuf, M., Nandi, S., See, P., Gokhan, S., Mehler, M.F., Conway, S.J., Ng, L.G., Stanley, E.R., Samokhvalov, I.M., Merad, M., 2010. Fate Mapping Analysis Reveals That Adult Microglia Derive from Primitive Macrophages. Science. 330**,** 841-845.

Giulian, D., Lachman, L.B., 1985. Interleukin-1 stimulation of astroglial proliferation after brain injury. Science. 228**,** 497-499.

Giulian, D., Baker, T.J., Shih, L.C.N., Lachman, L.B., 1986. Interleukin-1 of the central-nervous-system is produced by ameboid microglia. Journal of Experimental Medicine. 164**,** 594-604.

Giulian, D., Ingeman, J.E., 1988. Colony-Stimulating Factors as promoters of ameboid microglia. Journal of Neuroscience. 8**,** 4707-4717.

Giunti, D., Parodi, B., Cordano, C., Uccelli, A., de Rosbo, N.K., 2014. Can we switch microglia's phenotype to foster neuroprotection? Focus on multiple sclerosis. Immunology. 141**,** 328-339.

Goldshmit, Y., Bourne, J.A., 2010. Upregulation of EphA4 on Astrocytes Potentially Mediates Astrocytic Gliosis after Cortical Lesion in the Marmoset Monkey. Journal of Neurotrauma. 27**,** 1321-1332.

Goldshmit, Y., Spanevello, M.D., Tajouri, S., Li, L., Rogers, F., Pearse, M., Galea, M., Bartlett, P.F., Boyd, A.W., Turnley, A.M., 2011. EphA4 Blockers Promote Axonal Regeneration and Functional Recovery Following Spinal Cord Injury in Mice. Plos One. 6.

Gomez, R., Romero, R., Ghezzi, F., Yoon, B.H., Mazor, M., Berry, S.M., 1998. The fetal inflammatory response syndrome. American Journal of Obstetrics and Gynecology. 179**,** 194-202.

Gomez-Cambronero, J., Horn, J., Paul, C.C., Baumann, M.A., 2003. Granulocyte-macrophage colony-stimulating factor is a chemoattractant cytokine for human neutrophils: Involvement of the ribosomal p70 S6 kinase signaling pathway. Journal of Immunology. 171**,** 6846-6855.

Goslin, K., Banker, G., 1990. Rapid changes in the distribution of gap-43 correlate with the expression of neuronal polarity during normal development and under experimental conditions. Journal of Cell Biology. 110**,** 1319-1331.

Graeber, M.B., Kreutzberg, G.W., 1986. Astrocytes increase in glial fibrillary acidic protein during retrograde changes of facial motor neurons. Journal of Neurocytology. 15**,** 363-373.

Graeber, M.B., Streit, W.J., Kreutzberg, G.W., 1988a. Axotomy of the rat facial-nerve leads to increased CR3 complement receptor expression by activated microglial cells. Journal of Neuroscience Research. 21**,** 18-24.

Graeber, M.B., Streit, W.J., Kreutzberg, G.W., 1988b. The microglial cytoskeleton - vimentin is localized within activated cells insitu. Journal of Neurocytology. 17**,** 573-580.

Graeber, M.B., Tetzlaff, W., Streit, W.J., Kreutzberg, G.W., 1988c. Microglial cells but not astrocytes undergo mitosis following rat facial-nerve axotomy. Neuroscience Letters. 85**,** 317-321.

Graeber, M.B., Streit, W.J., Kreutzberg, G.W., 1989. Formation of microglia-derived brain macrophages is blocked by Adriamycin. Acta Neuropathologica. 78**,** 348-358.

Grafstein, B., 1975. Nerve-cell body response to axotomy. Experimental Neurology. 48**,** 32-51.

Grill, R., Murai, K., Blesch, A., Gage, F.H., Tuszynski, M.H., 1997a. Cellular delivery of neurotrophin-3 promotes corticospinal axonal growth and partial functional recovery after spinal cord injury. Journal of Neuroscience. 17**,** 5560-5572.

Grill, R.J., Blesch, A., Tuszynski, M.H., 1997b. Robust growth of chronically injured spinal cord axons induced by grafts of genetically modified NGF-secreting cells. Experimental Neurology. 148**,** 444-452.

Grosheva, M., Guntinas-Lichius, O., Arnhold, S., Skouras, E., Kuerten, S., Streppel, M., Angelova, S.K., Wewetzer, K., Radtke, C., Dunlop, S.A., Angelov, D.N., 2008. Bone marrow-derived mesenchymal stem cell transplantation does not improve quality of muscle reinnervation or recovery of motor function after facial nerve transection in rats. Biological Chemistry. 389**,** 873-888.

Grumet, M., 1991. Cell adhesion molecules and their subgroups in the nervous system. Current opinion in neurobiology. 1**,** 370-6.

Guest, J., Herrera, L.P., Qian, T., 2006. Rapid recovery of segmental neurological function in a tetraplegic patient following transplantation of fetal olfactory bulb-derived cells. Spinal Cord. 44**,** 135-142.

Guest, J.D., Hesse, D., Schnell, L., Schwab, M.E., Bunge, M.B., Bunge, R.P., 1997. Influence of IN-1 antibody and acidic FGF-fibrin glue on the response of injured corticospinal tract axons to human Schwann cell grafts. Journal of Neuroscience Research. 50**,** 888-905.

Guillemin, G., Boussin, F.D., leGrand, R., Croitoru, J., Coffigny, H., Dormont, D., 1996. Granulocyte macrophage colony stimulating factor stimulates in vitro proliferation of astrocytes derived from simian mature brains. Glia. 16**,** 71-80.

Guntinas-Lichius, O., Effenberger, K., Angelov, D.N., Klein, J., Streppel, M., Stennert, E., Neiss, W.F., 2000. Delayed rat facial nerve repair leads to accelerated and enhanced muscle reinnervation with reduced collateral axonal sprouting during a definite denervation period using a cross-anastomosis paradigm. Experimental Neurology. 162**,** 98-111.

Gutierrez, H., O'Keeffe, G.W., Gavalda, R., Gallagher, D., Davies, A.M., 2008. Nuclear factor kappa B signaling either stimulates or inhibits neurite growth depending on the phosphorylation status of p65/RelA. Journal of Neuroscience. 28**,** 8246-8256.

Gutmann, E., Guttmann, L., Medawar, P.B., Young, J.Z., 1942. The rate of regeneration of nerve. Journal of Experimental Biology. 19**,** 14-44.

Ha, Y., Kim, Y.S., Cho, J.M., Yoon, S.H., Park, S.R., Yoon, D.H., Kim, E.Y., Park, H.C., 2005. Role of granulocyte-macrophage colony-stimulating factor in preventing apoptosis and improving functional outcome in experimental spinal cord contusion injury. Journal of Neurosurgery-Spine. 2**,** 55-61.

Hacein-Bey-Abina, S., von Kalle, C., Schmidt, M., Le Deist, F., Wulffraat, N., McIntyre, E., Radford, I., Villeval, J.L., Fraser, C.C., Cavazzana-Calvo, M., Fischer, A., 2003. A serious adverse event after successful gene therapy for X-linked severe combined immunodeficiency. New England Journal of Medicine. 348**,** 255-256.

Hadlock, T., Lindsay, R., Edwards, C., Smitson, C., Weinberg, J., Knox, C., Heaton, J.T., 2010. The Effect of Electrical and Mechanical Stimulation on the Regenerating Rodent Facial Nerve. Laryngoscope. 120**,** 1094-1102.

Hagberg, H., Peebles, D., Mallard, C., 2002. Models of white matter injury: Comparison of infectious, hypoxic-ischemic, and excitotoxic insults. Mental Retardation and Developmental Disabilities Research Reviews. 8**,** 30-38.

Hailer, N.P., Bechmann, I., Heizmann, S., Nitsch, R., 1997. Adhesion molecule expression on phagocytic microglial cells following anterograde degeneration of perforant path axons. Hippocampus. 7**,** 341-349.

Hains, B.C., Black, J.A., Waxman, S.G., 2003. Primary cortical motor neurons undergo apoptosis after axotomizing spinal cord injury. Journal of Comparative Neurology. 462**,** 328-341.

Hamilton, J.A., 1993. Colony Stimulating Factors, cytokines and Monocyte-macrophages - some controversies. Immunology Today. 14**,** 18-24.

Hamilton, J.A., 2002. GM-CSF in inflammation and autoimmunity. Trends in Immunology. 23**,** 403-408.

Hamilton, T.A., Ohmori, Y., Tebo, J.M., Kishore, R., 1999. Regulation of macrophage gene expression by pro- and anti-inflammatory cytokines. Pathobiology. 67**,** 241-244.

Han, J.H., Ulevitch, R.J., 2005. Limiting inflammatory responses during activation of innate immunity. Nature Immunology. 6**,** 1198-1205.

Hanz, S., Perlson, E., Willis, D., Zheng, J.Q., Massarwa, R., Huerta, J.J., Koltzenburg, M., Kohler, M., van-Minnen, J., Twiss, J.L., Fainzilber, M., 2003. Axoplasmic importins enable retrograde injury signaling in lesioned nerve. Neuron. 40**,** 1095-1104.

Hara, M., Takasu, M., Watanabe, K., Noda, A., Takagi, T., Suzuki, Y., Yoshida, J., 2000. Protein kinase inhibition by fasudil hydrochloride promotes neurological recovery after spinal cord injury in rats. Journal of Neurosurgery. 93**,** 94-101.

Harel, N.Y., Song, K.-H., Tang, X., Strittmatter, S.M., 2010. Nogo Receptor Deletion and Multimodal Exercise Improve Distinct Aspects of Recovery in Cervical Spinal Cord Injury. Journal of Neurotrauma. 27**,** 2055-2066.

Harvey, P.J., Grochmal, J., Tetzlaff, W., Gordon, T., Bennett, D.J., 2005. An investigation into the potential for activity-dependent regeneration of the rubrospinal tract after spinal cord injury. European Journal of Neuroscience. 22**,** 3025-3035.

Hausmann, E.H.S., Berman, N.E.J., Wang, Y.Y., Meara, J.B., Wood, G.W., Klein, R.M., 1998. Selective chemokine mRNA expression following brain injury. Brain Research. 788**,** 49-59.

Hauwel, M., Furon, E., Canova, C., Griffiths, M., Neal, J., Gasque, P., 2005. Innate (inherent) control of brain infection, brain inflammation and brain repair: the role of microglia, astrocytes, "protective" glial stem cells and stromal ependymal cells. Brain Research Reviews. 48**,** 220-233.

Hay, N., Sonenberg, N., 2004. Upstream and downstream of mTOR. Genes & Development. 18**,** 1926-1945.

Hayashi, K., Ohta, S., Kawakami, Y., Toda, M., 2009. Activation of dendritic-like cells and neural stem/progenitor cells in injured spinal cord by GM-CSF. Neuroscience Research. 64**,** 96-103.

Hayashi, M., Ueyama, T., Tamaki, T., Senba, E., 1997. Expression of neurotrophin and IL-1-beta mRNAs following spinal cord injury and the effects of methylprednisolone treatment. Acta Anatomica Nipponica. 72**,** 209-213.

Hayes, G.M., Woodroofe, M.N., Cuzner, M.L., 1987. Microglia are the major cell type expressing MHC Class-II in human white matter. Journal of the Neurological Sciences. 80**,** 25-37.

Heaton, J.T., Kowaleski, J.M., Bermejo, R., Zeigler, H.P., Ahlgren, D.J., Hadlock, T.A., 2008. A system for studying facial nerve function in rats through simultaneous bilateral monitoring of eyelid and whisker movements. Journal of Neuroscience Methods. 171**,** 197-206.

Herdegen, T., Kummer, W., Fiallos, C.E., Leah, J., Bravo, R., 1991. Expression of c-jun, jun-b and jun-d proteins in rat nervous-system following transection of vagus nerve and cervical sympathetic trunk. Neuroscience. 45**,** 413-422.

Herdegen, T., Blume, A., Buschmann, T., Georgakopoulos, E., Winter, C., Schmid, W., Hsieh, T.F., Zimmermann, M., Gass, P., 1997. Expression of activating transcription factor-2, serum response factor and cAMP/Ca response element binding protein in the adult rat brain following generalized seizures, nerve fibre lesion and ultraviolet irradiation. Neuroscience. 81**,** 199-212.

Herdegen, T., Claret, F.X., Kallunki, T., Martin-Villalba, A., Winter, C., Hunter, T., Karin, M., 1998. Lasting N-terminal phosphorylation of c-Jun and activation of c-Jun N-terminal kinases after neuronal injury. Journal of Neuroscience. 18**,** 5124-5135.

Herman, R., He, J., D'Luzansky, S., Willis, W., Dilli, S., 2002. Spinal cord stimulation facilitates functional walking in a chronic, incomplete spinal cord injured. Spinal Cord. 40**,** 65-68.

Hermanson, M., Olsson, T., Westermark, B., Funa, K., 1995. PDGF and its receptors following facial-nerve axotomy in rats - expression in neurons and surrounding glia. Experimental Brain Research. 102**,** 415-422.

Herrmann, J.E., Shah, R.R., Chan, A.F., Zheng, B., 2010. EphA4 deficient mice maintain astroglial-fibrotic scar formation after spinal cord injury. Experimental Neurology. 223**,** 582-598.

Heumann, R., Korsching, S., Bandtlow, C., Thoenen, H., 1987. Changes of nerve Growth-Factor synthesis in nonneuronal cells in response to sciatic-nerve transection. Journal of Cell Biology. 104**,** 1623-1631.

Hickey, W.F., Kimura, H., 1988. Perivascular microglial cells of the cns are bone-marrow derived and present antigen invivo. Science. 239**,** 290-292.

Hickey, W.F., Hsu, B.L., Kimura, H., 1991. Lymphocyte-t entry into the Central-Nervous-System. Journal of Neuroscience Research. 28**,** 254-260.

Hill, C.E., Beattie, M.S., Bresnahan, J.C., 2001. Degeneration and sprouting of identified descending supraspinal axons after contusive spinal cord injury in the rat. Experimental Neurology. 171**,** 153-169.

Hirasawa, T., Ohsawa, K., Imai, Y., Ondo, Y., Akazawa, C., Uchino, S., Kohsaka, S., 2005. Visualization of microglia in living tissues using Iba1-EGFP transgenic mice. Journal of Neuroscience Research. 81**,** 357-362.

Hirata, A., Masaki, T., Motoyoshi, K., Kamakura, K., 2002. Intrathecal administration of nerve growth factor delays GAP 43 expression and early phase regeneration of adult rat peripheral nerve. Brain Research. 944**,** 146-156.

Hochreiter-Hufford, A., Ravichandran, K.S., 2013. Clearing the Dead: Apoptotic Cell Sensing, Recognition, Engulfment, and Digestion. Cold Spring Harbor Perspectives in Biology. 5.

Hofstetter, C.P., Holmstrom, N.A.V., Lilja, J.A., Schweinhardt, P., Hao, J.X., Spenger, C., Wiesenfeld-Hallin, Z., Kurpad, S.N., Frisen, J., Olson, L., 2005. Allodynia limits the usefulness of intraspinal neural stem cell grafts; directed differentiation improves outcome. Nature Neuroscience. 8**,** 346-353.

Hohn, A., Leibrock, J., Bailey, K., Barde, Y.A., 1990. Identification and characterization of a novel member of the nerve growth-factor Brain-Derived Neurotrophic Factor family. Nature. 344**,** 339-341.

Hol, E.M., Schwaiger, F.W., Werner, A., Schmitt, A., Raivich, G., Kreutzberg, G.W., 1999. Regulation of the LIM-type homeobox gene islet-1 during neuronal regeneration. Neuroscience. 88**,** 917-925.

Holmes, F.E., Mahoney, S., King, V.R., Bacon, A., Kerr, N.C.H., Pachnis, V., Curtis, R., Priestley, J.V., Wynick, D., 2000. Targeted disruption of the galanin gene reduces the number of sensory neurons and their regenerative capacity. Proceedings of the National Academy of Sciences of the United States of America. 97**,** 11563-11568.

Holmin, S., Soderlund, J., Biberfeld, P., Mathiesen, T., 1998. Intracerebral inflammation after human brain contusion. Neurosurgery. 42**,** 291-298.

Holmin, S., Mathiesen, T., 2000. Intracerebral administration of interleukin-1 beta and induction of inflammation, apoptosis, and vasogenic edema. Journal of Neurosurgery. 92**,** 108-120.

Holstege, G., 1991. Descending motor pathways and the spinal motor system - limbic and nonlimbic components. Role of the Forebrain in Sensation and Behavior, Vol. 87.

Holtmaat, A., Oestreicher, A.B., Gispen, W.H., Verhaagen, J., 1998. Manipulation of gene expression in the mammalian nervous system: application in the study of neurite outgrowth and neuroregeneration-related proteins. Brain Research Reviews. 26**,** 43-71.

Hoogewoud, F., Hamadjida, A., Wyss, A.F., Mir, A., Schwab, M.E., Belhaj-Saif, A., Rouiller, E.M., 2013. Comparison of functional recovery of manual dexterity after unilateral spinal cord lesion or motor cortex lesion in adult macaque monkeys. Frontiers in neurology. 4**,** 101-101.

Hooper, D.C., Morimoto, K., Bette, M., Weihe, E., Koprowski, H., Dietzschold, B., 1998. Collaboration of antibody and inflammation in clearance of rabies virus from the central nervous system. Journal of Virology. 72**,** 3711-3719.

Hopkins, S.J., Rothwell, N.J., 1995. Cytokines and the Nervous-System .1. Expression and recognition. Trends in Neurosciences. 18**,** 83-88.

Horai, R., Asano, M., Sudo, K., Kanuka, H., Suzuki, M., Nishihara, M., Takahashi, M., Iwakura, Y., 1998. Production of mice deficient in genes for interleukin (IL)-1 alpha, IL-1 beta, IL-1 alpha/beta, and IL-1 receptor antagonist shows that IL-1 beta is crucial in turpentine-induced fever development and glucocorticoid secretion. Journal of Experimental Medicine. 187**,** 1463-1475.

Hossain-Ibrahim, M.K., Rezajooi, K., MacNally, J.K., Mason, M.R.J., Lieberman, A.R., Anderson, P.N., 2006. Effects of lipopolysaccharide-induced inflammation on expression of growth-associated genes by corticospinal neurons. Bmc Neuroscience. 7.

Hossain-Ibrahim, M.K., Rezajooi, K., Stallcup, W.B., Lieberman, A.R., Anderson, P.N., 2007. Analysis of axonal regeneration in the central and peripheral nervous systems of the NG2-deficient mouse. Bmc Neuroscience. 8.

Houle, J.D., Jin, Y., 2001. Chronically injured supraspinal neurons exhibit only modest axonal dieback in response to a cervical hemisection lesion. Experimental Neurology. 169**,** 208-217.

Hristova, M., Cuthill, D., Zbarsky, V., Acosta-Saltos, A., Wallace, A., Blight, K., Buckley, S.M.K., Peebles, D., Heuer, H., Waddington, S.N., Raivich, G., 2010. Activation and Deactivation of Periventricular White Matter Phagocytes During Postnatal Mouse Development. Glia. 58**,** 11-28.

Hu, L.Y., Sun, Z.G., Wen, Y.M., Cheng, G.Z., Wang, S.L., Zhao, H.B., Zhang, X.R., 2010. ATP-Mediated Protein Kinase B Akt/Mammalian Target Of Rapamycin mTOR/P70 ribosomal S6 Protein p70S6 Kinase signaling pathway activation promotes improvement of locomotor function after spinal cord injury in rats. Neuroscience. 169**,** 1046-1062.

Hu, P., McLachlan, E.M., 2003. Distinct functional types of macrophage in dorsal root ganglia and spinal nerves proximal to sciatic and spinal nerve transections in the rat. Experimental Neurology. 184**,** 590-605.

Hu, S.X., Sheng, W.S., Peterson, P.K., Chao, C.C., 1995. Cytokine modulation of murine microglial cell Superoxide production. Glia. 13**,** 45-50.

Huang, H.Y., Chen, L., Wang, H.M., Xiu, B., Li, B.C., Wang, R., Zhang, J., Zhang, F., Gu, Z., Li, Y., Song, Y.L., Hao, W., Pang, S.Y., Sun, J.Z., 2003. Influence of patients' age on functional recovery after transplantation of olfactory ensheathing cells into injured spinal cord injury. Chinese Medical Journal. 116**,** 1488-1491.

Huang, X., Kim, J.-M., Kong, T.H., Park, S.R., Ha, Y., Kim, M.H., Park, H., Yoon, S.H., Park, H.C., Park, J.O., Min, B.-H., Choi, B.H., 2009. GM-CSF inhibits glial scar formation and shows long-term protective effect after spinal cord injury. Journal of the Neurological Sciences. 277**,** 87-97.

Hudmon, A., Choi, J.-S., Tyrrell, L., Black, J.A., Rush, A.M., Waxman, S.G., Dib-Hajj, S.D., 2008. Phosphorylation of sodium channel Na(v)1.8 by p38 mitogen-activated protein kinase increases current density in dorsal root ganglion neurons. Journal of Neuroscience. 28**,** 3190-3201.

Hurley, S.D., Walter, S.A., Semple-Rowland, S.L., Streit, W.J., 1999. Cytokine transcripts expressed by microglia in vitro are not expressed by ameboid microglia of the developing rat central nervous system. Glia. 25**,** 304-309.

Hutson, T.H., Verhaagen, J., Yanez-Munoz, R.J., Moon, L.D.F., 2012. Corticospinal tract transduction: a comparison of seven adeno-associated viral vector serotypes and a non-integrating lentiviral vector. Gene Therapy. 19**,** 49-60.

Hynds, D.L., Snow, D.M., 1999. Neurite outgrowth inhibition by chondroitin sulfate proteoglycan: Stalling/stopping exceeds turning in human neuroblastoma growth cones. Experimental Neurology. 160**,** 244-255.

Hynes, R.O., Lander, A.D., 1992. Contact and adhesive specificities in the associations, migrations, and targeting of cells and axons. Cell. 68**,** 303-322.

Ide, C., 1996. Peripheral nerve regeneration. Neuroscience Research. 25**,** 101-121.

Imai, Y., Ibata, I., Ito, D., Ohsawa, K., Kohsaka, S., 1996. A novel gene iba1 in the major histocompatibility complex class III region encoding an EF hand protein expressed in a monocytic lineage. Biochemical and Biophysical Research Communications. 224**,** 855-862.

Inder, T.E., Huppi, P.S., Warfield, S., Kikinis, R., Zientara, G.P., Barnes, P.D., Jolesz, F., Volpe, J.J., 1999. Periventricular white matter injury in the premature infant is followed by reduced cerebral cortical gray matter volume at term. Annals of Neurology. 46**,** 755-760.

Irwin, N., Li, Y.M., O'Toole, J.E., Benowitz, L.I., 2006. Mst3b, a purine-sensitive Ste20-like protein kinase, regulates axon outgrowth. Proceedings of the National Academy of Sciences of the United States of America. 103**,** 18320-18325.

Ito, D., Imai, Y., Ohsawa, K., Nakajima, K., Fukuuchi, Y., Kohsaka, S., 1998. Microglia-specific localisation of a novel calcium binding protein, Iba1. Brain research. Molecular brain research. 57**,** 1-9.

Ito, M., Kudo, M., 1994. Reinnervation by axon collaterals from single facial motoneurons to multiple muscle targets following axotomy in the adult guinea-pig. Acta Anatomica. 151**,** 124-130.

Ito, Y., Sakagami, H., Kondo, H., 1996. Enhanced gene expression for phosphatidylinositol 3-kinase in the hypoglossal motoneurons following axonal crush. Molecular Brain Research. 37**,** 329-332.

Iwanami, A., Kaneko, S., Nakamura, M., Kanemura, Y., Mori, H., Kobayashi, S., Yamasaki, M., Momoshima, S., Ishii, H., Ando, K., Tanioka, Y., Tamaoki,

N., Nomura, T., Toyama, Y., Okano, H., 2005. Transplantation of human neural stem cells for spinal cord injury in primates. Journal of Neuroscience Research. 80**,** 182-190.

Jack, C.S., Arbour, N., Manusow, J., Montgrain, V., Blain, M., McCrea, E., Shapiro, A., Antel, J.P., 2005. TLR signaling tailors innate immune responses in human microglia and astrocytes. Journal of Immunology. 175**,** 4320-4330.

Jacob, J.M., McQuarrie, I.G., 1996. Assembly of microfilaments and microtubules from axonally transported actin and tubulin after axotomy. Journal of Neuroscience Research. 43**,** 412-419.

Jacobowitz, D.M., Cole, J.T., McDaniel, D.P., Pollard, H.B., Watson, W.D., 2012. Microglia activation along the corticospinal tract following traumatic brain injury in the rat: A neuroanatomical study. Brain Research. 1465**,** 80-89.

Jain, A., Brady-Kalnay, S.M., Bellamkonda, R.V., 2004. Modulation of Rho GTPase activity alleviates chondroitin sulfate proteoglycan-dependent inhibition of neurite extension. Journal of Neuroscience Research. 77**,** 299-307.

Jakeman, L.B., Reier, P.J., 1991. Axonal projections between fetal spinal-cord transplants and the adult-rat spinal-cord - a neuroanatomical tracing study of local interactions. Journal of Comparative Neurology. 307**,** 311-334.

Jankowski, M.P., Cornuet, P.K., McIlwrath, S., Koerber, H.R., Albers, K.M., 2006. SRY-box containing gene 11 (Sox11) transcription factor is required for neuron survival and neurite growth. Neuroscience. 143**,** 501-514.

Jankowski, M.P., McIlwrath, S.L., Jing, X., Cornuet, P.K., Salerno, K.M., Koerber, H.R., Albers, K.M., 2009. Sox11 transcription factor modulates peripheral nerve regeneration in adult mice. Brain Research. 1256**,** 43-54.

Janzer, R.C., 1993. The blood-brain-barrier - cellular basis. Journal of Inherited Metabolic Disease. 16**,** 639-647.

Jenkins, R., Hunt, S.P., 1991. Long-term increase in the levels of c-jun messenger-RNA and jun protein-like immunoreactivity in motor and sensory neurons following axon damage. Neuroscience Letters. 129**,** 107-110.

Ji, B., Case, L.C., Liu, K., Shao, Z., Lee, X., Yang, Z., Wang, J., Tian, T., Shulga-Morskaya, S., Scott, M., He, Z., Relton, J.K., Mi, S., 2008. Assessment of functional recovery and axonal sprouting in oligodendrocyte-myelin glycoprotein (OMgp) null mice after spinal cord injury. Molecular and Cellular Neuroscience. 39**,** 258-267.

Jiang, J.G., Zarnegar, R., 1997. A novel transcriptional regulatory region within the core promoter of the hepatocyte growth factor gene is responsible for its inducibility by cytokines via the C/EBP family of transcription factors. Molecular and Cellular Biology. 17**,** 5758-5770.

Jimenez-Diaz, L., Geranton, S.M., Passmore, G.M., Leith, J.L., Fisher, A.S., Berliocchi, L., Sivasubramaniam, A.K., Sheasby, A., Lumb, B.M., Hunt, S.P., 2008. Local Translation in Primary Afferent Fibers Regulates Nociception. Plos One. 3.

Jin, Y., Tessler, A., Fischer, I., Houle, J.D., 2000. Fibroblasts genetically modified to produce BDNF support regrowth of chronically injured serotonergic axons. Neurorehabilitation and Neural Repair. 14**,** 311-317.

Jin, Y., Fischer, I., Tessler, A., Houle, J.D., 2002. Transplants of fibroblasts genetically modified to express BDNF promote axonal regeneration from supraspinal neurons following chronic spinal cord injury. Experimental Neurology. 177**,** 265-275.

Jones, L.L., Kreutzberg, G.W., Raivich, G., 1998. Transforming growth factor beta's 1, 2 and 3 inhibit proliferation of ramified microglia on an astrocyte monolayer. Brain Research. 795**,** 301-306.

Jones, L.L., Liu, Z.Q., Shen, J., Werner, A., Kreutzberg, G.W., Raivich, G., 2000. Regulation of the cell adhesion molecule CD44 after nerve transection and direct trauma to the mouse brain. Journal of Comparative Neurology. 426**,** 468-492.

Josephson, A., Widenfalk, J., Widmer, H.W., Olson, L., Spenger, C., 2001. NOGO mRNA expression in adult and fetal human and rat nervous tissue and in weight drop injury. Experimental Neurology. 169**,** 319-328.

Kadhim, H., Tabarki, B., Verellen, G., De Prez, C., Rona, A.M., Sebire, G., 2001. Inflammatory cytokines in the pathogenesis of periventricular leukomalacia. Neurology. 56**,** 1278-1284.

Kalil, K., Schneider, G.E., 1975. Retrograde cortical and axonal changes following lesions of pyramidal tract. Brain Research. 89**,** 15-27.

Kao, C.C., Chang, L.W., Bloodworth, J.M.B., 1977. Electron-microscopic observations of mechanisms of terminal club formation in transected spinal-cord axons. Journal of Neuropathology and Experimental Neurology. 36**,** 140-156.

Karanth, S., Yang, G., Yeh, J., Richardson, P.M., 2006. Nature of signals that initiate the immune response during Wallerian degeneration of peripheral nerves. Experimental Neurology. 202**,** 161-166.

Karimi-Abdolrezaee, S., Eftekharpour, E., Wang, J., Morshead, C.M., Fehlings, M.G., 2006. Delayed transplantation of adult neural precursor cells promotes remyelination and functional neurological recovery after spinal cord injury. Journal of Neuroscience. 26**,** 3377-3389.

Keirstead, H.S., Nistor, G., Bernal, G., Totoiu, M., Cloutier, F., Sharp, K., Steward, O., 2005. Human embryonic stem cell-derived oligodendrocyte progenitor cell transplants remyelinate and restore locomotion after spinal cord injury. Journal of Neuroscience. 25**,** 4694-4705.

Kempf, A., Schwab, M.E., 2013. Nogo-A Represses Anatomical and Synaptic Plasticity in the Central Nervous System. Physiology. 28**,** 151-163.

Kendall, G.S., Hirstova, M., Horn, S., Dafou, D., Acosta-Saltos, A., Almolda, B., Zbarsky, V., Rumajogee, P., Heuer, H., Castellano, B., Pfeffer, K., Nedospasov, S.A., Peebles, D.M., Raivich, G., 2011. TNF gene cluster deletion abolishes lipopolysaccharide-mediated sensitization of the neonatal brain to hypoxic ischemic insult. Laboratory Investigation. 91**,** 328-341.

Kenney, A.M., Kocsis, J.D., 1998. Peripheral axotomy induces long-term c-Jun amino-terminal kinase-1 activation and activator protein-1 binding activity by c-Jun and junD in adult rat dorsal root ganglia in vivo. Journal of Neuroscience. 18**,** 1318-1328.

Kerschensteiner, M., Schwab, M.E., Lichtman, J.W., Misgeld, T., 2005. In vivo imaging of axonal degeneration and regeneration in the injured spinal cord. Nature Medicine. 11**,** 572-577.

Kershman, J., 1939. Genesis of microglia in the human brain. Archives of Neurology and Psychiatry. 42**,** 24-50.

Khajah, M., Millen, B., Cara, D.C., Waterhouse, C., McCafferty, D.M., 2011. Granulocyte-macrophage colony-stimulating factor (GM-CSF): a chemoattractive agent for murine leukocytes in vivo. Journal of Leukocyte Biology. 89**,** 945-953.

Kiefer, R., Lindholm, D., Kreutzberg, G.W., 1993. Interleukin-6 and transforming Growth-Factor-Beta-1 messenger-RNAs are induced in rat facial nucleus following motoneuron axotomy. European Journal of Neuroscience. 5**,** 775-781.

Kim, J.E., Li, S.X., GrandPre, T., Qiu, D., Strittmatter, S.M., 2003. Axon regeneration in young adult mice lacking Nogo-A/B. Neuron. 38**,** 187-199.

Kim, Y.M., Brinkmann, M.M., Paquet, M.E., Ploegh, H.L., 2008. UNC93B1 delivers nucleotide-sensing toll-like receptors to endolysosomes. Nature. 452**,** 234-U80.

Kirsch, M., Terheggen, U., Hofmann, H.D., 2003. Ciliary neurotrophic factor is an early lesion-induced retrograde signal for axotomized facial motoneurons. Molecular and Cellular Neuroscience. 24**,** 130-138.

Kitamura, Y., Taniguchi, T., Kimura, H., Nomura, Y., Gebicke-Haerter, P.J., 2000. Interleukin-4-inhibited mRNA expression in mixed rat glial and in isolated microglial cultures. Journal of Neuroimmunology. 106**,** 95-104.

Klein, M.A., Frigg, R., Flechsig, E., Raeber, A.J., Kalinke, U., Bluethmann, H., Bootz, F., Suter, M., Zinkernagel, R.M., Aguzzi, A., 1997a. A crucial role for B cells in neuroinvasive scrapie. Nature. 390**,** 687-690.

Klein, M.A., Moller, J.C., Jones, L.L., Bluethmann, H., Kreutzberg, G.W., Raivich, G., 1997b. Impaired neuroglial activation in interleukin-6 deficient mice. Glia. 19**,** 227-233.

Kloss, C.U.A., Kreutzberg, G.W., Raivich, G., 1997. Proliferation of ramified microglia on an astrocyte monolayer: Characterization of stimulatory and inhibitory cytokines. Journal of Neuroscience Research. 49**,** 248-254.

Kloss, C.U.A., Werner, A., Klein, M.A., Shen, J., Menuz, K., Probst, C., Kreutzberg, G.W., Raivich, G., 1999. Integrin family of cell adhesion molecules in the injured brain: Regulation and cellular localization in the normal and regenerating mouse facial motor nucleus. Journal of Comparative Neurology. 411**,** 162-178.

Kneubuhl, J., Steward, O., 2008. Spinal cord injury does not lead to extensive degeneration of corticospinal tract axons in the medullary pyramid. Society for Neuroscience Abstract Viewer and Itinerary Planner. 38.

Knox, C.J., Hohman, M.H., Kleiss, I.J., Weinberg, J.S., Heaton, J.T., Hadlock, T.A., 2013. Facial nerve repair: Fibrin Adhesive Coaptation versus Epineurial Suture Repair in a Rodent Model. Laryngoscope. 123**,** 1618-1621.

Koda, M., Okada, S., Nakayama, T., Koshizuka, S., Kamada, T., Nishio, Y., Someya, Y., Yoshinaga, K., Okawa, A., Moriya, H., Yamazaki, M., 2005. Hematopoietic stem cell and marrow stromal cell for spinal cord injury in mice. Neuroreport. 16**,** 1763-1767.

Kong, T., Choi, J.-K., Park, H., Choi, B.H., Snyder, B.J., Bukhari, S., Kim, N.-K., Huang, X., Park, S.R., Park, H.C., Ha, Y., 2009. Reduction in programmed cell death and improvement in functional outcome of transient focal cerebral ischemia after administration of granulocyte-macrophage colony-stimulating factor in rats. Journal of Neurosurgery. 111**,** 155-163.

Kosel, S., Egensperger, R., Bise, K., Arbogast, S., Mehraein, P., Graeber, M.B., 1997. Long-lasting perivascular accumulation of major histocompatibility complex class II positive lipophages in the spinal cord of stroke patients:

possible relevance for the immune privilege of the brain. Acta Neuropathologica. 94**,** 532-538.

Koshizuka, S., Okada, S., Okawa, A., Koda, M., Murasawa, M., Hashimoto, M., Kamada, T., Yoshinaga, K., Murakami, M., Moriya, H., Yamazaki, M., 2004. Transplanted hematopoietic stem cells from bone marrow differentiate into neural lineage cells and promote functional recovery after spinal cord injury in mice. Journal of Neuropathology and Experimental Neurology. 63**,** 64-72.

Kostovic, I., Rakic, P., 1990. Developmental history of the transient subplate zone in the visual and somatosensory cortex of the macaque monkey and human brain. Journal of Comparative Neurology. 297**,** 441-470.

Kreutzberg, G.W., Graeber, M.B., Streit, W.J., 1989. Neuron - glial relationship during regeneration of motor-neurons. Metabolic Brain Disease. 4**,** 81-85.

Kreutzberg, G.W., 1995. Reaction of the neuronal cell body to axonal damage. In The Axon: Structure, function and pathophysiology. Oxford University Press.

Kreutzberg, G.W., 1996. Microglia: A sensor for pathological events in the CNS. Trends in Neurosciences. 19**,** 312-318.

Krikorian, J.G., Guth, L., Donati, E.J., 1981. Origin of the connective-tissue scar in the transected rat spinal-cord. Experimental Neurology. 72**,** 698-707.

Kruger, R.R., Aurandt, J., Guan, K.L., 2005. Semaphorins command cells to move. Nature Reviews Molecular Cell Biology. 6**,** 789-800.

Kuang, R.Z., Kalil, K., 1990. Branching patterns of corticospinal axon arbors in the rodent. Journal of Comparative Neurology. 292**,** 585-598.

Kubota, T., Okumura, A., Hayakawa, F., Kato, T., Itomi, K., Kuno, K., Watanabe, K., 2002. Combination of neonatal electroencephalography and ultrasonography: sensitive means of early diagnosis of periventricular leukomalacia. Brain & Development. 24**,** 698-702.

Kullander, K., Croll, S.D., Zimmer, M., Pan, L., McClain, J., Hughes, V., Zabski, S., DeChiara, T.M., Klein, R., Yancopoulos, G.D., Gale, N.W., 2001. Ephrin-B3 is the midline barrier that prevents corticospinal tract axons from recrossing, allowing for unilateral motor control. Genes & Development. 15**,** 877-888.

Kullander, K., Klein, R., 2002. Mechanisms and functions of EPH and ephrin signalling. Nature Reviews Molecular Cell Biology. 3**,** 475-486.

Kumaratilake, L.M., Ferrante, A., Jaeger, T., Rzepczyk, C., 1996. GM-CSF-induced priming of human neutrophils for enhanced phagocytosis and

killing of asexual blood stages of Plasmodium falciparum: Synergistic effects of GM-CSF and TNF. Parasite Immunology. 18**,** 115-123.

Kunkel-Bagden, E., Schnell, L., Dai, H.N., Gao, D., Schwab, M.E., Bregman, B.S., 1993. Does the regrowth of injured corticospinal fibers elicited by antibodies to neurite growth inhibitors lead to recovery of motor function? Society for Neuroscience Abstracts. 19**,** 681-681.

Kurkowska-Jastrzebska, I., Wronska, A., Kohutnicka, M., Czlonkowski, A., Czlonkowska, A., 1999. Inflammatory reaction following 1-methyl-4-phenyl-1,2,3,6-tetrahydropyridine intoxication in mouse. Experimental Neurology. 156**,** 50-61.

Kwon, B.K., Liu, J., Messerer, C., Kobayashi, N.R., McGraw, J., Oschipok, L., Tetzlaff, W., 2002. Survival and regeneration of rubrospinal neurons 1 year after spinal cord injury. Proceedings of the National Academy of Sciences of the United States of America. 99**,** 3246-3251.

Lalancette-Hebert, M., Gowing, G., Simard, A., Weng, Y.C., Kriz, J., 2007. Selective ablation of proliferating microglial cells exacerbates ischemic injury in the brain. Journal of Neuroscience. 27**,** 2596-2605.

Lang, R.A., Metcalf, D., Cuthbertson, R.A., Lyons, I., Stanley, E., Kelso, A., Kannourakis, G., Williamson, D.J., Klintworth, G.K., Gonda, T.J., Dunn, A.R., 1987. Transgenic mice expressing a hematopoietic growth-factor gene (GM-CSF) develop accumulations of macrophages, blindness, and a fatal syndrome of tissue-damage. Cell. 51**,** 675-686.

Lassmann, H., Ammerer, H.P., Kulnig, W., 1978. Ultrastructural sequence of myelin degradation .1. Wallerian degeneration in rat optic-nerve. Acta Neuropathologica. 44**,** 91-102.

Laywell, E.D., Dorries, U., Bartsch, U., Faissner, A., Schachner, M., Steindler, D.A., 1992. Enhanced expression of the developmentally regulated extracellular-matrix molecule Tenascin following adult brain injury. Proceedings of the National Academy of Sciences of the United States of America. 89**,** 2634-2638.

Lechpammer, M., Manning, S.M., Samonte, F., Nelligan, J., Sabo, E., Talos, D.M., Volpe, J.J., Jensen, F.E., 2008. Minocycline treatment following hypoxic/ischaemic injury attenuates white matter injury in a rodent model of periventricular leucomalacia. Neuropathology and Applied Neurobiology. 34**,** 379-393.

Ledeboer, A., Breve, J.J.P., Poole, S., Tilders, F.J.H., Van Dam, A.M., 2000. Interleukin-10, interleukin-4, and transforming growth factor-beta differentially regulate lipopolysaccharide-induced production of pro-inflammatory cytokines and nitric oxide in co-cultures of rat astroglial and microglial cells. Glia. 30**,** 134-142.

Lee, J.K., Geoffroy, C.G., Chan, A.F., Tolentino, K.E., Crawford, M.J., Leal, M.A., Kang, B., Zheng, B., 2010. Assessing Spinal Axon Regeneration and Sprouting in Nogo-, MAG-, and OMgp-Deficient Mice. Neuron. 66**,** 663-670.

Lee, N., Neitzel, K.L., Devlin, B.K., MacLennan, A.J., 2004a. STAT3 phosphorylation in injured axons before sensory and motor neuron nuclei: Potential role for STAT3 as a retrograde signaling transcription factor. Journal of Comparative Neurology. 474**,** 535-545.

Lee, S.C., Liu, W., Brosnan, C.F., Dickson, D.W., 1994. GM-CSF promotes proliferation of human fetal and adult microglia in primary cultures. Glia. 12**,** 309-318.

Lee, S.M., Yune, T.Y., Kim, S.J., Park, D.W., Lee, Y.K., Kim, Y.C., Oh, Y.J., Markelonis, G.J., Oh, T.H., 2003. Minocycline reduces cell death and improves functional recovery after traumatic spinal cord injury in the rat. Journal of Neurotrauma. 20**,** 1017-1027.

Lee, Y.B., Nagai, A., Kim, S.U., 2002a. Cytokines, chemokines, and cytokine receptors in human microglia. Journal of Neuroscience Research. 69**,** 94-103.

Lee, Y.S., Hsiao, I., Lin, V.W., 2002b. Peripheral nerve grafts and aFGF restore partial hindlimb function in adult paraplegic rats. Journal of Neurotrauma. 19**,** 1203-1216.

Lee, Y.S., Lin, C.Y., Robertson, R.T., Hsiao, I., Lin, V.W., 2004b. Motor recovery and anatomical evidence of axonal regrowth in spinal cord-repaired adult rats. Journal of Neuropathology and Experimental Neurology. 63**,** 233-245.

Legacy, J., Hanea, S., Theoret, J., Smith, P.D., 2013. Granulocyte macrophage colony-stimulating factor promotes regeneration of retinal ganglion cells in vitro through a mammalian target of rapamycin-dependent mechanism. Journal of Neuroscience Research. 91**,** 771-779.

Lehnardt, S., Lachance, C., Patrizi, S., Lefebvre, S., Follett, P.L., Jensen, F.E., Rosenberg, P.A., Volpe, J.J., Vartanian, T., 2002. The toll-like receptor TLR4 is necessary for lipopolysaccharide-induced oligodendrocyte injury in the CNS. Journal of Neuroscience. 22**,** 2478-2486.

Leinster, V.H.L., Joy, M.T., Vuononvirta, R.E., Bolsover, S.R., Anderson, P.N., 2013. ErbB1 epidermal growth factor receptor is a valid target for reducing the effects of multiple inhibitors of axonal regeneration. Experimental Neurology. 239**,** 82-90.

Leon, S., Yin, Y.Q., Nguyen, J., Irwin, N., Benowitz, L.I., 2000. Lens injury stimulates axon regeneration in the mature rat optic nerve. Journal of Neuroscience. 20**,** 4615-4626.

Leong, S.K., Ling, E.A., 1992. Ameboid and ramified microglia - their interrelationship and response to brain injury. Glia. 6**,** 39-47.

Leong, S.K., Ling, E.A., Fan, D.P., 1995. Glial reaction after pyramidotomy in mice and rats. Neurodegeneration. 4**,** 403-413.

Levi, A.D.O., Dancausse, H., Li, X.M., Duncan, S., Horkey, L., Oliviera, M., 2002. Peripheral nerve grafts promoting central nervous system regeneration after spinal cord injury in the primate. Journal of Neurosurgery. 96**,** 197-205.

Leviton, A., Paneth, N., 1990. White matter damage in preterm newborns - an epidemiologic perspective. Early Human Development. 24**,** 1-22.

Li, W.W.Y., Yew, D.T.W., Chuah, M.I., Leung, P.C., Tsang, D.S.C., 1994. Axonal sprouting in the hemisected adult-rat spinal-cord. Neuroscience. 61**,** 133-139.

Li, Y., Raisman, G., 1995. Sprouts from cut corticospinal axons persist in the presence of astrocytic scarring in long-term lesions of the adult-rat spinal-cord. Experimental Neurology. 134**,** 102-111.

Li, Y., Field, P.M., Raisman, G., 1997. Repair of adult rat corticospinal tract by transplants of olfactory ensheathing cells. Science. 277**,** 2000-2002.

Li, Y., Decherchi, P., Raisman, G., 2003. Transplantation of olfactory ensheathing cells into spinal cord lesions restores breathing and climbing. Journal of Neuroscience. 23**,** 727-731.

Lieberman, A.R., 1971. The axon reaction: a review of the principal features of perikaryal responses to axon injury. International review of neurobiology. 14**,** 49-124.

Liebscher, T., Schnell, L., Schnell, D., Scholl, J., Schneider, R., Gullo, M., Fouad, K., Mir, A., Rausch, M., Kindler, D., Hamers, F.P.T., Schwab, M.E., 2005. Nogo-A antibody improves regeneration and locomotion of spinal cord-injured rats. Annals of Neurology. 58**,** 706-719.

Lin, L., Chan, S.O., 2003. Perturbation of CD44 function affects chiasmatic routing of retinal axons in brain slice preparations of the mouse retinofugal pathway. European Journal of Neuroscience. 17**,** 2299-2312.

Linda, H., Risling, M., Cullheim, S., 1985. Dendraxons in regenerating motoneurons in the cat - do dendrites generate new axons after central axotomy. Brain Research. 358**,** 329-333.

Lindholm, D., Heumann, R., Meyer, M., Thoenen, H., 1987. Interleukin-1 regulates synthesis of nerve growth-factor in nonneuronal cells of rat sciatic-nerve. Nature. 330**,** 658-659.

Lindholm, T., Skold, M.K., Suneson, A., Carlstedt, T., Cullheim, S., Risling, M., 2004. Semaphorin and neuropilin expression in motoneurons after intraspinal motoneuron axotomy. Neuroreport. 15**,** 649-654.

Lindwall, C., Dahlin, L., Lundborg, G., Kanje, M., 2004. Inhibition of c-Jun phosphorylation reduces axonal outgrowth of adult rat nodose ganglia and dorsal root ganglia sensory neurons. Molecular and Cellular Neuroscience. 27**,** 267-279.

Lindwall, C., Kanje, M., 2005. Retrograde axonal transport of JNK signaling molecules influence injury induced nuclear changes in p-c-Jun and ATF3 in adult rat sensory neurons. Molecular and Cellular Neuroscience. 29**,** 269-282.

Lips, K., Stichel, C.C., Muller, H.W., 1995. Restricted appearance of tenascin and chondroitin sulfate proteoglycans after transection and sprouting of adult-rat postcommissural fornix. Journal of Neurocytology. 24**,** 449-464.

Liu, B.P., Strittmatter, S.M., 2001. Semaphorin-mediated axonal guidance via Rho-related G proteins. Current Opinion in Cell Biology. 13**,** 619-626.

Liu, K., Lu, Y., Lee, J.K., Samara, R., Willenberg, R., Sears-Kraxberger, I., Tedeschi, A., Park, K.K., Jin, D., Cai, B., Xu, B., Connolly, L., Steward, O., Zheng, B., He, Z., 2010. PTEN deletion enhances the regenerative ability of adult corticospinal neurons. Nature Neuroscience. 13**,** 1075-U64.

Liu, L., Persson, J.K.E., Svensson, M., Aldskogius, H., 1998. Glial cell responses, complement, and clusterin in the central nervous system following dorsal root transection. Glia. 23**,** 221-238.

Liu, X.H., Kato, H., Nakata, N., Kogure, K., Kato, K., 1993. AN immunohistochemical study of copper-zinc Superoxide-Dismutase and manganese Superoxide-Dismutase in rat hippocampus after transient cerebral-ischemia. Brain Research. 625**,** 29-37.

Liu, Y., Kim, D.H., Himes, B.T., Chow, S.Y., Schallert, T., Murray, M., Tessler, A., Fischer, I., 1999. Transplants of fibroblasts genetically modified to express BDNF promote regeneration of adult rat rubrospinal axons and recovery of forelimb function. Journal of Neuroscience. 19**,** 4370-4387.

Liva, S.M., Kahn, M.A., Dopp, J.M., de Vellis, J., 1999. Signal transduction pathways induced by GM-CSF in microglia: Significance in the control of proliferation. Glia. 26**,** 344-352.

Loddick, S.A., Wong, M.L., Bongiorno, P.B., Gold, P.W., Licinio, J., Rothwell, N.J., 1997. Endogenous interleukin-1 receptor antagonist is neuroprotective. Biochemical and Biophysical Research Communications. 234**,** 211-215.

Long-Smith, C.M., Collins, L., Toulouse, A., Sullivan, A.M., Nolan, Y.M., 2010. Interleukin-1 beta contributes to dopaminergic neuronal death induced by lipopolysaccharide-stimulated rat glia in vitro. Journal of Neuroimmunology. 226**,** 20-26.

Lorber, B., Howe, M.L., Benowitz, L.I., Irwin, N., 2009. Mst3b, an Ste20-like kinase, regulates axon regeneration in mature CNS and PNS pathways. Nature Neuroscience. 12**,** 1407-1414.

Lu, J., Feron, F., Ho, S.H., Mackay-Sim, A., Waite, P.M.E., 2001a. Transplantation of nasal olfactory tissue promotes partial recovery in paraplegic adult rats. Brain Research. 889**,** 344-357.

Lu, P., Blesch, A., Tuszynski, M.H., 2001b. Neurotrophism without neurotropism: BDNF promotes survival but not growth of lesioned corticospinal neurons. Journal of Comparative Neurology. 436**,** 456-470.

Lu, X., Richardson, P.M., 1991. Inflammation near the nerve-cell body enhances axonal regeneration. Journal of Neuroscience. 11**,** 972-978.

Lu, X., Richardson, P.M., 1993. Responses of macrophages in rat dorsal-root ganglia following peripheral-nerve injury. Journal of Neurocytology. 22**,** 334-341.

Lu, X., Richardson, P.M., 1995. Changes in neuronal messenger-rnas induced by a local inflammatory reaction. Journal of Neuroscience Research. 41**,** 8-14.

Luo, L.Q., O'Leary, D.D.M., 2005. Axon retraction and degeneration in development and disease. Annual Review of Neuroscience. 28**,** 127-156.

Luskin, M.B., Shatz, C.J., 1985. Studies of the earliest generated cells of the cats visual-cortex - cogeneration of subplate and marginal zones. Journal of Neuroscience. 5**,** 1062-1075.

Ma, W., Bisby, M.A., 1998. Increased activation of nuclear factor kappa B in rat lumbar dorsal root ganglion neurons following partial sciatic nerve injuries. Brain Research. 797**,** 243-254.

Mackinnon, S.E., Dellon, A.L., Obrien, J.P., 1991. Changes in nerve-fiber numbers distal to a nerve repair in the rat sciatic-nerve model. Muscle & Nerve. 14**,** 1116-1122.

Madsen, P.W., Yezierski, R.P., Holets, V.R., 1994. Syringomyelia - clinical observations and experimental studies. Journal of Neurotrauma. 11**,** 241-254.

Magill, C.K., Tong, A., Kawamura, D., Hayashi, A., Hunter, D.A., Parsadanian, A., Mackinnon, S.E., Myckatyn, T.M., 2007. Reinnervation of the tibialis anterior following sciatic nerve crush injury: A confocal microscopic study in transgenic mice. Experimental Neurology. 207**,** 64-74.

Makwana, M., Raivich, G., 2005. Molecular mechanisms in successful peripheral regeneration. Febs Journal. 272**,** 2628-2638.

Makwana, M., Jones, L.L., Cuthill, D., Heuer, H., Bohatschek, M., Hristova, M., Friedrichsen, S., Ormsby, I., Bueringer, D., Koppius, A., Bauer, K., Doetschman, T., Raivich, G., 2007. Endogenous transforming growth factor beta 1 suppresses inflammation and promotes survival in adult CNS. Journal of Neuroscience. 27**,** 11201-11213.

Makwana, M., Serchov, T., Hristova, M., Bohatschek, M., Gschwendtner, A., Kalla, R., Liu, Z., Heumann, R., Raivich, G., 2009. Regulation and function of neuronal GTP-Ras in facial motor nerve regeneration. Journal of Neurochemistry. 108**,** 1453-1463.

Makwana, M., Werner, A., Acosta-Saltos, A., Gonitel, R., Pararajasingham, A., Ruff, C., Rumajogee, P., Cuthill, D., Galiano, M., Bohatschek, M., Wallace, A.S., Anderson, P.N., Mayer, U., Behrens, A., Raivich, G., 2010. Peripheral Facial Nerve Axotomy in Mice Causes Sprouting of Motor Axons Into Perineuronal Central White Matter: Time Course and Molecular Characterization. Journal of Comparative Neurology. 518**,** 699-721.

Malipiero, U.V., Frei, K., Fontana, A., 1990. Production of hematopoietic colony-stimulating factors by astrocytes. Journal of Immunology. 144**,** 3816-3821.

Mangano, E.N., Peters, S., Litteljohn, D., So, R., Bethune, C., Bobyn, J., Clarke, M., Hayley, S., 2011. Granulocyte macrophage-colony stimulating factor protects against substantia nigra dopaminergic cell loss in an environmental toxin model of Parkinson's disease. Neurobiology of Disease. 43**,** 99-112.

Martin, M.R., Lodge, D., 1977. Morphology of facial nucleus of rat. Brain Research. 123**,** 1-12.

Martinez, F.O., Sica, A., Mantovani, A., Locati, M., 2008. Macrophage activation and polarization. Frontiers in Bioscience-Landmark. 13**,** 453-461.

Martini, R., Schachner, M., 1988. Immunoelectron microscopic localization of neural cell-adhesion molecules (L1, N-Cam, and Myelin-Associated Glycoprotein) in regenerating adult-mouse sciatic-nerve. Journal of Cell Biology. 106**,** 1735-1746.

Mason, M.R.J., Lieberman, A.R., Grenningloh, G., Anderson, P.N., 2002. Transcriptional upregulation of SCG10 and CAP-23 is correlated with regeneration of the axons of peripheral and central neurons in vivo. Molecular and Cellular Neuroscience. 20**,** 595-615.

Mason, M.R.J., Lieberman, A.R., Anderson, P.N., 2003. Corticospinal neurons up-regulate a range of growth-associated genes following intracortical, but not spinal, axotomy. European Journal of Neuroscience. 18**,** 789-802.

Matsui, T., Motoki, Y., Yoshida, Y., 2013. Hypothermia Reduces Toll-Like Receptor 3-Activated Microglial Interferon-beta and Nitric Oxide Production. Mediators of Inflammation. 7.

Mausberg, A.K., Jander, S., Reichmann, G., 2009. Intracerebral Granulocyte-Macrophage Colony-Stimulating Factor Induces Functionally Competent Dendritic Cells in the Mouse Brain. Glia. 57**,** 1341-1350.

Maxwell, W.L., Follows, R., Ashhurst, D.E., Berry, M., 1990. The response of the cerebral hemisphere of the rat to injury .1. The mature rat. Philosophical Transactions of the Royal Society of London Series B-Biological Sciences. 328**,** 479.

McBride, R.L., Feringa, E.R., Garver, M.K., Williams, J.K., 1989. Prelabeled red nucleus and sensorimotor cortex neurons of the rat survive 10 and 20 weeks after spinal-cord transection. Journal of Neuropathology and Experimental Neurology. 48**,** 568-576.

McBride, R.L., Livingston, V.C., Harper, W.B., Feringa, E.R., 1991. Comparison of retrograde fluorogold and horseradish-peroxidase labeling of corticospinal neurons after spinal-cord transection. Journal of Neuropathology and Experimental Neurology. 50**,** 331-331.

McClellan, A.D., 1994. Functional regeneration and restoration of locomotor-activity following spinal-cord transection in the lamprey. In Neural Regeneration. Progress in Brain Research, Vol. 103, F.J. Seil, pp. 203-217.

McCord, J.M., 1987. Oxygen-derived radicals - a link between reperfusion injury and inflammation. Federation Proceedings. 46**,** 2402-2406.

McDonald, J.W., Liu, X.Z., Qu, Y., Liu, S., Mickey, S.K., Turetsky, D., Gottlieb, D.I., Choi, D.W., 1999. Transplanted embryonic stem cells survive, differentiate and promote recovery in injured rat spinal cord. Nature Medicine. 5**,** 1410-1412.

McGeer, P.L., Kawamata, T., Walker, D.G., Akiyama, H., Tooyama, I., McGeer, E.G., 1993. Microglia in degenerative neurological disease. Glia. 7**,** 84-92.

McGill, J.L., Nonnecke, B.J., Lippolis, J.D., Reinhardt, T.A., Sacco, R.E., 2013. Differential chemokine and cytokine production by neonatal bovine gamma delta T-cell subsets in response to viral toll-like receptor agonists and in vivo respiratory syncytial virus infection. Immunology. 139**,** 227-244.

McKenna, J.E., Whishaw, I.Q., 1999. Complete compensation in skilled reaching success with associated impairments in limb synergies, after dorsal column lesion in the rat. Journal of Neuroscience. 19**,** 1885-1894.

McKeon, R.J., Schreiber, R.C., Rudge, J.S., Silver, J., 1991. Reduction of neurite outgrowth in a model of glial scarring following cns injury is correlated with the expression of inhibitory molecules on reactive astrocytes. Journal of Neuroscience. 11**,** 3398-3411.

McKeon, R.J., Hoke, A., Silver, J., 1995. Injury-induced proteoglycans inhibit the potential for laminin-mediated axon growth on astrocytic scars. Experimental Neurology. 136**,** 32-43.

McKerracher, L., David, S., Jackson, D.L., Kottis, V., Dunn, R.J., Braun, P.E., 1994. Identification of myelin-associated glycoprotein as a major myelin-derived inhibitor of neurite growth. Neuron. 13**,** 805-811.

McLaughlin, P., Zhou, Y., Ma, T., Liu, J., Zhang, W., Hong, J.S., Kovacs, M., Zhang, J., 2006. Proteomic analysis of microglial contribution to mouse strain-dependent dopaminergic neurotoxicity. Glia. 53**,** 567-582.

McQualter, J.L., Darwiche, R., Ewing, C., Onuki, M., Kay, T.W., Hamilton, J.A., Reid, H.H., Bernard, C.C.A., 2001. Granulocyte macrophage colony-stimulating factor: A new putative therapeutic target in multiple sclerosis. Journal of Experimental Medicine. 194**,** 873-881.

McQuarrie, I.G., Grafstein, B., Gershon, M.D., 1977. Axonal regeneration in rat sciatic-nerve - effect of a conditioning lesion and of DBCAMP. Brain Research. 132**,** 443-453.

McQuillen, P.S., DeFreitas, M.F., Zada, G., Shatz, C.J., 2002. A novel role for p75NTR in subplate growth cone complexity and visual thalamocortical innervation. Journal of Neuroscience. 22**,** 3580-3593.

McQuillen, P.S., Sheldon, R.A., Shatz, C.J., Ferriero, D.M., 2003. Selective vulnerability of subplate neurons after early neonatal hypoxia-ischemia. Journal of Neuroscience. 23**,** 3308-3315.

McQuillen, P.S., Ferriero, D.M., 2005. Perinatal subplate neuron injury: Implications for cortical development and plasticity. Brain Pathology. 15**,** 250-260.

Means, E.D., Anderson, D.K., Nicolosi, G., Gaudsmith, J., 1978. Micro-vascular perfusion experimental spinal-cord injury. Surgical Neurology. 9**,** 353-360.

Mekada, A., Sasahara, M., Yamada, E., Kani, K., Hazama, F., 1998. Platelet-derived growth factor B-chain expression in the rat retina and optic nerve: distribution and changes after transection of the optic nerve. Vision Research. 38**,** 3031-3039.

Meller, K., 1987. Early structural-changes in the axoplasmic cytoskeleton after axotomy studied by cryofixation. Cell and Tissue Research. 250**,** 663-672.

Melton, L.M., Keith, A.B., Davis, S., Oakley, A.E., Edwardson, J.A., Morris, C.M., 2003. Chronic glial activation, neurodegeneration, and APP immunoreactive deposits following acute administration of double-stranded RNA. Glia. 44**,** 1-12.

Merianda, T.T., Lin, A.C., Lam, J.S.Y., Vuppalanchi, D., Willis, D.E., Karin, N., Holt, C.E., Twiss, J.L., 2009. A functional equivalent of endoplasmic reticulum and Golgi in axons for secretion of locally synthesized proteins. Molecular and Cellular Neuroscience. 40**,** 128-142.

Merline, M., Kalil, K., 1990. Cell-death of corticospinal neurons is induced by axotomy before but not after innervation of spinal targets. Journal of Comparative Neurology. 296**,** 506-516.

Merrill, J.E., Kono, D.H., Clayton, J., Ando, D.G., Hinton, D.R., Hofman, F.M., 1992. Inflammatory leukocytes and cytokines in the peptide-induced disease of Experimental Allergic Encephalomyelitis in SJL and B10.PL mice. Proceedings of the National Academy of Sciences of the United States of America. 89**,** 574-578.

Merson, T.D., Binder, M.D., Kilpatrick, T.J., 2010. Role of Cytokines as Mediators and Regulators of Microglial Activity in Inflammatory Demyelination of the CNS. Neuromolecular Medicine. 12**,** 99-132.

Metcalf, D., Moore, J.G., 1988. Divergent disease patterns in granulocyte macrophage colony-stimulating factor transgenic mice associated with different transgene insertion sites. Proceedings of the National Academy of Sciences of the United States of America. 85**,** 7767-7771.

Metcalf, D., 1989. The molecular control of cell-division, differentiation commitment and maturation in hematopoietic-cells. Nature. 339**,** 27-30.

Metcalf, D., 2008. Hematopoietic cytokines. Blood. 111**,** 485-491.

Metz, G.A., Whishaw, I.Q., 2002. Cortical and subcortical lesions impair skilled walking in the ladder rung walking test: a new task to evaluate fore- and hindlimb stepping, placing, and co-ordination. Journal of Neuroscience Methods. 115**,** 169-179.

Meyer, M., Matsuoka, I., Wetmore, C., Olson, L., Thoenen, H., 1992. Enhanced synthesis of Brain-Derived Neurotrophic Factor in the lesioned peripheral-nerve - different mechanisms are responsible for the regulation of bdnf and ngf messenger-RNA. Journal of Cell Biology. 119**,** 45-54.

Mikule, K., Sunpaweravong, S., Gatlin, J.C., Pfenninger, K.H., 2003. Eicosanoid activation of protein kinase C epsilon - Involvement in growth cone repellent signaling. Journal of Biological Chemistry. 278**,** 21168-21177.

Mills, C.D., Kincaid, K., Alt, J.M., Heilman, M.J., Hill, A.M., 2000. M-1/M-2 macrophages and the Th1/Th2 paradigm. Journal of Immunology. 164**,** 6166-6173.

Miranda, J.D., White, L.A., Marcillo, A.E., Willson, C.A., Jagid, J., Whittemore, S.R., 1999. Induction of Eph B3 after spinal cord injury. Experimental Neurology. 156**,** 218-222.

Mirski, R., Reichert, F., Klar, A., Rotshenker, S., 2003. Granulocyte macrophage colony stimulating factor (GM-CSF) activity is regulated by a GM-CSF binding molecule in Wallerian degeneration following injury to peripheral nerve axons. Journal of Neuroimmunology. 140**,** 88-96.

Mitsui, T., Fischer, I., Shurnsky, J.S., Murray, M., 2005. Transplants of fibroblasts expressing BDNF and NT-3 promote recovery of bladder and hindlimb function following spinal contusion injury in rats. Experimental Neurology. 194**,** 410-431.

Mocchetti, I., Wrathall, J.R., 1995. Neurotrophic factors in Central-Nervous-System trauma. Journal of Neurotrauma. 12**,** 853-870.

Moisse, K., Volkening, K., Leystra-Lantz, C., Welch, I., Hill, T., Strong, M.J., 2009. Divergent patterns of cytosolic TDP-43 and neuronal progranulin expression following axotomy: Implications for TDP-43 in the physiological response to neuronal injury. Brain Research. 1249**,** 202-211.

Moller, J.C., Klein, M.A., Haas, S., Jones, L.L., Kreutzberg, G.W., Raivich, G., 1996. Regulation of thrombospondin in the regenerating mouse facial motor nucleus. Glia. 17**,** 121-132.

Moneta, M.E., Gehrmann, J., Topper, R., Banati, R.B., Kreutzberg, G.W., 1993. Cell-adhesion molecule expression in the regenerating rat facial nucleus. Journal of Neuroimmunology. 45**,** 203-206.

Monier, A., Evrard, P., Gressens, P., Verney, C., 2006. Distribution and differentiation of microglia in the human encephalon during the first two trimesters of gestation. Journal of Comparative Neurology. 499**,** 565-582.

Monier, A., Adle-Biassette, H., Delezoide, A.-L., Evrard, P., Gressens, P., Verney, C., 2007. Entry and distribution of microglial cells in human embryonic and

fetal cerebral cortex. Journal of Neuropathology and Experimental Neurology. 66**,** 372-382.

Monnier, P.P., Sierra, A., Schwab, J.M., Henke-Fahle, S., Mueller, B.K., 2003. The Rho/ROCK pathway mediates neurite growth-inhibitory activity associated with the chondroitin sulfate proteoglycans of the CNS glial scar. Molecular and Cellular Neuroscience. 22**,** 319-330.

Moon, L.D.F., Asher, R.A., Rhodes, K.E., Fawcett, J.W., 2001. Regeneration of CNS axons back to their target following treatment of adult rat brain with chondroitinase ABC. Nature Neuroscience. 4**,** 465-466.

Morris, J.H., Hudson, A.R., Weddell, G., 1972. Study of degeneration and regeneration in divided rat sciatic nerve based on electron-microscopy .2. Development of regenerating unit. Zeitschrift Fur Zellforschung Und Mikroskopische Anatomie. 124**,** 103.

Morrow, D.R., Campbell, G., Lieberman, A.R., Anderson, P.N., 1993. Differential regenerative growth of CNS axons into tibial and peroneal nerve grafts in the thalamus of adult-rats. Experimental Neurology. 120**,** 60-69.

Mukhopadhyay, G., Doherty, P., Walsh, F.S., Crocker, P.R., Filbin, M.T., 1994. A novel role for myelin-associated glycoprotein as an inhibitor of axonal regeneration. Neuron. 13**,** 757-767.

Murashov, A.K., Haq, I.U., Hill, C., Park, E., Smith, M., Wang, X., Wang, X.Y., Goldberg, D.J., Wolgemuth, D.J., 2001. Crosstalk between p38, Hsp25 and Akt in spinal motor neurons after sciatic nerve injury. Molecular Brain Research. 93**,** 199-208.

Nadeau, S., Hein, P., Fernandes, K.J.L., Peterson, A.C., Miller, F.D., 2005. A transcriptional role for C/EBP beta in the neuronal response to axonal injury. Molecular and Cellular Neuroscience. 29**,** 525-535.

Nagy, J.I., Price, M.L., Staines, W.A., Lynn, B.D., Granholm, A.C., 1998. The hyaluronan receptor RHAMM in noradrenergic fibers contributes to axon growth capacity of locus coeruleus neurons in an intraocular transplant model. Neuroscience. 86**,** 241-255.

Nansen, A., Christensen, J.P., Ropke, C., Marker, O., Scheynius, A., Thomsen, A.R., 1998. Role of interferon-gamma in the pathogenesis of LCMV-induced meningitis: unimpaired leucocyte recruitment, but deficient macrophage activation in interferon-gamma knock-out mice. Journal of Neuroimmunology. 86**,** 202-212.

Naveilhan, P., ElShamy, V.M., Emfors, P., 1997. Differential regulation of mRNAs for GDNF and its receptors Ret and GDNFR alpha after sciatic nerve lesion in the mouse. European Journal of Neuroscience. 9**,** 1450-1460.

Neal, J.W., Singhrao, S.K., Jasani, B., Newman, G.R., 1996. Immunocytochemically detectable metallothionein is expressed by astrocytes in the ischaemic human brain. Neuropathology and Applied Neurobiology. 22**,** 243-247.

Nedergaard, M., Ransom, B., Goldman, S.A., 2003. New roles for astrocytes: Redefining the functional architecture of the brain. Trends in Neurosciences. 26**,** 523-530.

Neher, J.J., Neniskyte, U., Zhao, J.-W., Bal-Price, A., Tolkovsky, A.M., Brown, G.C., 2011. Inhibition of Microglial Phagocytosis Is Sufficient To Prevent Inflammatory Neuronal Death. Journal of Immunology. 186**,** 4973-4983.

Neher, J.J., Emmrich, J.V., Fricker, M., Mander, P.K., Thery, C., Brown, G.C., 2013. Phagocytosis executes delayed neuronal death after focal brain ischemia. Proceedings of the National Academy of Sciences of the United States of America. 110**,** E4098-E4107.

Neniskyte, U., Neher, J.J., Brown, G.C., 2011. Neuronal Death Induced by Nanomolar Amyloid beta Is Mediated by Primary Phagocytosis of Neurons by Microglia. Journal of Biological Chemistry. 286**,** 39904-39913.

Neniskyte, U., Brown, G.C., 2013. Lactadherin/MFG-E8 is essential for microglia-mediated neuronal loss and phagoptosis induced by amyloid beta. Journal of Neurochemistry. 126**,** 312-317.

Neumann, H., Kotter, M.R., Franklin, R.J.M., 2009. Debris clearance by microglia: an essential link between degeneration and regeneration. Brain. 132**,** 288-295.

Neumann, S., Woolf, C.J., 1999. Regeneration of dorsal column fibers into and beyond the lesion site following adult spinal cord injury. Neuron. 23**,** 83-91.

Nguyen, Q.T., Sanes, J.R., Lichtman, J.W., 2002. Pre-existing pathways promote precise projection patterns. Nature Neuroscience. 5**,** 861-867.

Niederost, B., Oertle, T., Fritsche, J., McKinney, R.A., Bandtlow, C.E., 2002. Nogo-A and myelin-associated glycoprotein mediate neurite growth inhibition by antagonistic regulation of RhoA and Rac1. Journal of Neuroscience. 22**,** 10368-10376.

Nikulina, E., Tidwell, J.L., Dai, H.N., Bregman, B.S., Filbin, M.T., 2004. The phosphodiesterase inhibitor rolipram delivered after a spinal cord lesion promotes axonal regeneration and functional recovery. Proceedings of the National Academy of Sciences of the United States of America. 101**,** 8786-8790.

Nimmerjahn, A., Kirchhoff, F., Helmchen, F., 2005. Resting microglial cells are highly dynamic surveillants of brain parenchyma in vivo. Science. 308**,** 1314-1318.

Nimmervoll, B., White, R., Yang, J.-W., An, S., Henn, C., Sun, J.-J., Luhmann, H.J., 2013. LPS-Induced Microglial Secretion of TNF alpha Increases Activity-Dependent Neuronal Apoptosis in the Neonatal Cerebral Cortex. Cerebral Cortex. 23**,** 1742-1755.

Nurse, C.A., Macintyre, L., Diamond, J., 1984. Reinnervation of the rat touch dome restores the merkel cell-population reduced after denervation. Neuroscience. 13**,** 563-571.

Obrien, M.F., Lenke, L.G., Lou, J., Bridwell, K.H., Joyce, M.E., 1994. Astrocyte response and transforming growth-factor-beta localization in acute spinal-cord injury. Spine. 19**,** 2321-2330.

Ogawa, Y., Sawamoto, K., Miyata, T., Miyao, S., Watanabe, M., Nakamura, M., Bregman, B.S., Koike, M., Uchiyama, Y., Toyama, Y., Okano, H., 2002. Transplantation of in vitro-expanded fetal neural progenitor cells results in neurogenesis and functional recovery after spinal cord contusion injury in adult rats. Journal of Neuroscience Research. 69**,** 925-933.

Olson, J.K., Miller, S.D., 2004. Microglia initiate central nervous system innate and adaptive immune responses through multiple TLRs. Journal of Immunology. 173**,** 3916-3924.

Oltvai, Z.N., Milliman, C.L., Korsmeyer, S.J., 1993. BCL-2 heterodimerizes in-vivo with a conserved homolog, bax, that accelerates programmed cell-death. Cell. 74**,** 609-619.

Ono, K., Suzuki, H., Sawada, M., 2010. Delayed neural damage is induced by iNOS-expressing microglia in a brain injury model. Neuroscience Letters. 473**,** 146-150.

Oudega, M., Rosano, C., Sadi, D., Wood, P.M., Schwab, M.E., Hagg, T., 2000. Neutralizing antibodies against neurite growth inhibitor NI-35/250 do not promote regeneration of sensory axons in the adult rat spinal cord. Neuroscience. 100**,** 873-883.

Owada, Y., Utsunomiya, A., Yoshimoto, T., Kondo, H., 1997. Expression of mRNA for Akt, serine-threonine protein kinase, in the brain during development and its transient enhancement following axotomy of hypoglossal nerve. Journal of Molecular Neuroscience. 9**,** 27-33.

Pallini, R., Fernandez, E., Sbriccoli, A., 1988. Retrograde degeneration of corticospinal axons following transection of the spinal-cord in rats - a quantitative study with anterogradely transported horseradish-peroxidase. Journal of Neurosurgery. 68**,** 124-128.

Panegyres, P.K., Hughes, J., 1998. The neuroprotective effects of the recombinant interleukin-1 receptor antagonist rhIL-1ra after excitotoxic stimulation with kainic acid and its relationship to the amyloid precursor protein gene. Journal of the Neurological Sciences. 154**,** 123-132.

Pang, Y., Cai, Z., Rhodes, P.G., 2003. Disturbance of oligodendrocyte development, hypomyelination and white matter injury in the neonatal rat brain after intracerebral injection of lipopolysaccharide. Brain research. Developmental brain research. 140**,** 205-14.

Papez, J.W., 1927. Subdivisions of the facial nucleus. Journal of Comparative Neurology. 43**,** 159-191.

Park, C., Lee, S., Cho, I.H., Lee, H.K., Kim, D., Choi, S.Y., Oh, S.B., Park, K., Kim, J.S., Lee, S.J., 2006. TLR3-mediated signal induces proinflammatory cytokine and chemokine gene expression in astrocytes: Differential signaling mechanisms of TLR3-induced IP-10 and IL-8 gene expression. Glia. 53**,** 248-256.

Park, K.K., Liu, K., Hu, Y., Smith, P.D., Wang, C., Cai, B., Xu, B., Connolly, L., Kramvis, I., Sahin, M., He, Z., 2008. Promoting Axon Regeneration in the Adult CNS by Modulation of the PTEN/mTOR Pathway. Science. 322**,** 963-966.

Pasquale, E.B., 2005. EPH receptor signalling casts a wide net on cell behaviour. Nature Reviews Molecular Cell Biology. 6**,** 462-475.

Pasquale-Styles, M., Marcillo, A., Norenberg, M.D., 2003. Retrograde degeneration of the corticospinal tract in human spinal cord injury. Journal of Neuropathology and Experimental Neurology. 62**,** 568-568.

Pasterkamp, R.J., Verhaagen, J., 2001. Emerging roles for semaphorins in neural regeneration. Brain Research Reviews. 35**,** 36-54.

Pasterkarnp, R.J., Verhaagen, J., 2006. Semaphorins in axon regeneration: developmental guidance molecules gone wrong? Philosophical Transactions of the Royal Society B-Biological Sciences. 361**,** 1499-1511.

Patodia, S., Raivich, G., 2012a. Role of transcription factors in peripheral nerve regeneration. Frontiers in molecular neuroscience. 5**,** 8-8.

Patodia, S., Raivich, G., 2012b. Downstream effector molecules in successful peripheral nerve regeneration. Cell and Tissue Research. 349**,** 15-26.

Patro, I.K., Amit, Shrivastava, M., Bhumika, S., Patro, N., 2010. Poly I:C induced microglial activation impairs motor activity in adult rats. Indian Journal of Experimental Biology. 48**,** 104-109.

Patro, N., Singh, K., Patro, I., 2013. Differential microglial and astrocytic response to bacterial and viral infection in the developing hippocampus of neonatal rats. Indian Journal of Experimental Biology. 51**,** 606-614.

Pattison, M.J., MacKenzie, K.F., Elcombe, S.E., Arthur, J.S.C., 2013. IFN beta autocrine feedback is required to sustain TLR induced production of MCP-1 in macrophages. Febs Letters. 587**,** 1496-1503.

Pearse, D.D., Marcillo, A.E., Oudega, M., Lynch, M.P., Wood, P.M., Bunge, M.B., 2004a. Transplantation of Schwann cells and olfactory ensheathing glia after spinal cord injury: Does pretreatment with methylprednisolone and interleukin-10 enhance recovery? Journal of Neurotrauma. 21**,** 1223-1239.

Pearse, D.D., Pereira, F.C., Marcillo, A.E., Bates, M.L., Berrocal, Y.A., Filbin, M.T., Bunge, M.B., 2004b. cAMP and Schwann cells promote axonal growth and functional recovery after spinal cord injury. Nature Medicine. 10**,** 610-616.

Peebles, D.M., Miller, S., Newman, J.P., Scott, R., Hanson, M.A., 2003. The effect of systemic administration of lipopolysaccharide on cerebral haemodynamics and oxygenation in the 0.65 gestation ovine fetus in utero. Bjog-an International Journal of Obstetrics and Gynaecology. 110**,** 735-743.

Peeva, G.P., Angelova, S.K., Guntinas-Lichius, O., Streppel, M., Irintchev, A., Schuetz, U., Popratiloff, A., Savaskan, N.E., Braeuer, A.U., Alvanou, A., Nitsch, R., Angelov, D.N., 2006. Improved outcome of facial nerve repair in rats is associated with enhanced regenerative response of motoneurons and augmented neocortical plasticity. European Journal of Neuroscience. 24**,** 2152-2162.

Pekny, M., Stanness, K.A., Eliasson, C., Betsholtz, C., Janigro, D., 1998. Impaired induction of blood-brain barrier properties in aortic endothelial cells by astrocytes from GFAP-deficient mice. Glia. 22**,** 390-400.

Peltier, D.C., Simms, A., Farmer, J.R., Miller, D.J., 2010. Human Neuronal Cells Possess Functional Cytoplasmic and TLR-Mediated Innate Immune Pathways Influenced by Phosphatidylinositol-3 Kinase Signaling. Journal of Immunology. 184**,** 7010-7021.

Perlson, E., Hanz, S., Ben-Yaakov, K., Segal-Ruder, Y., Seger, R., Fainzilber, M., 2005. Vimentin-dependent spatial translocation of an activated MAP kinase in injured nerve. Neuron. 45**,** 715-726.

Pernet, V., Schwab, M.E., 2012. The role of Nogo-A in axonal plasticity, regrowth and repair. Cell and Tissue Research. 349**,** 97-104.

Perry, R.B.-T., Doron-Mandel, E., Iavnilovitch, E., Rishal, I., Dagan, S.Y., Tsoory, M., Coppola, G., McDonald, M.K., Gomes, C., Geschwind, D.H., Twiss,

J.L., Yaron, A., Fainzilber, M., 2012. Subcellular Knockout of Importin beta 1 Perturbs Axonal Retrograde Signaling. Neuron. 75**,** 294-305.

Perry, V.H., Gordon, S., 1987. Modulation of cd4 antigen on macrophages and microglia in rat-brain. Journal of Experimental Medicine. 166**,** 1138-1143.

Perry, V.H., Brown, M.C., 1992. Role of macrophages in peripheral-nerve degeneration and repair. Bioessays. 14**,** 401-406.

Perry, V.H., Andersson, P.B., Gordon, S., 1993. Macrophages and inflammation in the central-nervous-system. Trends in Neurosciences. 16**,** 268-273.

Phillips, M.J., Needham, M., Weller, R.O., 1997. Role of cervical lymph nodes in autoimmune encephalomyelitis in the Lewis rat. Journal of Pathology. 182**,** 457-464.

Plant, G.W., Christensen, C.L., Oudega, M., Bunge, M.B., 2003. Delayed transplantation of olfactory ensheathing glia promotes sparing/regeneration of supraspinal axons in the contused adult rat spinal cord. Journal of Neurotrauma. 20**,** 1-16.

Pleasure, D., Soulika, A., Singh, S.K., Gallo, V., Bannerman, P., 2006. Inflammation in white matter: Clinical and pathophysiological aspects. Mental Retardation and Developmental Disabilities Research Reviews. 12**,** 141-146.

Poggi, S.H., Park, J., Toso, L., Abebe, D., Roberson, R., Woodard, J.E., Spong, C.Y., 2005. No phenotype associated with established lipopolysaccharide model for cerebral palsy. American Journal of Obstetrics and Gynecology. 192**,** 727-733.

Pollock, G., Pennypacker, K.R., Memet, S., Israel, A., Saporta, S., 2005. Activation of NF-kappa B in the mouse spinal cord following sciatic nerve transection. Experimental Brain Research. 165**,** 470-477.

Ponomarev, E.D., Shriver, L.P., Maresz, K., Pedras-Vasconcelos, J., Verthelyi, D., Dittel, B.N., 2007. GM-CSF production by autoreactive T cells is required for the activation of microglial cells and the onset of experimental autoimmune encephalomyelitis. Journal of Immunology. 178**,** 39-48.

Popovich, P.G., Streit, W.J., Stokes, B.T., 1993. Differential expression of MHC Class-II antigen in the contused rat spinal-cord. Journal of Neurotrauma. 10**,** 37-46.

Popovich, P.G., Wei, P., Stokes, B.T., 1997. Cellular inflammatory response after spinal cord injury in Sprague-Dawley and Lewis rats. Journal of Comparative Neurology. 377**,** 443-464.

Popovich, P.G., Guan, Z., Wei, P., Huitinga, I., van Rooijen, N., Stokes, B.T., 1999. Depletion of hematogenous macrophages promotes partial hindlimb recovery and neuroanatomical repair after experimental spinal cord injury. Experimental Neurology. 158**,** 351-365.

Popovich, P.G., Guan, Z., McGaughy, V., Fisher, L., Hickey, W.F., Basso, D.M., 2002. The neuropathological and behavioral consequences of intraspinal microglial/macrophage activation. Journal of Neuropathology and Experimental Neurology. 61**,** 623-633.

Pratt, L., Ni, L., Ponzio, N.M., Jonakait, G.M., 2013. Maternal inflammation promotes fetal microglial activation and increased cholinergic expression in the fetal basal forebrain: role of interleukin-6. Pediatric Research. 74**,** 393-401.

Prekeris, R., Klumperman, J., Chen, Y.A., Scheller, R.H., 1998. Syntaxin 13 mediates cycling of plasma membrane proteins via tubulovesicular recycling endosomes. Journal of Cell Biology. 143**,** 957-971.

Price, D.J., Aslam, S., Tasker, L., Gillies, K., 1997. Fates of the earliest generated cells in the developing murine neocortex. Journal of Comparative Neurology. 377**,** 414-422.

Prinz, M., Mildner, A., 2011. Microglia in the CNS: Immigrants from Another World. Glia. 59**,** 177-187.

Qin, Q.Y., Baudry, M., Liao, G.H., Noniyev, A., Galeano, J., Bi, X.N., 2009. A Novel Function for p53: Regulation of Growth Cone Motility through Interaction with Rho Kinase. Journal of Neuroscience. 29**,** 5183-5192.

Quelle, F.W., Sato, N., Witthuhn, B.S., Inhorn, R.C., Eder, M., Miyajima, A., Griffin, J.D., Ihle, J.N., 1994. JAK2 associates with the Beta(c) chain of the receptor far Granulocyte-Macrophage Colony-Stimulating Factor, and its activation requires the membrane-proximal region. Molecular and Cellular Biology. 14**,** 4335-4341.

Quinta, H.R., Pasquini, J.M., Rabinovich, G.A., Pasquini, L.A., 2014. Glycan-dependent binding of galectin-1 to neuropilin-1 promotes axonal regeneration after spinal cord injury. Cell Death and Differentiation. 21**,** 941-955.

Rahim, A.A., Wong, A.M.S., Howe, S.J., Buckley, S.M.K., Acosta-Saltos, A.D., Elston, K.E., Ward, N.J., Philpott, N.J., Cooper, J.D., Anderson, P.N., Waddington, S.N., Thrasher, A.J., Raivich, G., 2009. Efficient gene delivery to the adult and fetal CNS using pseudotyped non-integrating lentiviral vectors. Gene Therapy. 16**,** 509-520.

Raivich, G., Gehrmann, J., Kreutzberg, G.W., 1991a. Increase of Macrophage Colony-Stimulating Factor and Granulocyte-Macrophage Colony-

Stimulating Factor receptors in the regenerating rat facial nucleus. Journal of Neuroscience Research. 30**,** 682-686.

Raivich, G., Hellweg, R., Kreutzberg, G.W., 1991b. NGF receptor mediated reduction in axonal ngf uptake and retrograde transport following sciatic-nerve injury and during regeneration. Neuron. 7**,** 151-164.

Raivich, G., Gehrmann, J., Graeber, M.B., Kreutzberg, G.W., 1993. Quantitative immunohistochemistry in the rat facial nucleus with i-125 iodinated secondary antibodies and insitu autoradiography - nonlinear binding characteristics of primary monoclonal and polyclonal antibodies. Journal of Histochemistry & Cytochemistry. 41**,** 579-592.

Raivich, G., Morenoflores, M.T., Moller, J.C., Kreutzberg, G.W., 1994. Inhibition of posttraumatic microglial proliferation in a genetic model of Macrophage-Colony-Stimulating Factor deficiency in the mouse. European Journal of Neuroscience. 6**,** 1615-1618.

Raivich, G., Bluethmann, H., Kreutzberg, G.W., 1996. Signaling molecules and neuroglial activation in the injured central nervous system. Keio Journal of Medicine. 45**,** 239-247.

Raivich, G., Haas, S., Werner, A., Klein, M.A., Kloss, C., Kreutzberg, G.W., 1998a. Regulation of MCSF receptors on microglia in the normal and injured mouse central nervous system: A quantitative immunofluorescence study using confocal laser microscopy. Journal of Comparative Neurology. 395**,** 342-358.

Raivich, G., Jones, L.L., Kloss, C.U.A., Werner, A., Neumann, H., Kreutzberg, G.W., 1998b. Immune surveillance in the injured nervous system: T-Lymphocytes invade the axotomized mouse facial motor nucleus and aggregate around sites of neuronal degeneration. Journal of Neuroscience. 18**,** 5804-5816.

Raivich, G., Bohatschek, M., Kloss, C.U.A., Werner, A., Jones, L.L., Kreutzberg, G.W., 1999. Neuroglial activation repertoire in the injured brain: graded response, molecular mechanisms and cues to physiological function. Brain Research Reviews. 30**,** 77-105.

Raivich, G., Liu, Z.Q., Kloss, C.U.A., Labow, M., Bluethmann, H., Bohatschek, M., 2002. Cytotoxic potential of proinflammatory cytokines: combined deletion of TNF receptors TNFR1 and TNFR2 prevents motoneuron cell death after facial axotomy in adult mouse. Experimental Neurology. 178**,** 186-193.

Raivich, G., Bohatschek, M., Da Costa, C., Iwata, O., Galiano, M., Hristova, M., Nateri, A.S., Makwana, M., Riera-Sans, L., Wolfer, D.P., Lipp, H.P., Aguzzi, A., Wagner, E.F., Behrens, A., 2004. The AP-1 transcription factor c-jun is required for efficient axonal regeneration. Neuron. 43**,** 57-67.

Raivich, G., Makwana, M., 2007. The making of successful axonal regeneration: Genes, molecules and signal transduction pathways. Brain Research Reviews. 53**,** 287-311.

Raivich, G., 2011. Transcribing the path to neurological recovery-From early signals through transcription factors to downstream effectors of successful regeneration. Annals of Anatomy-Anatomischer Anzeiger. 193**,** 248-258.

Ramer, L.M., Au, E., Richter, M.W., Liu, J., Tetzlaff, W., Roskams, A.J., 2004. Peripheral olfactory ensheathing cells reduce scar and cavity formation and promote regeneration after spinal cord injury. Journal of Comparative Neurology. 473**,** 1-15.

Ramirez, L.F., Kalil, K., 1985. Critical stages for growth in the development of cortical-neurons. Journal of Comparative Neurology. 237**,** 506-518.

Ramon-Cueto, A., Cordero, M.I., Santos-Benito, F.F., Avila, J., 2000. Functional recovery of paraplegic rats and motor axon regeneration in their spinal cords by olfactory ensheathing glia. Neuron. 25**,** 425-435.

RamonyCajal, 1928. Degeneration and Regeneration of the Nervous System. Vol., Hafner Publishing Co, New York.

Ransohoff, R.M., Perry, V.H., 2009. Microglial Physiology: Unique Stimuli, Specialized Responses. Annual Review of Immunology. 27**,** 119-145.

Rapalino, O., Lazarov-Spiegler, O., Agranov, E., Velan, G.J., Yoles, E., Fraidakis, M., Solomon, A., Gepstein, R., Katz, A., Belkin, M., Hadani, M., Schwartz, M., 1998. Implantation of stimulated homologous macrophages results in partial recovery of paraplegic rats. Nature Medicine. 4**,** 814-821.

Rappolee, D.A., Werb, Z., 1992. Macrophage-derived growth factors. Current topics in microbiology and immunology. 181**,** 87-140.

Re, F.B., Belyanskaya, S.L., Riese, R.J., Cipriani, B., Fischer, F.R., Granucci, F., Ricciardi-Castagnoli, P., Brosman, C., Stern, L.J., Strominger, J.L., Santambrogio, L., 2002. Granulocyte-macrophage colony-stimulating factor induces an expression program in neonatal microglia that primes them for antigen presentation. Journal of Immunology. 169**,** 2264-2273.

Reddy, P.H., Manczak, M., Zhao, W., Nakamura, K., Bebbington, C., Yarranton, G., Mao, P., 2009. Granulocyte-macrophage colony-stimulating factor antibody suppresses microglial activity: implications for anti-inflammatory effects in Alzheimer's Disease and multiple sclerosis. Journal of Neurochemistry. 111**,** 1514-1528.

Reier, P.J., Houle, J.D., 1988. The glial scar: its bearing on axonal elongation and transplantation approaches to CNS repair. Advances in neurology. 47**,** 87-138.

Reier, P.J., Stokes, B.T., Thompson, F.J., Anderson, D.K., 1992. Fetal cell grafts into resection and contusion compression injuries of the rat and cat spinal-cord. Experimental Neurology. 115**,** 177-188.

Relton, J.K., Rothwell, N.J., 1992. Interleukin-1 receptor antagonist inhibits ischemic and excitotoxic neuronal damage in the rat
. Brain Research Bulletin. 29**,** 243-246.

Ren, Z., Chen, X., Yang, J., Kress, B.T., Tong, J., Liu, H., Takano, T., Zhao, Y., Nedergaard, M., 2013. Improved axonal regeneration after spinal cord injury in mice with conditional deletion of ephrin B2 under the GFAP promoter. Neuroscience. 241**,** 89-99.

Rezaie, P., Male, D., 1999. Colonisation of the developing human brain and spinal cord by microglia: A review. Microscopy Research and Technique. 45**,** 359-382.

Rezaie, P., Dean, A., 2002. Periventricular leukomalacia, inflammation and white matter lesions within the developing nervous system. Neuropathology. 22**,** 106-132.

Richardson, P.M., McGuinness, U.M., Aguayo, A.J., 1980. Axons from cns neurons regenerate into pns grafts. Nature. 284**,** 264-265.

Richardson, P.M., McGuinness, U.M., Aguayo, A.J., 1982. Peripheral-nerve autografts to the rat spinal-cord - studies with axonal tracing methods. Brain Research. 237**,** 147-162.

Richardson, P.M., Issa, V.M.K., 1984. Peripheral injury enhances central regeneration of primary sensory neurons. Nature. 309**,** 791-793.

Richardson, P.M., Issa, V.M.K., Aguayo, A.J., 1984. Regeneration of long spinal axons in the rat. Journal of Neurocytology. 13**,** 165-182.

Richardson, P.M., Verge, V.M.K., 1987. Axonal regeneration in dorsal spinal roots is accelerated by peripheral axonal transection. Brain Research. 411**,** 406-408.

Richmond, F.J.R., Gladdy, R., Creasy, J.L., Kitamura, S., Smits, E., Thomson, D.B., 1994. Efficacy of 7 retrograde tracers, compared in multiple-labeling studies of feline motoneurons. Journal of Neuroscience Methods. 53**,** 35-46.

Riddell, J.S., Enriquez-Denton, M., Toft, A., Fairless, R., Barnett, S.C., 2004. Olfactory ensheathing cell grafts have minimal influence on regeneration at the dorsal root entry zone following rhizotomy. Glia. 47**,** 150-167.

Ridet, J.L., Malhotra, S.K., Privat, A., Gage, F.H., 1997. Reactive astrocytes: cellular and molecular cues to biological function. Trends in Neurosciences. 20**,** 570-577.

Rishal, I., Fainzilber, M., 2010. Retrograde signaling in axonal regeneration. Experimental Neurology. 223**,** 5-10.

Risling, M., Fried, K., Linda, H., Cullheim, S., Meier, M., 1992. Changes in nerve growth-factor receptor-like immunoreactivity in the spinal-cord after ventral funiculus lesion in adult cats. Journal of Neurocytology. 21**,** 79-93.

Robey, E., Allison, J.P., 1995. T-cell activation - integration of signals from the antigen receptor and costimulatory molecules. Immunology Today. 16**,** 306-310.

Robinson, G.A., 1996. Changes in the expression of transcription factors ATF-2 and Fra-2 after axotomy and during regeneration in rat retinal ganglion cells. Molecular Brain Research. 41**,** 57-64.

Romero, R., Avila, C., Santhanam, U., Sehgal, P.B., 1990. Amniotic-fluid interleukin-6 in preterm labor - association with infection. Journal of Clinical Investigation. 85**,** 1392-1400.

Roth, P., Stanley, E.R., 1992. The biology of CSF-1 and its receptor. Current topics in microbiology and immunology. 181**,** 141-67.

Rozwarski, D.A., Diederichs, K., Hecht, R., Boone, T., Karplus, P.A., 1996. Refined crystal structure and mutagenesis of human granulocyte-macrophage colony-stimulating factor. Proteins-Structure Function and Genetics. 26**,** 304-313.

Rubartelli, A., Lotze, M.T., 2007. Inside, outside, upside down: damage-associated molecular-pattern molecules (DAMPs) and redox. Trends in Immunology. 28**,** 429-436.

Rubio, N., Sierra, A., 1993. Interleukin-6 production by brain-tissue and cultured astrocytes infected with theilers murine encephalomyelitis virus. Glia. 9**,** 41-47.

Ruff, C.A., Staak, N., Patodia, S., Kaswich, M., Rocha-Ferreira, E., Da Costa, C., Brecht, S., Makwana, M., Fontana, X., Hristova, M., Rumajogee, P., Galiano, M., Bohatschek, M., Herdegen, T., Behrens, A., Raivich, G., 2012. Neuronal c-Jun is required for successful axonal regeneration, but the effects of phosphorylation of its N-terminus are moderate. Journal of Neurochemistry. 121**,** 607-618.

Ruitenberg, M.J., Levison, D.B., Lee, S.V., Verhaagen, J., Harvey, A.R., Plant, G.W., 2005. NT-3 expression from engineered olfactory ensheathing glia promotes spinal sparing and regeneration. Brain. 128**,** 839-853.

Rutschman, R., Lang, R., Hesse, M., Ihle, J.N., Wynn, T.A., Murray, P.J., 2001. Cutting edge: Stat6-dependent substrate depletion regulates nitric oxide production. Journal of Immunology. 166**,** 2173-2177.

Saliba, E., Marret, S., 2001. Cerebral white matter damage in the preterm infant: pathophysiology and risk factors. Seminars in neonatology : SN. 6**,** 121-33.

Sallerfors, B., 1994. Endogenous production and peripheral-blood levels of Granulocyte-Macrophage (GM) and Granulocyte (G) Colony-Stimulating Factors. Leukemia & Lymphoma. 13**,** 235-247.

Sawada, M., Kondo, N., Suzumura, A., Marunouchi, T., 1989. Production of Tumor Necrosis Factor-alpha by microglia and astrocytes in culture. Brain Research. 491**,** 394-397.

Sawada, M., Suzumura, A., Yamamoto, H., Marunouchi, T., 1990. Activation and proliferation of the isolated microglia by Colony Stimulating Factor-I and possible involvement of Protein Kinase-C. Brain Research. 509**,** 119-124.

Schaebitz, W.-R., Krueger, C., Pitzer, C., Weber, D., Laage, R., Gassler, N., Aronowski, J., Mier, W., Kirsch, F., Dittgen, T., Bach, A., Sommer, C., Schneider, A., 2008. A neuroprotective function for the hematopoietic protein granulocyte-macrophage colony stimulating factor (GM-CSF). Journal of Cerebral Blood Flow and Metabolism. 28**,** 29-43.

Schallenberg, M., Charalambous, P., Thanos, S., 2012. GM-CSF protects rat photoreceptors from death by activating the SRC-dependent signalling and elevating anti-apoptotic factors and neurotrophins. Graefes Archive for Clinical and Experimental Ophthalmology. 250**,** 699-712.

Schermer, C., Humpel, C., 2002. Granulocyte macrophage-colony stimulating factor activates microglia in rat cortex organotypic brain slices. Neuroscience Letters. 328**,** 180-184.

Schluter, D., Kaefer, N., Hof, H., Wiestler, O.D., DeckertSchluter, M., 1997. Expression pattern and cellular origin of cytokines in the normal and Toxoplasma gondii-infected murine brain. American Journal of Pathology. 150**,** 1021-1035.

Schluter, D., Bertsch, D., Frei, K., Hubers, S.B., Wiestler, O.D., Hof, H., Fontana, A., Deckert-Schluter, M., 1998. Interferon-gamma antagonizes transforming growth factor-beta(2)-mediated immunosuppression in murine Toxoplasma encephalitis. Journal of Neuroimmunology. 81**,** 38-48.

Schmidtmayer, J., Jacobsen, C., Miksch, G., Sievers, J., 1994. Blood monocytes and spleen macrophages differentiate into microglia-like cells on monolayers of astrocytes - membrane currents. Glia. 12**,** 259-267.

Schmitt, A.B., Brook, G.A., Buss, A., Nacimiento, W., Noth, J., Kreutzberg, G.W., 1998. Dynamics of microglial activation in the spinal cord after cerebral infarction are revealed by expression of MHC class II antigen. Neuropathology and Applied Neurobiology. 24**,** 167-176.

Schnell, L., Schwab, M.E., 1990. Axonal regeneration in the rat spinal-cord produced by an antibody against myelin-associated neurite growth-inhibitors. Nature. 343**,** 269-272.

Schnell, L., Schwab, M.E., 1993. Sprouting and regeneration of lesioned corticospinal tract fibers in the adult-rat spinal-cord. European Journal of Neuroscience. 5**,** 1156-1171.

Schroeter, M., Zickler, P., Denhardt, D.T., Hartung, H.P., Jander, S., 2006. Increased thalamic neurodegeneration following ischaemic cortical stroke in osteopontin-deficient mice. Brain. 129**,** 1426-1437.

Schuettauf, F., Zurakowski, D., Quinto, K., Varde, M.A., Besch, D., Laties, A., Anderson, R., Wen, R., 2005. Neuroprotective effects of cardiotrophin-like cytokine on retinal ganglion cells. Graefes Archive for Clinical and Experimental Ophthalmology. 243**,** 1036-1042.

Schwab, J.M., Brechtel, K., Mueller, C.A., Failli, V., Kaps, H.P., Tuli, S.K., Schluesener, H.J., 2006. Experimental strategies to promote spinal cord regeneration - an integrative perspective. Progress in Neurobiology. 78**,** 91-116.

Schwaiger, F.W., Hager, G., Schmitt, A.B., Horvat, A., Streif, R., Spitzer, C., Gamal, S., Breuer, S., Brook, G.A., Nacimiento, W., Kreutzberg, G.W., 2000. Peripheral but not central axotomy induces changes in Janus kinases (JAK) and signal transducers and activators of transcription (STAT). European Journal of Neuroscience. 12**,** 1165-1176.

Schwartz, J.P., Nishiyama, N., 1994. Neurotrophic factor gene-expression in astrocytes during development and following injury. Brain Research Bulletin. 35**,** 403-407.

Schwartz, M., Butovsky, O., Bruck, W., Hanisch, U.K., 2006. Microglial phenotype: is the commitment reversible? Trends in Neurosciences. 29**,** 68-74.

Schweigreiter, R., Walmsley, A.R., Niederost, B., Zimmermann, D.R., Oertle, T., Casademunt, E., Frentzel, S., Dechant, G., Mir, A., Bandtlow, C.E., 2004. Versican V2 and the central inhibitory domain of Nogo-A inhibit neurite

growth via p75(NTR)/NgR-independent pathways that converge at RhoA. Molecular and Cellular Neuroscience. 27**,** 163-174.

Scumpia, P.O., Kelly, S.M., Reeves, W.H., Stevens, B.R., 2005. Double-stranded RNA signals antiviral and inflammatory programs and dysfunctional glutamate transport in TLR3-expressing astrocytes. Glia. 52**,** 153-162.

Seif, G.I., Nomura, H., Tator, C.H., 2007. Retrograde axonal degeneration ("Dieback") in the corticospinal tract after transection injury of the rat spinal cord: A Confocal Microscopy study. Journal of Neurotrauma. 24**,** 1513-1528.

Seijffers, R., Allchorne, A.J., Woolf, C.J., 2006. The transcription factor ATF-3 promotes neurite outgrowth. Molecular and Cellular Neuroscience. 32**,** 143-154.

Seilhean, D., Kobayashi, K., He, Y., Uchihara, T., Rosenblum, O., Katlama, C., Bricaire, F., Duyckaerts, C., Hauw, J.J., 1997. Tumor necrosis factor-alpha, microglia and astrocytes in AIDS dementia complex. Acta Neuropathologica. 93**,** 508-517.

Semba, K., Egger, M.D., 1986. The facial motor-nerve of the rat - control of vibrissal movement and examination of motor and sensory components. Journal of Comparative Neurology. 247**,** 144-158.

Sendtner, M., Dittrich, F., Hughes, R.A., Thoenen, H., 1994. Actions of cntf and neurotrophins on degenerating motoneurons - preclinical studies and clinical implications. Journal of the Neurological Sciences. 124**,** 77-83.

Sendtner, M., Gotz, R., Holtmann, B., Thoenen, H., 1997. Endogenous ciliary neurotrophic factor is a lesion factor for axotomized motoneurons in adult mice. Journal of Neuroscience. 17**,** 6999-7006.

Shapiro, L., Love, J., Colman, D.R., 2007. Adhesion molecules in the nervous system: Structural insights into function and diversity. In Annual Review of Neuroscience. Annual Review of Neuroscience, Vol. 30, ed.^eds., pp. 451-474.

Sheng, J.G., Mrak, R.E., Griffin, W.S.T., 1997. Glial-neuronal interactions in Alzheimer disease: Progressive association of IL-1 alpha(+) microglia and S100 beta(+) astrocytes with neurofibrillary tangle stages. Journal of Neuropathology and Experimental Neurology. 56**,** 285-290.

Shepherd, G.M.G., Harris, K.M., 1998. Three-dimensional structure and composition of CA3 - CA1 axons in rat hippocampal slices: Implications for presynaptic connectivity and compartmentalization. Journal of Neuroscience. 18**,** 8300-8310.

Shi, Y.F., Liu, C.H., Roberts, A.I., Das, J.T., Xu, G.W., Ren, G.W., Zhang, Y.Y., Zhang, L.Y., Yuan, Z.R., Tan, H.S.W., Das, G.H., Devadas, S., 2006. Granulocyte-macrophage colony-stimulating factor (GM-CSF) and T-cell responses: what we do and don't know. Cell Research. 16**,** 126-133.

Shibayama, M., Kuchiwaki, H., Inao, S., Yoshida, K., Ito, M., 1996. Intercellular adhesion molecule-1 expression on glia following brain injury: Participation of interleukin-1 beta. Journal of Neurotrauma. 13**,** 801-808.

Shihabuddin, L.S., Horner, P.J., Ray, J., Gage, F.H., 2000. Adult spinal cord stem cells generate neurons after transplantation in the adult dentate gyrus. Journal of Neuroscience. 20**,** 8727-8735.

Shokouhi, B.N., Wong, B.Z.Y., Siddiqui, S., Lieberman, A.R., Campbell, G., Tohyama, K., Anderson, P.N., 2010. Microglial responses around intrinsic CNS neurons are correlated with axonal regeneration. Bmc Neuroscience. 11**,** 15.

Sierra, A., Abiega, O., Shahraz, A., Neumann, H., 2013. Janus-faced microglia: beneficial and detrimental consequences of microglial phagocytosis. Frontiers in Cellular Neuroscience. 7.

Silbereis, J.C., Huang, E.J., Back, S.A., Rowitch, D.H., 2010. Towards improved animal models of neonatal white matter injury associated with cerebral palsy. Disease Models & Mechanisms. 3**,** 678-688.

Silver, R.M., Edwin, S.S., Trautman, M.S., Simmons, D.L., Branch, D.W., Dudley, D.J., Mitchell, M.D., 1995. Bacterial lipopolysaccharide-mediated fetal death - production of a newly recognized form of inducible cyclooxygenase (cox-2) in murine decidua in response to lipopolysaccharide. Journal of Clinical Investigation. 95**,** 725-731.

Singh, A., Balasubramanian, S., Murray, M., Lemay, M., Houle, J., 2011. Role of Spared Pathways in Locomotor Recovery after Body-Weight-Supported Treadmill Training in Contused Rats. Journal of Neurotrauma. 28**,** 2405-2416.

Sinis, N., Horn, F., Genchev, B., Skouras, E., Merkel, D., Angelova, S.K., Kaidoglou, K., Michael, J., Pavlov, S., Igelmund, P., Schaller, H.-E., Irintchev, A., Dunlop, S.A., Angelov, D.N., 2009. Electrical stimulation of paralyzed vibrissal muscles reduces endplate reinnervation and does not promote motor recovery after facial nerve repair in rats. Annals of Anatomy-Anatomischer Anzeiger. 191**,** 356-370.

Sivron, T., Schwartz, M., 1995. Glial-cell types, lineages, and response to injury in rat and fish - implications for regeneration. Glia. 13**,** 157-165.

Smith, G.M., Hale, J.H., 1997. Macrophage/microglia regulation of astrocytic tenascin: Synergistic action of transforming growth factor-beta and basic fibroblast growth factor. Journal of Neuroscience. 17**,** 9624-9633.

Smiththomas, L.C., Fokseang, J., Stevens, J., Du, J.S., Muir, E., Faissner, A., Geller, H.M., Rogers, J.H., Fawcett, J.W., 1994. An inhibitor of neurite outgrowth produced by astrocytes. Journal of Cell Science. 107**,** 1687-1695.

Snow, D.M., Lemmon, V., Carrino, D.A., Caplan, A.I., Silver, J., 1990. Sulfated proteoglycans in astroglial barriers inhibit neurite outgrowth invitro. Experimental Neurology. 109**,** 111-130.

Song, H.J., Ming, G.L., Poo, M.M., 1997. CAMP-induced switching in turning direction of nerve growth cones. Nature. 388**,** 275-279.

Spira, M.E., Oren, R., Dormann, A., Gitler, A.D., 2003. Critical calpain-dependent ultrastructural alterations underlie the transformation of an axonal segment into a growth cone after axotomy of cultured Aplysia neurons. Journal of Comparative Neurology. 457**,** 293-312.

Stammers, A.T., Liu, J., Kwon, B.K., 2012. Expression of Inflammatory Cytokines Following Acute Spinal Cord Injury in a Rodent Model. Journal of Neuroscience Research. 90**,** 782-790.

Stanley, E., Lieschke, G.J., Grail, D., Metcalf, D., Hodgson, G., Gall, J.A.M., Maher, D.W., Cebon, J., Sinickas, V., Dunn, A.R., 1994. Granulocyte/Macrophage Colony-Stimulating Factor-deficient mice show no major perturbation of hematopoiesis but develop a characteristic pulmonary pathology. Proceedings of the National Academy of Sciences of the United States of America. 91**,** 5592-5596.

Steelman, A.J., Li, J., 2011. Poly(I:C) promotes TNF alpha/TNFR1-dependent oligodendrocyte death in mixed glial cultures. Journal of Neuroinflammation. 8.

Stichel, C.C., Hermanns, S., Luhmann, H.J., Lausberg, F., Niermann, H., D'Urso, D., Servos, G., Hartwig, H.G., Muller, H.W., 1999. Inhibition of collagen IV deposition promotes regeneration of injured CNS axons. European Journal of Neuroscience. 11**,** 632-646.

Stirling, D.P., Khodarahmi, K., Liu, J., McPhail, L.T., McBride, C.B., Steeves, J.D., Ramer, M.S., Tetzlaff, W., 2004. Minocycline treatment reduces delayed oligodendrocyte death, attenuates axonal dieback, and improves functional outcome after spinal cord injury. Journal of Neuroscience. 24**,** 2182-2190.

Stobart, J.L., Anderson, C.M., 2013. Multifunctional role of astrocytes as gatekeepers of neuronal energy supply. Frontiers in Cellular Neuroscience. 7.

Stoica, B.A., Faden, A.I., 2010. Cell Death Mechanisms and Modulation in Traumatic Brain Injury. Neurotherapeutics. 7**,** 3-12.

Stoll, G., Muller, H.W., 1999. Nerve injury, axonal degeneration and neural regeneration: Basic insights. Brain Pathology. 9**,** 313-325.

Strauss, S., Otten, U., Joggerst, B., Pluss, K., Volk, B., 1994. Increased levels of Nerve Growth-Factor (NGF) protein and messenger-rna and reactive gliosis following kainic acid injection into the rat striatum. Neuroscience Letters. 168**,** 193-196.

Streit, W.J., Kreutzberg, G.W., 1988. Response of endogenous glial-cells to motor neuron degeneration induced by toxic Ricin. Journal of Comparative Neurology. 268**,** 248-263.

Streit, W.J., Graeber, M.B., Kreutzberg, G.W., 1989a. Expression of ia-antigen on perivascular and microglial cells after sublethal and lethal motor neuron injury. Experimental Neurology. 105**,** 115-126.

Streit, W.J., Graeber, M.B., Kreutzberg, G.W., 1989b. Peripheral-nerve lesion produces increased levels of major histocompatibility complex antigens in the Central Nervous-System. Journal of Neuroimmunology. 21**,** 117-123.

Streit, W.J., Semple-Rowland, S.L., Hurley, S.D., Miller, R.C., Popovich, P.G., Stokes, B.T., 1998. Cytokine mRNA profiles in contused spinal cord and axotomized facial nucleus suggest a beneficial role for inflammation and gliosis. Experimental Neurology. 152**,** 74-87.

Streit, W.J., Hurley, S.D., McGraw, T.S., Semple-Rowland, S.L., 2000. Comparative evaluation of cytokine profiles and reactive gliosis supports a critical role for interleukin-6 in neuron-glia signaling during regeneration. Journal of Neuroscience Research. 61**,** 10-20.

Streppel, M., Azzolin, N., Dohm, S., Guntinas-Lichius, O., Haas, C., Grothe, C., Wevers, A., Neiss, W.F., Angelov, D.N., 2002. Focal application of neutralizing antibodies to soluble neurotrophic factors reduces collateral axonal branching after peripheral nerve lesion. European Journal of Neuroscience. 15**,** 1327-1342.

Strittmatter, S.M., Fankhauser, C., Huang, P.L., Mashimo, H., Fishman, M.C., 1995. Neuronal pathfinding is abnormal in mice lacking the neuronal growth cone protein GAP-43. Cell. 80**,** 445-452.

Sunderland, S., 1947. Rate of regeneration of motor fibers in the ulnar and sciatic nerves. Archives of Neurology and Psychiatry. 58**,** 7-13.

Sung, J.K., Miao, L., Calvert, J.W., Huang, L.X., Harkey, H.L., Zhang, J.H., 2003. A possible role of RhoA/Rho-kinase in experimental spinal cord injury in rat. Brain Research. 959**,** 29-38.

Suzumura, A., Mezitis, S.G.E., Gonatas, N.K., Silberberg, D.H., 1987. MHC antigen expression on bulk isolated macrophage-microglia from newborn mouse-brain - induction of IA-antigen expression by Gamma-Interferon. Journal of Neuroimmunology. 15**,** 263-278.

Svensson, M., Mattsson, P., Aldskogius, H., 1994. A bromodeoxyuridine labeling study of proliferating cells in the brain-stem following hypoglossal nerve transection. Journal of Anatomy. 185**,** 537-542.

Svigos, J.M., 2001. The fetal inflammatory response syndrome and cerebral palsy: yet another challenge and dilemma for the obstetrician. Australian & New Zealand Journal of Obstetrics & Gynaecology. 41**,** 170-176.

Szczepanik, A.M., Fishkin, R.J., Rush, D.K., Wilmot, C.A., 1996. Effects of chronic intrahippocampal infusion of lipopolysaccharide in the rat. Neuroscience. 70**,** 57-65.

Tabakow, P., Raisman, G., Fortuna, W., Czyz, M., Huber, J., Li, D., Szewczyk, P., Okurowski, S., Miedzybrodzki, R., Czapiga, B., Salomon, B., Halon, A., Li, Y., Lipiec, J., Kulczyk, A., Jarmundowicz, W., 2014. Functional regeneration of supraspinal connections in a patient with transected spinal cord following transplantation of bulbar olfactory ensheathing cells with peripheral nerve bridging. Cell Transplant.

Tabata, H., Nakajima, K., 2001. Efficient in utero gene transfer system to the developing mouse brain using electroporation: Visualization of neuronal migration in the developing cortex. Neuroscience. 103**,** 865-872.

Tahraoui, S.L., Marret, S., Bodenant, C., Leroux, P., Dommergues, M.A., Evrard, P., Gressens, P., 2001. Central role of microglia in neonatal excitotoxic lesions ef the murine periventricular white matter. Brain Pathology. 11**,** 56-71.

Takami, T., Oudega, M., Bates, M.L., Wood, P.M., Kleitman, N., Bunge, M.B., 2002. Schwann cell but not olfactory ensheathing glia transplants improve hindlimb locomotor performance in the moderately contused adult rat thoracic spinal cord. Journal of Neuroscience. 22**,** 6670-6681.

Takeda, A., Kimpara, T., Onodera, H., Itoyama, Y., Shibahara, S., Kogure, K., 1996. Regional difference in induction of heme oxygenase-1 protein following rat transient forebrain ischemia. Neuroscience Letters. 205**,** 169-172.

Takeuchi, H., Jin, S., Wang, J., Zhang, G., Kawanokuchi, J., Kuno, R., Sonobe, Y., Mizuno, T., Suzumura, A., 2006. Tumor necrosis factor-alpha induces neurotoxicity via glutamate release from hemichannels of activated microglia in an autocrine manner. Journal of Biological Chemistry. 281**,** 21362-21368.

Takizawa, S., Matsushima, K., Shinohara, Y., Ogawa, S., Komatsu, N., Utsunomiya, H., Watanabe, K., 1994. Immunohistochemical localization of glutathione-peroxidase in infarcted human brain. Journal of the Neurological Sciences. 122**,** 66-73.

Tanaka, H., Yamashita, T., Yachi, K., Fujiwara, T., Yoshikawa, H., Tohyama, M., 2004. Cytoplasmic p21(Cip1/WAF1) enhances axonal regeneration and functional recovery after spinal cord injury in rats. Neuroscience. 127**,** 155-164.

Tanaka, K., Zhang, Q.L., Webster, H.D., 1992. Myelinated fiber regeneration after sciatic-nerve crush - morphometric observations in young-adult and aging mice and the effects of macrophage suppression and conditioning lesions. Experimental Neurology. 118**,** 53-61.

Tang, B.L., 2003. Inhibitors of neuronal regeneration: mediators and signaling mechanisms. Neurochemistry International. 42**,** 189-203.

Tanigawa, N., Saito, T., Ogawa, K., Iida, H., 2005. Origin of regenerated axons in nerve bypass grafts. Journal of Neurotrauma. 22**,** 605-612.

Taocheng, J.H., Nagy, Z., Brightman, M.W., 1987. Tight junctions of brain endothelium in vitro are enhanced by astroglia. Journal of Neuroscience. 7**,** 3293-3299.

Taylor, D.L., Jones, F., Kubota, E., Pocock, J.M., 2005. Stimulation of microglial metabotropic glutamate receptor mGlu2 triggers tumor necrosis factor alpha-induced neurotoxicity in concert with microglial-derived fas ligand. Journal of Neuroscience. 25**,** 2952-2964.

Taylor, L., Jones, L., Tuszynski, M.H., Blesch, A., 2006. Neurotrophin-3 gradients established by lentiviral gene delivery promote short-distance axonal bridging beyond cellular grafts in the injured spinal cord. Journal of Neuroscience. 26**,** 9713-9721.

Tedeschi, A., Nguyen, T., Puttagunta, R., Gaub, P., Di Giovanni, S., 2009. A p53-CBP/p300 transcription module is required for GAP-43 expression, axon outgrowth, and regeneration. Cell Death and Differentiation. 16**,** 543-554.

Teng, Y.D., Lavik, E.B., Qu, X.L., Park, K.I., Ourednik, J., Zurakowski, D., Langer, R., Snyder, E.Y., 2002. Functional recovery following traumatic spinal cord injury mediated by a unique polymer scaffold seeded with neural stem

cells. Proceedings of the National Academy of Sciences of the United States of America. 99**,** 3024-3029.

Teng, Y.D., Choi, H., Onario, R.C., Zhu, S., Desilets, F.C., Lan, S.M., Woodard, E.J., Snyder, E.Y., Eichler, M.E., Friedlander, R.M., 2004. Minocycline inhibits contusion-triggered mitochondrial cytochrome c release and mitigates functional deficits after spinal cord injury. Proceedings of the National Academy of Sciences of the United States of America. 101**,** 3071-3076.

Terman, J.R., Mao, T.Y., Pasterkamp, R.J., Yu, H.H., Kolodkin, A.L., 2002. MICALs, a family of conserved flavoprotein oxidoreductases, function in plexin-mediated axonal repulsion. Cell. 109**,** 887-900.

Tetzlaff, W., Bisby, M.A., Kreutzberg, G.W., 1988a. Changes in cytoskeletal proteins in the rat facial nucleus following axotomy. Journal of Neuroscience. 8**,** 3181-3189.

Tetzlaff, W., Graeber, M.B., Bisby, M.A., Kreutzberg, G.W., 1988b. Increased glial fibrillary acidic protein-synthesis in astrocytes during retrograde reaction of the rat facial nucleus. Glia. 1**,** 90-95.

Tetzlaff, W., Alexander, S.W., Miller, F.D., Bisby, M.A., 1991. Response of facial and rubrospinal neurons to axotomy - changes in messenger-RNA expression for cytoskeletal proteins and GAP-43. Journal of Neuroscience. 11**,** 2528-2544.

Thallmair, M., Metz, G.A.S., Z'Graggen, W.J., Raineteau, O., Kartje, G.L., Schwab, M.E., 1998. Neurite growth inhibitors restrict plasticity and functional recovery following corticospinal tract lesions. Nature Neuroscience. 1**,** 124-131.

Thored, P., Heldmann, U., Gomes-Leal, W., Gisler, R., Darsalia, V., Taneera, J., Nygren, J.M., Jacobsen, S.-E.W., Ekdahl, C.T., Kokaia, Z., Lindvall, O., 2009. Long-Term Accumulation of Microglia with Proneurogenic Phenotype Concomitant with Persistent Neurogenesis in Adult Subventricular Zone After Stroke. Glia. 57**,** 835-849.

Thuret, S., Moon, L.D.F., Gage, F.H., 2006. Therapeutic interventions after spinal cord injury. Nature Reviews Neuroscience. 7**,** 628-643.

Tofaris, G.K., Patterson, P.H., Jessen, K.R., Mirsky, R., 2002. Denervated Schwann cells attract macrophages by secretion of leukemia inhibitory factor (LIF) and monocyte chemoattractant protein-1 in a process regulated by interleukin-6 and LIF. Journal of Neuroscience. 22**,** 6696-6703.

Tokita, Y., Keino, H., Matsui, F., Aono, S., Ishiguro, H., Higashiyama, S., Oohira, A., 2001. Regulation of neuregulin expression in the injured rat brain and cultured astrocytes. Journal of Neuroscience. 21**,** 1257-1264.

Tosolini, A.P., Morris, R., 2012. Spatial characterization of the motor neuron columns supplying the rat forelimb. Neuroscience. 200**,** 19-30.

Toth, C.C., Willis, D., Twiss, J.L., Walsh, S., Martinez, J.A., Liu, W.-Q., Midha, R., Zochodne, D.W., 2009. Locally Synthesized Calcitonin Gene-Related Peptide Has a Critical Role in Peripheral Nerve Regeneration. Journal of Neuropathology and Experimental Neurology. 68**,** 326-337.

Toulmond, S., Rothwell, N.J., 1995. Interleukin-1 receptor antagonist inhibits neuronal damage caused by fluid percussion injury in the rat. Brain Research. 671**,** 261-266.

Town, T., Jeng, D., Alexopoulou, L., Tan, J., Flavell, R.A., 2006. Microglia recognize double-stranded RNA via TLR3. Journal of Immunology. 176**,** 3804-3812.

Trapp, B.D., Peterson, J., Ransohoff, R.M., Rudick, R., Mork, S., Bo, L., 1998. Axonal transection in the lesions of multiple sclerosis. New England Journal of Medicine. 338**,** 278-285.

Trojanowski, J.Q., Lee, V.M.Y., Schlaepfer, W.W., 1984. Neurofilament breakdown products in degenerating rat and human peripheral-nerves. Annals of Neurology. 16**,** 349-355.

Tsacopoulos, M., Magistretti, P.J., 1996. Metabolic coupling between glia and neurons. Journal of Neuroscience. 16**,** 877-885.

Tseng, G.F., Wang, Y.J., Lai, Q.C., 1996. Perineuronal microglial reactivity following proximal and distal axotomy of rat rubrospinal neurons. Brain Research. 715**,** 32-43.

Tuszynski, M.H., Gabriel, K., Gage, F.H., Suhr, S., Meyer, S., Rosetti, A., 1996. Nerve growth factor delivery by gene transfer induces differential outgrowth of sensory, motor, and noradrenergic neurites after adult spinal cord injury. Experimental Neurology. 137**,** 157-173.

Uno, H., Matsuyama, T., Akita, H., Nishimura, H., Sugita, M., 1997. Induction of tumor necrosis factor-alpha in the mouse hippocampus following transient forebrain ischemia. Journal of Cerebral Blood Flow and Metabolism. 17**,** 491-499.

Unsicker, K., Meier, C., Krieglstein, K., Sartor, B.M., Flanders, K.C., 1996. Expression, localization, and function of transforming growth factor-beta s in embryonic chick spinal cord, hindbrain, and dorsal root ganglia. Journal of Neurobiology. 29**,** 262-276.

Urakubo, A., Jarskog, L.F., Lieberman, J.A., Gilmore, J.H., 2001. Prenatal exposure to maternal infection alters cytokine expression in the placenta, amniotic fluid, and fetal brain. Schizophrenia Research. 47**,** 27-36.

Vallee, R.B., Bloom, G.S., 1991. Mechanisms of fast and slow axonal-transport. Annual Review of Neuroscience. 14**,** 59-92.

van der Veen, R.C., Hinton, D.R., Incardonna, F., Hofman, F.M., 1997. Extensive peroxynitrite activity during progressive stages of central nervous system inflammation. Journal of Neuroimmunology. 77**,** 1-7.

van Meerloo, J., Kaspers, G.J.L., Cloos, J., 2011. Cell Sensitivity Assays: The MTT Assay. In Cancer Cell Culture: Methods and Protocols, Second Edition. Methods in Molecular Biology, Vol. 731, I.A. Cree. Humana Press Inc, Totowa, pp. 237-245.

Van Meeteren, N.L.U., Eggers, R., Lankhorst, A.J., Gispen, W.H., Hamers, F.P.T., 2003. Locomotor recovery after spinal cord contusion injury in rats is improved by spontaneous exercise. Journal of Neurotrauma. 20**,** 1029-1037.

van Rossum, D., Hilbert, S., Strassenburg, S., Hanisch, U.-K., Brueck, W., 2008. Myelin-phagocytosing macrophages in isolated sciatic and optic nerves reveal a unique reactive phenotype. Glia. 56**,** 271-283.

Varol, C., Landsman, L., Fogg, D.K., Greenshtein, L., Gildor, B., Margalit, R., Kalchenko, V., Geissmann, F., Jung, S., 2007. Monocytes give rise to mucosal, but not splenic, conventional dendritic cells. Journal of Experimental Medicine. 204**,** 171-180.

Vaudano, E., Campbell, G., Anderson, P.N., Davies, A.P., Woolhead, C., Schreyer, D.J., Lieberman, A.R., 1995. The effects of a lesion or a peripheral-nerve graft on GAP-43 up-regulation in the adult-rat brain - an in-situ hybridization and immunocytochemical study. Journal of Neuroscience. 15**,** 3594-3611.

Vavrek, R., Girgis, J., Tetzlaff, W., Hebert, G.W., Fouad, K., 2006. BDNF promotes connections of corticospinal neurons onto spared descending interneurons in spinal cord injured rats. Brain. 129**,** 1534-1545.

Verdrengh, M., Tarkowski, A., 1998. Granulocyte-macrophage colony-stimulating factor in Staphylococcus aureus-induced arthritis. Infection and Immunity. 66**,** 853-855.

Verma, P., Chierzi, S., Codd, A.M., Campbell, D.S., Meyer, R.L., Holt, C.E., Fawcett, J.W., 2005. Axonal protein synthesis and degradation are necessary for efficient growth cone regeneration. Journal of Neuroscience. 25**,** 331-342.

Vidovic, M., Sparacio, S.M., Elovitz, M., Benveniste, E.N., 1990. Induction and regulation of Class-II Major Histocompatibility Complex messenger-RNA expression in astrocytes by Interferon-Gamma and Tumor-Necrosis-Factor-Alpha. Journal of Neuroimmunology. 30**,** 189-200.

Vincent, V.A.M., Tilders, F.J.H., VanDam, A.M., 1997. Inhibition of endotoxin-induced nitric oxide synthase production in microglial cells by the presence of astroglial cells: A role for transforming growth factor beta. Glia. 19**,** 190-198.

Volpe, J.J., 2009. Brain injury in premature infants: a complex amalgam of destructive and developmental disturbances. Lancet Neurology. 8**,** 110-124.

von Meyenburg, J., Brosamle, C., Metz, G.A.S., Schwab, M.E., 1998. Regeneration and sprouting of chronically injured corticospinal tract fibers in adult rats promoted by NT-3 and the mAb IN-1, which neutralizes myelin-associated neurite growth inhibitors. Experimental Neurology. 154**,** 583-594.

Vroemen, M., Aigner, L., Winkler, J., Weidner, N., 2003. Adult neural progenitor cell grafts survive after acute spinal cord injury and integrate along axonal pathways. European Journal of Neuroscience. 18**,** 743-751.

Wahl, S.M., Feldman, G.M., McCarthy, J.B., 1996. Regulation of leukocyte adhesion and signaling in inflammation and disease. Journal of Leukocyte Biology. 59**,** 789-796.

Wang, K.C., Koprivica, V., Kim, J.A., Sivasankaran, R., Guo, Y., Neve, R.L., He, Z.G., 2002. Oligodendrocyte-myelin glycoprotein is a Nogo receptor ligand that inhibits neurite outgrowth. Nature. 417**,** 941-944.

Wang, X., Rousset, C.I., Hagberg, H., Mallard, C., 2006. Lipopolysaccharide-induced inflammation and perinatal brain injury. Seminars in Fetal & Neonatal Medicine. 11**,** 343-353.

Wang, X., Hellgren, G., Lofqvist, C., Li, W., Hellstrom, A., Hagberg, H., Mallard, C., 2009. White Matter Damage After Chronic Subclinical Inflammation in Newborn Mice. Journal of Child Neurology. 24**,** 1171-1178.

Wang, X.K., Barone, F.C., Aiyar, N.V., Feuerstein, G.Z., 1997. Interleukin-1 receptor and receptor antagonist gene expression after focal stroke in rats. Stroke. 28**,** 155-161.

Wannier, T., Schmidlin, E., Bloch, J., Rouiller, E.M., 2005. A unilateral section of the corticospinal tract at cervical level in primate does not lead to measurable cell loss in motor cortex. Journal of Neurotrauma. 22**,** 703-717.

Weidner, N., Ner, A., Salimi, N., Tuszynski, M.H., 2001. Spontaneous corticospinal axonal plasticity and functional recovery after adult central nervous system injury. Proceedings of the National Academy of Sciences of the United States of America. 98**,** 3513-3518.

Wekerle, H., Linington, C., Lassmann, H., Meyermann, R., 1986. Cellular immune reactivity within the CNS. Trends in Neurosciences. 9**,** 271-277.

Werner, A., Kloss, C.U.A., Walter, J., Kreutzberg, G.W., Raivich, G., 1998. Intercellular adhesion molecule-1 (ICAM-1) in the mouse facial motor nucleus after axonal injury and during regeneration. Journal of Neurocytology. 27**,** 219-232.

Werner, A., Willem, M., Jones, L.L., Kreutzberg, G.W., Mayer, U., Raivich, G., 2000. Impaired axonal regeneration in alpha 7 integrin-deficient mice. Journal of Neuroscience. 20**,** 1822-1830.

Whishaw, I.Q., Nonneman, A.J., Kolb, B., 1981. Environmental constraints on motor abilities used in grooming, swimming, and eating by decorticate rats. Journal of Comparative and Physiological Psychology. 95**,** 792-804.

Whishaw, I.Q., Oconnor, W.T., Dunnett, S.B., 1986. The contributions of motor cortex, nigrostriatal dopamine and caudate-putamen to skilled forelimb use in the rat. Brain. 109**,** 805-843.

Whishaw, I.Q., Kolb, B., 1988. Sparing of skilled forelimb reaching and corticospinal projections after neonatal motor cortex removal or hemidecortication in the rat - support for the kennard doctrine. Brain Research. 451**,** 97-114.

Whishaw, I.Q., Pellis, S.M., 1990. The structure of skilled forelimb reaching in the rat - a proximally driven movement with a single distal rotatory component. Behavioural Brain Research. 41**,** 49-59.

Whishaw, I.Q., Pellis, S.M., Gorny, B.P., Pellis, V.C., 1991. The impairments in reaching and the movements of compensation in rats with motor cortex lesions - an end-point, videorecording, and movement notation analysis. Behavioural Brain Research. 42**,** 77-91.

Whishaw, I.Q., Dringenberg, H.C., Pellis, S.M., 1992. Spontaneous forelimb grasping in free feeding by rats - motor cortex aids limb and digit positioning. Behavioural Brain Research. 48**,** 113-125.

Whishaw, I.Q., Pellis, S.M., Gorny, B., Kolb, B., Tetzlaff, W., 1993. Proximal and distal impairments in rat forelimb use in reaching follow unilateral pyramidal tract lesions. Behavioural Brain Research. 56**,** 59-76.

Whishaw, I.Q., Gorny, B., 1996. Does the red nucleus provide the tonic support against which fractionated movements occur? A study on forepaw movements used in skilled reaching by the rat. Behavioural Brain Research. 74**,** 79-90.

Whishaw, I.Q., Gorny, B., Sarna, J., 1998. Paw and limb use in skilled and spontaneous reaching after pyramidal tract, red nucleus and combined lesions in the rat: behavioral and anatomical dissociations. Behavioural Brain Research. 93**,** 167-183.

Wiktor-Jedrzejczak, W., Bartocci, A., Ferrante, A.W., Ahmedansari, A., Sell, K.W., Pollard, J.W., Stanley, E.R., 1990. Total absence of colony-stimulating factor 1 in the macrophage-deficient osteopetrotic (OP OP) mouse. Proceedings of the National Academy of Sciences of the United States of America. 87**,** 4828-4832.

Williams, S.E., Mann, F., Erskine, L., Sakurai, T., Wei, S.N., Rossi, D.J., Gale, N.W., Holt, C.E., Mason, C.A., Henkemeyer, M., 2003. Ephrin-B2 and EphB1 mediate retinal axon divergence at the optic chiasm. Neuron. 39**,** 919-935.

Willis, D., Li, K.W., Zheng, J.Q., Chang, J.H., Smit, A., Kelly, T., Merianda, T.T., Sylvester, J., van Minnen, J., Twiss, J.L., 2005. Differential transport and local translation of cytoskeletal, injury-response, and neurodegeneration protein mRNAs in axons. Journal of Neuroscience. 25**,** 778-791.

Wolpaw, J.R., 2006. Treadmill training after spinal cord injury - Good but not better. Neurology. 66**,** 466-467.

Wong, G.H.W., Bartlett, P.F., Clarklewis, I., Battye, F., Schrader, J.W., 1984. Inducible expression of H-2 and IA antigens on brain-cells. Nature. 310**,** 688-691.

Wong, L.F., Goodhead, L., Prat, C., Mitrophanous, K.A., Kingsman, S.M., Mazarakis, N.D., 2006. Lentivirus-mediated gene transfer to the central nervous system: Therapeutic and research applications. Human Gene Therapy. 17**,** 1-9.

Wu, D., Huang, W., Richardson, P.M., Priestley, J.V., Liu, M., 2008. TRPC4 in rat dorsal root ganglion neurons is increased after nerve injury and is necessary for neurite outgrowth. Journal of Biological Chemistry. 283**,** 416-426.

Wu, S.F., Suzuki, Y., Ejiri, Y., Noda, T., Bai, H.L., Kitada, M., Kataoka, K., Ohta, M., Chou, H., Ide, C., 2003. Bone marrow stromal cells enhance differentiation of cocultured neurosphere cells and promote regeneration of injured spinal. Journal of Neuroscience Research. 72**,** 343-351.

Xu, M., Ng, Y.K., Leong, S.K., 1998. Induction of microglial reaction and expression of nitric oxide synthase I in the nucleus dorsalis and red nucleus following lower thoracic spinal cord hemisection. Brain Research. 808**,** 23-30.

Xu, X.M., Guenard, V., Kleitman, N., Bunge, M.B., 1995. Axonal regeneration into schwann cell-seeded guidance channels grafted into transected adult-rat spinal-cord. Journal of Comparative Neurology. 351**,** 145-160.

Yamamoto, M., Raisman, G., Li, Y., 2009. Loss of directed fore-limb reaching after destruction of spinal grey matter. Brain Research. 1265**,** 47-52.

Yan, Q., Wang, J., Matheson, C.R., Urich, J.L., 1999. Glial cell line-derived neurotrophic factor (GDNF) promotes the survival of axotomized retinal ganglion cells in adult rats: Comparison to and combination with brain-derived neurotrophic factor (BDNF). Journal of Neurobiology. 38**,** 382-390.

Yanez-Munoz, R.J., Balaggan, K.S., MacNeil, A., Howe, S.J., Schmidt, M., Smith, A.J., Buch, P., MacLaren, R.E., Anderson, P.N., Barker, S.E., Duran, Y., Bartholomae, C., von Kalle, C., Heckenlively, J.R., Kinnon, C., Ali, R.R., Thrasher, A.J., 2006. Effective gene therapy with nonintegrating lentiviral vectors. Nature Medicine. 12**,** 348-353.

Yang, G.Y., Liu, X.H., Kadoya, C., Zhao, Y.J., Mao, Y., Davidson, B.L., Betz, A.L., 1998. Attenuation of ischemic inflammatory response in mouse brain using an adenoviral vector to induce overexpression of interleukin-1 receptor antagonist. Journal of Cerebral Blood Flow and Metabolism. 18**,** 840-847.

Yang, J.T., Rayburn, H., Hynes, R.O., 1993. Embryonic mesodermal defects in alpha(5) integrin-deficient mice. Development. 119**,** 1093-1105.

Yang, P., Wen, H.Z., Ou, S., Cui, J., Fan, D.H., 2012. IL-6 promotes regeneration and functional recovery after cortical spinal tract injury by reactivating intrinsic growth program of neurons and enhancing synapse formation. Experimental Neurology. 236**,** 19-27.

Yick, L.W., Wu, W.T., So, K.F., Yip, H.K., Shum, D.K.Y., 2000. Chondroitinase ABC promotes axonal regeneration of Clarke's neurons after spinal cord injury. Neuroreport. 11**,** 1063-1067.

Yick, L.W., Cheung, P.T., So, K.F., Wu, W.T., 2003. Axonal regeneration of Clarke's neurons beyond the spinal cord injury scar after treatment with chondroitinase ABC. Experimental Neurology. 182**,** 160-168.

Yick, L.W., So, K.F., Cheung, P.T., Wu, W.T., 2004. Lithium chloride reinforces the regeneration-promoting effect of chondroitinase ABC on rubrospinal neurons after spinal cord injury. Journal of Neurotrauma. 21**,** 932-943.

Yin, Y., Leon, S., Hu, M., Irwin, N., Benowitz, L.I., 2000. Macrophage activation in the eye stimulates retinal ganglion cell survival and axon regeneration in the mature rat optic nerve. Society for Neuroscience Abstracts. 26**,** Abstract No.-229.7.

Yin, Y.Q., Henzl, M.T., Lorber, B., Nakazawa, T., Thomas, T.T., Jiang, F., Langer, R., Benowitz, L.I., 2006. Oncomodulin is a macrophage-derived signal for axon regeneration in retinal ganglion cells. Nature Neuroscience. 9**,** 843-852.

Yoneyama, M., Fujita, T., 2010. Recognition of viral nucleic acids in innate immunity. Reviews in Medical Virology. 20**,** 4-22.

Yoo, S., Nguyen, M.P., Fukuda, M., Bittner, G.D., Fishman, H.M., 2003. Plasmalemmal sealing of transected mammalian neurites is a gradual process mediated by Ca2+-regulated proteins. Journal of Neuroscience Research. 74**,** 541-551.

Yoon, B.H., Jun, J.K., Romero, R., Park, K.H., Gomez, R., Choi, J.H., Kim, I.O., 1997a. Amniotic fluid inflammatory cytokines (interleukin-6, interleukin-1 beta, and tumor necrosis factor-alpha), neonatal brain white matter lesions, and cerebral palsy. American Journal of Obstetrics and Gynecology. 177**,** 19-26.

Yoon, B.H., Romero, R., Kim, C.J., Koo, J.N., Choe, G., Syn, H.C., Chi, J.G., 1997b. High expression of tumor necrosis factor-alpha and interleukin-6 in periventricular leukomalacia. American Journal of Obstetrics and Gynecology. 177**,** 406-411.

Z'Graggen, W.J., Metz, G.A.S., Kartje, G.L., Thallmair, M., Schwab, M.E., 1998. Functional recovery and enhanced corticofugal plasticity after unilateral pyramidal tract lesion and blockade of myelin-associated neurite growth inhibitors in adult rats. Journal of Neuroscience. 18**,** 4744-4757.

Zagrebelsky, M., Buffo, A., Skerra, A., Schwab, M.E., Strata, P., Rossi, F., 1998. Retrograde regulation of growth-associated gene expression in adult rat Purkinje cells by myelin-associated neurite growth inhibitory proteins. Journal of Neuroscience. 18**,** 7912-7929.

Zhang, X., Xin, N., Tong, L., Tong, X.-J., 2013. Electrical stimulation enhances peripheral nerve regeneration after crush injury in rats. Molecular Medicine Reports. 7**,** 1523-1527.

Zhang, Y., Campbell, G., Anderson, P.N., Martini, R., Schachner, M., Lieberman, A.R., 1995. Molecular-basis of interactions between regenerating adult-rat thalamic axons and schwann-cells in peripheral-nerve grafts .1. Neural cell-adhesion molecules. Journal of Comparative Neurology. 361**,** 193-209.

Zhang, Y., Tohyama, K., Winterbottom, J.K., Haque, N.S.K., Schachner, M., Lieberman, A.R., Anderson, P.N., 2001. Correlation between putative inhibitory molecules at the dorsal root entry zone and failure of dorsal root axonal regeneration. Molecular and Cellular Neuroscience. 17**,** 444-459.

Zhang, Z.G., Chopp, M., Goussev, A., Powers, C., 1998. Cerebral vessels express interleukin 1 beta after focal cerebral ischemia. Brain Research. 784**,** 210-217.

Zheng, J.Q., Kelly, T.K., Chang, B.S., Ryazantsev, S., Rajasekaran, A.K., Martin, K.C., Twiss, J.L., 2001. A functional role for intra-axonal protein synthesis during axonal regeneration from adult sensory neurons. Journal of Neuroscience. 21**,** 9291-9303.

Zhi, Y., Lu, Q., Zhang, C.W., Yip, H.K., So, K.F., Cui, Q., 2005. Different optic nerve injury sites result in different responses of retinal ganglion cells to brain-derived neurotrophic factor but not neurotrophin-4/5. Brain Research. 1047**,** 224-232.

Zhou, T.H., Ling, K., Guo, J., Zhou, H., Wu, Y.L., Jing, Q., Ma, L., Pei, G., 2000. Identification of a human brain-specific isoform of mammalian STE20-like kinase 3 that is regulated by cAMP-dependent protein kinase. Journal of Biological Chemistry. 275**,** 2513-2519.